Cocrystals Mitigate the Effect of pH on Solubility and Dissolution of Basic Drugs

by

Yitian Marguerite Chen

A dissertation submitted in partial fulfillment
of the requirements for the degree of
Doctor of Philosophy
(Pharmaceutical Sciences)
in the University of Michigan
2017

Doctoral Committee:

Professor Naír Rodríguez-Hornedo, Chair
Professor Gordon L. Amidon
Research Professor Gregory E. Amidon
Professor Adam J. Matzger

Yitian Marguerite Chen

yitian@umich.edu

ORCID iD: 0000-0002-6539-1861

ACKNOWLEDGEMENTS

I would like to acknowledge all the individuals who have supported and encouraged me during my graduate studies. First and foremost, I would like to extend my sincerest gratitude toward my advisor, Dr. Naír Rodríguez-Hornedo. It has been such a privilege to study and train under her instruction. Her extensive knowledge and abundant enthusiasm for science has been and will continue to be an inspiration to me. Her constant challenges for me to think harder, dig deeper, and see further have exponentially improved my ability to critically think and solve problems over the years. I could not have become the scientist I am today without her training and encouragement. I would also like to thank my dissertation committee members, Dr. Gordon Amidon, Dr. Gregory Amidon, and Dr. Adam Matzger for their valuable insights and helpful suggestions for improvement. Dr. Greg Amidon has, on numerous occasions, advised and supported me in both thesis research and career development.

I would like to thank all my fellow lab members, past and present, for their support throughout the years. My graduate school experience would not be the same without Katie Cavanagh, Nicholas Waltz, Dr. Gislaine Kuminek, Dr. Fengjuan Cao, Dr. Maya Lipert, and Dr. Lilly Roy. I was also extremely fortunate to have the opportunity to work with many visiting students over the years, especially Paola Borba and Alanny Rocha. I would also like to extend my gratitude to our undergraduate student, Vinod Raman, who has worked on the precipitation model tirelessly with me earlier this year. All of you have made my journey through graduate school enjoyable, and I will treasure these friendships and memories for many years to come.

This research has been made possible by the financial support from many sources including the National Institute of General Medical Sciences of the National Institutes of Health (R01GM107146), the Gordon and Pamela Amidon Fellowship in Pharmaceutics, the Norman Weiner Graduate Scholarship, the Warner-Lambert/Parke-Davis Fellowship, and the Graduate Student Instructor (GSI) program at the University of Michigan, College of Pharmacy.

Lastly, I would like to thank my family and friends for their support over the years. I want to thank my parents for encouraging me to seek higher education after my undergraduate degree. I know and deeply appreciate the sacrifices they have made for me to be where I am today. A special acknowledgment goes to my fiancé, Angelo, for his patience and unconditional support in the past years. He has always been there to help me get back on track whenever I feel lost and overwhelmed. His family deserves special thanks for essentially "adopting" me as one of their own, and they were always there whenever I needed anything. I want to thank Laura Radecki and Therese Roth for showing me that I am stronger than I realized, literally. Finally, I want to thank Katherine and Caitlan, who never allowed geographical distances to diminish our friendships, and they will always be just a phone call, an email, or a road trip away.

TABLE OF CONTENTS

LIST OF FIGURES

LIST OF TABLES

ABSTRACT

Pharmaceutical cocrystals are emerging as a useful strategy for enhancing solubility, dissolution, and bioavailability for poorly water-soluble drugs. One of the most important properties of cocrystals is their fine-tunable solubility. This property enables cocrystals to increase or decrease solubility. Cocrystal solubility is the result of intricate chemical interactions between cocrystal solution components and conditions such as additives and pH. Without the critical knowledge of cocrystal solution behavior and the underlying solution interactions, studying cocrystals is a trial and error exercise that can be time consuming. This dissertation determines the mechanisms by which the cocrystal solubility is influenced by pH and solubilizing agents and investigates the relationship between cocrystal supersaturation index and conversion kinetics.

The objectives of this work are to (1) determine the effect of pH and solubilizing agents on cocrystal solubility, supersaturation index, and dissolution, (2) derive mathematical equations that describe cocrystal solubility and supersaturation index behavior based on solution equilibria of cocrystal dissociation, component ionization, and component solubilization, (3) investigate the relationship between cocrystal supersaturation index and risk of solution-mediated conversion, and (4) assess the ability of cocrystals to generate and maintain supersaturation.

Three cocrystals (1:1 stochiometric ratio) composed of a basic drug, ketoconazole (KTZ), and acidic coformers, adipic acid (ADP), fumaric acid (FUM), and succinic acid (SUC), were used as model compounds. While KTZ has shown orders of magnitude decreases in solubility

and dissolution as pH increases from 1 to 7, the cocrystal solubility increases with respect to drug at pH above pH_{max} (pH_{max} range 3.6 to 3.8). Cocrystal solubility advantage (SA), also referred to as the supersaturation index, increased from 1 at pH_{max} to between 900 and 6000 at pH 6.5. This range of SA translated into cocrystals that sustain supersaturation levels to different extents or not at all. SA values ranged from 5 to 13 (FeSSIF), 13 to 36 (blank FeSSIF), 221 to 1418 (FaSSIF), and 440 to 3118 (blank FaSSIF). Maximum supersaturation with respect to drug and AUC ratio of cocrystal to drug during dissolution showed that cocrystals exhibited superior dissolution behavior over drug in all media except for the cocrystal with the highest SA (3118, KTZ-FUM in blank FaSSIF). Cocrystals showed the highest supersaturation (22 to 30) and AUC ratio (10 to 16) values in FaSSIF. Supersaturation and AUC ratio increased with SA in FaSSIF, and they leveled off at SA between 460 and 1400. The lowest supersaturation (1.5) and AUC ratio (1.6) values were observed in FeSSIF, where cocrystals were fully dissolved and no drug precipitation occurred. pH-shift dissolution studies also showed that the cocrystal C_{max} and AUC values exhibited less sensitivity to gastric pH than the drug. KTZ was also observed to undergo liquid-liquid phase separation when high levels of supersaturation (about 150) were generated by rapid pH-shift from 2 to 6.5. These metastable forms exhibited higher solubility compared to the crystalline form, and their formation appeared to delay crystallization. Formation of such metastable phases may increase oral absorption.

CHAPTER 1

INTRODUCTION

Oral administration is the preferred way for dosing a drug product due to its noninvasiveness and convenience.[1] Generally, an orally administered drug must be absorbed from the GI tract into the systemic circulation in order to reach its intended target site, and this process is determined by the ability of the drug molecules to dissolve in the GI fluid and permeate the intestinal gut membrane.[1-2] The Biopharmaceutics Classification System (BCS) uses these two parameters, aqueous solubility and permeability, to define and describe oral absorption of drugs.[2] For BCS Class II compounds, defined as having low solubility but high permeability, dissolution is the rate-limiting step for oral absorption, and improving their solubility can potentially improve their absorption.[2-3] Pharmaceutical scientists explored many methods in attempt to improve the solubility of a poorly soluble drug including generating different solid forms of the drug such as polymorphs, amorphous materials, salts, and cocrystals.[4-5]

Recently, cocrystals have gathered a lot of interest in the pharmaceutical industry due to their potential to improve drug *in vitro* and *in vivo* performances by increasing solubility, dissolution, and therefore bioavailability.[4-14] Cocrystals are a class of multicomponent solid forms that contains two or more molecular components that are solids at room temperature (unlike solvates) in a single homogenous crystalline phase with well-defined stoichiometry.[5, 9, 15-20] The availability of a large variety of coformers offers flexibility in cocrystal composition and

stoichiometry for a single drug, and cocrystal solution behavior can be fine-tuned based on the molecular interactions in solution.[5, 15, 21-23]

Cocrystals are supersaturating drug delivery systems (SDDS) and can generate supersaturation in solution relative to drug solubility in solution.[11, 15, 21] A major challenge for cocrystals with very high solubility advantages (with respect toref drug) is the risk of rapid solution-mediated transformation to the less soluble, more thermodynamically stable drug form. This can lead to little or no improvement in dissolution and bioavailability despite the high cocrystal solubility advantage.[9, 21] Generally, the higher the solubility and solubility advantage (SA) of a cocrystal, the greater the risk of failure during its kinetic measurements.[15, 21] Cocrystal SA and stability relative to drug can be manipulated with pH and solubilizing agents with proper understanding of cocrystal solution behavior.[15, 21, 23-26]

This chapter introduces some basic concepts and current understanding of cocrystal solubility, ionization, and solubilization through relevant cocrystal solution chemistry. Research objectives will be in the conclusion of this chapter.

Cocrystal Formation and Design

Pharmaceutical cocrystals are formed by supramolecular synthons of two or more components formed through molecular associations of the component functional groups, and the carboxylic acid moieties are amongst the most common functional groups used in the crystal engineering of cocrystals.[27-28] Figure 1.1 demonstrates some of the common hydrogen bonding interactions between different functional groups.[27]

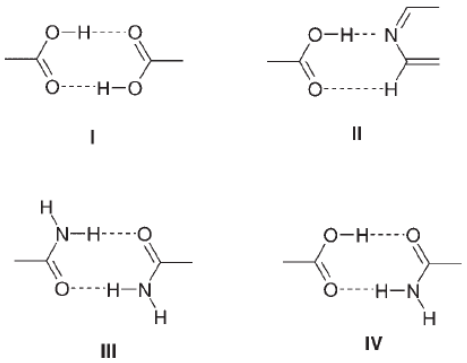

Figure 1.1. Common supramolecular synthons formed via hydrogen bonding between carboxylic acid and amide groups.[27]

Figure 1.2 illustrates some of the common multicomponent solid forms used for modification of drug properties. Cocrystals, being crystalline in structure, have stability advantage over amorphous materials, and cocrystal formation is much more predictable and less restrictive when compared to producing particular polymorphs of a material.[5] Although salts can rival cocrystals in the ability to modify the solubility of a drug, salts require acidic and basic components that have ΔpK_a greater than 2 or 3 in order to form, while cocrystals can form between neutral compounds as well as ionizable ones.[5, 15, 18] Cocrystals also differ from solvates in that all of the cocrystal components are solids at room temperature.[5, 15]

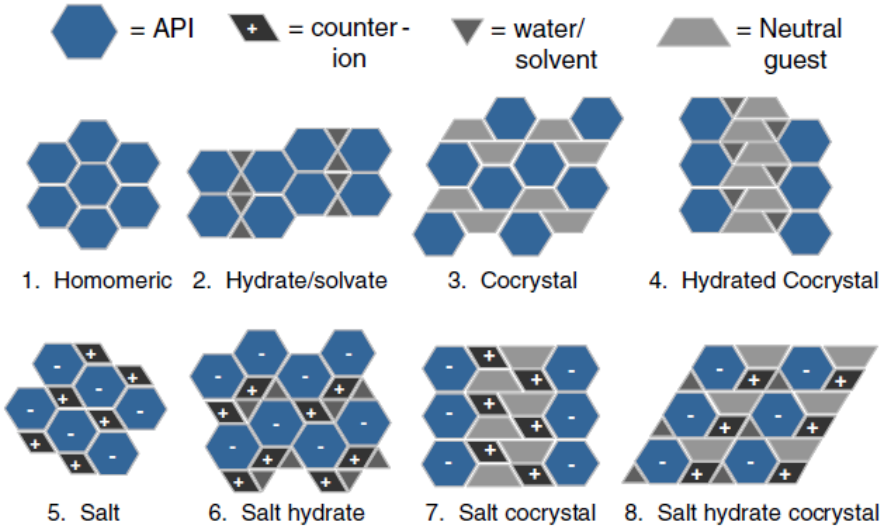

Figure 1.2. Comparison of multicomponent solid form modifications that can be used to alter the properties of a drug.[15, 29]

While coformers can be selected based on their functional group(s) potential to hydrogen bond with the drug substance, cocrystal formation is not guaranteed.[15, 28] Thus, cocrystal discovery is done empirically with selected coformers under conditions that optimize cocrystallization. Cocrystals screening and synthesis can be carried out by using a variety of methods such as slow evaporation, co-grinding, sublimation, melt crystallization, and solvent drop grinding.[5, 15, 19, 27, 30-33] Some of the limitations of cocrystal screening methods include the crystallization of single components instead of cocrystal, difficulty in scaling-up, and large amount of materials and time required. The reaction crystallization method (RCM) is particularly useful for synthesis and screening of cocrystals, and it is based on generating supersaturation with respect to cocrystal where the solution is at or below saturation with respect to its components.[15, 34]

Similar to salts, cocrystal solubility behavior is governed by solution compositions and exhibits solubility product behavior.[9, 35-36] RCM takes advantage of this solubility product behavior to generate supersaturation with respect to cocrystal in solvent systems where the cocrystals are more soluble and thermodynamically unstable compared to the drug. Consider a 1:1 (stochiometric ratio) cocrystal AB, its dissolution/precipitation in solution can be described by the following reaction,

$$AB_{cocrystal} \overset{K_{sp}}{\rightleftharpoons} A_{solution} + B_{solution} \tag{1.1}$$

where $AB_{cocrystal}$ represents the solid cocrystal, $A_{solution}$ and $B_{solution}$ represent the drug and coformer dissolved in aqueous solution, respectively. The solubility product, K_{sp}, is the equilibrium constant of this reaction.

$$K_{sp} = [A][B] \tag{1.2}$$

The terms in brackets represent concentration of the cocrystal component.

The supersaturation, σ, with respect to the cocrystal AB is described by

$$\sigma = \left(\frac{[A][B]}{K_{sp}} \right)^{1/2} \tag{1.3}$$

Figure 1.3 demonstrates how RCM generates supersaturation with respect to cocrystal and forms cocrystal in solution, by simply dissolving its components and changing their concentrations in solution.[15, 34]

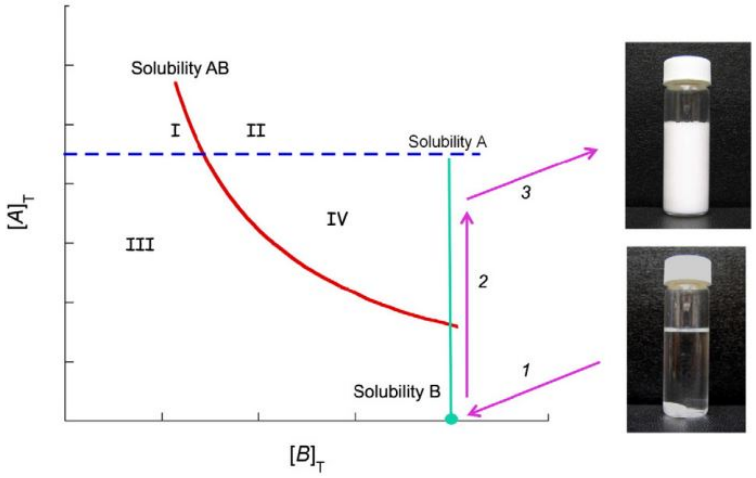

Figure 1.3 Schematic phase solubility diagram indicating regions where cocrystal can form or dissolve and a possible cocrystal formation pathway. Lines represent solubilities of drug A, coformer B, and cocrystal AB. Cocrystal solubility decreases with coformer concentration $[B]_T$. The subscript T represents analytical or total concentrations. The arrows represent a path along which only cocrystal can crystallize. Region I: solution is supersaturated with respect to drug, and cocrystal can convert to drug. Region II: solution is supersaturated with respect to both drug and cocrystal, and both can crystallize. Region III: solution is below saturation and drug, cocrystal, and coformer dissolve. Region IV: solution is supersaturated with respect to cocrystal, and drug can convert to cocrystal. Crystallization pathway involves: (1) solution saturated with respect to coformer (the most soluble component in this example), (2) dissolution of drug, and (3) cocrystal formation.[15]

At region IV (high excess coformer B concentration and supersaturated with respect to cocrystal AB) the cocrystal solubility is lower than that of the drug, and therefore the cocrystal is the thermodynamically stable form. Manipulating the solution condition so that it resembles

region IV on the diagram would maximize the likelihood of synthesizing and obtaining the cocrystal through precipitation of the least soluble crystalline form from solution. RCM has the advantages of that the cocrystal formation is not limited by different solubilities of its components, the range of solvents that can be used for cocrystallization is expanded, and cocrystals can be generated on both small and large scales.[15, 34]

Lattice and Solvation Energy of Cocrystals

Solubility is the thermodynamic equilibrium of a solute between two phases, in this case a solid and liquid phase, and the solubility enhancement of a material is based on the free energy of solution, which includes both lattice energy and solvation energy.[21, 37]

$$\Delta G_{solution} = \Delta G_{lattice} + \Delta G_{solvation} \quad (1.4)$$

In order for solubilization or dissolution to occur, the first step involves breaking the intermolecular bonds in both the solid (solute) and the solvent within themselves, and then followed by forming solute-solvent intermolecular bonds.[21, 37] The interaction of the solute-solvent must be stronger than the solute-solute and solvent-solvent bonds in order for a solid to dissolve in solution.[21] Under ideal conditions where all the intermolecular forces are equivalent (solute-solute = solvent-solvent = solute-solvent), the strength of the solute crystal lattice determines solubility.[5, 21] Formation of amorphous solids, polymorphs, solvates, salts, and cocrystals all reduce the lattice energy of the solid material in order to improve solubility. Realistically, ideal solutions are quite unusual, and therefore lattice energy alone cannot define the solubility of a material.[5, 21, 38-39]

In aqueous environments, solvation energy, rather than lattice energy, is generally the key determining factor for the solubility of a poorly soluble drug compound and its cocrystals,

especially if the drug is hydrophobic.[3, 9, 21, 25, 40] Solvation energy is based on solvent-solute interactions, and therefore it can vary greatly based on the hydrophobicity of the drug molecule and the nature of the solvent (organic vs. aqueous). In the case of a cocrystal, the coformer can decrease the solvation barrier to an extent that is proportional to the pure coformer solubility.[9, 15] The linear correlation between the aqueous solubility of coformer and cocrystal is why highly soluble coformers are usually selected to screen for cocrystals for solubility enhancement.

Cocrystal Solubility and Transition Points

Cocrystals have the versatility to fine-tune solubility, and their solubility is highly dependent on the solution phase interactions of cocrystal components.[5, 9, 15, 23, 41] Considering that cocrystals are composed of multiple components of large diversity, the molecular interactions in the solution phase can play an important role in determining cocrystal solubility.[9, 15, 21] As cocrystal dissolves in solution, the components dissociate and interact with the solution environment via ionization, partition, and complexation (figure 1.4).[9, 21, 41-42] These solution interactions will then influence the equilibrium solubility of the cocrystal.

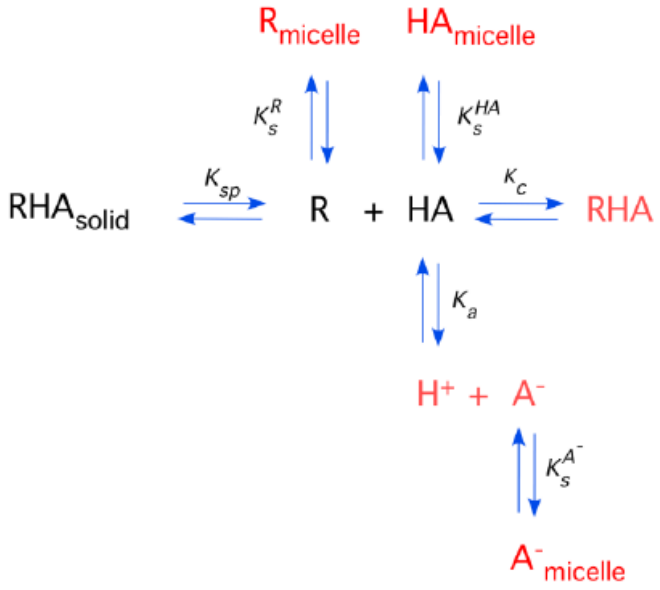

Figure 1.4. Cocrystal solution phase interactions for a cocrystal RHA of a non-ionizable drug (R) and weakly acidic conformer (HA) and associated equilibria commonly encountered by pharmaceutical dosage forms, such as dissociation, complexation, ionization, and micellar solubilization. K_{sp} represents the cocrystal solubility product, K_a is the ionization constant, K_c is the complexation constant and K_s^{HA}, $K_s^{A^-}$, K_s^R are the micellar solubilization constants for HA, A^-, and R, respectively.[5, 15, 21]

Due to different solubility-pH and solubilization behaviors exhibited by cocrystals from its parent drug, it is not uncommon for a cocrystal to be less, equal, or more soluble than the drug depending on solution conditions.[15, 21, 23-24, 26, 39, 42-43] There are a few key cocrystal solubility transition points that define the thermodynamic stability regions of a cocrystal, and at above or below which the cocrystal SA with respect to drug is reversed.[15, 24] Cocrystal transition points can be induced by pH, drug solubilizing agents, and coformer concentration in solution (figure 1.5), and they are defined by pH_{max}, CSC/S*, and K_{eu}, respectively.[15, 23-24, 26] These transitions points and the factors that affects them will be discussed in more detail in the following sections.

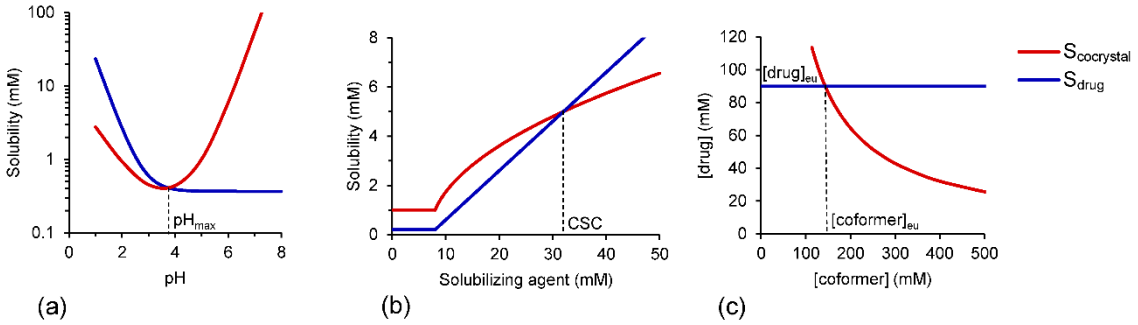

Figure 1.5. Cocrystal solubility can be fine-tuned by (a) pH, (b) drug solubilizing agents, and (c) coformer concentration. Solution conditions change the cocrystal solubility relative to drug solubility and so the cocrystal thermodynamic stability. The cocrystal is thermodynamically stable when $S_{cocrystal} \leq S_{drug}$. The cocrystal solubility advantage over drug ($S_{cocrystal}/S_{drug}$) when $S_{cocrystal} > S_{drug}$ is however critical to achieve higher drug concentrations during cocrystal dissolution.[15]

Cocrystal Ionization and pH_{max}

Pharmaceutical cocrystals often composed of drugs and coformers with different ionization properties. These components can be nonionic, acidic, basic, amphoteric, or zwitterionic.[5, 15, 21, 23, 25, 41, 44-45] The wide range of drug and coformer ionization properties results in cocrystals with a great variety of solubility-pH behavior, even for cocrystals of the same drug. It is imperative to acknowledge and understand that cocrystal solubility behaviors exhibit vastly different pH-dependence than that of the drug, and proper understanding of this behavior is essential for cocrystal characterization.

The solution phase interactions in figure 1.4 can be described by the following equilibrium reactions and corresponding constants for 1:1 cocrystal RHA, where R represents a non-ionizable drug and HA represents a weakly acidic coformer.[21, 41] The cocrystal dissolves in aqueous solution according to its K_{sp}

$$RHA_{cocrystal} \overset{K_{sp}}{\rightleftharpoons} R_{aq} + HA_{aq} \tag{1.5}$$

$$K_{sp} = [R][HA] \tag{1.6}$$

The monoprotic acidic coformer dissociates according to its ionization constant, K_a

$$HA_{aq} \overset{K_a}{\rightleftharpoons} A^-_{aq} + H^+_{aq} \tag{1.7}$$

$$K_a = \frac{[A^-]_{aq}[H^+]_{aq}}{[HA]_{aq}} \tag{1.8}$$

Under stoichiometric conditions, the solubility of the cocrystal ($S_{cocrystal}$) as a function of pH would be equal to the total concentration (T) of drug or coformer

$$S_{cocrystal} = [R]_T = [A]_T \tag{1.9}$$

Substituting in the appropriate equilibrium constants, the cocrystal solubility can be described by

$$S_{cocrystal} = \sqrt{K_{sp}\left(1 + \frac{K_a}{[H^+]}\right)} \tag{1.10}$$

Sometimes, cocrystals can exhibit a solubility transition point with respect to solution pH, called the pH_{max}.[5, 15, 21, 23, 26, 41] It is also known as the Gibbs pH, and it is not unique to cocrystals, but also commonly used to characterize pharmaceutical salts.[46-48] The pH_{max} is an important parameter that identifies stability region of cocrystals. At pH_{max}, both cocrystal and drug solid phases are thermodynamically stable and can coexist in equilibrium with solution.[21, 26, 41]

Figure 1.6 demonstrates the solubility-pH profiles of cocrystals with various ionization properties and how they differ from that of the parent drug. In figure 1.6a and 1.6b, the non-ionizable drug (R) does not exhibit solubility-pH dependence, as can be seen that the drug solubility is constant regardless of solution pH. However, the cocrystals exhibit solubility-pH dependence based on the coformer ionization properties, with the acidic coformer (H_2A) leading to cocrystal solubility increase with pH in figure 1.6a, and the amphoteric coformer (HAB) resulting in a U-shaped solubility in the pH range plotted (figure 1.6b). A cocrystal composed of

a basic drug (B) and acidic coformer (H_2A) also exhibit U-shaped solubility-pH profile, although in this case, both drug and coformer ionizations contribute to this phenomenon (figure 1.6c). In the last case, represented by figure 1.6d, an acidic coformer (H_2X) causes a steeper increase in cocrystal solubility at pH > 4, leading to an intersection of cocrystal and drug ($^-ABH^+$) solubility. This intersection, where the cocrystal and drug solubility are equal, is the transition point pH_{max}.[39, 41, 43] In the case of gabapentin-3-hydroxybenzoic acid cocrystal (figure 1.6d), at solution pH < pH_{max}, the drug is more soluble than the cocrystal, but at pH > pH_{max}, this relationship reverses, and the cocrystal becomes more soluble than the drug.

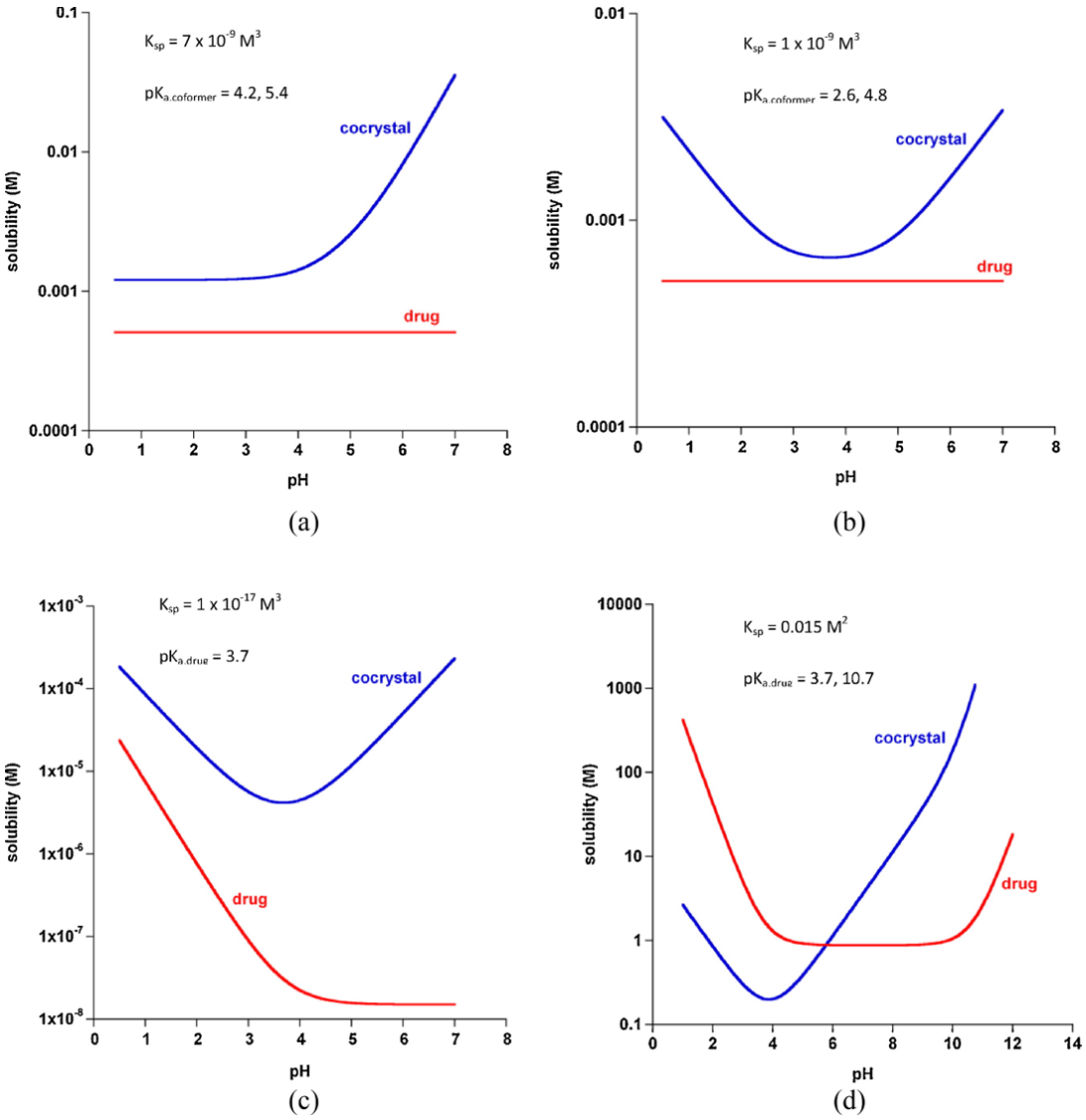

Figure 1.6. Cocrystals modulate the solubility dependence on pH as a result of the ionization properties of cocrystal components: (a) 2:1 R_2H_2A cocrystal, (b) 2:1 R_2HAB cocrystal, (c) 2:1 B_2H_2A cocrystal, and (d) 1:1 $^{-}ABH^{+}H_2X$ cocrystal. Plots were generated from experimentally determined K_a and K_{sp} values of (a) carbamazepine-succinic acid,[12] (b) carbamazepine-4-aminobenzoic acid hydrate,[41] (c) itraconazole-L-tartaric acid,[49] (d) gabapentin-3-hydroxybenzoic acid.[43] This plot shows that cocrystals can impart pH-dependent solubility to non-ionizable drugs, and modulate pH sensitivity of ionizable drugs.[41] Cocrystals can also exhibit a pH_{max} as shown for the gabapentin-3-hydroxybenzoic acid.[5, 41]

Figure 1.7 demonstrates the solubility-pH profiles of nevirapine (NVP) and its cocrystals with acidic coformers of saccharin (SAC), maleic acid (MLE), and salicylic acid (SLC).[23] The NVP cocrystals are generally more soluble than the drug, and the cocrystal solubility advantage

over drug is highly dependent on pH. At pH 1, the weakly basic drug NVP is highly soluble, and as solution pH increases, NVP solubility decreases until it reaches a constant value at pH above 4.[23] The NVP cocrystals, with the additional influence of the acidic coformers, exhibit U-shaped solubility dependence on pH. NVP-SAC and NVP-SLC have pH_{max} values at pH 1.1 and 1.7, respectively.[23] As pH nears the pH_{max}, the cocrystal SA ($S_{cocrystal}/S_{drug}$) approaches 1, meaning little or no advantage. Frequently, solution pH is ignored in the evaluation of cocrystal solubility and dissolution measurements, but NVP cocrystals demonstrated that even small variations in pH can cause large changes in cocrystal solubility and solubility advantage over drug.

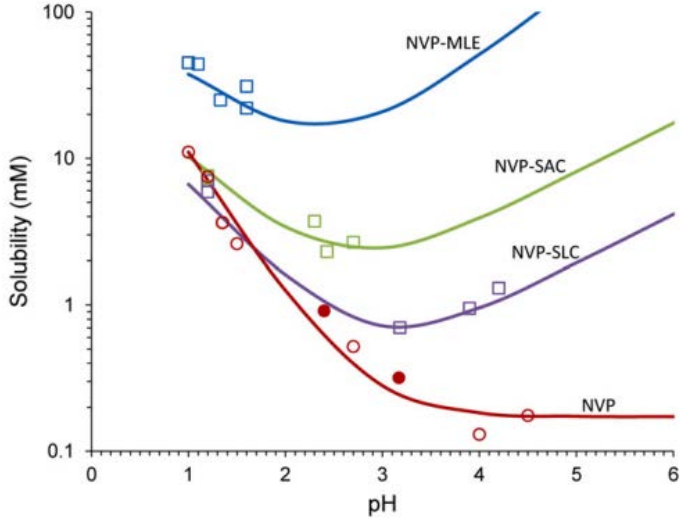

Figure 1.7. Solubility of the basic drug NVP and its cocrystals with acidic coformers: (1:1) cocrystal NVP-MLE, and (2:1) NVP-SAC and NVP-SLC as a function of pH. The symbols represent solubilities determined from the solutions saturated with NVP and/or cocrystal at 25ºC. The pH values correspond to equilibrium pH. As pH increased, the cocrystal and drug solubility curves approach each other and intersect at pH_{max}. The pH value at the intersection of the drug and cocrystal (NVP-SAC and NVP-SLC) solubility curves corresponds to pH_{max} or transition point above which a less soluble cocrystal becomes more soluble than drug. The curves were calculated from cocrystal and drug solubility-pH dependence according to equations $S^{1:1}_{cocrystal} = \sqrt{K_{sp}(1 + 10^{pK_{a,D} - pH})(1 + 10^{pH - pK_{a1,CF}} + 10^{2pH - pK_{a1,CF} - pK_{a2,CF}})}$ and $S^{2:1}_{cocrystal} = 2\sqrt[3]{\frac{K_{sp}}{4}(1 + 10^{pK_{a,D} - pH})^2(1 + 10^{pH - pK_{a1,CF}})}$ and cocrystal K_{sp} values 1.96 x 10^{-5} M^2, 1.05 x 10^{-10} M^3, and 3.63 x 10^{-11} M^3 for NVP-MLE (1:1), NVP-SAC (2:1), and NVP-SLC

(2:1), respectively. The symbols represent: NVP solubility (NVP hydrate-open circles, NVP anhydrous-filled circles) and cocrystal solubilities from eutectic points (squares).[15, 23]

Cocrystal Solubilization, S, and CSC*

Figure 1.4 also describes cocrystal solution phase interaction with drug solubilizing agents. In the presence of surfactant micelles, the non-ionizable drug R can partition into the hydrophobic micellar core, according to the micellar solubilization constant of the drug, K_S^R.[26, 42]

$$R_{aq} + M \overset{K_S^R}{\rightleftharpoons} R_m \tag{1.11}$$

$$K_s^R = \frac{[R]_m}{[R]_{aq}[M]} \tag{1.12}$$

Subscript "aq" refers to drug or coformer dissolved in the aqueous phase, subscript "m" refers to drug and coformer in the micellar pseudophase, and "[M]" represents surfactant micelle concentration, which is equal to the total surfactant concentration minus the critical micellar concentration (CMC).

The non-ionized and ionized coformer (HA and A^-) can also partition into surfactant micelles according to their micellar solubilization constant, K_S^{HA} and $K_S^{A^-}$.[26]

$$HA_{aq} + M \overset{K_S^{HA}}{\rightleftharpoons} HA_m \tag{1.13}$$

$$K_s^{HA} = \frac{[HA]_m}{[HA]_{aq}[M]} \tag{1.14}$$

$$A_{aq}^- + M \overset{K_S^{A-}}{\rightleftharpoons} A_m^- \tag{1.15}$$

$$K_s^{A^-} = \frac{[A^-]_m}{[A^-]_{aq}[M]} \tag{1.16}$$

The assumption is that micellar solubilization, or the partition of drug and coformer species into the surfactant micelles, is independent.[42] The mass balance for cocrystal components in solution can be expressed as:[41-42, 50]

$$[R]_T = [R]_{aq} + [R]_m \tag{1.17}$$

$$[A]_T = [HA]_{aq} + [HA]_m + [A^-]_m \tag{1.18}$$

By combining equations 1.6, 1.9, 1.17, and 1.18, and substituting in appropriate equilibrium constants, the cocrystal solubility in the presence of micellar surfactant can be derived as

$$S_{cocrystal,T} = \sqrt{K_{sp}(1+K_s^R[M])(1+\frac{K_a}{[H^+]}+K_s^{HA}[M]+\frac{K_a}{[H^+]}K_s^{A^-}[M])} \tag{1.19}$$

where $S_{cocrystal,T}$ represents the total cocrystal solubility in aqueous and micellar environments. The drug solubility in surfactant solutions can be described by

$$S_{drug,T} = [R]_{aq}(1+K_s^R[M]) \tag{1.20}$$

where $S_{drug,,T}$ represents the total drug solubility.

Based on the relationship presented in equation 1.19, if the surfactant micelles solubilize the drug to a higher extent compared to the coformer, cocrystal solubility will exhibit a non-linear dependence on surfactant concentration (figure 1.8). This can lead to a solubility transition point based on surfactant concentration.[42] This transition point induced by surfactants is defined by CSC (critical solubilization concentration) and S*.[24, 26, 42]

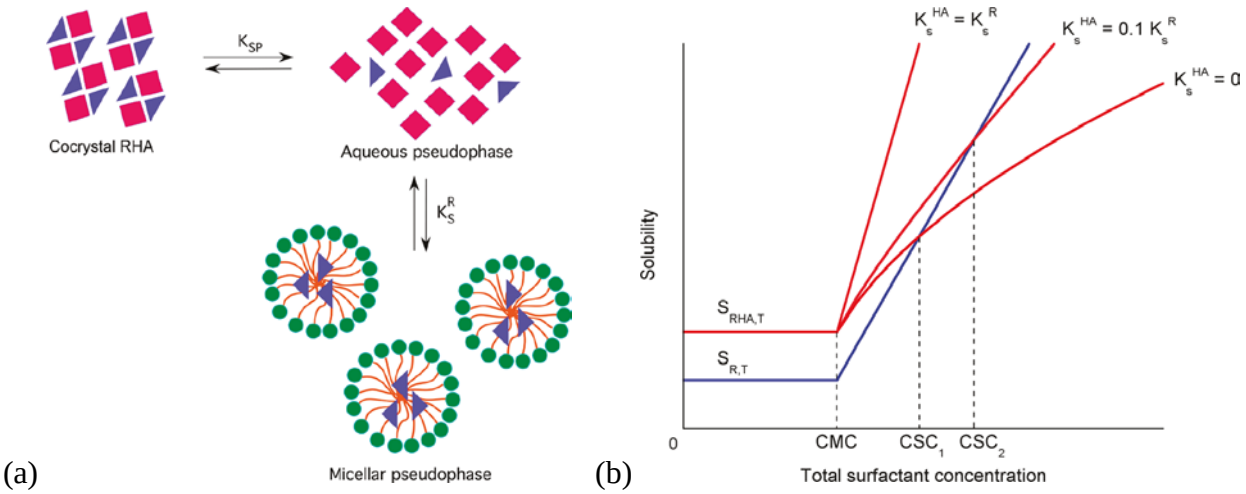

Figure 1.8. (a) Schematic illustration of the equilibria between the cocrystal phase and its components in the aqueous and micellar pseudophases. This scheme represents micellar solubilization of one cocrystal component (drug), leading to excess coformer in the aqueous pseudophase and in this way stabilizing the cocrystal phase. (b) Schematic representation of the cocrystal (RHA) and drug (R) solubility with respect to the total surfactant concentrations according to equations 1.19 and 1.20. Differential solubilization of cocrystal components represented by the relative values of K_s^{HA} and K_s^R leads to nonlinear cocrystal solubility dependence and to intersection of the cocrystal and drug solubility curves. CSC refers to the critical stabilization concentration, at which both cocrystal and drug are thermodynamically stable.[42]

In the presence of a drug solubilizing agent, a cocrystal can display higher, equal, or lower solubility than the parent drug with respect to the solubilizing agent concentration.[26, 42, 51] The preferential solubilization of the drug over the coformer by the solubilizing agent is responsible for this behavior.[26, 42, 51] Generally, pharmaceutical cocrystals are composed of a hydrophobic drug and a hydrophilic coformer, and therefore the drug will be more solubilized by the solubilizing agents in solution.[21, 24, 26, 42, 51-52] As solubilizing agent concentration increases in solution, the drug solubility increases at a higher rate than the cocrystal, and this can lead to an intersection of the solubility curves of cocrystals and drug. This point of intersection is a cocrystal transition point characterized by the solubilizing agent concentration (CSC) and the solubility of the drug and cocrystal at the transition point (S*).[15, 24] S* can be described by the following equation.

$$S_{cocrystal,T} = S_{drug,T} = S^* = \frac{(S_{cocrystal,aq})^m}{(S_{drug,aq})^n} \quad (1.21)$$

The values of superscripts "m" and "n" are derived from the stoichiometry of the cocrystal, where m = 2 and n = 1 for 1:1 cocrystals, and m = 3 and n = 2 for 2:1 cocrystals.[15]

CSC value is dependent on the effectiveness of the solubilizing agent, but the S* value is independent of solubilizing agents as long as the coformer is not solubilized.[15, 24] A stronger drug solubilizing agent (larger drug K_s value) would result in a lower CSC value for the cocrystal compared to a weaker one (smaller K_s value).[24] Unlike the CSC, the value of S* is constant.[24] S* is governed by the aqueous solubility of the cocrystal and drug in aqueous solutions, as can be seen in equation 1.21.[24] The concept of this cocrystal transition point, CSC and S*, is illustrated in figure 1.9.

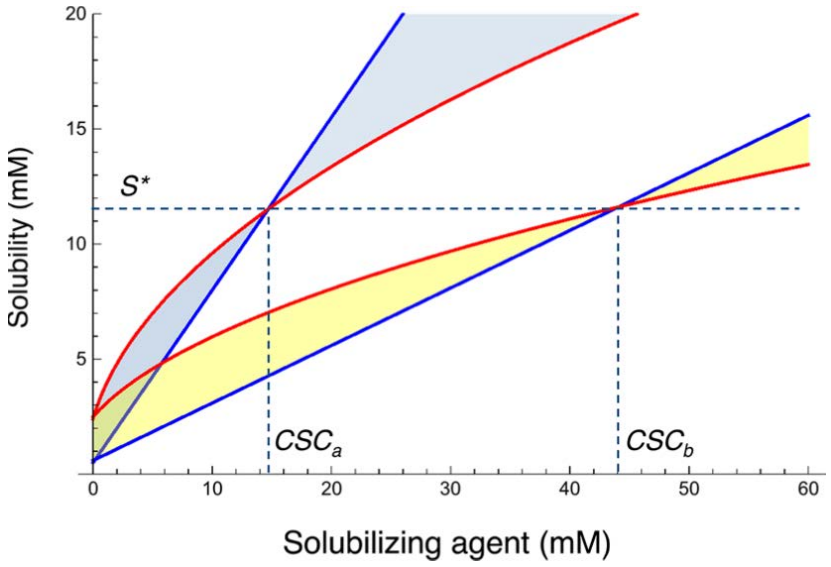

Figure 1.9. Transition point (S* and CSC) for a cocrystal (red line) and its constituent drug (blue line) in two different solubilizing agent, *a* and *b*. S* is constant, and CSC varies with the extent of drug solubilizing by the solubilizing agent. Drug is solubilized to a greater extent by *a* than by *b*, and thus $CSC_a < CSC_b$. The curves were generated from equations 1.20 and 1.23 with parameter values $S_{drug,aq}$ = 0.5 mM, $S_{cocrystal,aq}$ = 2.4 mM (K_{sp} = 5.76 mM^2), and K_s^{drug}= 1.5 mM^{-1} and 0.5 mM^{-1} for solubilizing agents *a* and *b*, respectively.[24]

Cocrystal SR and SA

When the solubilizing agent impact on coformer solubility is negligible, equation 1.19 can be simplified to

$$S_{cocrystal,T} = \sqrt{K_{sp}(1 + K_s^{drug}[M])} \tag{1.22}$$

where drug solubilization constant is represented by K_s^{drug}. Equation 1.22 can be rewritten in terms of $S_{cocrystal,aq}$, which is the cocrystal solubility in aqueous phase.[24]

$$S_{cocrystal,T} = S_{cocrystal,aq}\sqrt{1 + K_s^{drug}[M]} \tag{1.23}$$

By combining equations 1.20 and 1.23, the relationship between cocrystal and drug solubilization ratios can be established[24]

$$\left(\frac{S_T}{S_{aq}}\right)_{cocrystal} = \sqrt{\left(\frac{S_T}{S_{aq}}\right)_{drug}} \tag{1.24}$$

where S_{aq} is the aqueous solubility, sum of non-ionized and ionized forms, of drug and cocrystal.

For a 2:1 cocrystal (drug:coformer), the relationship becomes[24]

$$\left(\frac{S_T}{S_{aq}}\right)_{cocrystal} = \left(\frac{S_T}{S_{aq}}\right)_{drug}^{2/3} \tag{1.25}$$

A general form of the equation for cocrystal A_xB_y can be written as[24]

$$\left(\frac{S_T}{S_{aq}}\right)_{cocrystal} = \left(\frac{S_T}{S_{aq}}\right)_{drug}^{\frac{x}{x+y}} \tag{1.26}$$

where A and B are the cocrystal constituents, drug and coformer, and x and y are the stoichiometric molar ratios. At the transition point, equation 1.24 can be rewritten in term of S*

$$\left(\frac{S^*}{S_{aq}}\right)_{cocrystal} = \sqrt{\left(\frac{S^*}{S_{aq}}\right)_{drug}} \tag{1.27}$$

solve for S* the equation becomes, [24]

$$S^* = \frac{\left(S_{cocrystal,aq}\right)^2}{S_{drug,aq}} \tag{1.28}$$

Equation 1.28 shows that S* value is determined by the drug and cocrystal aqueous solubilities at a given pH and temperature for a 1:1 cocrystal.[15, 24]

Solubilization ratio (SR) is defined as the total solubility in surfactant media ($S_T = S_{aq} + S_s$) divided by the aqueous solubility (S_{aq}), where S_s represents the cocrystal/drug solubilized by solubilizing agents.[24, 52]

$$SR \equiv \left(\frac{S_T}{S_{aq}}\right) \tag{1.29}$$

Replacing the term SR into equations 1.24, 1.25, and 1.26, the equations simplifies to

$$SR_{cocrystal} = \sqrt{SR_{drug}} \tag{1.30}$$

$$SR_{cocrystal} = (SR_{drug})^{2/3} \tag{1.31}$$

$$SR_{cocrystal} = (SR_{drug})^{\frac{x}{x+y}} \tag{1.32}$$

The relationships based on equations 1.30 to 1.32 only hold when the solubilizing agent solubilizes the drug but not the coformer, and this can be justified due to pharmaceutical cocrystals are generally composed of hydrophobic drugs and hydrophilic coformers. In the absence of any experiments of cocrystal solubility, the simple equation 1.32 can give a general idea of cocrystal behavior in media containing solubilizing agents.

The relationships between $SR_{cocrystal}$ and SR_{drug} is shown in figure 1.10 for a 1:1 and 2:1 (drug:coformer) cocrystal.

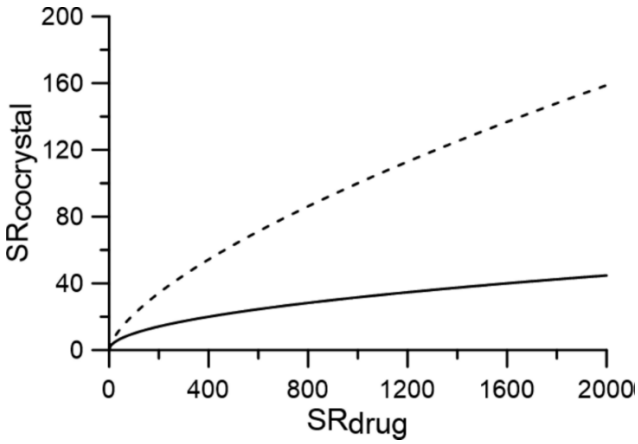

Figure 1.10. Dependence of $SR_{cocrystal}$ on SR_{drug} according to equations 1.30 and 1.31 for cocrystal stoichiometries 1:1 (—) and 2:1 (- - -), using typical range of SR_{drug} values.[24]

Due to preferential solubilization of the drug, $SR_{cocrystal}$ is smaller than SR_{drug}, and SR for a 1:1 cocrystal is lower than SR for a 2:1 cocrystal.[24] Since cocrystal solubility increases at a slower rate than that of the drug with solubilizing agent concentrations, a cocrystal that possesses higher solubility in aqueous solution can become less soluble than the drug when a certain amount of solubilizing agent is added to the solution.[24, 26, 42] This demonstrates the importance of understanding how solubilizing agents affects drug and cocrystal differently when examine cocrystal solution properties in the presence of additives or excipients.

Cocrystal solubility advantage over drug (SA), also known as the supersaturation index of the cocrystal, is dependent on drug solubilization ratio[15]

$$\left(\frac{S_{cocrystal}}{S_{drug}}\right)_T = \frac{\left(\frac{S_{cocrystal}}{S_{drug}}\right)_{aq}}{\sqrt{\left(\frac{S_T}{S_{aq}}\right)_{drug}}} \tag{1.33}$$

or

$$SA = \frac{SA_{aq}}{\sqrt{SR_{drug}}} \tag{1.34}$$

SA_{aq} is the aqueous cocrystal solubility advantage in the absence of drug solubilization (SR_{drug} = 1). Cocrystal SA values can be fine-tuned with drug solubilization, through the incorporation of any solubilizing agents such as polymers, surfactants, or lipids that preferentially solubilizes the drug over coformer.[15] Equation 1.34 can be rewritten in logarithmic form and plotted in figure 1.11.

$$\log(SA) = \log(SA_{aq}) - \frac{1}{2}\log(SR_{drug}) \tag{1.35}$$

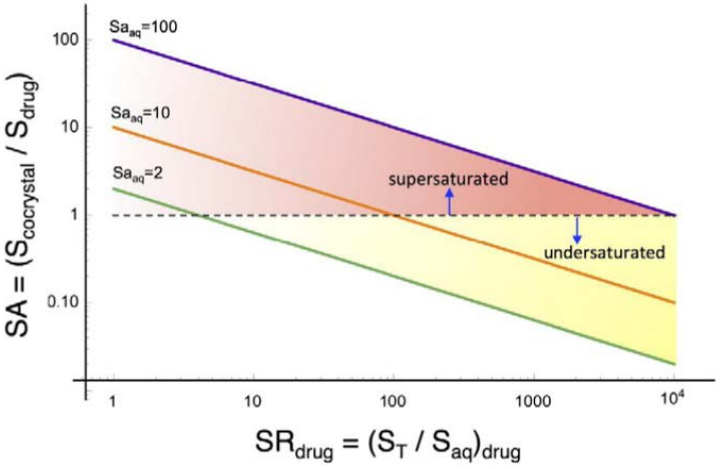

Figure 1.11. Cocrystal solubility advantage over drug or supersaturation index (SA) decreases in a predictable way with increasing (SR_{drug}). The full lines represent (1:1) cocrystals with SA_{aq} = 2, 10, and 100. The dashed line indicates SA = 1. The intersection of the cocrystal SA and SA = 1 line represents the SR_{drug} at which $S_{cocrystal} = S_{drug}$, and identifies transition points, which in these examples are at SR_{drug} = 4, 100, and 10,000 for the corresponding cocrystals, Below the SR_{drug} limit, the cocrystal is more soluble than the drug but becomes less soluble than the drug above this SR_{drug} value.[15]

Figure 1.11 shows the drug solubilization regions where the cocrystal is more, equal, or less soluble than the drug. The intersections of the cocrystal SA line with the dotted line (SA = 1) defines the regions where cocrystals can generate supersaturation (SR_{drug} < intersection).[15] A cocrystal with lower SA_{aq} will require a lower SR_{drug} at the transition point, meaning that the cocrystal SA can be eliminated with low level of drug solubilization by pharmaceutical additives. The assumptions here include that 1) the coformer is not solubilized by the drug solubilizing

agent 2) no other solution phase interactions occur between the drug, coformer, and additives.[15] Solubilization of the coformers will cause deviations in this relationship, which can be quantified by a factor ε.[15, 24] Consider a weakly monoprotic acidic coformer,

$$\varepsilon = \frac{\left(1+10^{pH-pK_{a,coformer}} + K_s^{coformer}[M]\right)}{(1+10^{pH-pK_{a,coformer}})} \tag{1.36}$$

and for a 1:1 cocrystal solubilization becomes

$$SR_{cocrystal} = \sqrt{\varepsilon(SR_{drug})} \tag{1.37}$$

If the coformer is not solubilized, the $K_s^{coformer} = 0$, and ε would be equal to 1, turning equation 1.37 to 1.30.[15, 24] The simple equations enable one to get an initial approximation and evaluation of cocrystals, and can provide guidance for further selection, analysis, and formulation of these cocrystals under the right conditions.

Cocrystal Eutectic Point and K_{eu}

The cocrystal eutectic point has been well established in the literature as an important transition point that characterizes the cocrystal thermodynamic stability relative to its components.[9, 12, 35, 53] At the eutectic point, both drug and cocrystal solid phases coexist in solution at equilibrium.[9] Generally the equilibrium of drug and cocrystal solid phases is used since drug is usually the least soluble component. Since the solution is saturated with two phases (drug and cocrystal), the eutectic concentrations are independent of the mass ratio of the solid phases at the eutectic.[21] The eutectic concentrations of drug and coformer can lead to information regarding cocrystal solubility under stoichiometric conditions. Cocrystal eutectic constant, K_{eu}, is the ratio of coformer to drug activities (*a*) at the eutectic point and can be approximated by the concentration ratio as:[15, 53]

$$K_{eu} = \frac{a_{coformer,eu}}{a_{drug,eu}} \approx \frac{[coformer]_{eu,T}}{[drug]_{eu,T}} \tag{1.38}$$

K_{eu} can also be expressed in terms of the cocrystal to drug solubility ratio ($S_{cocrystal}/S_{drug}$) under stoichiometric solution conditions for a 1:1 cocrystal:[15, 23]

$$K_{eu}^{1:1} = \left(\frac{S_{cocrystal}}{S_{drug}} \right)^2 \tag{1.39}$$

For a 2:1 cocrystal, the K_{eu} equation becomes:[15, 23]

$$K_{eu}^{2:1} = 0.5 \left(\frac{S_{cocrystal}}{S_{drug}} \right)^3 \tag{1.40}$$

Figure 1.12 uses 1:1 and 2:1 cocrystals of nevirapine with acidic coformers as examples to illustrate the relationships between K_{eu} and cocrystal SA ($S_{cocrystal}/S_{drug}$).

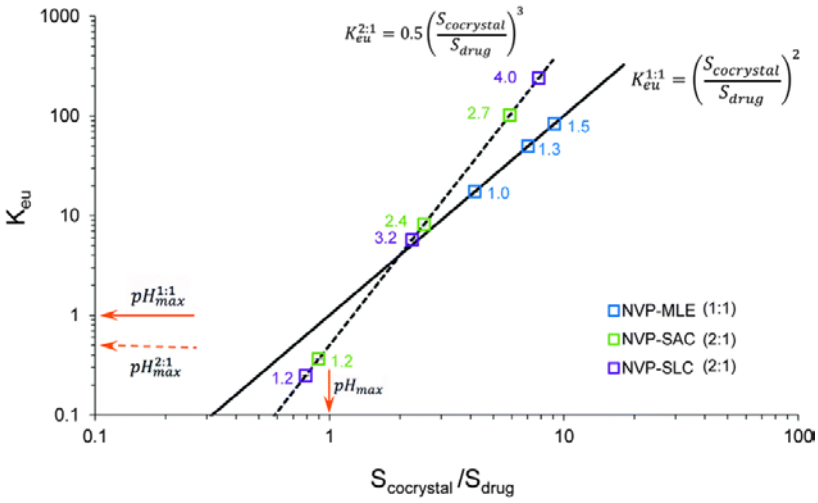

Figure 1.12. Predicted and experimental values of K_{eu} and cocrystal solubility advantage ($S_{cocrystal}/S_{drug}$) for 1:1 NVP-MLE and 2:1 NVP-SAC and NVP-SLC cocrystals. K_{eu} is a key indicator of $S_{cocrystal}/S_{drug}$. K_{eu} dependence on pH reveals the cocrystal pH_{max} as well as the cocrystal increase in solubility over drug as pH increases. At pH_{max}, $K_{eu} = 1$ for 1:1 cocrystals and $K_{eu} = 0.5$ for 2:1 cocrystals. Log axes are used due to the large range of values. Symbols represent experimental values. Numbers next to data points indicate pH at eutectic point or equilibrium pH. Lines were generated according to equations 1.39 and 1.40. Solid lines represent 1:1 cocrystals and dashed lines 2:1 cocrystals.[23]

K_{eu} is an indicator of the thermodynamic stability region(s) in the cocrystal phase diagram, and its value is dependent on solution chemistry including cocrystal stoichiometry, component ionization, and solution conditions.[9, 15, 21] For example, for a 1:1 cocrystal, $K_{eu} > 1$ indicates that the cocrystal is more soluble and thermodynamically unstable with respect to the drug.[15] If K_{eu} value for the 1:1 cocrystal decreases to less than 1, then the thermodynamic stability reverses and the cocrystal becomes more stable (less soluble) than the drug.[15] When $K_{eu} = 1$ for a 1:1 cocrystal, it indicates that the cocrystal solubility is equal to that of the drug. Similarly, for a 2:1 cocrystal, $K_{eu} > 0.5$ indicates the cocrystal is thermodynamically unstable, while $K_{eu} < 0.5$ indicates the cocrystal is more stable.[15] The pH of the solution and the presence of solubilizing agents can influence cocrystal K_{eu}, solubility, and thermodynamic stability.[23, 25-26, 53]

Figure 1.13 illustrates the phase solubility diagrams and the eutectic points for a stable cocrystal (cocrystal 1) and a metastable cocrystal (cocrystal 2) with respect to drug.[15] The coformer solubility is assumed to be much higher than that of the drug, and the curves indicate cocrystal solubility product behavior as a function of its component concentrations according to K_{sp} = [drug][coformer]. Cocrystal 1 exhibits lower solubility compared to drug, and its solubility can be measured by suspending solid cocrystals in solution without concerns for cocrystal to drug conversion. For metastable cocrystal 2, where determining their solubility in solution is challenging due to solution-mediated transformation, eutectic measurement provides an alternative way to accurately assess the cocrystal's thermodynamic solubility. To measure cocrystal solubility at the eutectic point, the drug and cocrystal solid phases are suspended in solution over sufficient time to allow the system to come to equilibrium. Once it is confirmed

that both drug and cocrystal solid phases are present, the solution concentrations of both drug and coformer are measured and used to evaluate cocrystal (stoichiometric) solubility.

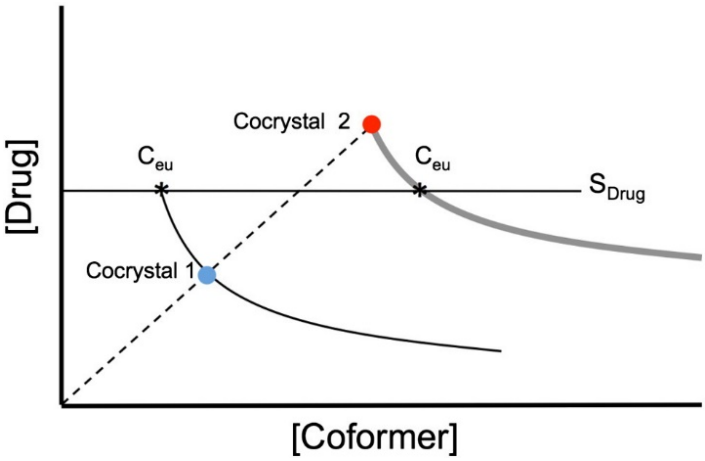

Figure 1.13. Schematic phase diagram indicating the eutectic points (*) where cocrystal and drug solid are in equilibrium with solution.[9] C_{eu} represents the eutectic concentrations of drug and conformer. Two different cocrystals are considered based on their stability with respect to drug under stoichiometric conditions: a stable cocrystal (cocrystal 1) and metastable (cocrystal 2) where the cocrystal generates supersaturation with respect to drug. Drug solubility is indicated and is much lower than the solubility of the conformer, which is not shown. The circle represents the solubility of cocrystals under stoichiometric conditions. The dashed line illustrates stoichiometric concentrations of cocrystal components which dissolution could follow. This line represents a drug to coformer ratio equal to the cocrystal stoichiometric ratio of the components.[15]

Cocrystal Dissolution and Supersaturation Index (SA)

Cocrystallization can potentially provide huge solubility enhancements to drugs, but supersaturation with respect to the most stable, least soluble component (usually the drug) can also lead to solution-mediated conversion from cocrystal to drug.[11, 15, 21] The rate of cocrystal conversion is affected by factors such as the solubility of drug and cocrystal, dissolution rate, supersaturation level with respect to drug, and crystallization rate of drug.[9, 15, 21] Cocrystal conversion to drug under these conditions can be so rapid that no dissolution advantage can be observed. This can lead to incorrect interpretations of cocrystal dissolution results for a highly soluble cocrystal, if the thermodynamic solubility/stability of the cocrystal is not considered.

Despite the potential failures of kinetic measurement (dissolution), it is often the first approach used when evaluating a cocrystal. Since most pharmaceutical cocrystals are designed to be more soluble than the drug, they are susceptible to solution-mediated phase transformation. If conversion occurs during dissolution, cocrystals will not be able to reach its true solubility, as figure 1.14 illustrates. The maximum drug concentration achieved (C_{max}) is determined by cocrystal dissolution and drug crystallization rate, and not a reliable solubility indicator for highly soluble cocrystals.[21] If the drug C_{max} from a kinetic measurement is used to evaluate the solubility of a cocrystal, one could underestimate the cocrystal solubility. Therefore, the most reliable way to evaluate cocrystal solubility is through eutectic measurement, which would establish the true solubility and the thermodynamic stability region(s) of the cocrystal. Understanding the thermodynamic behavior of a cocrystal allows one to gain insights for its kinetic behavior, and manages the conversion rate by manipulating the cocrystal SA.

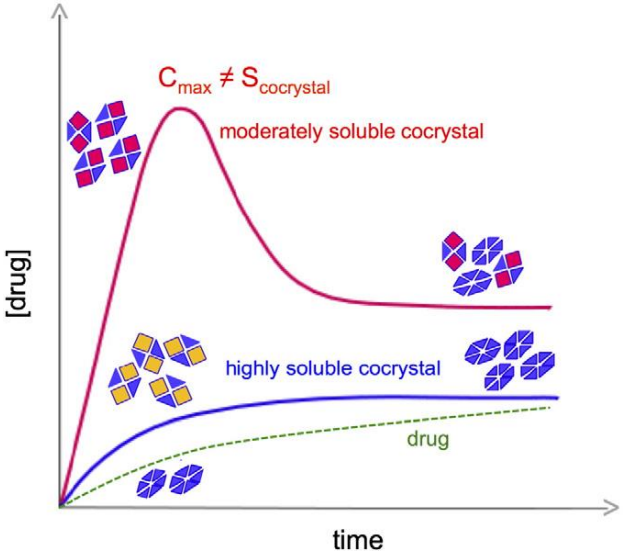

Figure 1.14. Dissolution methods may provide C_{max} for moderately soluble cocrystals and may not detect highly soluble cocrystals. As cocrystals dissolve and drug precipitates, drug concentrations can reach a maximum in the case of moderately soluble cocrystals, whereas highly soluble cocrystals may undergo such rapid conversion that eludes detection and drug concentration is maintained close to or at the drug solubility.[15, 21]

The rate at which a cocrystal converts to drug can be reduced by decreasing the SA of the cocrystal with respect to drug. Solubilizing agents that preferentially solubilize the drug over the coformer can be used as additives to reduce cocrystal SA.[15, 24, 26, 52] Cocrystal solubilization behavior in the presence of solubilizing agents were presented in detail in the previous sections and would not be explained again here. This section instead focuses on the effect of the solubilizing agent and reduction of SA on the kinetic dissolution and conversion behavior of cocrystals.

Physiologically Relevant Surfactants

Physiologically relevant surfactants such as bile salts present in the GI tract can solubilize drug and cocrystals. Cocrystal dissolution in fed-state simulated intestinal fluid (FeSSIF) and in aqueous buffer of the same pH (FeSSIF without surfactants) showed how the surfactants present in FeSSIF helped to prevent or slow cocrystal conversion to drug and improved dissolution performance. Powder dissolution studies of indomethacin-saccharin (IND-SAC) and piroxicam-saccharin (PXC-SAC) cocrystals were conducted to determine the impact of SA on the dissolution profile, supersaturation during dissolution, and transformation kinetics. IND-SAC was predicted to have SA value of 220 in pH 5 buffer, and this SA value is reduced in FeSSIF to be about 57.[54] This large reduction of SA lowered the driving force for cocrystal transformation in FeSSIF compared to aqueous buffer, and can lead to slower cocrystal conversion to drug.

IND-SAC achieved and maintained higher drug concentrations during dissolution in FeSSIF compared to buffer (figure 1.15). In the absence of surfactants, IND-SAC achieved peak concentration at around 10 minutes, and then rapidly decreased until, by the end of the experiment, the IND concentration (0.034 mM) was close to the solubility of IND (0.023 mM).[54] The final solid phases in aqueous buffer showed a mixture of drug and cocrystal, indicating the

cocrystal, IND-SAC, had transformed during dissolution. However, in FeSSIF, the final solid phase remains pure IND-SAC, indicating no solution-mediated transformation had occurred during the 4-hour dissolution period.

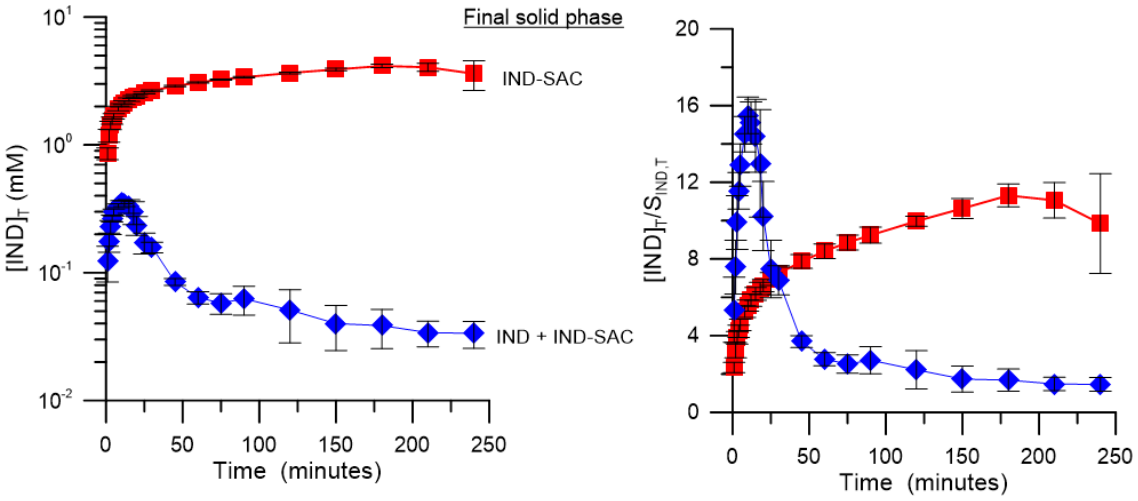

Figure 1.15. IND-SAC dissolution in FeSSIF (red square) and buffer (blue diamonds) at 25°C. (a) $[IND]_T$ vs time profile for dissolution and (b) supersaturation generated by IND-SAC during dissolution ($[IND]_T/S_T^{IND}$).[15, 54]

PXC-SAC is 520 times more soluble than PXC drug in buffer, and 370 times more soluble than the drug in FeSSIF.[54] Similar to IND-SAC dissolutions, powder dissolution of PXC-SAC achieved and maintained higher drug concentration in FeSSIF compared to buffer (figure 1.16). The final solid phases indicated that the cocrystal had transformed to PXC(H), which is the hydrated form of PXC, in buffer, while in FeSSIF no such transformation was observed. For both IND-SAC and PXC-SAC cocrystals, dissolution in FeSSIF yielded higher drug concentrations than in aqueous buffer. Cocrystal SA values were reduced in FeSSIF compared to in buffer, and SA was shown to be a good indicator for cocrystal to drug conversion for these systems. Decrease in cocrystal SA from aqueous buffer to FeSSIF led to sustained supersaturation of drug and slower conversions.[54] This also shows that very high SA values may not be ideal for a supersaturation drug delivery system, such as cocrystals, due to the potential of

rapid transformation which could eliminate all dissolution advantage to the parent drug. A balance must be struck between solubility and solution stability in order to fully exploit the advantage offered by cocrystals.

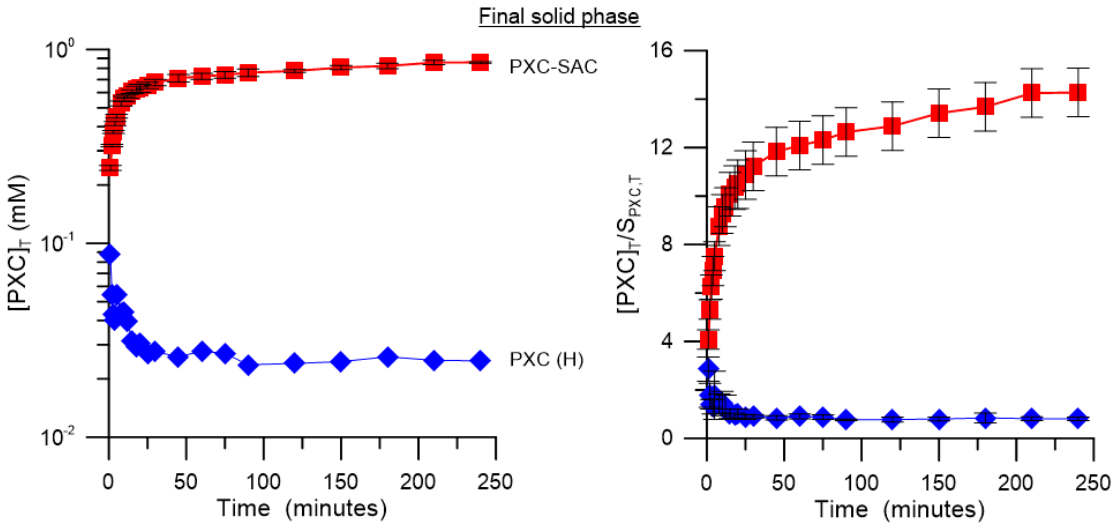

Figure 1.16. PXC-SAC dissolution in FeSSIF (red squares) and buffer (blue diamonds) at 25°C. (a) $[PXC]_T$ vs time profile for dissolution from cocrystal and (b) supersaturation generated by PXC-SAC during dissolution ($[PXC]_T/S_T^{PXC}$).[15, 54]

Synthetic Additives

Danazol-vanillin cocrystal (DNZ-VAN) has SA value of 280 with respect to DNZ drug in aqueous buffer, while DNZ cocrystal with 4-hydroxybenzoic acid (DNZ-HBA) has an even higher SA value of 660 in the same media.[52, 54] However, this large SA can generate very high levels of drug supersaturations in solution, and increase the driving force for cocrystal conversation and drug precipitation during dissolution studies.[11, 15, 21] In some cases, this can result in cocrystals demonstrating no dissolution advantage despite large solubility advantages with respect to drug. Cocrystal SA can be reduced not only by physiologically relevant surfactants, but also synthetic drug solubilizing agents. For example, SA values for DNZ-HBA and DNZ-VAN is reduced by FeSSIF surfactants to 28 and 14, respectively.[54] When 150mM of

Tween 80 was added to FeSSIF media, DNZ-HBA SA value was further reduced to 7.7, and DNZ-VAN SA value was reduced to 5.3.[54] Powder dissolution of DNZ-VAN in FeSSIF and FeSSIF+150 mM Tween 80 demonstrated how the reduction of DNZ-VAN SA values influenced the dissolution behavior for this cocrystal (Figure 1.17).

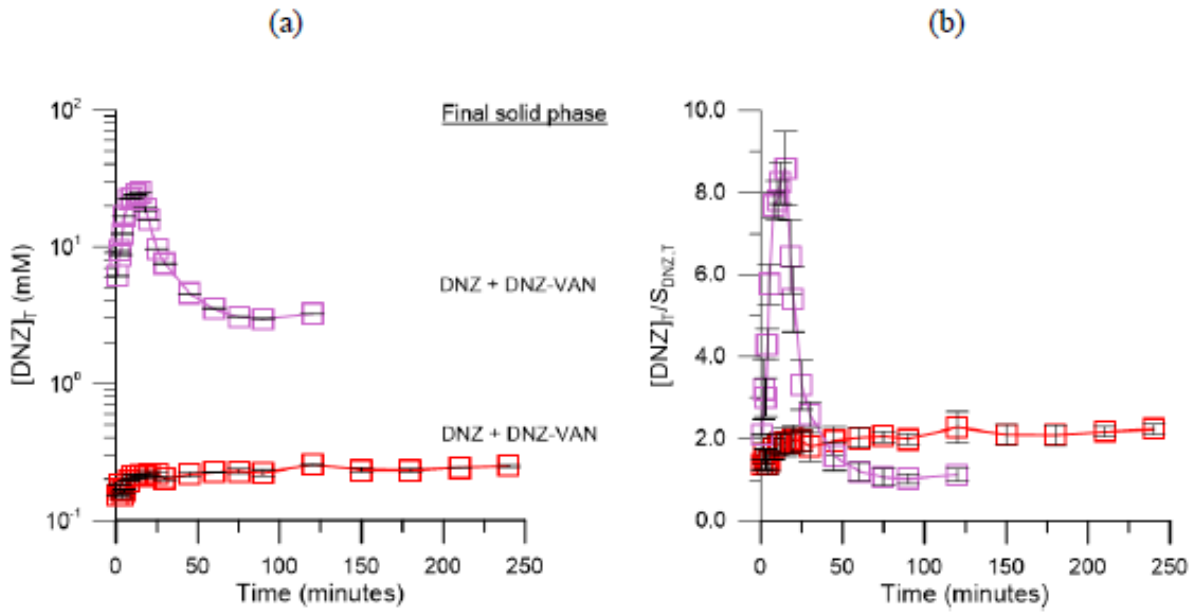

Figure 1.17. DNZ-VAN dissolution in FeSSIF (□) and FeSSIF + 150mM Tween 80 (□) at 25°C. (a) $[DNZ]_T$ vs time profile and (b) supersaturation generated by DNZ-VAN during dissolution ($[DNZ]_T/S_{DNZ,T}$). The pH of both media had an initial and final pH of 5.00.[54]

A study of DNZ-VAN cocrystal published in 2013 by Scott Childs and colleagues demonstrated the effect of vitamin E-TPGS (D-α-Tocopheryl polyethylene glycol 1000 succinate) and HPC (Klucel LF Pharm hydroxypropylcellulose) on this cocrystal *in vitro* and *in vivo* behavior (figure 1.18).[11] The "unformulated" (0.5% w/v PVP K-25) suspension of DNZ-VAN showed little improvement both in *in vitro* dissolution and *in vivo* bioavailability when compared to the drug polymorph. However, when 1% w/v of TPGS and 2% w/v of HPC were added to solution (formulated), the *in vitro* dissolution showed improvement for both drug and cocrystal. The "formulated" cocrystal achieved a maximum concentration of 0.35 mg/mL for DNZ during dissolution, which is about 5.5 times higher than DNZ drug under the same

condition.[11] The DNZ bioavailability (plasma concentration AUC) from the cocrystal in formulated aqueous suspension was improved by about 10 fold when compared to the drug polymorph under the same conditions.[11] The results suggested that the presence of the solubilizing agents (TPGS and HPC) was able to enhance both DNZ drug and DNZ-VAN cocrystal solubility and dissolution, and decreased the rate of cocrystal conversion allowing higher bioavailability of DNZ to be achieved.

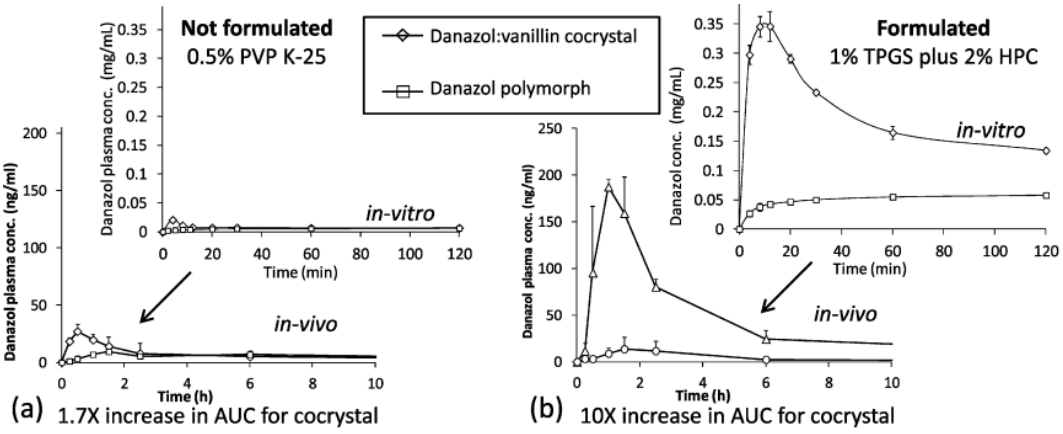

Figure 1.18. *In vitro* dissolution data and *in vivo* plasma concentration for the danazol cocrystal and polymorph, shown for the unformulated suspension (a) containing 0.5% PVP K-25 as a suspending agent, and the formulated suspension (b) containing 1% TPGS and 2% HPC.[11]

Effect of Interfacial pH on Cocrystal Dissolution

For BCS class II drugs (low solubility, high permeability) dissolution is the rate limiting step in absorption.[2] Based on the Noyes-Whitney and Nernst-Brunner equation, the dissolution rate is dependent on the properties of the dissolving components, such as solubility and diffusion.[55-56] Cocrystals can alter the solubility of the parent drug, which can lead to alterations in dissolution rate. Cocrystal components can have different ionization properties, and one drug can form cocrystals with a large variety of coformers with different ionization properties. Different ionization properties can alter the pH at the dissolving solid surface (interfacial pH)

compared to the bulk solution, which can influence the cocrystal solubility at the interface.[57] Interfacial pH and dissolution rate for a substance is determined by the concentration of the species at the interface. The component concentrations at the dissolving surface are dependent on both the solubility and diffusion coefficients of each component.[57] Since drug components tend to have much higher molecular weight than the coformers, the drug component are expected to have slower diffusion than the coformer. This difference in diffusion coefficients between drug and coformer species causes unequal, or non-stoichiometric, concentrations of cocrystal components at the dissolving surface, affecting cocrystal solubility.[57]

It was found that the dissolution of cocrystal is heavily influenced by the interfacial pH instead of the bulk solution pH (figure 1.19).[15, 57] Cocrystals with ionizable components can modulate the pH microenvironment at the dissolving interface by self-buffering. Within the buffering region of the cocrystal components, the interfacial pH is not expected to change as bulk pH changes. The flux dependence for drug and coformer would follow the interfacial pH conditions instead of bulk pH. Carbamazepine (CBZ) is a non-ionizable drug, and therefore cannot alter the interfacial pH from the bulk, and its flux is independent of both bulk and interfacial pH. However, CBZ cocrystals with acidic coformers, saccharin (SAC) and salicylic acid (SLC), imparted the ability to buffer the pH at the dissolving interface when the bulk pH is increase above the coformer pK_a values.[57] Without the knowledge of interfacial pH, one might expect that the dissolution rates of both cocrystals would be purely dependent on the bulk pH. Due to the pH buffering effect of the coformers, the interfacial pH plateaus as bulk pH increases, causing the flux of the cocrystals to plateau in the buffering region.[57]

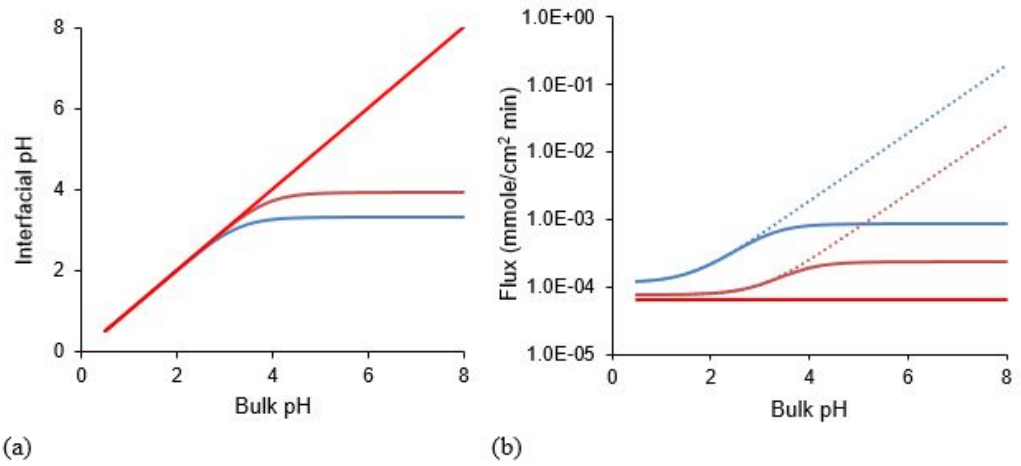

Figure 1.19. Interfacial pH (a) and flux (b) of CBZ (red) and its two cocrystals, CBZ-SAC (blue) and CBZ-SLC (orange) predicted using developed mass transport models as a function of bulk pH. The dotted lines in the flux plot represents the flux prediction with the assumption that interfacial pH is the same as bulk pH. The solubility product of CBZ-SLC is 1.00 mM^2 and CBZ-SAC is 0.4 mM^2. The pK_a values of SAC and SLC are 1.6 and 3.0, respectively.[57]

pH-Dependent Dissolution and Bioavailability of Basic Drugs

Poorly water soluble basic drugs often rely on the acidity of the gastric compartment to dissolve and then be absorbed in the intestine. Elevated pH in the stomach, either due to disease, food intake, or medication, can have serious negative impact on the oral absorption and bioavailability for this type of drugs.[58-64] The pH-dependent solubility, dissolution, and absorption behavior of basic drugs can lead to highly variable and/or poor bioavailability, causing difficulty in oral dosing.

Ketoconazole (KTZ) is a basic drug with poor aqueous solubility.[59, 62-63, 65-66] Figure 1.20 shows that KTZ was poorly absorbed when administered to healthy volunteers with cimetidine, which inhibits stomach acid production, and bicarbonate solution.[63] KTZ plasma levels in figure 1.20 show drastic improvements under acidic conditions.[63]

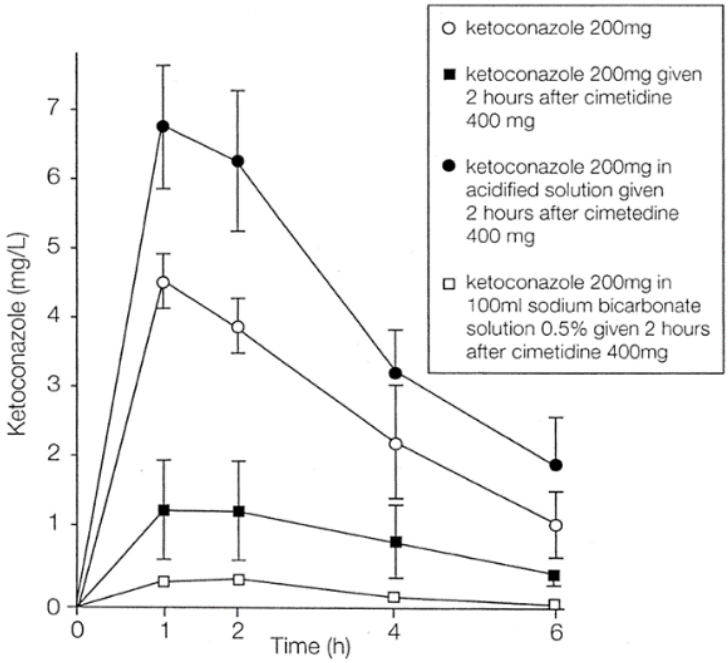

Figure 1.20. Ketoconazole plasma concentrations: Dependency on the gastric pH in healthy fasting volunteers.[62-63]

Another study conducted by Zhou et al. also shows high variability in dissolution and absorption behavior of KTZ based on pH.[59] KTZ tablets were able to fully dissolve in pH 1.2 media, but dissolution in pH 4.5 and pH 6.8 media only reached 43% and 4% after one hour.[59] Since it is a BCS class II compound (high intestinal permeability),[2, 67] KTZ oral absorption is limited by dissolution. Therefore, good correlation can be seen between its pH-dependent *in vitro* dissolution and *in vivo* absorption in beagle dogs (figure 1.2).[59] Solubility enhancement for such drugs can help reduce the negative impact of high pH on its bioavailability. Strategies to increase solubility include the use of additives (surfactants, lipids), amorphous formation, salt formation, and cocrystallization.[44, 46, 60, 68-69]

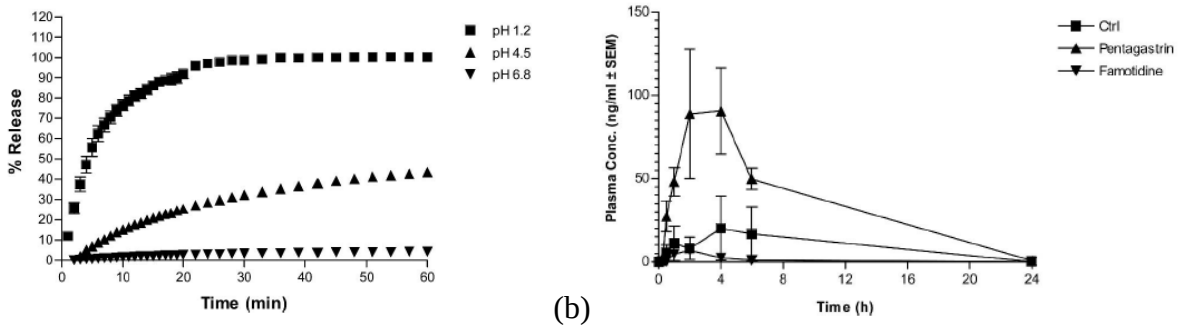

(a) (b)

Figure 1.21. (a) Ketoconazole pH-dependent dissolution release profile. Test was performed on ketoconazole tablets in 1000 mL of 0.1 N HCl, 0.05 M acetate buffer, and 0.05 M phosphate buffer, maintained at 37°C at a paddle rotation speed of 50 rpm for 1 h. Results are plotted as mean ± SD (n = 6). (b) Ketoconazole plasma profile in dogs, pH-dependent absorption. Results are control (no treatment), pentagastrin-, and famotidine-treated dogs shown as mean concentration (ng/ml, ± SEM, n = 4).[59]

Adachi et al. have shown that organic acids can act as pH-modifiers to enhance the *in vitro* dissolution and *in vivo* bioavailability of KTZ when incorporated as part of the formulation.[70] In 2013, Martin et al. discovered three cocrystals of KTZ with dicarboxylic acid coformers: fumaric acid (FUM), succinic acid (SUC), and adipic acid (ADP), along with a KTZ salt with oxalic acid.[44] Dissolution in DI water of the cocrystals and salt resulted in much higher drug concentrations compared to dissolution with pure drug.[44] The solubility and dissolution enhancement by these cocrystals (and salt) can lead to improvement in KTZ bioavailability, but further study and understanding of their solution behavior are needed to accurately assess their true potentials.

Statement of Dissertation Research

The purpose of this dissertation is to determine the ability and the mechanism by which cocrystals enhance solubility and dissolution behavior of basic drugs under elevated pH conditions. Cocrystals composed of ionizable components have been known to exhibit pH-dependent solubility behavior, which can differ from that of the parent drug. There remains a

lack of understanding of how pH influences cocrystal solubility, solubility advantage (SA), and thermodynamic stability relative to drug. Such knowledge is critical for the proper evaluation of a cocrystal both *in vitro* and *in* vivo. The main objective of this work is to develop mathematical models that describe cocrystal solubility behavior and establish thermodynamic parameters to explain cocrystal kinetic behavior including dissolution and solution-mediated conversion.

Chapter 2 investigates the influence of solution pH on the solubility and dissolution behavior of three cocrystals composed of a basic drug and acidic coformers in 1:1 stoichiometry: ketoconazole-adipic acid (KTZ-ADP), ketoconazole-fumaric acid (KTZ-FUM), and ketoconazole-succinic acid (KTZ-SUC). This chapter aims to show how cocrystallization can help reduce pH-sensitivity and improve solubility under high pH conditions for the basic drug. Previous work has shown that cocrystals with ionizable components can exhibit different solubility-pH behavior compared to the parent drug, and mathematical models have been derived to describe their solubility.[23, 25, 41, 43] KTZ cocrystals have a basic and an acidic component, and they are expected to behave quite differently from KTZ in aqueous solution. Mathematical equations that predict the solubility for KTZ drug and cocrystals were derived based on solution equilibria that consider component ionization and cocrystal dissociation. The equations can quantitatively predict drug and cocrystal solubility under a wide range of pH conditions, and the predicted values were validated with experimental solubility values. The cocrystals were found to exhibit very different solubility-pH profiles compared to the drug, leading to the existence of pH_{max} for each cocrystal. Above pH_{max}, KTZ cocrystals gain solubility and dissolution advantage over drug. The ability of these cocrystals to generate and sustain supersaturation of the drug during dissolution at $pH > pH_{max}$ was also investigated in this chapter.

Chapter 3 studies the combined effect of pH and drug solubilizing agents, specifically physiologically relevant surfactants, on KTZ cocrystal solubility and dissolution behavior. Previous work has shown that preferential solubilization of lipophilic drug over hydrophilic coformers can lead to reduced cocrystal SA values and impact drug supersaturation behavior during dissolution in surfactant containing media.[15, 24, 42, 50, 52] Cocrystal and drug solubility equations from Chapter 2 were expanded to take into account micellar solubilization of drug and coformer components. The predictions from the equations are in excellent agreement with experimentally measured solubility values. Cocrystal solubility enhancement by surfactant containing media (FaSSIF and FeSSIF) from the corresponding blank aqueous buffers was less pronounced than that of the pure drug. Decreases in the cocrystal SA values, also referred to as the supersaturation index of the cocrystal, can lead to slower solution-mediated transformation of cocrystal to drug and sustained supersaturation of drug during dissolution.

Chapter 4 evaluates the ability of KTZ cocrystals to generate and maintain drug supersaturation during pH-shift dissolution simulating conditions along the gastrointestinal tract, and assesses the potential of cocrystals to improve KTZ oral absorption under elevated gastric pH conditions. KTZ typically has good oral absorption when gastric pH is low, but it is known to perform poorly *in vitro* and *in vivo* when pH becomes elevated.[59, 63] KTZ drug and cocrystal dissolution behavior under different fasting gastric pH conditions were evaluated based on a novel pH-shift microdissolution method published by Mathias et al.[71] When initial (gastric) pH is low (pH 2), the drug and cocrystals have similar dissolution profiles that indicate full dissolution occurred in the initial media. Cocrystal dissolution studies conducted under high fasting gastric pH condition (initial pH 6) resulted in much higher KTZ solution concentrations and about 3-fold increase in drug AUC compared to pure drug dissolution. Cocrystal dissolution

behavior demonstrated less sensitivity to solution conditions compared to the parent drug, and this can lead to reductions of the negative impact from elevated pH on drug bioavailability.

The conclusions of this dissertation and future directions for this research are discussed in Chapter 5. Several of the chapters are being prepared for publication. Chapter 2 has been adapted and submitted for publication in *Crystal Growth and Design 2017*.

References

1. Lobenberg, R.; Vieira, M.; Amidon, G., Solubility as a limiting factor to drug absorption. In *Oral drug absorption prediction and assessment*, Jennifer B. Dressman, H. L., Ed. Marcel Dekker Inc.: 2000; Vol. 106, pp 137-154.

2. Amidon, G.; Lennernäs, H.; Shah, V.; Crison, J., A Theoretical Basis for a Biopharmaceutic Drug Classification: The Correlation of in Vitro Drug Product Dissolution and in Vivo Bioavailability. *Pharmaceutical Research* **1995,** *12* (3), 413-420.

3. Liu, R., *Water-insoluble drug formulation*. CRC Press: 2008.

4. Jung, M.-S.; Kim, J.-S.; Kim, M.-S.; Alhalaweh, A.; Cho, W.; Hwang, S.-J.; Velaga, S. P., Bioavailability of indomethacin-saccharin cocrystals. *Journal of Pharmacy and Pharmacology* **2010,** *62* (11), 1560-1568.

5. Thakuria, R.; Delori, A.; Jones, W.; Lipert, M. P.; Roy, L.; Rodríguez-Hornedo, N., Pharmaceutical cocrystals and poorly soluble drugs. *International Journal of Pharmaceutics* **2013,** *453* (1), 101-125.

6. Smith, A. J.; Kavuru, P.; Wojtas, L.; Zaworotko, M. J.; Shytle, R. D., Cocrystals of Quercetin with Improved Solubility and Oral Bioavailability. *Molecular Pharmaceutics* **2011,** *8* (5), 1867-1876.

7. Cheney, M. L.; Weyna, D. R.; Shan, N.; Hanna, M.; Wojtas, L.; Zaworotko, M. J., Coformer selection in pharmaceutical cocrystal development: A case study of a meloxicam aspirin cocrystal that exhibits enhanced solubility and pharmacokinetics. *Journal of Pharmaceutical Sciences* **2011,** *100* (6), 2172-2181.

8. Weyna, D. R.; Cheney, M. L.; Shan, N.; Hanna, M.; Zaworotko, M. J.; Sava, V.; Song, S.; Sanchez-Ramos, J. R., Improving Solubility and Pharmacokinetics of Meloxicam via Multiple-Component Crystal Formation. *Molecular Pharmaceutics* **2012,** *9* (7), 2094-2102.

9. Good, D. J.; Rodríguez-Hornedo, N. r., Solubility Advantage of Pharmaceutical Cocrystals. *Crystal Growth & Design* **2009,** *9* (5), 2252-2264.

10. McNamara, D. P.; Childs, S. L.; Giordano, J.; Iarriccio, A.; Cassidy, J.; Shet, M. S.; Mannion, R.; O'Donnell, E.; Park, A., Use of a Glutaric Acid Cocrystal to Improve Oral Bioavailability of a Low Solubility API. *Pharmaceutical Research* **2006,** *23* (8), 1888-1897.

11. Childs, S. L.; Kandi, P.; Lingireddy, S. R., Formulation of a Danazol Cocrystal with Controlled Supersaturation Plays an Essential Role in Improving Bioavailability. *Molecular Pharmaceutics* **2013,** *10* (8), 3112-3127.

12. Childs, S. L.; Rodriguez-Hornedo, N.; Reddy, L. S.; Jayasankar, A.; Maheshwari, C.; McCausland, L.; Shipplett, R.; Stahly, B. C., Screening strategies based on solubility and solution composition generate pharmaceutically acceptable cocrystals of carbamazepine. *CrystEngComm* **2008,** *10* (7), 856-864.

13. Childs, S. L.; Chyall, L. J.; Dunlap, J. T.; Smolenskaya, V. N.; Stahly, B. C.; Stahly, G. P., Crystal Engineering Approach To Forming Cocrystals of Amine Hydrochlorides with Organic Acids. Molecular Complexes of Fluoxetine Hydrochloride with Benzoic, Succinic, and Fumaric Acids. *Journal of the American Chemical Society* **2004,** *126* (41), 13335-13342.

14. Basavoju, S.; Boström, D.; Velaga, S., Indomethacin–Saccharin Cocrystal: Design, Synthesis and Preliminary Pharmaceutical Characterization. *Pharmaceutical Research* **2008,** *25* (3), 530-541.

15. Kuminek, G.; Cao, F.; Bahia de Oliveira da Rocha, A.; Gonçalves Cardoso, S.; Rodríguez-Hornedo, N., Cocrystals to facilitate delivery of poorly soluble compounds beyond-rule-of-5. *Advanced Drug Delivery Reviews* **2016,** *101*, 143-166.

16. Aakeroy, C. B.; Salmon, D. J., Building co-crystals with molecular sense and supramolecular sensibility. *CrystEngComm* **2005,** *7* (72), 439-448.

17. Jones, W.; Motherwell, W. D. S.; Trask, A. V., Pharmaceutical Cocrystals: An Emerging Approach to Physical Property Enhancement. *MRS Bulletin* **2006,** *31* (11), 875-879.

18. Childs, S. L.; Stahly, G. P.; Park, A., The Salt−Cocrystal Continuum: The Influence of Crystal Structure on Ionization State. *Molecular Pharmaceutics* **2007,** *4* (3), 323-338.

19. Shan, N.; Zaworotko, M. J., The role of cocrystals in pharmaceutical science. *Drug Discovery Today* **2008,** *13* (9–10), 440-446.

20. Aitipamula, S.; Banerjee, R.; Bansal, A. K.; Biradha, K.; Cheney, M. L.; Choudhury, A. R.; Desiraju, G. R.; Dikundwar, A. G.; Dubey, R.; Duggirala, N.; Ghogale, P. P.; Ghosh, S.; Goswami, P. K.; Goud, N. R.; Jetti, R. R. K. R.; Karpinski, P.; Kaushik, P.; Kumar, D.; Kumar, V.; Moulton, B.; Mukherjee, A.; Mukherjee, G.; Myerson, A. S.; Puri, V.; Ramanan, A.; Rajamannar, T.; Reddy, C. M.; Rodriguez-Hornedo, N.; Rogers, R. D.; Row, T. N. G.; Sanphui, P.; Shan, N.; Shete, G.; Singh, A.; Sun, C. C.; Swift, J. A.; Thaimattam, R.; Thakur, T. S.; Kumar Thaper, R.; Thomas, S. P.; Tothadi, S.; Vangala, V. R.; Variankaval, N.; Vishweshwar, P.;

Weyna, D. R.; Zaworotko, M. J., Polymorphs, Salts, and Cocrystals: What's in a Name? *Crystal Growth & Design* **2012,** *12* (5), 2147-2152.

21. Roy, L.; Lipert, M. P.; Rodriguez-Hornedo, N., Co-crystal Solubility and Thermodynamic Stability. In *Pharmaceutical Salts and Co-crystals*, The Royal Society of Chemistry: 2012; pp 247-279.

22. Aakeröy, C. B.; Fasulo, M. E.; Desper, J., Cocrystal or Salt: Does It Really Matter? *Molecular Pharmaceutics* **2007,** *4* (3), 317-322.

23. Kuminek, G.; Rodriguez-Hornedo, N.; Siedler, S.; Rocha, H. V. A.; Cuffini, S. L.; Cardoso, S. G., How cocrystals of weakly basic drugs and acidic coformers might modulate solubility and stability. *Chemical Communications* **2016,** *52* (34), 5832-5835.

24. Lipert, M. P.; Rodríguez-Hornedo, N., Cocrystal Transition Points: Role of Cocrystal Solubility, Drug Solubility, and Solubilizing Agents. *Molecular Pharmaceutics* **2015**.

25. Alhalaweh, A.; Roy, L.; Rodríguez-Hornedo, N.; Velaga, S. P., pH-Dependent Solubility of Indomethacin–Saccharin and Carbamazepine–Saccharin Cocrystals in Aqueous Media. *Molecular Pharmaceutics* **2012,** *9* (9), 2605-2612.

26. Huang, N.; Rodríguez-Hornedo, N., Engineering cocrystal solubility, stability, and pHmax by micellar solubilization. *Journal of Pharmaceutical Sciences* **2011,** *100* (12), 5219-5234.

27. Vishweshwar, P.; McMahon, J. A.; Bis, J. A.; Zaworotko, M. J., Pharmaceutical co-crystals. *Journal of Pharmaceutical Sciences* **2006,** *95* (3), 499-516.

28. Desiraju, G. R., Supramolecular Synthons in Crystal Engineering—A New Organic Synthesis. *Angewandte Chemie International Edition in English* **1995,** *34* (21), 2311-2327.

29. Schultheiss, N.; Newman, A., Pharmaceutical Cocrystals and Their Physicochemical Properties. *Crystal Growth & Design* **2009,** *9* (6), 2950-2967.

30. Trask, A. V.; Jones, W., Crystal Engineering of Organic Cocrystals by the Solid-State Grinding Approach. In *Organic Solid State Reactions: -/-*, Toda, F., Ed. Springer Berlin Heidelberg: Berlin, Heidelberg, 2005; pp 41-70.

31. Shan, N.; Toda, F.; Jones, W., Mechanochemistry and co-crystal formation: effect of solvent on reaction kinetics. *Chemical Communications* **2002,** (20), 2372-2373.

32. Weyna, D. R.; Shattock, T.; Vishweshwar, P.; Zaworotko, M. J., Synthesis and Structural Characterization of Cocrystals and Pharmaceutical Cocrystals: Mechanochemistry vs Slow Evaporation from Solution. *Crystal Growth & Design* **2009,** *9* (2), 1106-1123.

33. Lu, E.; Rodriguez-Hornedo, N.; Suryanarayanan, R., A rapid thermal method for cocrystal screening. *CrystEngComm* **2008,** *10* (6), 665-668.

34. Rodríguez-Hornedo, N.; Nehm, S. J.; Seefeldt, K. F.; Pagán-Torres, Y.; Falkiewicz, C. J., Reaction Crystallization of Pharmaceutical Molecular Complexes. *Molecular Pharmaceutics* **2006,** *3* (3), 362-367.

35. Nehm, S. J.; Rodríguez-Spong, B.; Rodríguez-Hornedo, N., Phase Solubility Diagrams of Cocrystals Are Explained by Solubility Product and Solution Complexation. *Crystal Growth & Design* **2005,** *6* (2), 592-600.

36. Jayasankar, A.; Reddy, L. S.; Bethune, S. J.; Rodríguez-Hornedo, N. r., Role of Cocrystal and Solution Chemistry on the Formation and Stability of Cocrystals with Different Stoichiometry. *Crystal Growth & Design* **2009,** *9* (2), 889-897.

37. Hildebrand, J. H., *Solubility*. The Chemical Catalog Com; New York: 1924.

38. Alhalaweh, A.; Sokolowski, A.; Rodríguez-Hornedo, N. r.; Velaga, S. P., Solubility Behavior and Solution Chemistry of Indomethacin Cocrystals in Organic Solvents. *Crystal Growth & Design* **2011,** *11* (9), 3923-3929.

39. Maheshwari, C.; André, V.; Reddy, S.; Roy, L.; Duarte, T.; Rodríguez-Hornedo, N., Tailoring aqueous solubility of a highly soluble compound via cocrystallization: effect of coformer ionization, pH max and solute–solvent interactions. *CrystEngComm* **2012,** *14* (14), 4801-4811.

40. Yalkowsky, S. H., *Solubility and solubilization in aqueous media*. American Chemical Society; Oxford University Press: 1999.

41. Bethune, S. J.; Huang, N.; Jayasankar, A.; Rodríguez-Hornedo, N. r., Understanding and Predicting the Effect of Cocrystal Components and pH on Cocrystal Solubility. *Crystal Growth & Design* **2009,** *9* (9), 3976-3988.

42. Huang, N.; Rodríguez-Hornedo, N. r., Effect of Micellar Solubilization on Cocrystal Solubility and Stability. *Crystal Growth & Design* **2010,** *10* (5), 2050-2053.

43. Reddy, L. S.; Bethune, S. J.; Kampf, J. W.; Rodríguez-Hornedo, N., Cocrystals and Salts of Gabapentin: pH Dependent Cocrystal Stability and Solubility. *Crystal Growth & Design* **2009,** *9* (1), 378-385.

44. Martin, F. A.; Pop, M. M.; Borodi, G.; Filip, X.; Kacso, I., Ketoconazole Salt and Co-crystals with Enhanced Aqueous Solubility. *Crystal Growth & Design* **2013,** *13* (10), 4295-4304.

45. Shayanfar, A.; Jouyban, A., Physicochemical characterization of a new cocrystal of ketoconazole. *Powder Technology* **2014,** *262*, 242-248.

46. Serajuddin, A. T. M., Salt formation to improve drug solubility. *Advanced Drug Delivery Reviews* **2007,** *59* (7), 603-616.

47. Stephenson, G. A.; Aburub, A.; Woods, T. A., Physical stability of salts of weak bases in the solid-state. *Journal of Pharmaceutical Sciences* **2011,** *100* (5), 1607-1617.

48. Thakral, N. K.; Behme, R. J.; Aburub, A.; Peterson, J. A.; Woods, T. A.; Diseroad, B. A.; Suryanarayanan, R.; Stephenson, G. A., Salt Disproportionation in the Solid State: Role of Solubility and Counterion Volatility. *Molecular Pharmaceutics* **2016,** *13* (12), 4141-4151.

49. Remenar, J. F.; Morissette, S. L.; Peterson, M. L.; Moulton, B.; MacPhee, J. M.; Guzmán, H. R.; Almarsson, Ö., Crystal Engineering of Novel Cocrystals of a Triazole Drug with 1,4-Dicarboxylic Acids. *Journal of the American Chemical Society* **2003,** *125* (28), 8456-8457.

50. Huang, N. C. Engineering cocrystal solubility and stability via ionization and micellar solubilization. University of Michigan, 2011.

51. Huang, N.; Rodríguez-Hornedo, N., Engineering cocrystal thermodynamic stability and eutectic points by micellar solubilization and ionization. *CrystEngComm* **2011,** *13* (17), 5409-5422.

52. Lipert, M. P.; Roy, L.; Childs, S. L.; Rodriguez-Hornedo, N., Cocrystal Solubilization in Biorelevant Media and its Prediction from Drug Solubilization. *Journal of Pharmaceutical Sciences* **2015**.

53. Good, D. J.; Rodríguez-Hornedo, N. r., Cocrystal Eutectic Constants and Prediction of Solubility Behavior. *Crystal Growth & Design* **2010,** *10* (3), 1028-1032.

54. Lipert, M. P. Predicting the Influence of Drug Solubilizing Agents on Cocrystal Solubility, Stability, and Transition Points. Dissertations and Theses, University of Michigan, 2015.

55. Dokoumetzidis, A.; Macheras, P., A century of dissolution research: From Noyes and Whitney to the Biopharmaceutics Classification System. *International Journal of Pharmaceutics* **2006,** *321* (1–2), 1-11.

56. Noyes, A. A.; Whitney, W. R., THE RATE OF SOLUTION OF SOLID SUBSTANCES IN THEIR OWN SOLUTIONS. *Journal of the American Chemical Society* **1897,** *19* (12), 930-934.

57. Cao, F.; Amidon, G. L.; Rodriguez-Hornedo, N.; Amidon, G. E., Mechanistic Analysis of Cocrystal Dissolution as a Function of pH and Micellar Solubilization. *Molecular Pharmaceutics* **2016,** *13* (3), 1030-1046.

58. McConnell, E. L.; Fadda, H. M.; Basit, A. W., Gut instincts: Explorations in intestinal physiology and drug delivery. *International Journal of Pharmaceutics* **2008,** *364* (2), 213-226.

59. Zhou, R.; Moench, P.; Heran, C.; Lu, X.; Mathias, N.; Faria, T. N.; Wall, D. A.; Hussain, M. A.; Smith, R. L.; Sun, D., pH-Dependent Dissolution in Vitro and Absorption in Vivo of Weakly Basic Drugs: Development of a Canine Model. *Pharmaceutical Research* **2005,** *22* (2), 188-192.

60. Brouwers, J.; Brewster, M. E.; Augustijns, P., Supersaturating drug delivery systems: The answer to solubility-limited oral bioavailability? *Journal of Pharmaceutical Sciences* **2009,** *98* (8), 2549-2572.

61. Mitra, A.; Kesisoglou, F., Impaired Drug Absorption Due to High Stomach pH: A Review of Strategies for Mitigation of Such Effect To Enable Pharmaceutical Product Development. *Molecular Pharmaceutics* **2013,** *10* (11), 3970-3979.

62. Dressman, J. B.; Reppas, C., In vitro–in vivo correlations for lipophilic, poorly water-soluble drugs. *European Journal of Pharmaceutical Sciences* **2000,** *11, Supplement 2*, S73-S80.

63. Van der Meer, J. W. M.; Keuning, J. J.; Scheijgrond, H. W.; Heykants, J.; Van Cutsem, J.; Brugmans, J., The influence of gastric acidity on the bio-availability of ketoconazole. *Journal of Antimicrobial Chemotherapy* **1980,** *6* (4), 552-554.

64. Budha, N. R.; Frymoyer, A.; Smelick, G. S.; Jin, J. Y.; Yago, M. R.; Dresser, M. J.; Holden, S. N.; Benet, L. Z.; Ware, J. A., Drug Absorption Interactions Between Oral Targeted Anticancer Agents and PPIs: Is pH-Dependent Solubility the Achilles Heel of Targeted Therapy? *Clinical Pharmacology & Therapeutics* **2012,** *92* (2), 203-213.

65. Galia, E.; Nicolaides, E.; Hörter, D.; Löbenberg, R.; Reppas, C.; Dressman, J. B., Evaluation of Various Dissolution Media for Predicting In Vivo Performance of Class I and II Drugs. *Pharmaceutical Research* **1998,** *15* (5), 698-705.

66. Buchanan, C. M.; Buchanan, N. L.; Edgar, K. J.; Ramsey, M. G., Solubilty and dissolution studies of antifungal drug:hydroxybutenyl-β-cyclodextrin complexes. *Cellulose* **2007,** *14* (1), 35-47.

67. Tsume, Y.; Mudie, D. M.; Langguth, P.; Amidon, G. E.; Amidon, G. L., The Biopharmaceutics Classification System: Subclasses for in vivo predictive dissolution (IPD) methodology and IVIVC. *European Journal of Pharmaceutical Sciences* **2014,** *57*, 152-163.

68. Brewster, M. E.; Vandecruys, R.; Verreck, G.; Peeters, J., Supersaturating drug delivery systems: effect of hydrophilic cyclodextrins and other excipients on the formation and stabilization of supersaturated drug solutions. *Die Pharmazie - An International Journal of Pharmaceutical Sciences* **2008,** *63* (3), 217-220.

69. Serajuddin, A. T. M., Solid dispersion of poorly water-soluble drugs: Early promises, subsequent problems, and recent breakthroughs. *Journal of Pharmaceutical Sciences* **1999,** *88* (10), 1058-1066.

70. Adachi, M.; Hinatsu, Y.; Kusamori, K.; Katsumi, H.; Sakane, T.; Nakatani, M.; Wada, K.; Yamamoto, A., Improved dissolution and absorption of ketoconazole in the presence of organic acids as pH-modifiers. *European Journal of Pharmaceutical Sciences* **2015,** *76* (Supplement C), 225-230.

71. Mathias, N. R.; Xu, Y.; Patel, D.; Grass, M.; Caldwell, B.; Jager, C.; Mullin, J.; Hansen, L.; Crison, J.; Saari, A.; Gesenberg, C.; Morrison, J.; Vig, B.; Raghavan, K., Assessing the Risk of pH-Dependent Absorption for New Molecular Entities: A Novel in Vitro Dissolution Test, Physicochemical Analysis, and Risk Assessment Strategy. *Molecular Pharmaceutics* **2013,** *10* (11), 4063-4073.

CHAPTER 2

COCRYSTALS MITIGATE NEGATIVE EFFECTS OF HIGH pH ON SOLUBILITY AND DISSOLUTION OF A BASIC DRUG

Introduction

Solubility and permeability are the major factors that govern the oral absorption of a drug according to the Biopharmaceutical Classification System (BCS).[1] For BCS class II drugs, which have low solubility and high permeability, drug dissolution *in vivo* is the rate controlling step in drug absorption.[1] Much focus has been placed on the enhancement of drug solubility in order to improve dissolution and bioavailability, and some of the approaches include amorphous forms, salts, and cocrystals.[2-6]

These supersaturating drug delivery systems generate supersaturated solutions with respect to the crystalline parent drug, which can in turn enhance absorption and bioavailability if sustained over sufficient period of time.[7] Cocrystals have gained much interest in recent decades due to their capability to incorporate both ionizable and non-ionizable drug/coformer components (unlike salts), their crystalline stability advantage over amorphous solids, and their ability to impart or alter solubility-pH dependence with coformers of different ionization properties.[5, 8-10]

While cocrystals are capable of increasing drug solubility by orders of magnitude, they often exhibit different ionization and solubilization behavior from their parent drugs, which alter the solubility enhancement by cocrystals based on solution conditions.[11-14] Therefore, in order to

comprehend cocrystal solubility, it is important to understand cocrystal solution phase interactions, such as component ionization and solubilization by additives. Previous work by our laboratory has shown that cocrystallization with saccharin has imparted solubility-pH dependence to non-ionizable drug carbamazepine and altered this dependence for acidic drug indomethacin.[9] Indomethacin-saccharin cocrystal went from being 13 times more soluble than the drug at pH 1 to 65 times more soluble at pH 3, while carbamazepine-saccharin cocrystal solubility advantage over carbamazepine dihydrate increased from 2 to 10 between pH 1 and 3.[9] These two cocrystals demonstrate that cocrystal solubility advantage over parent drug is not a constant value, but it is dependent on solution conditions such as pH.

Cocrystals of gabapentin and nevirapine can be more or less soluble than their parent drugs depending on solution pH.[10, 15] These cocrystals exhibit pH_{max} values, which is a solubility transition point between drug and cocrystal based on solution pH.[8, 10, 15] Similar to salts, pH_{max} is a parameter that identifies stability regions of a cocrystal and its parent drug.[2, 8, 16] At the pH_{max}, cocrystal and drug solubilities are equal, and both cocrystal and drug solid phases are thermodynamically stable and coexist in equilibrium with solution.[8] Cocrystals of the basic drug nevirapine with acidic coformers are less soluble than the drug below the pH_{max}, but become more soluble above the pH_{max}.[15] The nevirapine cocrystal study demonstrated that cocrystal solubility advantage over drug can be fine-tuned by changing solution pH.[15]

Weakly basic drugs often rely on low gastric pH to dissolve prior to transfer to the small intestine for absorption into the systemic circulation.[7, 17-18] Thus, elevated gastric pH, whether due to disease state, food, or medication, can negatively impact this type of drug's absorption and efficacy.[18-21] Ketoconazole (KTZ) is one such drug. KTZ is a lipophilic, BCS class II drug and is able to dissolve to a much higher extent under low pH conditions (< 3) compared to high

or neutral pH conditions.[1, 19, 22-23] Its poor solubility at neutral pH (~7) and high solubility-pH dependence result in variable oral absorption due to pH effect.[20, 22-23] Drug label of oral KTZ tablets warns that reduction in gastric acidity either due to achlorhydria condition caused by certain diseases or medications that suppress production or neutralize gastric acid can adversely affect the absorption of the drug.[24] Considering its use as an anti-fungal agent and that diseases such as gastric cancer and AIDS can cause elevated gastric pH conditions, it is essential to address the solubility-pH issue in order to ensure efficacy during treatment.[25-27]

In order to enhance its poor aqueous solubility, three new cocrystals and a salt of KTZ with dicarboxylic acids were synthesized and published by Martin et al. in 2013.[28] The three cocrystals are ketoconazole-fumaric acid (KTZ-FUM), ketoconazole-succinic acid (KTZ-SUC), and ketoconazole-adipic acid (KTZ-ADP), all of which are of 1:1 stoichiometric ratio.[28] In this fine article, the authors not only conducted solid-state characterization for the cocrystals (and salt) but also studied their dissolution behavior in water. The cocrystals were found to achieve much higher solution concentrations of KTZ (up to 100 times) during dissolution than that of the parent drug, and, somewhat surprisingly to us, none of the cocrystals transformed in solution during the dissolution experiment.[28] Highly soluble cocrystals are known to undergo solution-mediated conversion back to less soluble drug forms, which is why the most soluble cocrystal may not always generate high levels of supersaturation in solution.[8, 29] While studying this article we noticed that solution pH was not considered in their analysis, and this is important since pH is known to have profound effects on the solubility of ionizable drugs and cocrystals.[8-9, 11-12, 30]

This study focuses on the effect of pH on KTZ cocrystal solubility and dissolution. The study aims to (1) develop and validate mathematical models for predicting the solubility of KTZ

cocrystals, (2) compare solubility-pH behavior of cocrystals and pure drug, (3) determine the dissolution advantage of cocrystals as a function of pH, and (4) relate the dissolution-precipiation behavior of cocrystals to their solubility advantage, $SA = S_{cocrystal}/S_{drug}$.

Materials and Methods

Materials

Ketoconazole (lot # BS1203355108, 98% purity) was purchased from Bosche Scientific (New Brunswick, NJ) and used as received. Adipic acid (lot # 06807BE, 99% purity), succinic acid (lot # 037K0021, 99% purity), fumaric acid (lot # 09426EE, 99+% purity), acetic acid (lot # 074K3658, 99%), sodium acetate anhydrous (lot # 100K0272), dipotassium hydrogen phosphate (lot # 103H0287, ACS reagent), and sodium chloride (lot # 094K0183, ACS reagent) were purchased from Sigma-Aldrich (St. Louis, MO) and used as received.

HPLC grade methanol, HPLC grade 2-propanol, sodium phosphate monobasic (lot # 017316), and hydrochloric acid (lot # 2AJK15038, ACS grade) were purchased from Fisher Scientific (Fair Lawn, NJ). Acetone (ACS reagent 99.5%) and phosphoric acid (lot # B0506524, 85+%) were purchased from Acros Organics (NJ) and used as received. Trifluoroacetic acid (spectrophometric grade, 99%) was purchased from Aldrich Company (Milwaukee, WI). Sodium hydroxide pellets was purchased from J.T. Baker (Philipsburg, NJ). Water used in this study was filtered through a double deionized (DI) purification system (Milli Q Plus Water System) from Millipore Co. (Bedford, MA).

Cocrystal Synthesis

Cocrystals were prepared by reaction crystallization method at room temperature.[31-32] KTZ-FUM and KTZ-SUC were synthesized in acetone. KTZ-ADP was synthesized in 2-

propanol. Full conversion of drug to cocrystal was observed between 24 to 48 hours. The solid phases were verified by X-ray powder diffraction (XRPD) and differential scanning calorimetry (DSC), and the stoichiometries were verified by HPLC.

Media Preparation

Solubility media:

Phosphate buffers at pH 2.02 (± 0.02) and 8.04 (± 0.01) were prepared at concentrations of 12 mM and 100 mM, respectively, with the appropriate amount of phosphoric acid and dipotassium hydrogen phosphate. Acetate buffer at pH 5.00 (± 0.01) and concentration of 100 mM was prepared with sodium acetate anhydrous and acetic acid. pH 1.01 (± 0.01) HCl solution (100 mM) was prepared by diluting concentrated hydrochloric acid solution (~12 M). All buffers were prepared at room temperature with DI water filtered by Milli Q Plus Water System. 1 M NaOH and 1 M HCl solutions were used to adjust the pH of the buffer to target pH.

Dissolution media:

Dissolution media were prepared based on the conditions of fasted gastric, fasted intestinal, and fed intestinal pH published by Jantratid et al. without surfactants and pepsin.[33] pH 1.60 (± 0.01) buffer (34 mM) was prepared with the appropriate amount of NaCl and HCl solution. pH 5.00 (± 0.03) acetate buffer (144 mM) was prepared with the appropriate amount of NaOH (pellets), acetic acid, and NaCl. pH 6.50 (± 0.04) phosphate buffer (29 mM) was prepared with appropriate amount of NaOH (pellets), sodium phosphate monobasic ($NaH_2PO_4 \bullet H_2O$), and NaCl. The pH values of all dissolution media were adjusted to target pH with 1 M NaOH and 1 M HCl solutions. All media were prepared at room temperature with DI water filtered by Milli Q Plus Water System.

Drug Solubility

Drug solubility was measured by adding excess solid to 3 mL of solution media. The solutions were magnetically stirred and were kept in water bath at 25 ± 0.1°C over 96 hours. 0.5mL aliquots of the suspension were sampled every 24 hours. Collected samples were filtered via centrifuge through a 0.45 μm pore cellulose acetate membrane, and the pH of the solutions was measured. The concentrations of KTZ in the solutions were analyzed by HPLC after proper dilutions with the mobile phase.

Cocrystal Solubility

Method 1:

Equilibrium solubility of the KTZ cocrystals can be directly measured when the solution pH is below 3. Excess solid for each cocrystal was added to 3 mL of solution media, and the solution was magnetically stirred in water bath at 25 ± 0.1°C up to 96 hours. 0.5mL aliquots of the suspension were sampled every 24 hours and filtered via centrifuge through a 0.45 μm pore cellulose acetate membrane. The solid phases were analyzed by XRPD and DSC to ensure only cocrystal solid phases were present. The solution pH values were measured, and the cocrystal component concentrations were analyzed by HPLC after appropriate dilution with mobile phase.

Method 2:

At solution pH above 3, the equilibrium solubility of the cocrystals was determined at the eutectic point, where the drug and cocrystal solid phases are in equilibrium with the solution.[5, 8, 34] The eutectic points are approached by cocrystal dissolution, where 150 – 200 mg of cocrystal and 50 – 80 mg of KTZ were suspended in 3 mL of solution, and cocrystal precipitation, where 50 – 80 mg of cocrystal and 100 – 150 mg of KTZ were suspended in 3 mL of near saturated solution of coformer. The solutions were kept in water bath at 25 ± 0.1°C and magnetically

stirred for up to 96 hours. Solution samples (0.5 mL) were collected every 24 hours and were filtered via centrifuge through a 0.45 μm pore cellulose acetate membrane, and the pH values were measured. The solid phases were analyzed by XRPD and DSC to confirm both drug and cocrystal solid phases were present, indicating the solutions were at the eutectic point. The filtered solutions were then analyzed by HPLC after proper dilutions with the mobile phase.

Cocrystal and Drug Powder Dissolution

Powder dissolution of drug and cocrystal were conducted using an overhead stirrer with a glass propeller at 150 rpm over 3 hours. 30 mL of dissolution media were used to dissolve 30 mg of KTZ drug or 30 mg KTZ-equivalent amount of cocrystal. Both drug and cocrystal powders were sieved through mesh screens and particles between 106 – 125 μm size was used. The dissolution experiments were conducted in a water bath with temperature of 24.5 (± 0.5) °C. Solution pH was measured at the beginning and at the end of each dissolution run. Aliquots of 0.5 mL were taken with syringe at appropriate time points for up to 180 minutes (min). The solution samples were filtered with syringe filter with PVDF membrane of pore size of 0.45 μm. The solution concentrations of drug and coformers were analyzed with HPLC after proper dilution with mobile phase.

High Performance Liquid Chromatography (HPLC)

Solution concentrations of the drug and coformer were analyzed by a Waters HPLC equipped with a UV spectrometer detector. A Waters Atlantis C18 column with the dimension of 250 x 4.6 mm and 5 μm particle size was used for separation at ambient temperature. The flow rate was set at 1mL/min and the injection volume was 20 μL. For KTZ-ADP and KTZ-FUM cocrystals, the mobile phase used was composed of 60% methanol and 40% water with 0.1% trifluoroacetic acid (TFA). For KTZ-SUC cocrystal, different methods were used to

analyze each component due to poor separation of SUC peak from the solvent peak. The KTZ component of KTZ-SUC cocrystal was analyzed using mobile phase composed of 60% methanol and 40% water with 0.1% TFA. The SUC component was analyzed using a gradient method with flow rate of 1mL/min starting with mobile phase composed of 25% methanol and 75% water with 0.1% TFA. The composition changed to 80% methanol and 20% water with 0.1% TFA after 2.5 min then reverted back to 25% methanol and 75% water with 0.1% trifluoroacetic acid after 6 min. The wavelengths used for the analytes were as follows: 230 nm for KTZ, 220 nm for FUM, and 210 nm for SUC and ADP.

X-Ray Powder Diffraction (XRPD)

A Rigaku Miniflex X-ray diffractometer (Danverse, MA) using Cu-Kα radiation, a tube voltage of 30kV, and a tube current of 15mA was utilized for analysis and characterization of solid phases. Measurements were taken from 5° to 40° at a continuous scan rate of 2.5°/min.

Thermal Analysis

TA instrument differential scanning calorimetry (DSC) (Newark, DE) was used to analyze the collected solid phases from the solubility studies, after they were dried at room temperature. The heating rate of the experiments was 10°C/min under dry nitrogen atmosphere. Standard aluminum sample pans and lids were used for these measurements.

Results and Discussion

Cocrystal Experimental Solubility

Solubility of drug and cocrystal were measured under different solution pH conditions. Solution concentrations of drug and coformer at equilibrium (table 2.1) were used to determine stoichiometric cocrystal solubility ($S_{cc,T}$) at the corresponding pH with the following equation:

$$S_{cc,T} = \sqrt{[KTZ]_T[CF]_T} \quad (2.1)$$

where $[KTZ]_T$ and $[CF]_T$ represent total KTZ and total coformer concentrations, respectively. The subscript, T, indicates that the concentration includes all non-ionized and ionized species of drug or coformer. Thus, the total concentration of any ionizable cocrystal will change with solution pH.

Table 2.1. Cocrystal solubilities determined from KTZ and coformer concentrations in equilibrium with cocrystal and drug phases, or with cocrystal at corresponding pH.

Cocrystal	Initial pH	Equilibrium pH	Solid phase(s)	$[KTZ]_T$ [a] (mM)	$[CF]_T$ (mM)	$S_{cc,T}$ [b] (mM)
KTZ-ADP	1.01 ±0.01	2.66 ±0.01	KTZ-ADP	56.5 ±0.7	49 ±1	53 ±1
	2.02 ±0.02	3.37 ±0.02	KTZ + KTZ-ADP	15.2 ±0.9	6.6 ±0.3	10.0 ±0.7
	5.00 ±0.01	4.64 ±0.01	KTZ + KTZ-ADP	0.51 ±0.02	17.6 ±0.2	3.0 ±0.1
	8.04 ±0.01	5.04 ±0.01	KTZ + KTZ-ADP	0.188 ±0.004	66.9 ±0.5	3.5 ±0.1
KTZ-FUM	1.01 ±0.01	2.03 ±0.01	KTZ-FUM	49.09 ±0.04	47.0 ±0.6	48.0 ±0.6
	2.02 ±0.02	3.35 ±0.01	KTZ + KTZ-FUM	15.5 ±0.5	1.48 ±0.08	4.8 ±0.3
	5.00 ±0.01	4.34 ±0.01	KTZ + KTZ-FUM	1.09 ±0.06	22.6 ±0.8	5.0 ±0.3
	8.04 ±0.01	4.52 ±0.01	KTZ + KTZ-FUM	0.67 ±0.04	48 ±1	5.7 ±0.4
KTZ-SUC	1.01 ±0.01	2.52 ±0.01	KTZ-SUC	53.1 ±0.4	53.5 ±0.5	53.3 ±0.6
	2.02 ±0.02	3.36 ±0.01	KTZ + KTZ-SUC	15.35 ±0.08	6.12 ±0.06	9.7 ±0.1
	5.00 ±0.01	4.63 ±0.01	KTZ + KTZ-SUC	0.50 ±0.02	8 ±2	2.0 ±0.5
	8.04 ±0.01	5.05 ±0.01	KTZ + KTZ-SUC	0.21 ±0.01	45 ±1	3.1 ±0.2

a. Drug concentration is the drug solubility in solutions saturated with respect to cocrystal and drug phases.
b. Determined using equation 2.1.

KTZ concentrations decreased with increasing solution pH, while the acidic coformer solution concentrations increased with increasing pH. The self-buffering effect of the basic drug and acidic coformers caused the pH at equilibrium to fall within a narrower range (2.03 – 5.05) compared to the initial pH of the media (1.01 – 8.04). As the cocrystals dissolved in media of pH 1 and 2, high degrees of ionization of the basic drug elevated the pH of the solution, and the acidic coformers decreased the solution pH when the cocrystals were dissolved in pH 5 and pH 8 buffers. In this study, the equilibrium pH values have shown to change as much as 3.5 units from the initial media pH. This illustrates the importance of pH measurement during solubility studies involving ionizable components.

At pH < 3, KTZ cocrystals are less soluble than the drug and thermodynamically stable in solution. Cocrystal solid phase can be suspended under those pH conditions without the risk of conversion to drug. As pH increases to ≥ 4, the cocrystals become more soluble and less stable, which can lead to supersaturation and precipitation of the drug. This can result in underestimation of cocrystal solubility if only drug concentrations were measured. Measuring both drug and coformer concentrations at the cocrystal-drug eutectic point provides a simple alternative to assess cocrystal solubility. To confirm eutectic point was reached, one needs to ensure both drug and cocrystal solid phases are present at equilibrium. The solid phases in table 2.1 represent those present at equilibrium. The stoichiometric solubility of a cocrystal can then be calculated with component (non-ionized + ionized) eutectic concentrations using equation 2.1.

One may notice in table 2.1 that the drug and coformer concentrations measured in HCl solution (initial pH 1.01) were similar but not identical. In theory, dissolution of a 1:1 molar ratio cocrystal in the absence of conversion should result in the same drug and coformer solution concentrations. The small discrepancies could be from measurement errors, but they could also

come from impurities in the cocrystals used. This impurity refers to small amount of excess drug/coformer present to the cocrystal stoichiometry, and this can impact cocrystal solubility due to common ion effect.

The purity of the cocrystals used in the solubility studies were analyzed with XRPD, DSC, and HPLC. DSC and XRPD showed only cocrystal solid phases and did not indicate any impurities in terms of excess drug or coformers. HPLC analysis of the cocrystals was also used to check stochiometric ratios of drug and coformer. KTZ-FUM and KTZ-SUC drug to coformer ratio were found to be between 0.95 – 1.05 by HPLC. KTZ-ADP was found to have drug to coformer ratio of about 1.27 ± 0.02 by HPLC. Coformers ADP and SUC have poor UV absorbance which resulted in larger uncertainties in their concentrations analyzed by HPLC. SUC has shown approximately 2.5% error and ADP has about 3.8% error of their standard curves at the concentrations used for the analysis in the solubility study. FUM and KTZ standard curves has about 0.3% error at their concentrations used for analysis. By measuring both component concentrations and using equation 2.1 to determine cocrystal solubility, one can minimize errors caused by these analytical uncertainties and cocrystal impurities.

Inaccuracy in cocrystal solubility evaluation can result from (1) solution-mediated transformation of cocrystal to less soluble form and (2) common ion effect imparted by impurities in the form of one component in excess to its stoichiometry. These common problems can be avoided by assessing cocrystal solubility at the eutectic point and using both component concentrations to calculate the stoichiometric cocrystal solubility.

Cocrystal Solubility as a Function of K_{sp}, pK_a, and pH

Pharmaceutical cocrystals include a wide range of molecular components, and cocrystal solubility behavior can vary greatly based on component physicochemical properties. The

following equations were derived to describe KTZ drug and cocrystal solubility with consideration of solution pH, component ionization, and cocrystal dissociation. The details of their derivation can be found in appendix 2A.

KTZ drug solubility as a function of solution pH can be described by

$$S_{drug,T} = [KTZ]_T = S_{KTZ,0}(1+10^{pK_{a2,KTZ}-pH}+10^{pK_{a1,KTZ}+pK_{a2,KTZ}-2pH}) \quad (2.2)$$

where $S_{drug,T}$ represents KTZ solubility, $[KTZ]_T$ is the total (ionized + non-ionized) KTZ concentration in solution, $S_{KTZ,0}$ is the non-ionized KTZ concentration in solution, and $pK_{a,KTZ}$ represents KTZ ionization constant.

For a 1:1 cocrystal of KTZ and dicarboxylic acid coformer, the solubility can be described by equation:

$$S_{cc,T} = \sqrt{\frac{K_{sp}(1+10^{pK_{a2,KTZ}-pH}+10^{pK_{a1,KTZ}+pK_{a2,KTZ}-2pH})}{(1+10^{pH-pK_{a1,CF}}+10^{2pH-pK_{a1,CF}-pK_{a2,CF}})}} \quad (2.3)$$

where $S_{cc,T}$ is the cocrystal solubility, $K_{a,CF}$ represents the ionization constant for the coformer, K_{sp} is the solubility product of the cocrystal. With equations 2.2 and 2.3, KTZ cocrystal and drug solubilities can be quantitively predicted as a function of pH, $S_{KTZ,0}$, pK_a, and K_{sp} (figure 2.1). Parameter values of $S_{KTZ,0}$ and K_{sp} can be found in table 2.2.

K_{sp} describes the dissociation of cocrystal in solution into its components, and it is defined as the product of the non-ionized drug and coformer concentrations for a 1:1 cocrystal.[5, 32]

$$K_{sp} = [KTZ][CF] \quad (2.4)$$

In the absence of other solution phase interactions, cocrystal solubility is governed by K_{sp}, pK_a of the components, and solution pH.[11] pK_a values for KTZ and coformers (ADP, FUM, and SUC) are reported and can be obtained from literature.[35-38] Cocrystal K_{sp} values were

determined by linear regression based on equation 2.3 and are listed in table 2.2. Details can be found in appendix 2B.

Table 2.2. Cocrystal K_{sp} and intrinsic solubilities of cocrystals and drug at 25°C.

Drug/Cocrystal	K_{sp}[a] (M^2)	R^2	pK_{sp}[b]	S_0 [a,c] (mM)
KTZ	--	--	--	[a]$4.7(\pm0.2) \times 10^{-3}$
KTZ-ADP	$3.4(\pm0.2) \times 10^{-8}$	0.91	7.5	[c]$1.84 (\pm0.05) \times 10^{-1}$
KTZ-SUC	$2.7(\pm0.1) \times 10^{-8}$	0.77	7.6	[c]$1.64 (\pm0.03) \times 10^{-1}$
KTZ-FUM	$1.5(\pm0.2) \times 10^{-9}$	0.99	8.8	[c]$3.9 (\pm0.3) \times 10^{-2}$

a. K_{sp} and $S_{KTZ,0}$ determinations are shown in appendix 2B.
b. $pK_{sp} = -\log(K_{sp})$.
c. $S_{KTZ,0}$ is the intrinsic (non-ionized) solubility of KTZ; Cocrystal (1:1) intrinsic solubility calculated from $S_{cc,0} = \sqrt{K_{sp}}$. [5]

Out of the three cocrystals studied, KTZ-ADP has the highest K_{sp}, while KTZ-FUM has the lowest K_{sp}. In the absence of ionization, larger K_{sp} (or smaller pK_{sp}) indicates a more soluble cocrystal.[5] pK_{sp} values of 1:1 cocrystals of BCS class II drugs have been reported to be in the range of 1 to 9.[39] S_0 refers to the solubility of cocrystal and drug under non-ionized conditions. All three cocrystals exhibited higher S_0 values (between 8 and 39 times) compared to the drug.

Ionizable coformers, such as the acidic coformers of KTZ cocrystals, can alter cocrystal solubility behavior from that of the drug in aqueous environments. The influence of different ionization properties of drug and coformer on KTZ cocrystal solubility with respect to solution pH are illustrated in figure 2.1.

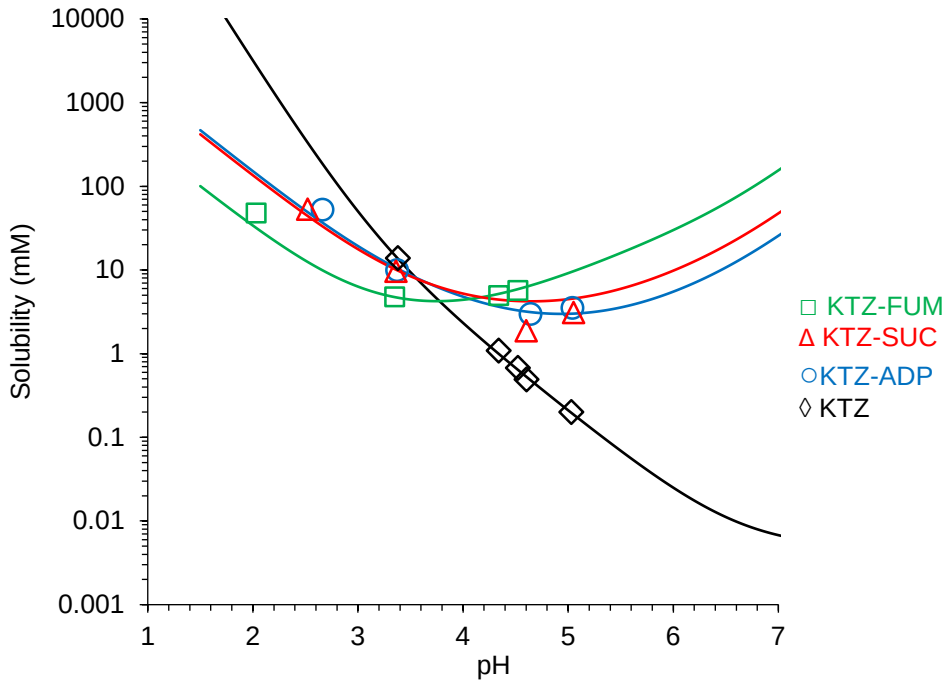

Figure 2.1. Predicted (lines) and experimental (symbols) KTZ cocrystal and drug solubilities as a function of pH. Predicted solubility-pH curves of KTZ drug and cocrystals were generated using equations 2.2 and 2.3 with parameters of component pK_a values (table 2.3), $S_{KTZ,0}$, and cocrystal K_{sp} values (table 2.2). Drug is represented in black and symbol "◊", KTZ-ADP is represented in blue and symbol "○", KTZ-FUM is represented in green and symbol "□", KTZ-SUC is represented in red and symbol "Δ". Cocrystal stoichiometric solubility values were determined experimentally using equation 2.1. pH values correspond to equilibrium pH. The standard errors for experimental solubility values are less than 4% and are within the experimental data points.

Solubility-pH profiles for KTZ drug and cocrystals were generated using equations 2.2 and 2.3 with corresponding parameter values of K_{sp}, pK_a, and $S_{KTZ,0}$ (figure 2.1). The cocrystal and drug solubility values obtained experimentally were plotted as data points and compared to the predicted solubility values. Excellent agreement between experimental and predicted solubility values demonstrated that the equations are effective in predicting drug and cocrystal solubilities.

Figure 2.1 illustrates the influence of solution pH on the solubility of KTZ and its three cocrystals: KTZ-ADP, KTZ-FUM, and KTZ-SUC. KTZ drug solubility decreases as pH

increases, while the cocrystals show U-shaped solubility-pH dependence due to the presence of both basic and acidic components. The acidic coformers caused the solubility of the cocrystals to be elevated at higher pH when compared to the parent drug. Cocrystallization with acidic coformers altered the solubility-pH profile of KTZ and reduced the magnitude of solubility variations as a result of solution pH. The self-buffering effect of the basic drug and acidic coformer narrowed the pH range in which the cocrystal equilibrium solubility could be experimentally determined. However, equation 2.3 enables quantitative prediction of cocrystal solubility at any pH, giving valuable insights for cocrystal solubility beyond the experimentally measurable pH range.

KTZ cocrystal solubility as a function of pH is largely governed by K_{sp} values and component ionization properties. KTZ-ADP and KTZ-SUC cocrystals have relatively similar K_{sp} and coformer pK_a values, which leads to similar solubility-pH behavior of the two cocrystals in the pH range studied. As pH increases to above 4.5, the difference between KTZ-ADP and KTZ-SUC solubilities becomes more noticeable as the effect of coformer ionization becomes more prominent. KTZ-FUM has the smallest K_{sp} out of the three cocrystals, and this contributed to it having the lowest solubility at $pH < 4$. However, because fumaric acid is the most acidic coformer (lowest pK_a values) and ionizes to a higher extent compared to the other coformers as pH increases, the fumaric acid cocrystal showed an earlier and steeper increase in solubility with pH. This resulted in KTZ-FUM solubility exhibiting the most variability with pH out of the three cocrystals.

In order to understand cocrystal solution behavior, one must first realize that cocrystal solubility is not a single number, and that it can exhibit drastically different behaviors than the parent drug based on the component properties. Cocrystal solubility is highly sensitive to

solution environment, in this case, the pH. KTZ cocrystals exhibited lower, equal, or higher solubility than the drug as solution pH increased from 1.5 to 7 in figure 2.1. This indicated the existence of solubility transition point, called the pH_{max}, which is the point of reversal in solubility advantage and relative stability for a cocrystal and its drug.[10, 15, 29] Cocrystal solubility advantage at pH above pH_{max} can lead to improvements in dissolution and oral absorption of KTZ in patients with elevated gastric pH.[22-23] The implications of this transition point will be discussed in more detail in the following section.

Cocrystal Solubility Advantage and pH_{max}

The intersections of cocrystal and drug solubility curves in figure 2.1 correspond to the pH_{max} of each cocrystal. pH_{max} is a solubility transition point with respect to pH, meaning that both cocrystal and drug solid phases coexist in equilibrium with solution at that particular pH value.[8, 11-12, 30] This is analogous to pH_{max} in salts, where the salt and free base/acid solubility curves intersect, and at which point both free base/acid and salt solid forms coexist in equilibrium with solution saturated with respect to both species.[2, 40-42]

pH_{max} identifies pH regions where a cocrystal is thermodynamically stable and where it can generate supersaturation with respect to drug solubility.[8, 12, 15, 30] KTZ cocrystals are thermodynamically stable at $pH < pH_{max}$, and they are less soluble than the parent drug under those solution conditions. As pH increases and surpasses pH_{max}, the relative stability of cocrystal and drug is reversed as the cocrystal becomes the more soluble form. KTZ cocrystal pH_{max} and the corresponding solubility values (table 2.3) were determined using MATLAB, with equations 2.2 and 2.3 and parameters including $S_{KTZ,0}$, cocrystal K_{sp}, and component pK_a values. Cocrystal solubility at pH_{max} ($S_{cc,pHmax}$) was calculated with equation 2.3 at $pH = pH_{max}$ for each cocrystal.

Table 2.3. KTZ cocrystal pH_{max}, $S_{cc,pHmax}$, and component pK_a values.

Cocrystal	pH_{max}	$S_{cc,pHmax}$ (mM)	Coformer pK_{a1}, pK_{a2}	Drug pK_{a1}, pK_{a2}[c]
KTZ-ADP	3.6	8.2	[a]4.44, 5.44	
KTZ-SUC	3.6	7.8	[b]4.00, 5.24	3.17, 6.63
KTZ-FUM	3.8	4.2	[b]2.85, 4.10	

a. From reference[38].
b. From reference[36].
c. From reference[35].

KTZ cocrystal pH_{max} values range from 3.6 to 3.8. The location of pH_{max} is dependent on cocrystal K_{sp} and component pK_a values. KTZ-ADP and KTZ-SUC cocrystals exhibited similar pH_{max} due to their similar K_{sp} and coformer pK_a. KTZ-FUM cocrystal has the lowest K_{sp} and coformer pK_a values out of the three cocrystals, and the combination resulted in a slightly higher pH_{max} for KTZ-FUM than the other cocrystals.

The influence of cocrystal K_{sp}/pK_{sp} and coformer pK_a on cocrystal pH_{max} is illustrated in the following figures generated using initial parameter values from KTZ-FUM (figure 2.2), KTZ-ADP (figure 2.3), and KTZ-SUC (figure 2.4). For simplicity, only the first pK_a of the coformers were altered in each figure to show the effects. The figures show that pH_{max} values are directly proportional to changes in pK_{sp} and coformer pK_a, while the $S_{cc,pHmax}$ values exhibit an inverse relationship with changes in pK_{sp} and coformer pK_a.

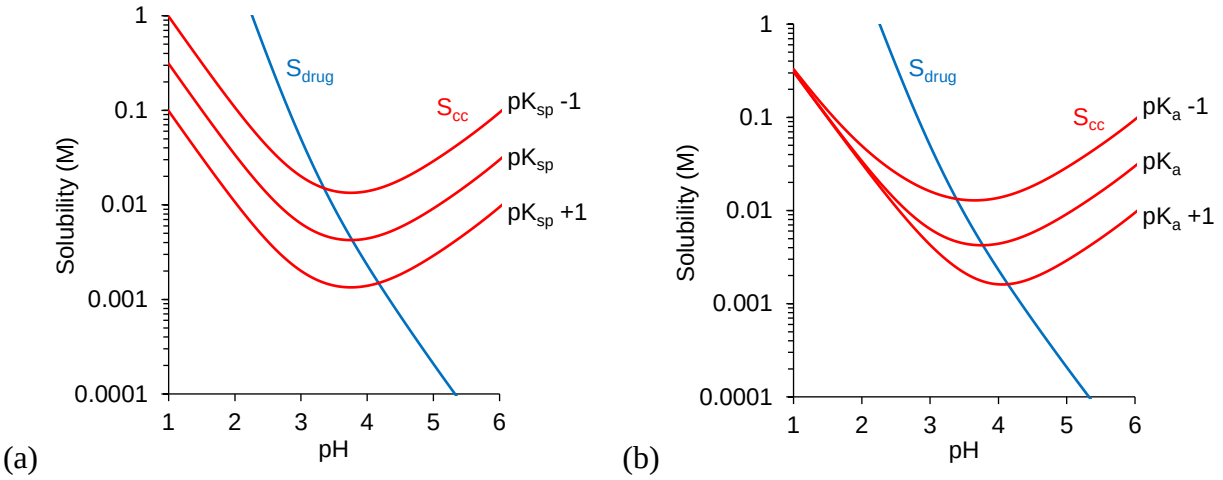

Figure 2.2. Influence of (a) cocrystal pK_{sp}, where $pK_{sp} = -\log(K_{sp})$ and (b) coformer pK_a ($pK_{a1,CF}$) on KTZ-FUM solubility and pH_{max}. Drug and cocrystal solubility curves were generated using equations 2.2 and 2.3 with the initial parameter values of $S_{KTZ,0} = 4.7 \times 10^{-6}$ M and KTZ-FUM pK_{sp}/K_{sp}, $pK_{a,KTZ}$, and $pK_{a,CF}$ values listed in tables 2.2 and 2.3. pK_{sp} value changes by 1 for every magnitude (10 fold) change of K_{sp}. Only $pK_{a1,CF}$ is altered while $pK_{a2,CF}$ and $pK_{a,KTZ}$ values are held constant in plot (b).

KTZ-FUM and its corresponding pK_{sp} and pK_a values were used in figure 2.2 to illustrate the effect of these parameters on cocrystal pH_{max}. With each unit change in pK_{sp}, the pH_{max} changed by ~ 0.4 unit, and $S_{cc,pHmax}$ changed between 3 - 3.5 fold, where $S_{cc,pHmax}$ value is more sensitive to decrease of pK_{sp}. One unit change of $pK_{a1,CF}$ resulted in ~ 0.4 unit change of pH_{max} and ~ 3 fold change of $S_{cc,pHmax}$.

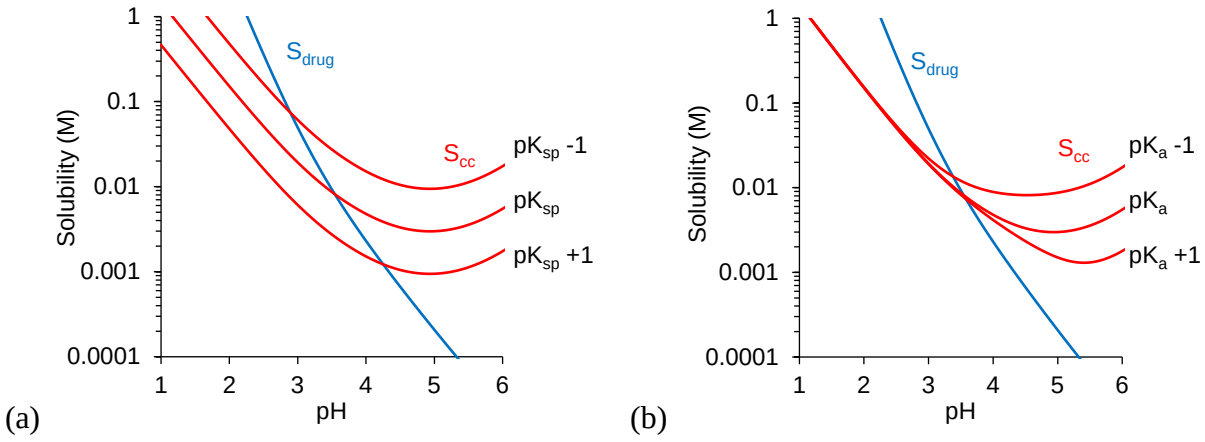

Figure 2.3. Influence of (a) cocrystal pK_{sp}, where $pK_{sp} = -\log(K_{sp})$, and (b) coformer pK_a ($pK_{a1,CF}$) on KTZ-ADP solubility and pH_{max}. Drug and cocrystal solubility curves were generated using equations 2.2 and 2.3 with the initial parameter values of $S_{KTZ,0} = 4.7 \times 10^{-6}$ M and KTZ-ADP pK_{sp}/K_{sp}, $pK_{a,KTZ}$, and $pK_{a,CF}$ listed in tables 2.2 and 2.3. Only the first pK_a of the coformer ($pK_{a1,CF}$) was altered in plot (b) while $pK_{a2,CF}$ remained unchanged.

The degree of pH_{max} and $S_{cc,pHmax}$ shift per unit change of pK_{sp} and pK_a are not the same for all cocrystals. KTZ-ADP in figure 2.3 shows that one unit change in pK_{sp} leads to ~ 0.7 unit change in pH_{max} and 7 – 9 fold change in $S_{cc,pHmax}$. Decreasing pK_{sp} has a larger impact on the value of $S_{cc,pHmax}$. For this cocrystal, the effect of increasing $pK_{a1,CF}$ on the pH_{max} and $S_{cc,pHmax}$ values is less pronounced in comparison to decreasing $pK_{a1,CF}$. One unit increase of $pK_{a1,CF}$ only changes pH_{max} and $S_{cc,pHmax}$ by ~ 0.03 unit and ~ 1.1 fold, whereas one unit decrease of $pK_{a1,CF}$ causes ~ 0.2 unit and ~ 2 fold changes in pH_{max} and $S_{cc,pHmax}$.

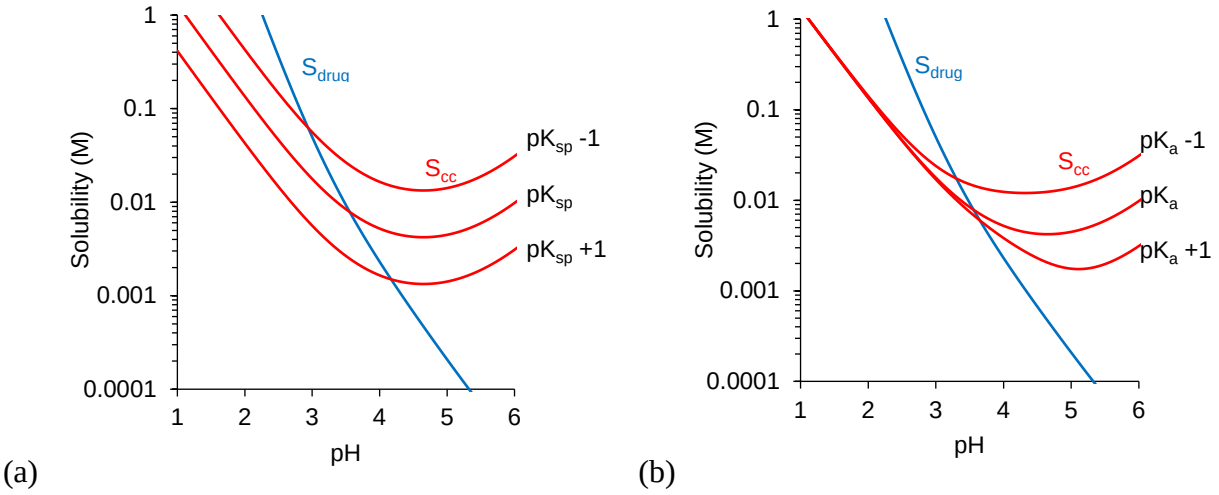

Figure 2.4. Influence of (a) cocrystal pK_{sp}, where $pK_{sp} = -\log(K_{sp})$, and (b) coformer pK_a ($pK_{a1,CF}$) on KTZ-SUC solubility and pH_{max}. Drug and cocrystal solubility curves were generated using equations 2.2 and 2.3 with the initial parameter values of $S_{KTZ,0} = 4.7 \times 10^{-6}$ M and KTZ-ADP pK_{sp}/K_{sp}, $pK_{a,KTZ}$, and $pK_{a,CF}$ listed in tables 2.2 and 2.3. Only the first pK_a of the coformer ($pK_{a1,CF}$) was altered in plot (b) while $pK_{a2,CF}$ remained unchanged.

KTZ-SUC pK_{sp} and $pK_{a,CF}$ values are similar to those of KTZ-ADP, leading to the two cocrystals exhibiting very similar behavior. Figure 2.4 shows that for every unit change in KTZ-SUC pK_{sp}, the pH_{max} changes by ~ 0.6 and $S_{cc,pHmax}$ changes by 5 – 8 fold. One unit increase of $pK_{a1,CF}$ causes ~ 0.1 and ~ 1.3 fold changes in pH_{max} and $S_{cc,pHmax}$ values, and decreasing $pK_{a1,CF}$ by the same magnitude leads to ~ 0.3 and ~ 2 fold changes in those values, respectively.

The figures 2.2, 2.3 and 2.4 show that altering pK_{sp} lead to parallel shifts of cocrystal solubility curves. Increasing pK_{sp} decreases the minimum cocrystal solubility value but have no influence on the pH at which it occurs. Changing coformer pK_a ($pK_{a1,CF}$) alters the curvature of cocrystal solubility-pH profiles, where increasing $pK_{a1,CF}$ led to lower values of minimum cocrystal solubility and delayed its occurrence with respect of pH.

Figure 2.5 illustrates the cocrystal solubility advantage over drug, defined as the ratio of cocrystal and drug solubility ($SA = S_{cc}/S_{drug}$), in the pH range between 1.5 and 7. Cocrystals exhibited no solubility advantage over drug ($SA \leq 1$) at or below pH_{max}. As pH increased to

above the pH_{max}, the cocrystals gained the ability to generate supersaturation with respect to the parent drug, and this can potentially lead to superior dissolution and even *in vivo* behavior. The cocrystal SA is expected to change quite dramatically with pH, as one can observe from figure 2.5. KTZ-FUM is predicted to be about 300 times LESS soluble than KTZ at pH 1.5 (SA ≈ 0.003) but would become more than 10,000 times MORE soluble than KTZ at pH 7 (SA > 10,000). Cocrystals KTZ-ADP and KTZ-SUC went from being 64 and 72 times less soluble to about 3,800 and 7,000 times more soluble than KTZ, respectively, in the same pH range.

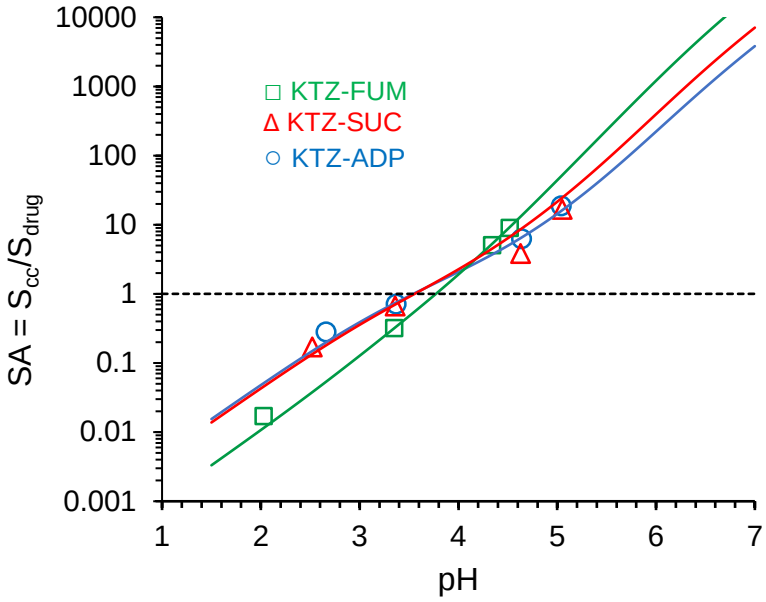

Figure 2.5. Cocrystal solubility advantage over drug (SA = S_{cc}/S_{drug}) as a function of pH. Solid lines represent predicted SA based on S_{drug} and S_{cc} values calculated using equation 2.2 and 2.3 and appropriate parameters. KTZ-ADP is represented in blue and with symbol "○". KTZ-FUM is represented in green and with symbol "□". KTZ-SUC is represented in red and with symbol "Δ". The dotted line represents where the cocrystal solubility and drug solubility are equal, and the cocrystal exhibit no solubility advantage over drug (SA = 1). The standard errors for SA values are less than 7% and are within the experimental data points.

The thermodynamic stability of KTZ drug and cocrystals can be altered by simply modifying solution pH. Proper understanding of cocrystal solution behavior is needed when designing and conducting solubility and dissolution experiments in order to avoid confusion.

The true solubility of these cocrystals might be underestimated if they undergo solution-mediated transformation during kinetic dissolution studies at pH > pH_{max}, and experiments conducted at pH < pH_{max} would not yield any solubility or dissolution advantage by the cocrystal. If cocrystal solubility-pH behavior is not understood, one may end up with contradicting results when attempting to correlate dissolution of these cocrystals under different solution conditions.

Our findings on cocrystal and drug solubilities are not in agreement with those reported in an earlier study.[28] Cocrystals were reported to be 75 to 100 times more soluble than KTZ, but the pH of the cocrystal and drug solutions were not considered during the comparison in that study.[28] The dissolution/solubility studies were conducted in water, and the final pH for each cocrystal was measured to be 3.8, 3.9, and 4.1 for KTZ-FUM, KTZ-ADP, and KTZ-SUC, respectively.[28] Unfortunately, the pH corresponding to KTZ solubility was not reported nor considered. A saturated solution of KTZ has a pH of about 8. KTZ is a basic compound and will increase the pH of aqueous solutions, in contrast to the cocrystals that will lower the pH as they have acidic coformers. Therefore, the comparison between cocrystal and drug solubility in is not representative of the true solubility advantage of the KTZ cocrystals, because the pH conditions were different.[28]

The previous study also reported that in spite of the high cocrystal solubility enhancement there was no conversion to the less soluble drug.[28] The reason for the lack of conversion is likely due to the pH during cocrystal solubility studies were very close to the pH_{max} (table 2.3), where drug and cocrystal are both thermodynamically stable. In fact, based on the final dissolution pH, KTZ-ADP and KTZ-SUC are only 1.7 and 2.5 times more soluble than the drug, respectively, while KTZ-FUM is equally soluble to the drug. The cocrystal

solubility/dissolution advantages are therefore much lower than the enhancements originally suggested by the authors of this fine publication.

Cocrystal K_{eu} and Solubility Advantage

In the previous sections, we have demonstrated how the eutectic point measurement enables the evaluation of cocrystal solubility in a solvent where the cocrystal is metastable.[5, 34] Aside from cocrystal solubility determination, the eutectic concentrations of drug and coformer can also be used to identify stability regions for the cocrystals. The eutectic constant (K_{eu}) is defined as the activity ratio (a) of coformer to drug at the eutectic point and can be approximated by the ratio of total coformer and drug concentrations.[5, 8, 29, 34]

$$K_{eu} \equiv \frac{a_{CF,eu}}{a_{drug,eu}} \approx \frac{[CF]_{eu,T}}{[drug]_{eu,T}} \qquad (2.5)$$

The terms $[CF]_{eu,T}$ and $[drug]_{eu,T}$ represent the total concentrations of coformer and drug at the eutectic, respectively.

KTZ cocrystal component eutectic concentrations between pH 3.3 and 5.1 (at equilibrium) are shown in figure 2.6.

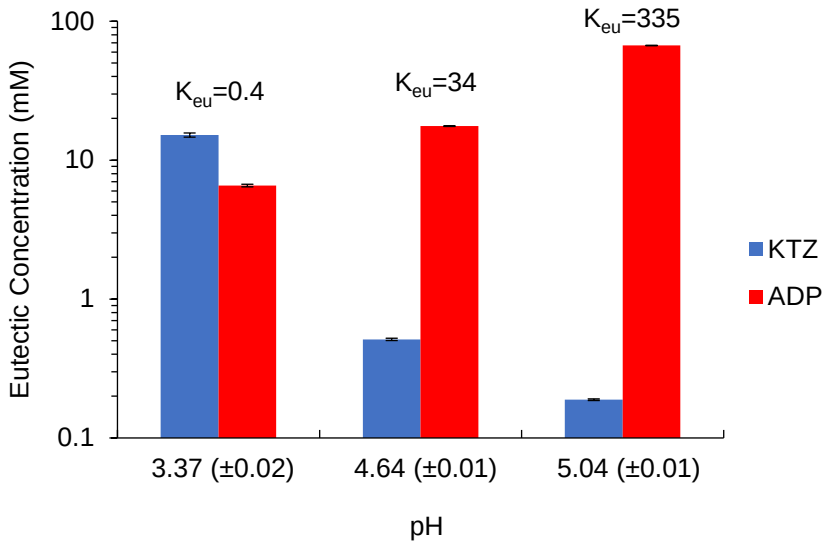

(a)

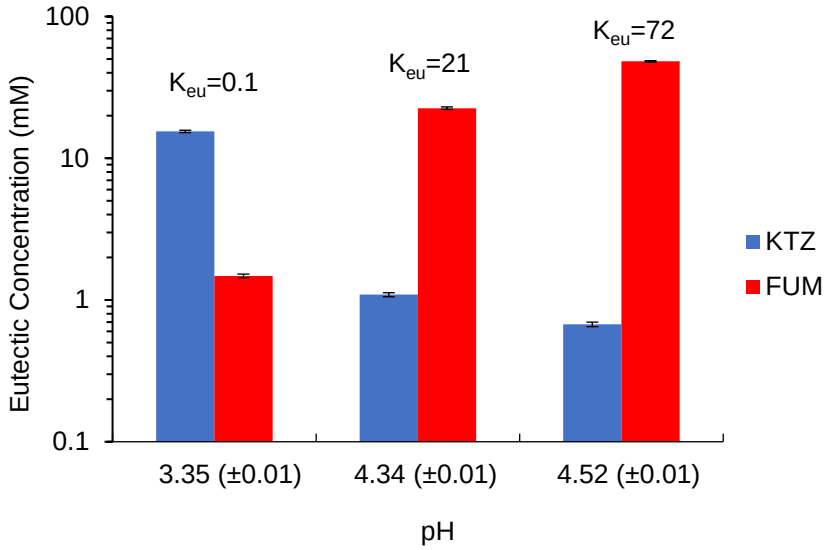

(b)

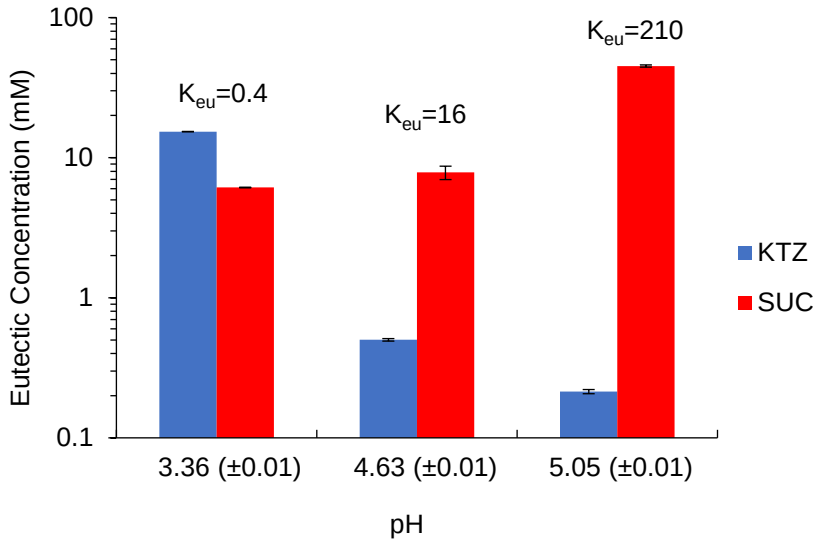

(c)

Figure 2.6. KTZ cocrystal component eutectic concentrations at different pH values indicate the relative thermodynamic stability of cocrystal to drug. (a) KTZ-ADP. (b) KTZ-FUM. (c) KTZ-SUC. X-axis values represent the solution pH at equilibrium, which has been altered from the initial media pH due to the buffering effect of drug and coformer. The initial media pH values are (from left to right) 2.02, 5.00, and 8.04. $K_{eu} < 1$ or $[coformer]_{eu} < [drug]_{eu}$ indicates that the cocrystal is less soluble than the drug at that given pH. As pH increases, this trend is reversed for all three cocrystals, indicating the existence of a solubility transition point, pH_{max}. Error bars on the columns indicate standard error.

The drug and coformer eutectic concentrations change with solution pH, and this led to changes in the K_{eu} values. At the lowest pH values (pH 3.35 – 3.37), $[KTZ]_{eu,T} > [CF]_{eu,T}$, resulting in $K_{eu} < 1$ and indicating that the cocrystal is less soluble and more stable compared to the drug. At higher pH values (pH 4.34 – 5.05), KTZ eutectic concentrations become less than that of the coformers. This resulted in K_{eu} values increasing to > 1, which indicated a reversal in the relative thermodynamic stability, and the cocrystals became more soluble than the drug. At pH_{max}, KTZ and CF eutectic concentrations are equal ($K_{eu} = 1$), and this indicates that the solubility of drug and cocrystal are equal. K_{eu} is a useful tool to assess cocrystal stability relative to drug, and it is easily accessible experimentally under equilibrium conditions.[9, 15, 34]

For a 1:1 cocrystal, regardless of ionization, cocrystal SA can be expressed in terms of eutectic concentrations of drug and coformer:[5, 9]

$$SA = \frac{S_{cc}}{S_{drug}} = \sqrt{\frac{[CF]_{eu}}{[drug]_{eu}}} \tag{2.6}$$

Combining equations 2.5 and 2.6, we get the relationship between K_{eu} and cocrystal SA:

$$K_{eu} = \left(\frac{S_{cc}}{S_{drug}} \right)^2 = SA^2 \tag{2.7}$$

The correlation between K_{eu} and SA is described by equation 2.7 and illustrated in figure 2.7, which showed excellent agreement between the predicted and observed behaviors.

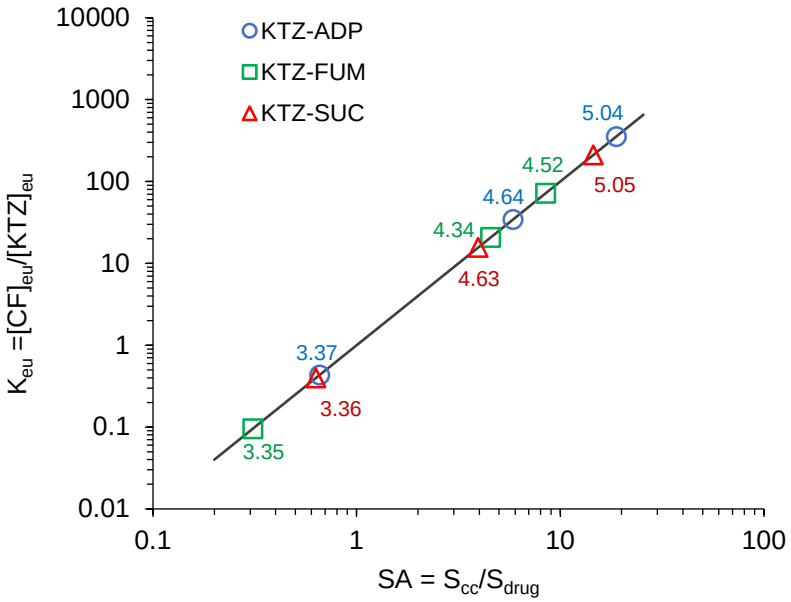

Figure 2.7. Predicted and experimental values of K_{eu} and cocrystal SA for KTZ-ADP, KTZ-FUM, and KTZ-SUC cocrystals. Prediction (dotted line) was generated using equation 2.7. The numbers by the symbols are pH values. Standard errors of K_{eu} values for most data points are less than 4%, except for K_{eu} standard error of KTZ-SUC at pH 4.63, which is 11%. Standard errors are within the experimental data points.

Cocrystal and Drug Dissolution

Powder dissolution studies of KTZ drug and cocrystals were conducted in aqueous buffer media at pH 1.60, 5.00, and 6.50 to represent the pH conditions in fasted gastric, fasted intestinal, and fed intestinal states.[33] Dissolution pH ranges from below to above the cocrystal pH_{max}. At pH > pH_{max}, the cocrystals gain solubility advantage over drug. The mass of pure drug and cocrystals used was 1 mg KTZ equivalent per mL (1.9 mM), which correspond to the oral dose of KTZ 200 mg if dissolved in 200 mL.[1, 24, 43-45] The dose is below KTZ solubility at pH 1.6, but at pH 5 and 6.5 it is 9 and 173 times above drug solubility. The dose is below cocrystal solubility at all pH values studied and will generate supersaturation with respect to KTZ above pH 4. This means that drug will fully dissolve at pH 1.6, and cocrystals will fully

dissolve at all pH values studied. Full dissolution of cocrystals can be confirmed by examining coformer concentrations during dissolution (appendix 2C).

Figure 2.8 shows that in general, the cocrystals outperformed the drug in pH 5 and pH 6.5 media and had similar performance to the drug in pH 1.6. Drug and cocrystals were fully dissolved in 20 min or less with similar dissolution profiles in pH 1.6 media. Percent drug dissolved in solution was calculated by multiplying the ratio of measured KTZ concentrations during dissolution to the fully dissolved concentration (~ 1.9 mM) with 100. In pH 5 media, cocrystal dissolutions showed that between 73% and 88% of the total KTZ (from cocrystals) were dissolved at corresponding C_{max}, which was huge improvements from the pure drug dissolution where only 11% of total KTZ was dissolved. In pH 6.5 media, KTZ-ADP and KTZ-SUC outperformed the drug, achieving about 13% drug dissolved at their C_{max}, whereas less than 1% dissolved during pure drug dissolution. KTZ-FUM dissolution in pH 6.5 exhibited high variabilities and showed little to no improvement from drug dissolution.

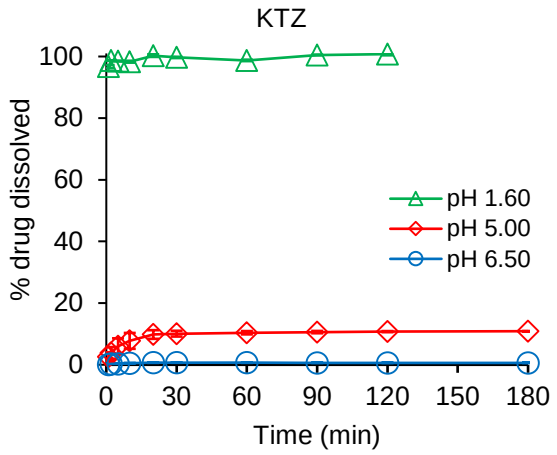

(a)

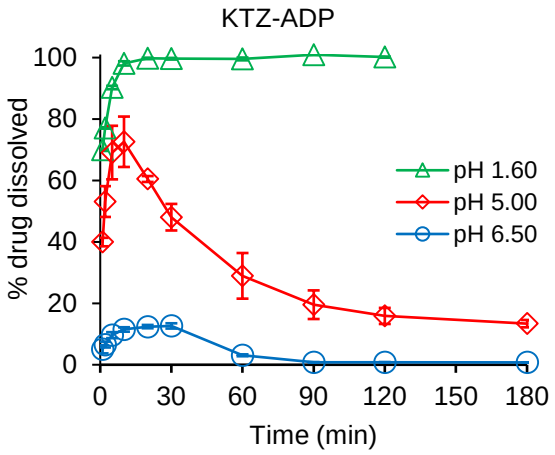

(b)

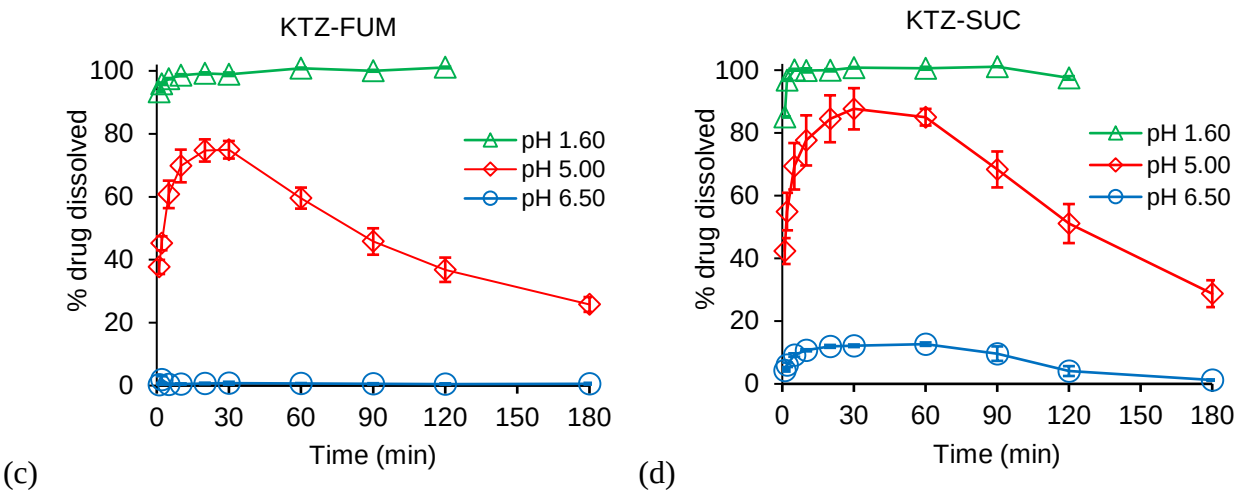

Figure 2.8. Percent KTZ dissolved during drug and cocrystals dissolution at initial pH values relevant to the pH of the fluid in the gastrointestinal tract. % drug dissolved was calculated from the ratio of measured KTZ in solution as a function of time to the theoretical concentration from the initial mass added, 100 × [KTZ] dissolved / [KTZ] total cocrystal or pure drug added. Legend indicate the initial pH of the dissolution media. Error bars indicate standard errors.

While cocrystal equilibrium solubility may be hundreds, even thousands, of times higher than that of the parent drug, the supersaturation level achieved by cocrystal dissolution may not be as high.[8] This is due to solution-mediated transformation of cocrystals back to its less soluble, more stable, drug form. The rate of conversion and level of drug concentration achieved through kinetic measurements depend on many factors, including cocrystal SA, also referred to as the supersaturation index, with respect to the parent drug.[7-8, 15, 29, 46] A highly soluble cocrystal can exhibit rapid solution-mediated transformation leading to no observable dissolution advantage over drug, while a less soluble cocrystal may be able to achieve and sustain a higher concentration over drug due to slower transformation.[7-8] Therefore, the concentration achieved during dissolution for a cocrystal may not always be proportional to its true solubility.

Influence of Cocrystal Supersaturation Index on Dissolution

KTZ supersaturation levels achieved during cocrystal dissolution are limited by conversion to the less soluble drug. Since cocrystals will experience the highest supersaturation

at the dissolving surface, where the solution is saturated with cocrystal,[47-48] we considered the supersaturation index (SA) as the driving force for cocrystal to drug conversion. As the SA value increases, the expected higher drug levels during cocrystal dissolution may be dampened by faster precipitation to the less soluble drug.

Cocrystal dissolution in pH 5 and 6.5 media decreased the pH of the solutions. Although these pH changes are relatively small (< 0.3 pH units in this study), they can lead to substantial changes in solubility and cocrystal SA values. Therefore, the maximum supersaturation (σ_{max}), defined as C_{max}/S_{drug}, and cocrystal SA in tables 2.4 and 2.5 were calculated using solubility values corresponding to the final dissolution pH instead of initial media pH.

Table 2.4. Cocrystal supersaturation index (SA), dissolution C_{max}, T_{max}, AUC, and maximum supersaturation (σ_{max}) in pH 6.5 media with standard errors.

	Final pH	SA[a]	KTZ C_{max} (mM)	KTZ T_{max} (min)	σ_{max} [a]	AUC (mM × min)
KTZ	6.48 ± 0.01	--	0.012 ± 0.001	--	--	2.11 ± 0.08
KTZ-ADP	6.23 ± 0.02	440	0.24 ± 0.03	30	14.7 ± 0.9	13.3 ± 0.5
KTZ-FUM	6.30 ± 0.09	3118	0.04 ± 0.03	2	2 ± 2	2.1 ± 0.4
KTZ-SUC	6.24 ± 0.05	822	0.24 ± 0.02	60	14.7 ± 0.6	26 ± 3

a. S_{cc} and S_{drug} values represent KTZ solubility at corresponding final pH of dissolution for each drug and cocrystal, calculated with equations 2.2 and 2.3.

Table 2.4 shows that KTZ-FUM dissolution in pH 6.5 media has a huge SA value (SA > 3,000) which might have led to rapid conversion to drug during dissolution, resulting in no dissolution advantage compared to that of the drug. KTZ-ADP and KTZ-SUC SA values are more modest in comparison (440 and 822, respectively), and they each achieved σ_{max} values of about 15 during dissolution. KTZ-SUC sustained supersaturation the longest (~ 2 hours), which

led to it having nearly two-fold higher AUC compared to the ADP cocrystal, even though they had similar C_{max} values.

Table 2.5. Cocrystal supersaturation index (SA), dissolution C_{max}, T_{max}, AUC, and maximum supersaturation (σ_{max}) in pH 5.0 media with standard errors.

	Final pH	SA[a]	KTZ C_{max} (mM)	KTZ T_{max} (min)	σ_{max} [a]	AUC (mM × min)
KTZ	5.01 ± 0.02	--	0.208 ± 0.001	--	--	35 ± 2
KTZ-ADP	4.94 ± 0.02	13	1.4 ± 0.3	10	5.9 ± 0.7	98 ± 9
KTZ-FUM	4.94 ± 0.06	36	1.41 ± 0.09	30	5.9 ± 0.2	160 ± 10
KTZ-SUC	4.99 ± 0.02	21	1.7 ± 0.2	30	7.8 ± 0.6	210 ± 20

a. S_{cc} and S_{drug} values represent KTZ solubility at corresponding final pH of dissolution for each drug and cocrystal, calculated with equations 2.2 and 2.3.

Table 2.5 shows that the cocrystal SA values were much smaller in pH 5 media (13 – 16) than in pH 6.5 media (440 – 3118). The C_{max} and AUC values from cocrystal dissolution were higher in pH 5 media than in pH 6.5 media, suggesting that the reduction of cocrystal SA also reduced cocrystal to drug conversion rate. The cocrystals achieved σ_{max} in the range of 6 to 8 with respect to drug during dissolution in pH 5 media. KTZ-SUC once again exhibited the best dissolution performance out of the three, achieving the highest C_{max} and AUC. KTZ-FUM achieved similar drug C_{max} and σ_{max} as KTZ-ADP during dissolution, but the AUC values of the two cocrystals indicate that the FUM cocrystal sustained supersaturation longer.

Dissolution of KTZ cocrystals demonstrated how having very large SA values may not be a desirable property for a cocrystal. Solution-mediated transformation of highly soluble cocrystals back to less soluble drug form can be accelerated as supersaturation level increases, leading to little or no dissolution advantage from the cocrystal. KTZ-FUM dissolution in pH 6.5 media is an excellent example of this.

In comparison to pure drug dissolution, cocrystal dissolution in media of different pH demonstrated less variation and higher drug concentrations (figure 2.9). In general, cocrystals outperformed the drug during dissolution, except KTZ-FUM in pH 6.5 buffer, where the conversion to drug was too rapid to allow for concentration enhancements. Higher drug concentrations and reduced variability at C_{max} in different media indicated that cocrystal *in vitro* dissolution behavior is less sensitive to pH compared to drug. This further implicates that these cocrystals may help reduce *in vivo* dissolution and absorption variability, and they can potentially improve drug bioavailability under elevated gastrointestinal pH conditions.

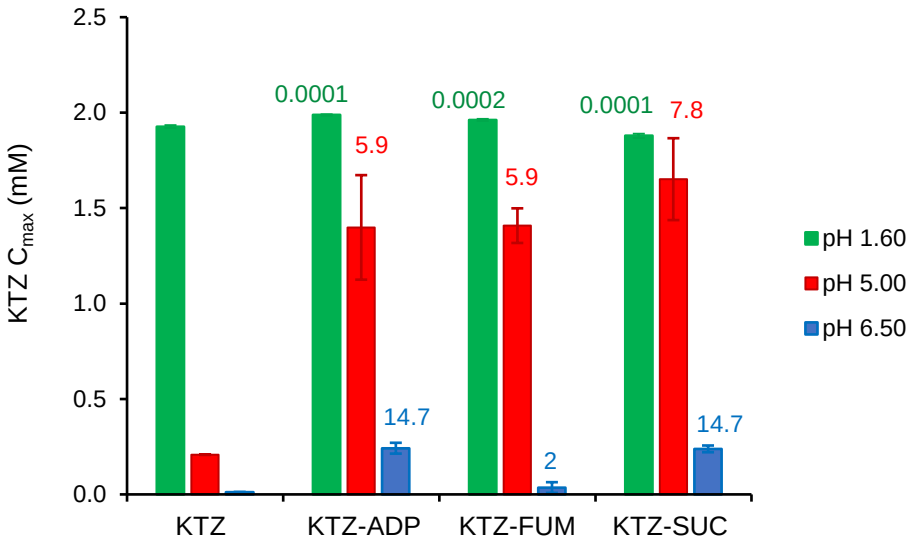

(a)

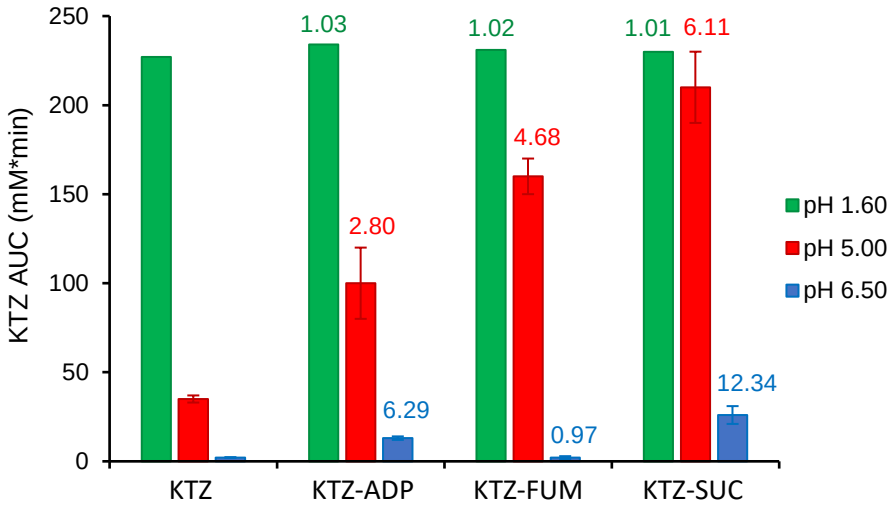

(b)

Figure 2.9. (a) C_{max} of KTZ during dissolution and (b) AUC of KTZ from 0 - 180 min for dissolution in pH 5.0 and 6.5 media, and from 0 – 120 min for dissolution in pH 1.6 media. Numbers on top of the columns represent (a) σ_{max} and (b) AUC ratio of cocrystal to drug ($AUC_{cc/drug}$). pH values in legend indicate initial media pH. Error bars indicate standard error.

The significance of cocrystal SA on the rate of conversion to drug can be appreciated in figure 2.10. Where σ_{max} indicates the highest supersaturation achieved by each cocrystal and the AUC ratio of cocrystal to drug indicates the cumulative drug exposure during cocrystal dissolution relative to the dissolution of pure drug.

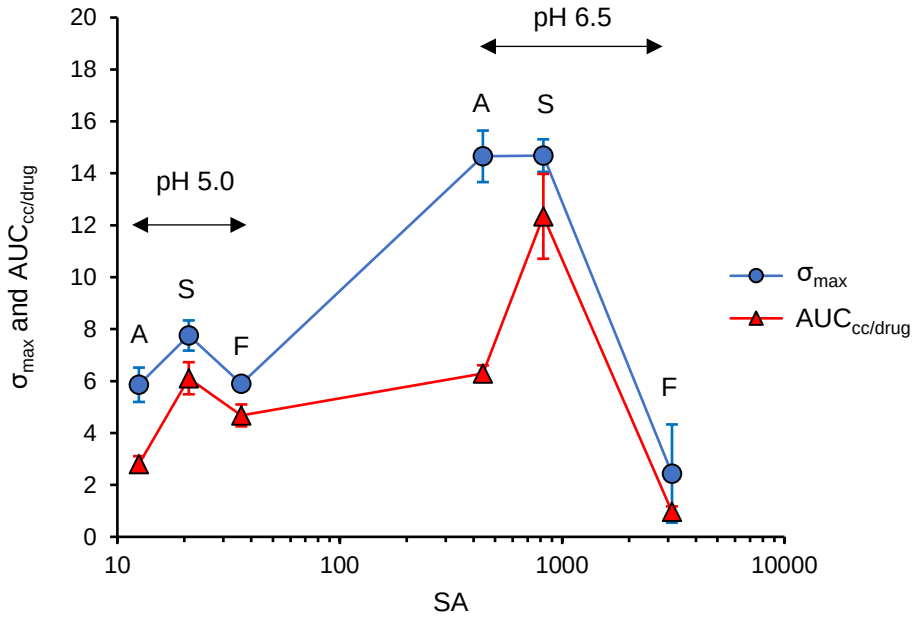

Figure 2.10. Cocrystal σ_{max} (○) and $AUC_{cc/drug}$ (Δ) as a function of cocrystal SA. Letters "A", "S", and "F" above the symbols represent cocrystals KTZ-ADP, KTZ-SUC, and KTZ-FUM, respectively. Error bars indicate standard error.

The range of SA values was found to be as low as 13 (ADP cocrystal, pH 5) and as high as 3,100 (FUM cocrystal, pH 6.5). Cocrystals with extremely high SA values, such as 3100 for KTZ-FUM in pH 6.5, are not expected to be able to sustain supersaturation in solution for very long. As can be observed in figure 2.10, this high SA value led to the lowest σ_{max} and $AUC_{cc/drug}$ values out of all the cocrystals and pH conditions. At pH 5, with cocrystal SA values between 13 and 40, enhancement in both σ_{max} and $AUC_{cc/drug}$ were observed. However, in pH 6.5, the much higher SA values between 440 and 3100 resulted in more variability in cocrystal dissolution behavior. KTZ-SUC achieved the highest σ_{max} and $AUC_{cc/drug}$ with SA of 822. Interestingly for KTZ-ADP, a lower SA (440) reached a high σ_{max} but a much lower $AUC_{cc/drug}$. It appeared that KTZ-SUC experienced the highest exposure levels with the slowest rate of conversion to drug among the three cocrystals. This might be a consequence of coformer effects on KTZ precipitation or cocrystal surface influence on nucleation mechanisms.

Conclusion

This work demonstrates that cocrystal solubility and dissolution are highly dependent on pH. Cocrystals of a weakly basic drug with acidic coformers dampen the negative effects of decreasing drug solubility with increasing pH. Solubility-pH dependence of cocrystals can be generated from determination of cocrystal K_{sp}. Different solubility-pH behavior exhibited by these cocrystals resulted in a pH_{max}, above which the cocrystal solubility and dissolution advantage over drug. Cocrystal K_{eu} can be used as a quick evaluation of cocrystal stability relative to drug. The equations presented in this work have demonstrated their ability to quantitatively predict solubility and to evaluate cocrystal supersaturation index under different solution pH conditions. SA is a useful in the interpretation of cocrystal dissolution-precipitation behavior, and is a meaningful parameter to assess the risk of cocrystal conversions.

Acknowledgement

Research reported in this publication was partially supported by the National Institute of General Medical Sciences of the National Institutes of Health under award number R01GM107146. The content is solely the responsibility of the authors and does not necessarily represent the official views of the National Institutes of Health. We also gratefully acknowledge partial financial support from the College of Pharmacy at the University of Michigan.

References

1. Amidon, G.; Lennernäs, H.; Shah, V.; Crison, J., A Theoretical Basis for a Biopharmaceutic Drug Classification: The Correlation of in Vitro Drug Product Dissolution and in Vivo Bioavailability. *Pharmaceutical Research* **1995,** *12* (3), 413-420.

2. Serajuddin, A. T. M., Salt formation to improve drug solubility. *Advanced Drug Delivery Reviews* **2007,** *59* (7), 603-616.

3. Serajuddin, A. T. M., Solid dispersion of poorly water-soluble drugs: Early promises, subsequent problems, and recent breakthroughs. *Journal of Pharmaceutical Sciences* **1999,** *88* (10), 1058-1066.

4. Hancock, B. C.; Zografi, G., Characteristics and significance of the amorphous state in pharmaceutical systems. *Journal of Pharmaceutical Sciences* **1997,** *86* (1), 1-12.

5. Good, D. J.; Rodríguez-Hornedo, N. r., Solubility Advantage of Pharmaceutical Cocrystals. *Crystal Growth & Design* **2009,** *9* (5), 2252-2264.

6. Thakuria, R.; Delori, A.; Jones, W.; Lipert, M. P.; Roy, L.; Rodríguez-Hornedo, N., Pharmaceutical cocrystals and poorly soluble drugs. *International Journal of Pharmaceutics* **2013,** *453* (1), 101-125.

7. Brouwers, J.; Brewster, M. E.; Augustijns, P., Supersaturating drug delivery systems: The answer to solubility-limited oral bioavailability? *Journal of Pharmaceutical Sciences* **2009,** *98* (8), 2549-2572.

8. Roy, L.; Lipert, M. P.; Rodriguez-Hornedo, N., Co-crystal Solubility and Thermodynamic Stability. In *Pharmaceutical Salts and Co-crystals*, The Royal Society of Chemistry: 2012; pp 247-279.

9. Alhalaweh, A.; Roy, L.; Rodríguez-Hornedo, N.; Velaga, S. P., pH-Dependent Solubility of Indomethacin–Saccharin and Carbamazepine–Saccharin Cocrystals in Aqueous Media. *Molecular Pharmaceutics* **2012,** *9* (9), 2605-2612.

10. Maheshwari, C.; André, V.; Reddy, S.; Roy, L.; Duarte, T.; Rodríguez-Hornedo, N., Tailoring aqueous solubility of a highly soluble compound via cocrystallization: effect of coformer ionization, pH max and solute–solvent interactions. *CrystEngComm* **2012,** *14* (14), 4801-4811.

11. Bethune, S. J.; Huang, N.; Jayasankar, A.; Rodríguez-Hornedo, N. r., Understanding and Predicting the Effect of Cocrystal Components and pH on Cocrystal Solubility. *Crystal Growth & Design* **2009,** *9* (9), 3976-3988.

12. Huang, N.; Rodríguez-Hornedo, N., Engineering cocrystal solubility, stability, and pHmax by micellar solubilization. *Journal of Pharmaceutical Sciences* **2011,** *100* (12), 5219-5234.

13. Lipert, M. P.; Rodríguez-Hornedo, N., Cocrystal Transition Points: Role of Cocrystal Solubility, Drug Solubility, and Solubilizing Agents. *Molecular Pharmaceutics* **2015**.

14. Huang, N.; Rodríguez-Hornedo, N. r., Effect of Micellar Solubilization on Cocrystal Solubility and Stability. *Crystal Growth & Design* **2010,** *10* (5), 2050-2053.

15. Kuminek, G.; Rodriguez-Hornedo, N.; Siedler, S.; Rocha, H. V. A.; Cuffini, S. L.; Cardoso, S. G., How cocrystals of weakly basic drugs and acidic coformers might modulate solubility and stability. *Chemical Communications* **2016,** *52* (34), 5832-5835.

16. Serajuddin, A. T.; Pudipeddi, M., *Salt selection strategies*. Wiley-VCH, Weinheim: 2002.

17. Dressman, J.; Berardi, R.; Dermentzoglou, L.; Russell, T.; Schmaltz, S.; Barnett, J.; Jarvenpaa, K., Upper Gastrointestinal (GI) pH in Young, Healthy Men and Women. *Pharmaceutical Research* **1990,** *7* (7), 756-761.

18. Hörter, D.; Dressman, J., Influence of physicochemical properties on dissolution of drugs in the gastrointestinal tract. *Advanced Drug Delivery Reviews* **2001,** *46* (1), 75-87.

19. Galia, E.; Nicolaides, E.; Hörter, D.; Löbenberg, R.; Reppas, C.; Dressman, J. B., Evaluation of Various Dissolution Media for Predicting In Vivo Performance of Class I and II Drugs. *Pharmaceutical Research* **1998,** *15* (5), 698-705.

20. Dressman, J. B.; Reppas, C., In vitro–in vivo correlations for lipophilic, poorly water-soluble drugs. *European Journal of Pharmaceutical Sciences* **2000,** *11, Supplement 2*, S73-S80.

21. Kostewicz, E. S.; Brauns, U.; Becker, R.; Dressman, J. B., Forecasting the Oral Absorption Behavior of Poorly Soluble Weak Bases Using Solubility and Dissolution Studies in Biorelevant Media. *Pharmaceutical Research* **2002,** *19* (3), 345-349.

22. Zhou, R.; Moench, P.; Heran, C.; Lu, X.; Mathias, N.; Faria, T. N.; Wall, D. A.; Hussain, M. A.; Smith, R. L.; Sun, D., pH-Dependent Dissolution in Vitro and Absorption in Vivo of Weakly Basic Drugs: Development of a Canine Model. *Pharmaceutical Research* **2005,** *22* (2), 188-192.

23. Van der Meer, J. W. M.; Keuning, J. J.; Scheijgrond, H. W.; Heykants, J.; Van Cutsem, J.; Brugmans, J., The influence of gastric acidity on the bio-availability of ketoconazole. *Journal of Antimicrobial Chemotherapy* **1980,** *6* (4), 552-554.

24. Nizoral (Ketoconazole) Tablets Drug Label. https://www.accessdata.fda.gov/drugsatfda_docs/label/2014/018533s041lbl.pdf.

25. Yasui, A.; Hoeft, S.; Stein, H.; DeMeester, T.; Bremner, R.; Nimura, Y., An Alkaline Stomach Is Common to Barrett's Esophagus and Gastric Carcinoma. In *Recent Advances in Diseases of the Esophagus*, Nabeya, K.-i.; Hanaoka, T.; Nogami, H., Eds. Springer Japan: 1993; pp 169-172.

26. Welage, L. S.; Carver, P. L.; Revankar, S.; Pierson, C.; Kauffman, C. A., Alterations in Gastric Acidity in Patients Infected with Human Immunodeficiency Virus. *Clinical Infectious Diseases* **1995,** *21* (6), 1431-1438.

27. Geraghty, J.; Thumbs, A.; Kankwatira, A.; Andrews, T.; Moore, A.; Malamba, R.; Mtunthama, N.; Hellberg, K.; Kalongolera, L.; O'Toole, P.; Varro, A.; Pritchard, D. M.; Gordon, M., Helicobacter pylori, HIV and Gastric Hypochlorhydria in the Malawian Population. *PLOS ONE* **2015,** *10* (8), e0132043.

28. Martin, F. A.; Pop, M. M.; Borodi, G.; Filip, X.; Kacso, I., Ketoconazole Salt and Co-crystals with Enhanced Aqueous Solubility. *Crystal Growth & Design* **2013,** *13* (10), 4295-4304.

29. Kuminek, G.; Cao, F.; Bahia de Oliveira da Rocha, A.; Gonçalves Cardoso, S.; Rodríguez-Hornedo, N., Cocrystals to facilitate delivery of poorly soluble compounds beyond-rule-of-5. *Advanced Drug Delivery Reviews* **2016,** *101*, 143-166.

30. Reddy, L. S.; Bethune, S. J.; Kampf, J. W.; Rodríguez-Hornedo, N., Cocrystals and Salts of Gabapentin: pH Dependent Cocrystal Stability and Solubility. *Crystal Growth & Design* **2009,** *9* (1), 378-385.

31. Rodríguez-Hornedo, N.; Nehm, S. J.; Seefeldt, K. F.; Pagán-Torres, Y.; Falkiewicz, C. J., Reaction Crystallization of Pharmaceutical Molecular Complexes. *Molecular Pharmaceutics* **2006,** *3* (3), 362-367.

32. Nehm, S. J.; Rodríguez-Spong, B.; Rodríguez-Hornedo, N., Phase Solubility Diagrams of Cocrystals Are Explained by Solubility Product and Solution Complexation. *Crystal Growth & Design* **2005,** *6* (2), 592-600.

33. Jantratid, E.; Janssen, N.; Reppas, C.; Dressman, J. B., Dissolution Media Simulating Conditions in the Proximal Human Gastrointestinal Tract: An Update. *Pharmaceutical Research* **2008,** *25* (7), 1663-1676.

34. Good, D. J.; Rodríguez-Hornedo, N. r., Cocrystal Eutectic Constants and Prediction of Solubility Behavior. *Crystal Growth & Design* **2010,** *10* (3), 1028-1032.

35. Avdeef, A., *Absorption and drug development solubility, permeability, and charge state*. 2nd ed.; John Wiley & Sons: Hoboken, N.J., 2012; p xli, 698 p.

36. Smith, R. M.; Martell, A. E.; SpringerLink, *Critical Stability Constants Second Supplement*. Springer US : Imprint: Springer: Boston, MA, 1989; p XVIII, 643 p.

37. Dean, J. A., *Handbook of organic chemistry*. McGraw-Hill: New York, 1987; p 1 v. (various pagings).

38. Serjeant, E. P.; Dempsey, B., *Ionisation constants of organic acids in aqueous solution*. Pergamon Press: Oxford ; New York, 1979; p xi, 989 p.

39. Kuminek, G., Cavanagh, K., Rodríguez-Hornedo, N., Measurement and mathematical relationships of cocrystal thermodynamic properties. In *Pharmaceutical Crystals: Science and Engineering*, John Wiley & Sons: 2017, Submitted.

40. Stahl, P. H.; Wermuth, C. G.; Stahl, P. H.; Wermuth, C. G., *Handbook of Pharmaceutical Salts: Properties, Selection, and Use*. 2002.

41. Avdeef, A., Solubility of sparingly-soluble ionizable drugs. *Advanced Drug Delivery Reviews* **2007,** *59* (7), 568-590.

42. Madhu Pudipeddi, A. T. M. S., David J. W. Grant, P. Heinrich Stahl, Solubility and Dissolution of Weak Acids, Bases, and Salts. In *Handbook of Pharmaceutical Salts: Properties, Selection, and Use*, 2nd, revised ed.; P. Heinrich Stahl, C. G. W., Ed. Wiley-VCH: Germany, 2011; pp 19-41.

43. Vertzoni, M.; Dressman, J.; Butler, J.; Hempenstall, J.; Reppas, C., Simulation of fasting gastric conditions and its importance for the in vivo dissolution of lipophilic compounds. *European Journal of Pharmaceutics and Biopharmaceutics* **2005,** *60* (3), 413-417.

44. Mudie, D. M.; Amidon, G. L.; Amidon, G. E., Physiological parameters for oral delivery and in vitro testing. *Molecular pharmaceutics* **2010,** *7* (5), 1388-1405.

45. P T Männistö, R. M., S Nykänen, U Lamminsivu, P Ottoila, Impairing effect of food on ketoconazole absorption. *Antimicrobial Agents and Chemotherapy* **1982,** *21* (5), 730-733.

46. Boistelle, R.; Astier, J. P., Crystallization mechanisms in solution. *Journal of Crystal Growth* **1988,** *90* (1), 14-30.

47. Nernst, W., Theorie der Reaktionsgeschwindigkeit in heterogenen systemen. *Z. Phys. Chem.* **1904,** *47*, 52-55.

48. Cao, F.; Amidon, G. L.; Rodriguez-Hornedo, N.; Amidon, G. E., Mechanistic Analysis of Cocrystal Dissolution as a Function of pH and Micellar Solubilization. *Molecular Pharmaceutics* **2016,** *13* (3), 1030-1046.

49. Guo, J.; Elzinga, P. A.; Hageman, M. J.; Herron, J. N., Rapid Throughput Screening of Apparent KSP values for Weakly Basic Drugs Using 96-Well Format. *Journal of Pharmaceutical Sciences* **2008,** *97* (6), 2080-2090.

50. Serajuddin, A. T. M.; Jarowski, C. I., Effect of diffusion layer pH and solubility on the dissolution rate of pharmaceutical bases and their hydrochloride salts I: Phenazopyridine. *Journal of Pharmaceutical Sciences* **1985,** *74* (2), 142-147.

Appendix 2A

KTZ Solubility as a Function of pH

The drug studied in this Chapter is ketoconazole (KTZ). Drug solubility can be described by the equilibrium of the solid drug KTZ with solution according to the following equilibrium expression:

$$KTZ_{crystal} \rightleftharpoons KTZ_{aq} \tag{2A.1}$$

where the dissolved drug, or the KTZ present in the aqueous phase, is expressed as KTZ_{aq}. KTZ is a dibasic drug, and can become ionized under certain aqueous conditions. Therefore, the total KTZ concentration ($[KTZ]_T$) in aqueous solution can be described by the sum of its non-ionized and ionized species in solution:

$$[KTZ]_T = [B]_{aq} + [BH^+]_{aq} + [BH_2^{2+}]_{aq} \tag{2A.2}$$

Where B, BH^+, and BH_2^{2+} are KTZ in its non-ionized, first protonated, and second protonated states. The subscripts T and aq denote the solubility and species in the aqueous phase, respectively. The non-ionized KTZ concentration in solution, $[B]_{aq}$, is also the intrinsic solubility of KTZ, which is expressed in later equations as $S_{KTZ,0}$.

The conjugate acids of the dibasic drug, KTZ, dissociate in solution according to their corresponding ionization constants

$$BH_{2,aq}^{2+} \overset{K_{a1,KTZ}}{\rightleftharpoons} H_{aq}^+ + BH_{aq}^+ \tag{2A.3}$$

$$K_{a1,KTZ} = \frac{[H^+]_{aq}[BH^+]_{aq}}{[BH_2^{2+}]_{aq}} \tag{2A.4}$$

$$BH_{aq}^+ \overset{K_{a2,KTZ}}{\rightleftharpoons} H_{aq}^+ + B_{aq} \tag{2A.5}$$

$$K_{a2,KTZ} = \frac{[H^+]_{aq}[B]_{aq}}{[BH^+]_{aq}} \quad (2A.6)$$

Substituting in relevant equilibria into the mass balance equation, KTZ solubility can be described by the equation:

$$S_{drug,T} = [KTZ]_T = S_{KTZ,0}(1 + \frac{[H^+]_{aq}}{K_{a2,KTZ}} + \frac{[H^+]_{aq}^2}{K_{a1,KTZ}K_{a2,KTZ}}) \quad (2A.7)$$

Equation 2A.7 can be expressed in terms of pH and pK_a

$$S_{drug,T} = S_{KTZ,0}(1 + 10^{pK_{a2,KTZ} - pH} + 10^{pK_{a1,KTZ} + pK_{a2,KTZ} - 2pH}) \quad (2A.8)$$

Acidic Coformer Ionization

Total concentration of diprotic acid coformer ($[CF]_T$) in aqueous solution can be described by the sum of its non-ionized and ionized species in solution (mass balance).

$$[CF]_T = [H_2A]_{aq} + [HA^-]_{aq} + [A^{2-}]_{aq} \quad (2A.9)$$

where H_2A represents the non-ionized form of coformer. HA^- and A^{2-} are the ionized species of the coformer.

The dicarboxylic acid coformer dissociates in solution according to its ionization constants:

$$H_2A_{aq} \overset{K_{a1,CF}}{\rightleftharpoons} H^+_{aq} + HA^-_{aq} \quad (2A.10)$$

$$K_{a1,CF} = \frac{[H^+]_{aq}[HA^-]_{aq}}{[H_2A]_{aq}} \quad (2A.11)$$

$$HA^-_{aq} \overset{K_{a2.CF}}{\rightleftharpoons} H^+_{aq} + A^{2-}_{aq} \quad (2A.12)$$

$$K_{a2,CF} = \frac{[H^+]_{aq}[A^{2-}]_{aq}}{[HA^-]_{aq}} \quad (2A.13)$$

Substituting in relevant equilibria into the mass balance equation, total coformer concentration in solution can be described by the equation:

$$[CF]_T = [H_2A]_{aq}(1+\frac{K_{a1,CF}}{[H^+]_{aq}}+\frac{K_{a1,CF}K_{a2,CF}}{[H^+]_{aq}^2}) \quad (2A.14)$$

Equation 2A.14 can be expressed in terms of pH and pK_a:

$$[CF]_T = [H_2A]_{aq}(1+10^{pH-pK_{a1,CF}}+10^{2pH-pK_{a1,CF}-pK_{a2,CF}}) \quad (2A.15)$$

Cocrystal Solubility as a Function of pH, pK_a, and K_{sp}

For 1:1 cocrystals of KTZ and dicarboxylic acid, the cocrystal solubility ($S_{cc,T}$) under stoichiometric condition can be described as:

$$S_{cc,T} = [KTZ]_T = [CF]_T \quad (2A.16)$$

Cocrystal dissociates in solution according to its solubility product, K_{sp}

$$KTZ\text{-}CF_{cocrystal} \overset{K_{sp}}{\rightleftharpoons} KTZ_{aq} + CF_{aq} \quad (2A.17)$$

$$K_{sp} = [KTZ][CF] = [B]_{aq}[H_2A]_{aq} \quad (2A.18)$$

where KTZ and CF refer to the non-ionized species of drug and coformer.

Considering cocrystal component mass balance (equations 2A.2 and 2A.9) and substituting in relevant equilibria, cocrystal solubility can be obtained:

$$S_{cc,T} = \sqrt{K_{sp}(1+\frac{[H^+]_{aq}}{K_{a2,KTZ}}+\frac{[H^+]_{aq}^2}{K_{a1,KTZ}K_{a2,KTZ}})(1+\frac{K_{a1,CF}}{[H^+]_{aq}}+\frac{K_{a1,CF}K_{a2,CF}}{[H^+]_{aq}^2})} \quad (2A.19)$$

Equation 2A.19 can be rewritten in terms of pH and pK_a:

$$S_{cc,T} = \sqrt{K_{sp}(1+10^{pK_{a2,KTZ}-pH}+10^{pK_{a1,KTZ}+pK_{a2,KTZ}-2pH})(1+10^{pH-pK_{a1,CF}}+10^{2pH-pK_{a1,CF}-pK_{a2,CF}})} \quad (2A.20)$$

Appendix 2B

Cocrystal K_{sp}

Equation 2A.20 can be linearized by squaring both sides.

$$S_{cc,T}^2 = K_{sp}(1+10^{pK_{a2,KTZ}-pH}+10^{pK_{a1,KTZ}+pK_{a2,KTZ}-2pH})(1+10^{pH-pK_{a1,CF}}+10^{2pH-pK_{a1,CF}-pK_{a2,CF}}) \quad (2B.1)$$

According to the relationship presented in equation 2B.1, by plotting the cocrystal solubility squared on the y-axis against the corresponding ionization terms of drug and coformer on the x-axis under difference pH conditions, the resulting slope of the line is the K_{sp} for the cocrystal (figure 2B.1).

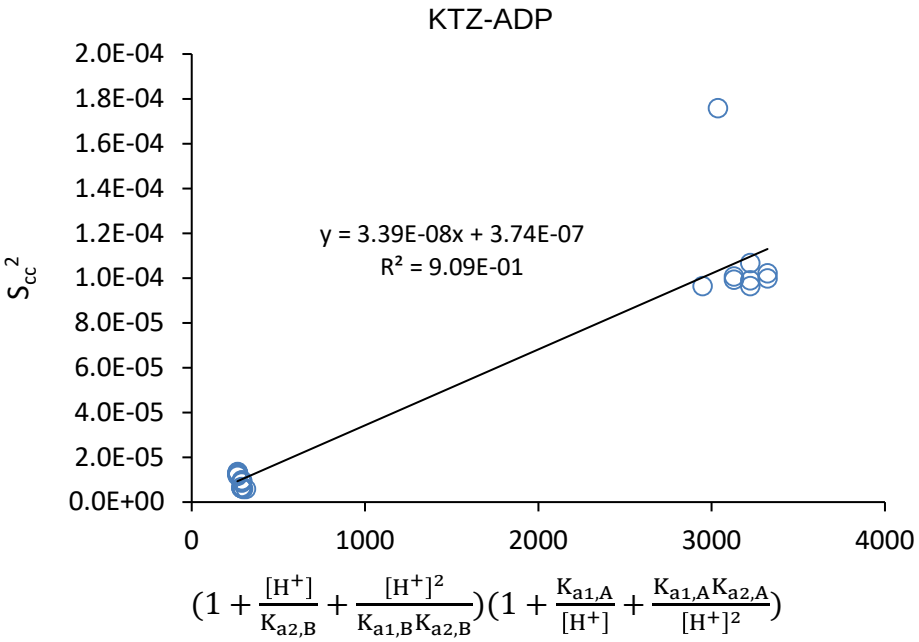

(a)

(b)

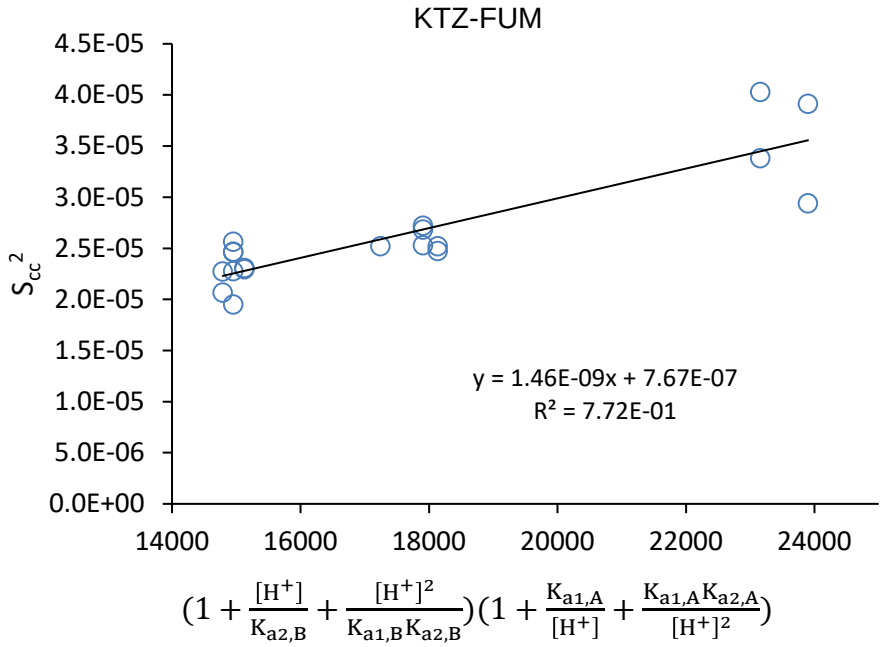

(c)

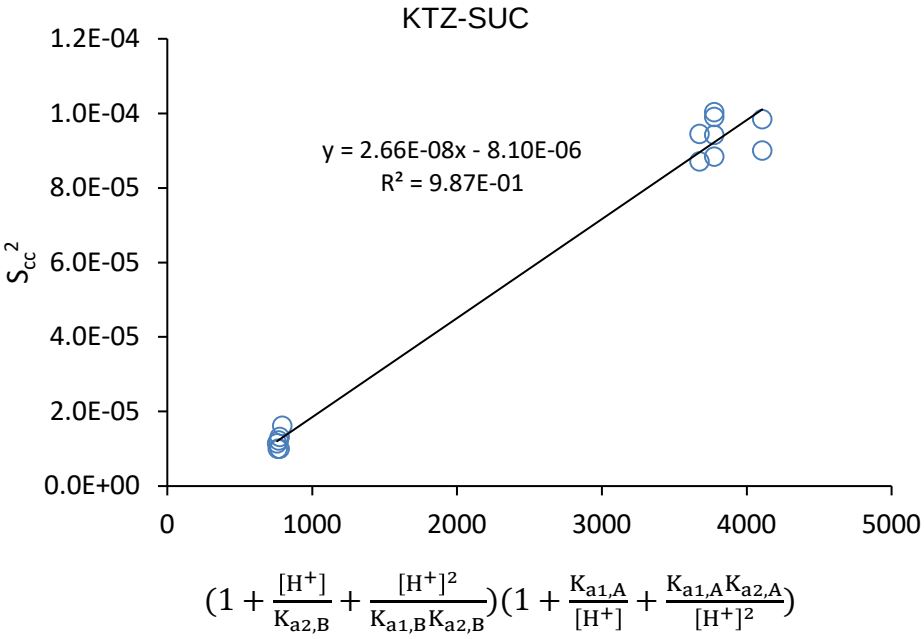

Figure 2B.1. Cocrystal K_{sp} determination from linear regression based on equation 2B.1, where K_{sp} is the slope of the regression line.

Under ideal conditions, cocrystal K_{sp} should be constant regardless of solution pH.

Equation 2.3 can be rearranged to solve for K_{sp} at each pH.

$$K_{sp} = \frac{S_{cc,T}^2}{(1+10^{pK_{a2,KTZ}-pH}+10^{pK_{a1,KTZ}+pK_{a2,KTZ}-2pH})(1+10^{pH-pK_{a1,CF}}+10^{2pH-pK_{a1,CF}-pK_{a2,CF}})} \quad (2B.2)$$

KTZ cocrystal K_{sp} values were determined for each pH condition studied. K_{sp} values calculated for each cocrystal under different pH conditions are summarized in table 2B.1 and compared to K_{sp} obtained from linear regression analysis.

Table 2B.1. Cocrystal K_{sp}.

	Media (initial pH)	Equilibrium pH	K_{sp} (M^2) calculated at each pH (eq. 2B.2)	Average K_{sp} calculated (M^2)	K_{sp} (M^2) linear regression
KTZ-ADP	Phosphate buffer (2.02 ±0.01)	3.37(±0.01)	3.1 (±0.1) x 10^{-8}	3 (±1) x 10^{-8}	3.4 (±0.2) x 10^{-8}
	Acetate buffer (5.00 ±0.01)	4.63(±0.03)	2.6 (±0.6) x 10^{-8}		
	Phosphate buffer (8.04 ±0.01)	5.04(±0.02)	4.8 (±0.2) x 10^{-8}		
KTZ-SUC	Phosphate buffer (2.02 ±0.01)	3.36(±0.01)	2.5 (±0.2) x 10^{-8}	2.1 (±0.5) x 10^{-8}	2.7 (±0.1) x 10^{-8}
	Phosphate buffer (8.04 ±0.01)	5.06(±0.01)	1.6 (±0.3) x 10^{-8}		
KTZ-FUM	Phosphate buffer (2.02 ±0.01)	3.35(±0.01)	1.5 (±0.1) x 10^{-9}	1.4 (±0.2) x 10^{-9}	1.5 (±0.2) x 10^{-9}
	Acetate buffer (5.00 ±0.01)	4.34(±0.02)	1.4 (±0.2) x 10^{-9}		
	Phosphate buffer (8.04 ±0.01)	4.53(±0.01)	1.5 (±0.3) x 10^{-9}		

K_{sp} of the KTZ cocrystals determined under different pH conditions showed some variability. Theoretically, K_{sp} should be a constant value that is based on the activities of cocrystal constituents.[5, 8] Under ideal conditions, the activities can be approximated by solution

concentrations of non-ionized drug and coformer, which was how the K_{sp} for KTZ cocrystals were estimated.[5, 8] It has been shown in the literature that the apparent K_{sp} of salts can vary with counter-ion concentration, solution pH, and ionic strength, due to the limitations of the determination method to account for all variables including ionic strength and pH.[49-50]

In the case of KTZ cocrystals, the apparent K_{sp} calculated for each cocrystal was usually the lowest at the pH where the measured cocrystal solubility was also the lowest, for example, KTZ-ADP in pH 5 acetate buffer (equilibrium pH = 4.63) and KTZ-SUC in pH 8 phosphate buffer (equilibrium pH = 5.06). KTZ-FUM equilibrium pH expanded a narrower range (3.35 - 4.53) compared to the other two cocrystals, and KTZ-FUM solubility changed very little (4.8 - 5.7 mM) in this pH region, which might help explain why its apparent K_{sp} values were the most consistent. The combined effect of cocrystal solubility (total concentration of drug and coformer in solution) and the extent of the ionization of its components influenced by solution pH may have contributed to the variability in apparent K_{sp}. The range of the apparent K_{sp} values for each KTZ cocrystal is less than 1 order of magnitude, which is consistent with reported variabilities of apparent K_{sp} determined for pharmaceutical salts under different counter-ion concentrations and pH conditions.[49]

Intrinsic Solubility of KTZ

The intrinsic (non-ionized) solubility of KTZ was not able to be measured directly due to the poor solubility of the basic drug at pH > 7 (figure 2B.2), which was below the quantification limit of the HPLC instrument used in this study. Therefore, KTZ solubility was measured, either as pure drug or at eutectic point with cocrystal, under different pH conditions and used to calculate the non-ionized drug solubility (table 2B.2).

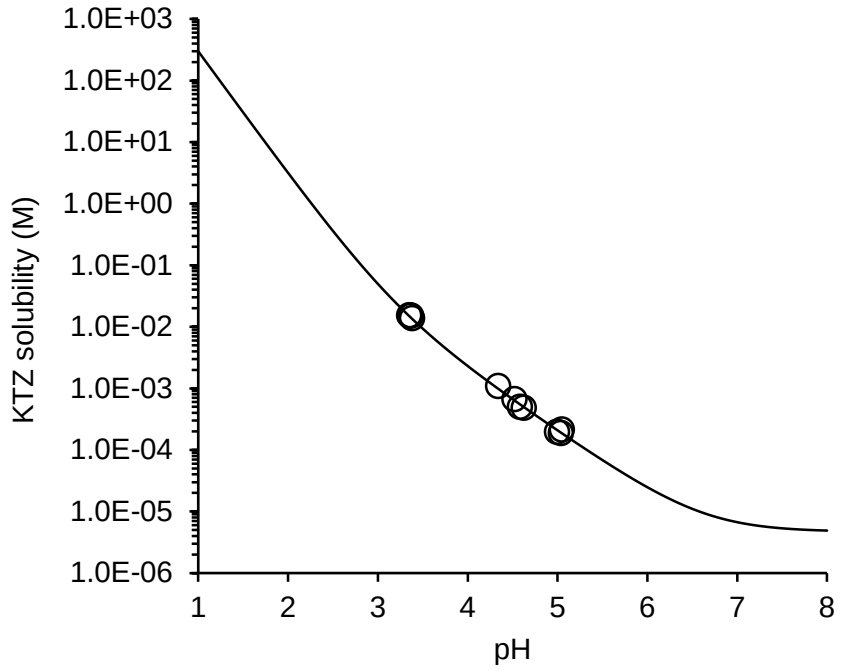

Figure 2B.2. KTZ solubility-pH profile generated with equation 2.1 and $S_{KTZ,0}$ = 4.7 x 10^{-6} M. Experimental solubility of KTZ at different pH is represented with data points. Standard errors are less than 4% and within the data points.

Table 2B.2. KTZ drug intrinsic solubility.

Media and initial pH	Equilibrium pH	Measurement type	$[KTZ]_T$ (M)	$[KTZ]_0$[a] (M)	Average $[KTZ]_0$ (M)
Phosphate buffer (2.02 ±0.01)	3.35 ±0.01	Eutectic	1.55 (±0.05) x 10^{-2}	4.88 x 10^{-6}	4.7 (±0.2) x 10^{-6}
	3.36 ±0.01	Eutectic	1.53 (±0.02) x 10^{-2}	4.92 x 10^{-6}	
	3.37 ±0.02	Eutectic	1.52 (±0.09) x 10^{-2}	5.10 x 10^{-6}	
	3.38 ±0.01	Single comp	1.382 (±0.004) x 10^{-2}	4.81 x 10^{-6}	
Acetate buffer (5.00 ±0.01)	4.34 ±0.01	Eutectic	1.09 (±0.04) x 10^{-3}	5.19 x 10^{-6}	
	4.58 ±0.01	Eutectic	5.01 (±0.08) x 10^{-4}	5.77 x 10^{-6}	
	4.62 ±0.05	Eutectic	4.9 (±0.2) x 10^{-4}	6.1 x 10^{-6}	
	5.00 ±0.02	Single comp	1.98 (±0.02) x 10^{-4}	4.44 x 10^{-6}	
Phosphate buffer (8.04 ±0.01)	4.52 ±0.01	Eutectic	6.7 (±0.4) x 10^{-4}	5.0 x 10^{-6}	
	5.04 ±0.01	Eutectic	1.89 (±0.04) x 10^{-4}	4.66 x 10^{-6}	
	5.05 ±0.01	Eutectic	2.1 (± 0.1) x 10^{-4}	5.4 x 10^{-6}	

a. $S_{KTZ,0}$ is calculated with experimental KTZ solubility and equation 2.1.

Appendix 2C

Cocrystal Dissolution in pH 6.5 Media

Both KTZ and coformer concentrations were measured to monitor the extent of cocrystal dissolution and conversion during dissolution (figure 2C.1).

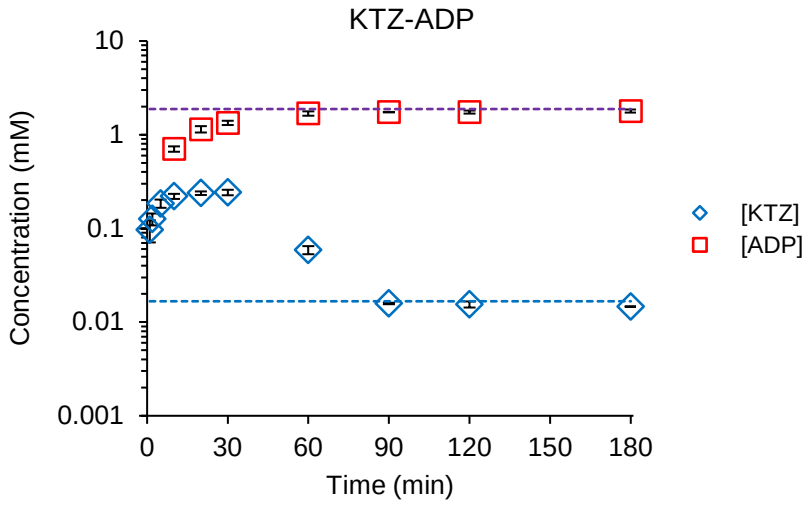

(a)

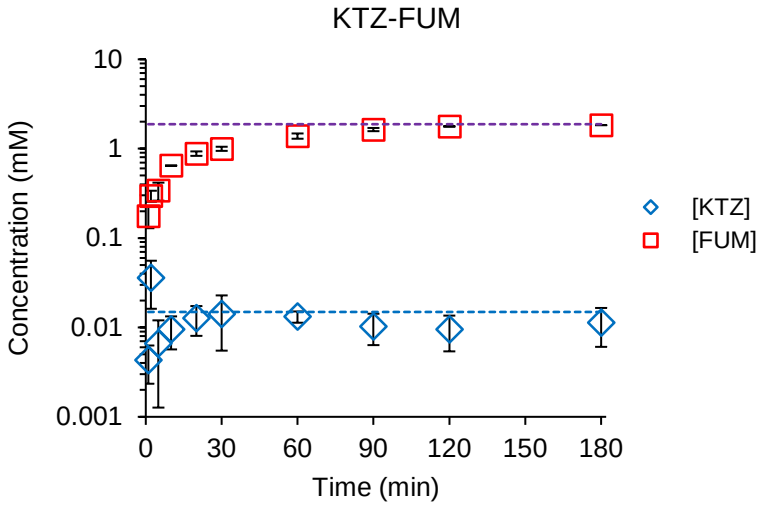

(b)

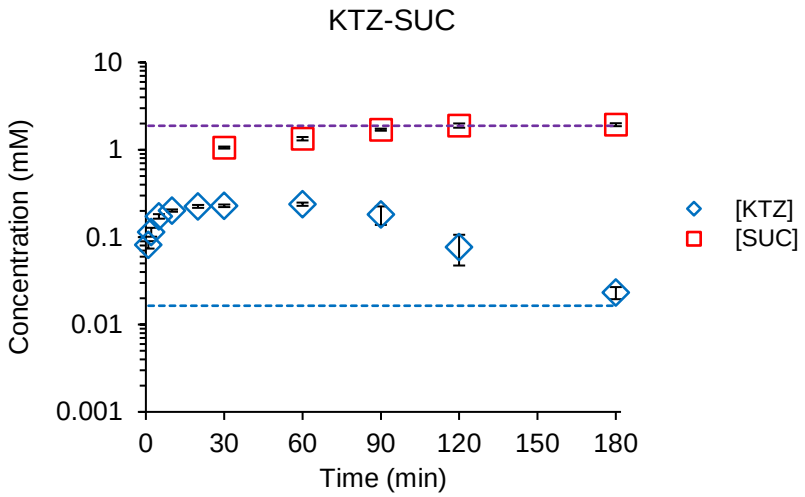

(c)

Figure 2C.1. KTZ cocrystal component concentrations during dissolution in pH 6.5 media. Purple dashed line indicates the concentration at which the cocrystal is fully dissolved. Blue dashed line indicates KTZ drug solubility. Error bars on the symbols indicate standard errors.

As cocrystal dissolved, both coformer and drug were released into the solution. The coformer concentration plateaued between 60 and 90 min, and the concentration at plateau indicated that the cocrystal added to solution was fully dissolved. KTZ concentration initially increased to reach C_{max}, then decreased as the rate of drug precipitation overtook the rate of cocrystal dissolution. The highly soluble coformers remained dissolved in solution, since the concentration used was below their solubility. The coformer concentration can be used to assess the extent of cocrystal dissolution. The poorly water soluble drug, however, was precipitating out of the solution as the cocrystals were dissolved.

Cocrystals have a larger impact on the bulk pH of the solution than the drug (figure 2C.2). KTZ drug has no or very little effect on pH, while the cocrystals decreased media pH (initial pH 6.50) by about 0.2 to 0.3 pH units during dissolution.

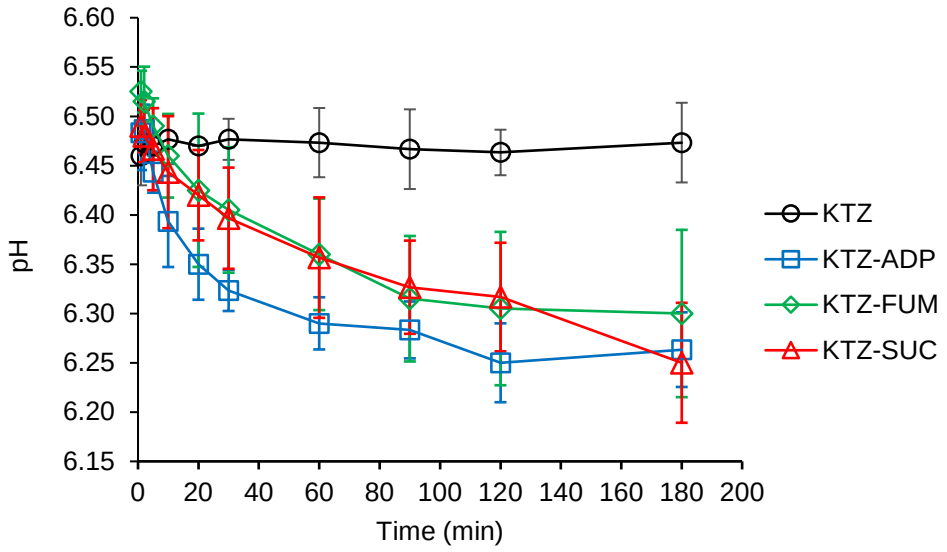

Figure 2C.2. Bulk pH as a function of time during KTZ drug and cocrystal dissolution in pH 6.5 media.

Cocrystal Dissolution in pH 5.0 Media

In pH 5.0 media (acetate buffer), the buffer species interfered with the UV absorbance of coformer SUC and ADP, and therefore their solution concentrations during dissolution were not able to be determined (figure 2C.3). However, the amount of solid used was below cocrystal solubility at the dissolution media pH, therefore the cocrystals were able to fully dissolve. KTZ-FUM was the only cocrystal in this media which coformer concentration could be measured, and FUM concentrations in figure 2C.3(b) indicate that the cocrystal was fully dissolved by 60 min. Drug precipitation also appeared slower in pH 5 media, allowing the solution to generate and maintain supersaturation with respect to KTZ solubility during dissolution.

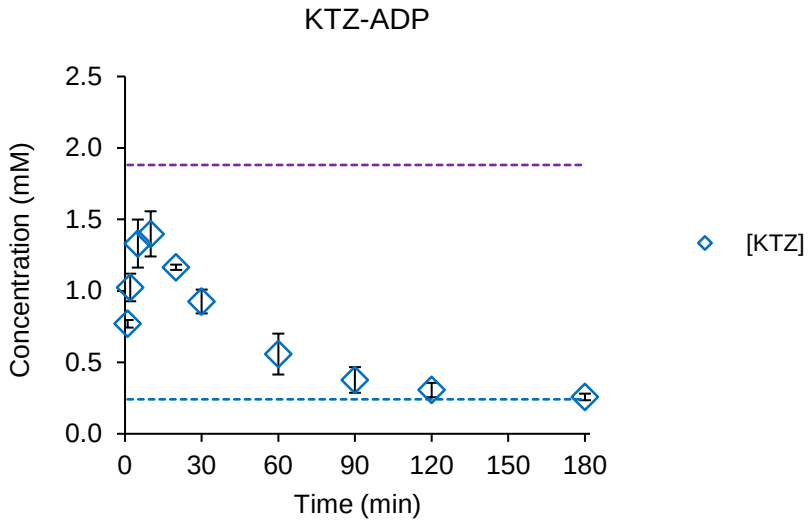
KTZ-ADP
Concentration (mM)
2.5
2.0
1.5
1.0
0.5
0.0
0
30
60
90
120
150
180
Time (min)
[KTZ]

(a)

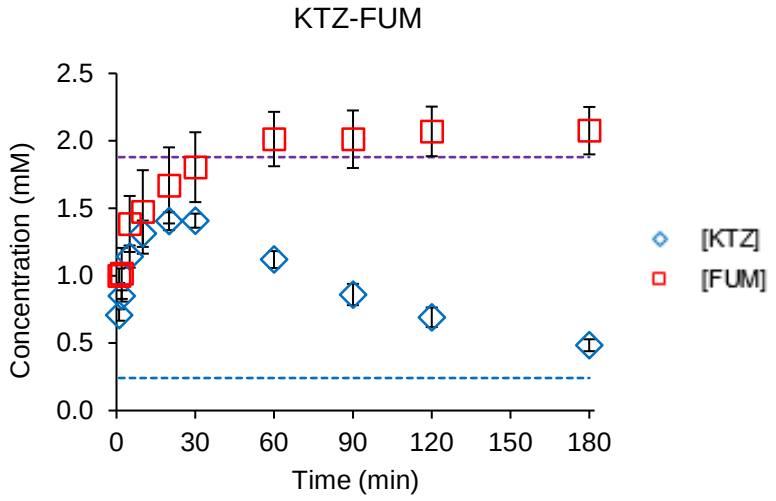
KTZ-FUM
Concentration (mM)
2.5
2.0
1.5
1.0
0.5
0.0
0
30
60
90
120
150
180
Time (min)
[KTZ]
[FUM]

(b)

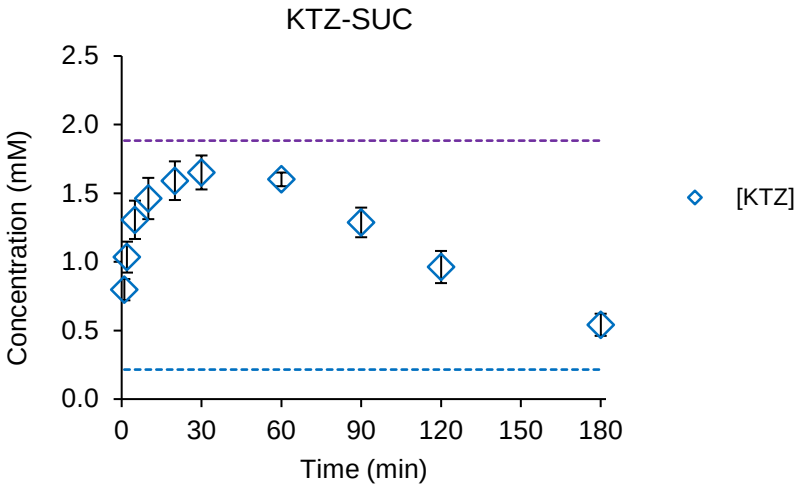

(c)

Figure 2C.3. KTZ cocrystal component concentrations during dissolution in pH 5.0 media. Purple dashed line indicates the concentration at which the cocrystal is fully dissolved. Blue dashed line indicates KTZ drug solubility. Error bars on the symbols indicate standard errors.

Figure 2C.4 shows that cocrystals and drug have very little impact on the bulk pH (< 0.1 unit change) during dissolution in pH 5 media.

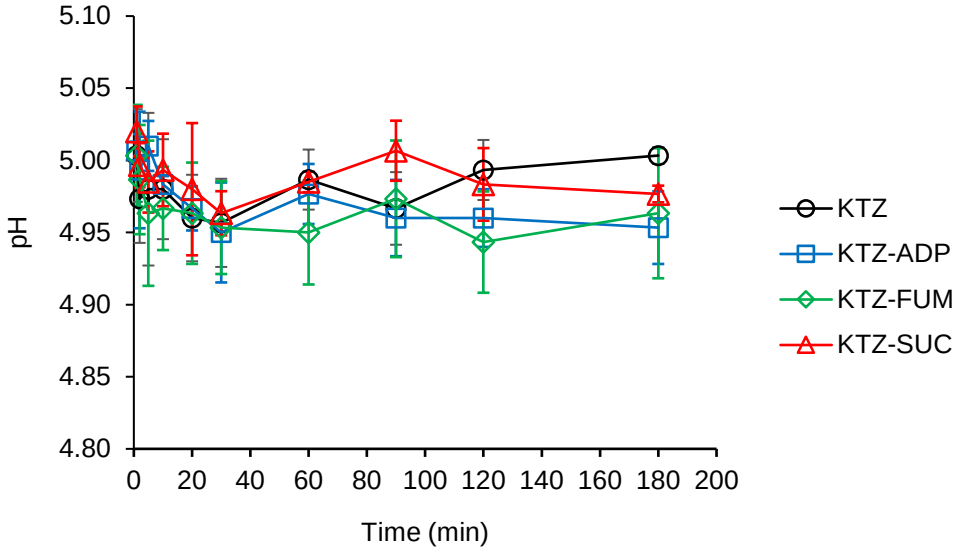

Figure 2C.4. Bulk pH as a function of time during KTZ drug and cocrystal dissolution in pH 5 media.

CHAPTER 3

EFFECT OF PHYSIOLOGICALLY RELEVANT SURFACTANTS ON COCRYSTAL SOLUBILITY AND DISSOLUTION

Introduction

Cocrystallization can enhance aqueous solubility of a poorly water soluble drug, which can lead to improvements in dissolution and bioavailability.[1-8] With a wide range of coformers to choose from, cocrystals of the same drug constituent can exhibit solution behavior as diverse as the coformer physicochemical properties.[2-3, 7, 9-11] Cocrystal solubility can be orders of magnitude above that of the parent drug. However, this huge solubility advantage can also lead to undesirable effects such as solution-mediated transformation of the cocrystal back to less soluble drug forms, which can prevent sustained supersaturation and lead to no observed dissolution advantage over the drug. Endogenous and synthetic solubilizing agents can reduce, and sometimes even eliminate, the solubility advantage (SA) of the cocrystal depending on the strength and concentration of the solubilizing agent. Reduction in cocrystal SA, also known as the supersaturation index, can help stabilize cocrystals in solution and achieve higher drug concentrations.

The mechanism by which drug solubilizing agents reduces the potential for cocrystal conversion in solution is through preferential solubilization of drug over coformer.[11-14] Most pharmaceutical cocrystals are composed of hydrophobic drugs and hydrophilic coformers, and the drug component is expected to be solubilized to a higher extent than the coformer when in

the presence of solubilizing agents such as surfactants and lipids.[12, 14-16] Rodriguez and coworkers have found that when only drug, but not coformer, is solubilized by a solubilizing agent, cocrystal (1:1 molar ratio) solubility exhibits a square-root dependence on solubilizing agent concentration, while the parent drug solubility has a linear dependence.[11-14, 16-18] This means that cocrystal solubility has a weaker dependence on solubilizing agent concentration compared to drug, which translates to reduced SA as solubilizing agent concentration increases.

Drug solubilizing agents can exist in many different forms including pharmaceutical additives, lipids from food, and bile salts present in the gastrointestinal (GI) tract. A drug or a cocrystal may encounter some, if not all, of these types of solubilizing agents during pharmaceutical development and oral dosing. FeSSIF (fed-state simulated intestinal fluid) and FaSSIF (fasted-state simulated intestinal fluid) media are frequently used in *in vitro* solubility and dissolution studies to evaluate solution properties of drugs, cocrystals, and various other solid forms.[19-24] FeSSIF and FaSSIF contain sodium taurocholate and lecithin, which can form mixed micelles in aqueous solutions and can solubilize cocrystal components based on their lipophilic properties.[19-20, 25] Proper understanding of solution phase interactions of cocrystal components is essential for accurate prediction and interpretation of cocrystal solution behavior under various *in vitro* and *in vivo* conditions. The purpose of the work presented here is to evaluate the effect of drug solubilizing agents on cocrystal solubility, supersaturation index (SA), and dissolution behavior.

The cocrystals studied in this chapter are 1:1 cocrystals of ketoconazole-adipic acid (KTZ-ADP), ketoconazole-fumaric acid (KTZ-FUM), and ketoconazole-succinic acid (KTZ-SUC). KTZ is a weakly basic compound with pK_a values of 3.17 and 6.63 (pK_a values determined with 0.15 M KCl background electrolyte at 25.0 ± 0.1°C and a blanket of heavy inert

gas of argon or nitrogen).[26] The coformers are all diprotic carboxylic acids, ADP pK_a values are 4.44 and 5.44, SUC pK_a values are 4.00 and 5.24, and FUM pK_a values are 2.85 and 4.10 at 25°C with 0.1 M ionic strength.[27-28] KTZ drug is also much more lipophilic ($logD_{7.4}$ = 3.83, determined with water saturated *n*-octanol and 50 mM phosphate buffer of pH 7.4) [26, 29] than the coformers (logP range between -0.59 and 0.46),[30] and KTZ has been shown to be solubilized by the surfactants present in FeSSIF and FaSSIF.[19, 31-33] In Chapter 2, we presented the effect of pH on the solubility and dissolution behavior of KTZ drug and cocrystals. Here we consider not only the effect of pH, but also the solubilization by physiologically relevant surfactant micelles. Equations have been derived in the past to predict cocrystal solubility behavior in the presence of solubilizing agents by Rodriguez and coworkers,[12-16] but no solubility equation of such has been derived for cocrystals of dibasic drug and diprotic acid coformers until now. It is expected that a cocrystal composed of hydrophobic drug and hydrophilic coformer will exhibit preferential solubilization of drug by these micellar systems. This can lead to lower SA, slower cocrystal to drug conversion, and sustained supersaturation of drug component during dissolution.

Theoretical

Drug Solubilization by Surfactant Micelles

The solubility of 1:1 cocrystals of KTZ, assuming solution complexation of cocrystal components is negligible, can be described by cocrystal dissociation, component ionization, and micellar solubilization of all solution species (ionized + non-ionized cocrystal components). Cocrystal dissolves in aqueous solutions and dissociates into its components according to K_{sp},

$$B-H_2A_{cocrystal} \overset{K_{sp}}{\rightleftharpoons} B_{aq} + H_2A_{aq} \tag{3.1}$$

where B is the basic drug KTZ, and H_2A is the diprotic acid coformer CF. Both are in their non-ionized forms. Subscript "aq" represents the drug and coformer species dissolved in the aqueous phase. Cocrystal K_{sp} is defined as the solubility product of non-ionized concentrations of drug and coformer

$$K_{sp} = [B]_{aq}[H_2A]_{aq} = [KTZ][CF] \tag{3.2}$$

where, KTZ and CF are the non-ionized species of the drug and coformer in solution, and they are equal to $[B]_{aq}$ and $[H_2A]_{aq}$, respectively.

Under stochiometric conditions, cocrystal solubility can be represented as

$$S_{cc,T} = [KTZ]_T = [CF]_T \tag{3.3}$$

where $S_{cc,T}$ is the cocrystal solubility, and subscript "T" denotes total solution concentration (ionized + non-ionized species in both aqueous and micellar pseudophases) of each cocrystal component.

Total KTZ in solution, $[KTZ]_T$, is the sum of its non-ionized (B) and ionized species (BH^+ and BH_2^{2+}) in both aqueous (aq) and micellar (m) pseudophases.

$$[KTZ]_T = [B]_T = [B]_{aq} + [BH^+]_{aq} + [BH_2^{2+}]_{aq} + [B]_m + [BH^+]_m + [BH_2^{2+}]_m \tag{3.4}$$

Ionization of the drug can be described by the following equilibria and associated ionization constants:

$$BH_{2,aq}^{2+} \overset{K_{a1,KTZ}}{\rightleftharpoons} H_{aq}^+ + BH_{aq}^+ \tag{3.5}$$

$$K_{a1,KTZ} = \frac{[H^+]_{aq}[BH^+]_{aq}}{[BH_2^{2+}]_{aq}} \tag{3.6}$$

$$BH_{aq}^+ \overset{K_{a2,KTZ}}{\rightleftharpoons} H_{aq}^+ + B_{aq} \tag{3.7}$$

$$K_{a2,KTZ} = \frac{[H^+]_{aq}[B]_{aq}}{[BH^+]_{aq}} \tag{3.8}$$

where $K_{a,KTZ}$ represents the ionization constant for the conjugate acid forms of KTZ. Micellar solubilization of the non-ionized and ionized drug species in solution is as follows:

$$B_{aq} + M \overset{K_S^B}{\rightleftharpoons} B_m \tag{3.9}$$

$$K_s^B = \frac{[B]_m}{[B]_{aq}[M]} \tag{3.10}$$

$$BH^+_{aq} + M \overset{K_S^{BH^+}}{\rightleftharpoons} BH^+_m \tag{3.11}$$

$$K_s^{BH^+} = \frac{[BH^+]_m}{[BH^+]_{aq}[M]} \tag{3.12}$$

$$BH^{2+}_{2,aq} + M \overset{K_S^{BH_2^{2+}}}{\rightleftharpoons} BH^{2+}_{2,m} \tag{3.13}$$

$$K_s^{BH_2^{2+}} = \frac{[BH_2^{2+}]_m}{[BH_2^{2+}]_{aq}[M]} \tag{3.14}$$

where M is the surfactant micelle and K_s is the solubilization constant. By substituting the appropriate equilibrium constants into equation 3.4, the drug solubility ($S_{drug,T}$) as a function of $[H^+]$ and micellar concentration can be expressed with the following equation

$$\begin{aligned} S_{drug,T} &= [KTZ]_T \\ &= [B]_{aq}\left(1 + [M]\left(K_s^B + \frac{K_s^{BH^+}[H^+]_{aq}}{K_{a2,KTZ}} + \frac{K_s^{BH_2^{2+}}[H^+]_{aq}^2}{K_{a1,KTZ}K_{a2,KTZ}}\right) + \frac{[H^+]_{aq}}{K_{a2,KTZ}} + \frac{[H^+]_{aq}^2}{K_{a1,KTZ}K_{a2,KTZ}}\right) \end{aligned} \tag{3.15}$$

Coformer Solubilization by Surfactant Micelles

The total coformer concentration ($[CF]_T$) in solution is the sum of the non-ionized (H_2A) and ionized (HA^- and A^{2-}) coformer species in the aqueous and micellar pseudophases.

$$[CF]_T = [A]_T = [H_2A]_{aq} + [HA^-]_{aq} + [A^{2-}]_{aq} + [H_2A]_m + [HA^-]_m + [A^{2-}]_m \quad (3.16)$$

The ionization and micellar solubilization of the diprotic acid coformer can be described by the following equilibria and corresponding ionization and solubilization constants:

$$H_2A_{aq} \overset{K_{a1,CF}}{\rightleftharpoons} H^+_{aq} + HA^-_{aq} \quad (3.17)$$

$$K_{a1,CF} = \frac{[H^+]_{aq}[HA^-]_{aq}}{[H_2A]_{aq}} \quad (3.18)$$

$$HA^-_{aq} \overset{K_{a2,CF}}{\rightleftharpoons} H^+_{aq} + A^{2-}_{aq} \quad (3.19)$$

$$K_{a2,CF} = \frac{[H^+]_{aq}[A^{2-}]_{aq}}{[HA^-]_{aq}} \quad (3.20)$$

$$H_2A_{aq} + M \overset{K_S^{H_2A}}{\rightleftharpoons} H_2A_m \quad (3.21)$$

$$K_S^{H_2A} = \frac{[H_2A]_m}{[H_2A]_{aq}[M]} \quad (3.22)$$

$$HA^-_{aq} + M \overset{K_S^{HA^-}}{\rightleftharpoons} HA^-_m \quad (3.23)$$

$$K_S^{HA^-} = \frac{[HA^-]_m}{[HA^-]_{aq}[M]} \quad (3.24)$$

$$A^{2-}_{aq} + M \overset{K_S^{A^{2-}}}{\rightleftharpoons} A^{2-}_m \quad (3.25)$$

$$K_s^{A^{2-}} = \frac{[A^{2-}]_m}{[A^{2-}]_{aq}[M]} \quad (3.26)$$

By substituting the appropriate equilibrium constants into equation 3.16, the total coformer concentration can be expressed as

$$[CF]_T = [H_2A]_{aq}\left(1+[M]\left(K_s^{H_2A}+\frac{K_S^{HA^-}K_{a1,CF}}{[H^+]_{aq}}+\frac{K_s^{A^{2-}}K_{a1,CF}K_{a2,CF}}{[H^+]_{aq}^2}\right)+\frac{K_{a1,CF}}{[H^+]_{aq}}+\frac{K_{a1,CF}K_{a2,CF}}{[H^+]_{aq}^2}\right) \quad (3.27)$$

where $[H_2A]_{aq}$ is the non-ionized coformer concentration in the aqueous pseudophase.

KTZ Cocrystal Solubility in Surfactant Media

In order to simplify equations 3.15 and 3.27, the total micellar solubilization constants for drug and coformer can be expressed as the following equations for KTZ drug,

$$K_{s,T}^{KTZ} = K_s^B + \frac{K_s^{BH^+}[H^+]_{aq}}{K_{a2,KTZ}} + \frac{K_s^{BH_2^{2+}}[H^+]_{aq}^2}{K_{a1,KTZ}K_{a2,KTZ}} \quad (3.28)$$

and for coformer,

$$K_{s,T}^{CF} = K_s^{H_2A} + \frac{K_s^{HA^-}K_{a1,CF}}{[H^+]_{aq}} + \frac{K_s^{A^{2-}}K_{a1,CF}K_{a2,CF}}{[H^+]_{aq}^2} \quad (3.29)$$

where $K_{s,T}$ is the total micellar solubilization constant incorporating all the non-ionized and ionized species of drug or coformer in solution. The value of $K_{s,T}$ is dependent on the type of solubilizing agent and solution condition such as pH.

Substituting equations 3.2, 3.15, 3.27, 3.28, and 3.29 into equation 3.3 and rearranging leads to the following expression for cocrystal solubility.

$$S_{cc,T} = \sqrt{\frac{K_{sp}\left(1+K_{s,T}^{KTZ}[M]+\frac{[H^+]_{aq}}{K_{a2,KTZ}}+\frac{[H^+]_{aq}^2}{K_{a1,KTZ}K_{a2,KTZ}}\right)}{\left(1+K_{s,T}^{CF}[M]+\frac{K_{a1,CF}}{[H^+]_{aq}}+\frac{K_{a1,CF}K_{a2,CF}}{[H^+]_{aq}^2}\right)}} \quad (3.30)$$

Equation 3.30 can be rewritten in terms of pK_a and pH:

$$S_{cc,T} = \sqrt{\frac{K_{sp}(1+K_{s,T}^{KTZ}[M]+10^{pK_{a2,KTZ}-pH}+10^{pK_{a1,KTZ}+pK_{a2,KTZ}-2pH})}{(1+K_{s,T}^{CF}[M]+10^{pH-pK_{a1,CF}}+10^{2pH-pK_{a1,CF}-pK_{a2,CF}})}} \quad (3.31)$$

Using equation 3.31, cocrystal solubility in the presence of surfactant micelles or other solubilizing agents can be quantitatively predicted with the knowledge of cocrystal K_{sp}, component pK_a, solution pH, micellar/solubilizing agent concentration, and component $K_{s,T}$ values at the corresponding pH.

Materials and Methods

Materials

Ketoconazole (lot # BS1203355108, 98% purity) was purchased from Bosche Scientific (New Brunswick, NJ) and used as received. Adipic acid (lot # 06807BE, 99% purity), succinic acid (lot # 037K0021, 99% purity), fumaric acid (lot # 09426EE, 99+% purity), acetic acid (lot # 074K3658, 99%), sodium acetate anhydrous (lot # 100K0272), dipotassium hydrogen phosphate (lot # 103H0287, ACS reagent), and sodium chloride (NaCl) (lot # 094K0183, ACS reagent) were purchased from Sigma-Aldrich (St. Louis, MO) and used as received. FaSSIF/FeSSIF/FaSSGF instant powder (lot# 01-1504-03NP) was purchased from Biorelevant.com (London, United Kingdom) and used as received.

HPLC grade methanol, HPLC grade 2-propanol, sodium phosphate monobasic ($NaH_2PO_4 \bullet H_2O$) (lot # 017316), and hydrochloric acid (lot # 2AJK15038, ACS grade) were purchased from Fisher Scientific (Fair Lawn, NJ). Acetone (ACS reagent 99.5%) and phosphoric acid (lot # B0506524, 85+%) were purchased from Acros Organics (NJ) and used as received. Trifluoroacetic acid (spectrophometric grade, 99%) was purchased from Aldrich Company (Milwaukee, WI). Sodium hydroxide pellets (NaOH) was purchased from J.T. Baker (Philipsburg, NJ). Water used in this study was filtered through a double deionized (DI) purification system (Milli Q Plus Water System) from Millipore Co. (Bedford, MA).

Cocrystal Synthesis

KTZ cocrystals (1:1 stoichiometric ratio) were prepared by reaction crystallization method at room temperature.[34-35] KTZ-FUM and KTZ-SUC cocrystals were synthesized in acetone. KTZ-ADP cocrystal was synthesized in 2-propanol. Full conversions to cocrystals were observed between 24 to 48 hours. The solid phases were characterized by X-ray powder diffraction (XRPD) and differential scanning calorimetry (DSC), and the stoichiometries were verified by HPLC.

Media Preparation

FaSSIF and FeSSIF media were prepared according to the method and composition described by Galia et al (table 3.1).[19]

Table 3.1. FaSSIF, FeSSIF, and blank media composition and pH.[19, 21]

	Blank FaSSIF	FaSSIF	Blank FeSSIF	FeSSIF
Sodium taurocholate	--	3 mM	--	15 mM
Lecithin	--	0.75 mM	--	3.75 mM
NaOH	8.7 mM	8.7 mM	101 mM	101 mM
$NaH_2PO_4 \bullet H_2O$	29 mM	29 mM	--	--
CH_3CO_2H	--	--	144 mM	144 mM
NaCl	106 mM	106 mM	203 mM	203 mM
pH	6.5	6.5	5.0	5.0

Blank FaSSIF (pH 6.50 phosphate buffer) was prepared at room temperature by dissolving 0.683 g of NaOH (pellets), 7.902 g of $NaH_2PO_4 \bullet H_2O$, and 12.372 g NaCl in 2 L of purified DI water. The pH was adjusted to 6.50 (± 0.04) with 1 M NaOH and 1 M HCl solutions. Blank FeSSIF (pH 5.00 acetate buffer) was prepared at room temperature by dissolving 8.089 g NaOH (pellets), 16.4 mL acetic acid, and 23.748g NaCl in 2 L of purified DI water. The pH was adjusted to 5.00 (± 0.03) with 1 M NaOH and 1 M HCl solutions. FaSSIF and FeSSIF media

were prepared by dissolving appropriate amount of FaSSIF/FeSSIF/FaSSGF powder in the blank media, then stored at room temperature and were used within 48 hours.

FeSSIF and FaSSIF media used here have the same surfactant compositions (sodium taurocholate + lecithin, 4:1 molar ratio).[20] FeSSIF media has 5 times higher surfactant concentration than FaSSIF and possesses a lower pH (pH 5 vs. pH 6.5, respectively).[20] The micellar concentration ([M]) is equal to the total surfactant concentration minus the critical micellar concentration (CMC). The CMC value for sodium taurocholate in the presence of lecithin in a 4:1 ratio, 0.1 M NaCl, at 25°C is reported to be 0.25 mM.[36-37] The micellar concentrations of FaSSIF and FeSSIF under the same solution conditions are 3.0 mM and 15 m M, respectively.[36-37]

Solubility Measurements

Cocrystal component solubility was measured by adding excess solid to 3 mL of solution media. The solutions were magnetically stirred and were kept in water bath at 25 ± 0.4°C for up to 96 hours. 0.5 mL aliquots of the suspension were sampled every 24 hours. Collected samples were filtered via centrifuge through a 0.45 μm pore cellulose acetate membrane, and the pH values of the solutions were measured. The concentrations of drug or coformer in the solutions were analyzed by HPLC.

The equilibrium solubility of each cocrystal was determined at the eutectic point, where the drug and cocrystal solid phases are in equilibrium with the solution.[3, 38] The eutectic points were approached by cocrystal dissolution, where 150 – 200 mg of cocrystal and 50 – 80 mg of KTZ were suspended in 3 mL of solution. The solutions were kept in water bath at 25 ± 0.1°C and magnetically stirred for up to 96 hours. Solution samples (0.5 mL) were collected every 24 hours and filtered via centrifuge through a 0.45 μm pore cellulose acetate membrane, and the pH

values were measured. The solid phases were analyzed by XRPD and DSC to confirm both drug and cocrystal solid phases were present, indicating that the solutions were at the eutectic point. The filtered solutions were then analyzed by HPLC after proper dilutions with the mobile phase.

Cocrystal and Drug Powder Dissolution

Powder dissolution studies of drug and cocrystals were conducted using an overhead stirrer with a glass propeller at 150 rpm over 3 hours. 30 mL of dissolution media was used to dissolve 30 mg of KTZ drug and 30 mg drug-equivalent mass of each cocrystal were used for each dissolution experiment. Both drug and cocrystal powders were sieved through mesh screens and the particle size between 106 and 125 μm was used. The dissolution media were kept in water bath with temperature of 24.5 (± 0.5) °C throughout the dissolution process. Solution pH was measured before and after the dissolution of KTZ and its cocrystals. Solution samples of 0.5 mL were taken at time points of 1, 2, 5, 10, 20, 30, 60, 90, 120, and 180 minutes (min) with a syringe. The solution samples were filtered using PVDF membrane syringe filters with pore size of 0.45 μm. The solution concentrations of drug and coformers were analyzed by HPLC after proper dilution with mobile phase.

X-Ray Powder Diffraction (XRPD)

A Rigaku Miniflex X-ray diffractometer (Danverse, MA0) using Cu-Kα radiation, a tube voltage of 30 kV, and a tube current of 15 mA was utilized for analysis and characterization of solid phases. Measurements were taken from 5° to 40° at a continuous scan rate of 2.5°/min.

Thermal Analysis

TA instrument differential scanning calorimetry (DSC) (Newark, DE) was used to analyze the collected solid phases from the solubility studies after they were dried at room

temperature. The heating rate of the experiments was 10°C/min under dry nitrogen atmosphere. Standard aluminum sample pans and lids were used for these measurements.

High Performance Liquid Chromatography (HPLC)

Solution concentrations of the drug and coformer were analyzed by a Waters HPLC equipped with a UV spectrometer detector. A Waters Atlantis C18 column with the dimension of 250 x 4.6 mm and 5 µm particle size was used for separation at ambient temperature. The flow rate was set at 1mL/min and the injection volume was 20 µL. For KTZ-ADP and KTZ-FUM cocrystals, the mobile phase used was composed of 60% methanol and 40% water with 0.1% trifluoroacetic acid (TFA). For KTZ-SUC cocrystal, different methods were used to analyze each component due to poor separation of SUC peak from the solvent peak. The KTZ component of KTZ-SUC cocrystal was analyzed using mobile phase composed of 60% methanol and 40% water with 0.1% TFA. The SUC component was analyzed using a gradient method with flow rate of 1mL/min starting with mobile phase composed of 25% methanol and 75% water with 0.1% TFA. The composition changed to 80% methanol and 20% water with 0.1% TFA after 2.5 min, then reverted back to 25% methanol and 75% water with 0.1% TFA after 6 min. The wavelengths used for the analytes were as follows: 230 nm for KTZ, 220 nm for FUM, and 210 nm for SUC and ADP.

Results and Discussion

Cocrystal Experimental Solubility

KTZ drug and cocrystal solubilities were measured in FaSSIF, FeSSIF, blank FaSSIF, and blank FeSSIF media, and all three cocrystals were found to be more soluble than the drug. This means that the cocrystals have the potential to generate supersaturation in solution with

respect to drug solubility and can undergo solution-mediated conversion. Therefore, cocrystal solubility was evaluated at the cocrystal and drug eutectic point, where both solid phases coexist in equilibrium with solution saturated with drug and cocrystal. KTZ and CF total (ionized + non-ionized) concentrations at eutectic are listed in table 3.2, and cocrystal stochiometric solubility values ($S_{cc,T}$) were determined with equation,

$$S_{cc,T} = \sqrt{[KTZ]_{eu,T}[CF]_{eu,T}} \tag{3.32}$$

where the subscript “eu” indicates eutectic point.

Table 3.2. Cocrystal stoichiometric solubility determined from KTZ and CF concentrations at the cocrystal and drug eutectic point. Error values are standard errors.

Cocrystal	Media[a]	pH_{eq} [b]	$[KTZ]_{eu,T}$ (mM)	$[CF]_{eu,T}$ (mM)	$S_{cc,T}$[c] (mM)
KTZ-ADP	blank FaSSIF	4.43 ± 0.02	0.71 ± 0.03	11.6 ± 0.9	2.87 ± 0.05
	FaSSIF	4.50 ± 0.02	0.93 ± 0.01	19.1 ± 0.1	4.21 ± 0.08
	blank FeSSIF	4.59 ± 0.02	0.50 ± 0.01	13.6 ± 0.7	2.60 ± 0.02
	FeSSIF	4.67 ± 0.03	2.49 ± 0.02	19.7 ± 0.7	7.0 ± 0.2
KTZ-FUM	blank FaSSIF	4.00 ± 0.01	1.99 ± 0.07	10.5 ± 0.4	4.56 ± 0.01
	FaSSIF	4.07 ± 0.02	2.52 ± 0.03	10.3 ± 0.2	5.10 ± 0.09
	blank FeSSIF	4.26 ± 0.07	1.09 ± 0.02	31.1 ± 0.3	5.82 ± 0.05
	FeSSIF	4.37 ± 0.04	1.89 ± 0.09	35 ± 3	8.1 ± 0.3
KTZ-SUC	blank FaSSIF	4.40 ± 0.01	0.75 ± 0.03	16 ± 2	3.4 ± 0.2
	FaSSIF	4.43 ± 0.03	1.01 ± 0.02	13.5 ± 0.1	3.68 ± 0.09
	blank FeSSIF	4.62 ± 0.01	0.48 ± 0.01	8.9 ± 0.4	2.07 ± 0.03
	FeSSIF	4.63 ± 0.01	2.59 ± 0.05	8.3 ± 0.7	4.6 ± 0.2

a. FaSSIF and blank FaSSIF initial pH = 6.50 ± 0.04. FeSSIF and blank FeSSIF initial pH = 5.00 ± 0.03.
b. pH at equilibrium.
c. Calculated with equation 3.32.

Since drug and cocrystal eutectic point was used for equilibrium solubility measurement, KTZ eutectic concentration is also the drug solubility at the corresponding pH and solution condition. As observed in table 3.2, KTZ eutectic concentrations/solubility values increased in surfactant containing media (FeSSIF and FaSSIF) from the corresponding blank media (≤ 440% increase). This indicates that KTZ is solubilized by sodium taurocholate and lecithin present in the biorelevant media. The effect of surfactants on coformer eutectic concentrations are less compared to that of the drug (≤ 65% increase).

Cocrystal stoichiometric solubility values were determined with KTZ and CF eutectic concentrations, and cocrystal solubility is higher than that of the drug for all three cocrystals under all media conditions used. In general, the enhancement of cocrystal solubility by surfactant containing media is less than that of the drug. This is because of the preferential solubilization of drug over coformer leading to non-linear increase in cocrystal solubility with surfactant concentration.[12-15] In most cases, for both drug and cocrystals, solubility increase was more pronounced from blank FeSSIF to FeSSIF compared to from blank FaSSIF to FaSSIF. FeSSIF contains more surfactants than FaSSIF, and this can contribute to larger solubility enhancements from blank FeSSIF to FeSSIF.

It is important to note that during the cocrystal solubility studies, acidic coformers caused the solution pH to decrease as equilibrium was reached. The pH alterations were very large in FaSSIF and blank FaSSIF media, with final pH decreased 2 - 2.5 pH units from the initial pH 6.5. KTZ-FUM cocrystal exhibited the lowest final pH of the three cocrystals, likely due to fumaric acid being the most acidic coformer (lowest pK_a values) and having the highest cocrystal solubility under the media conditions. In FeSSIF and blank FeSSIF, the changes in pH from

initial pH conditions (pH 5) were less pronounced, with < 0.8 pH unit decrease from initial pH for all cocrystal studies.

pH has a huge impact on cocrystal solubility, as was discussed in detail in Chapter 2. Equilibrium pH values in FaSSIF and blank FaSSIF (pH_{eq} range 4.00 – 4.50) for these cocrystals were slightly lower than their equilibrium pH values in FeSSIF and blank FeSSIF (pH_{eq} range 4.26 – 4.67). This resulted in more similar cocrystal solubility values than would be expected had the pH remained unchanged from the initial pH values of the media. On the other hand, solution pH changed very little during single component KTZ drug solubility studies (non-eutectic studies) as equilibrium was reached. Drug and cocrystal solubility and corresponding pH_{eq} values are shown in figure 3.1a.

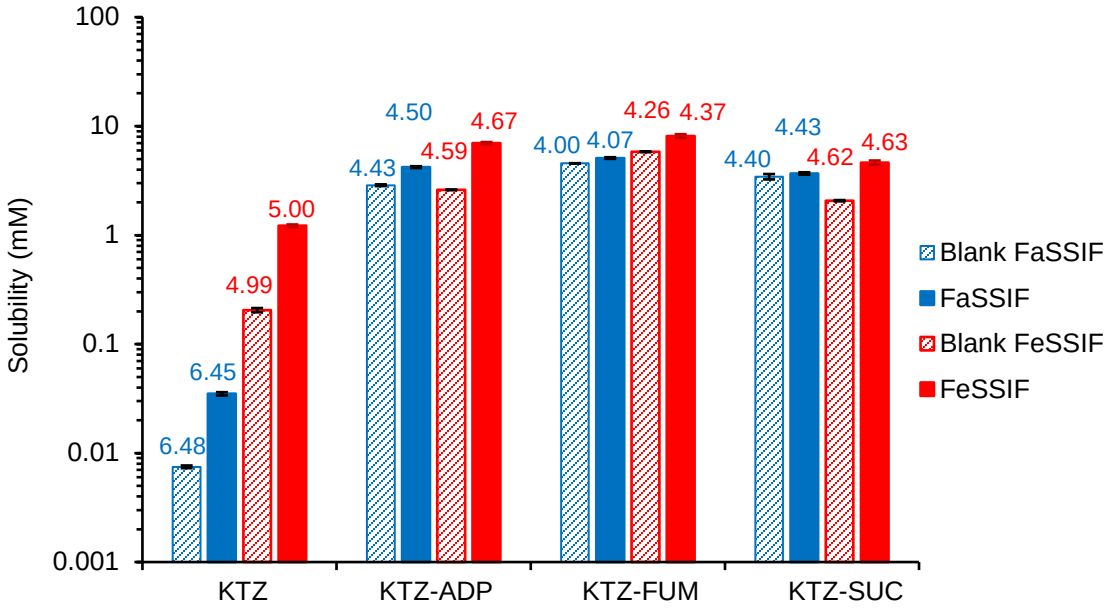

(a)

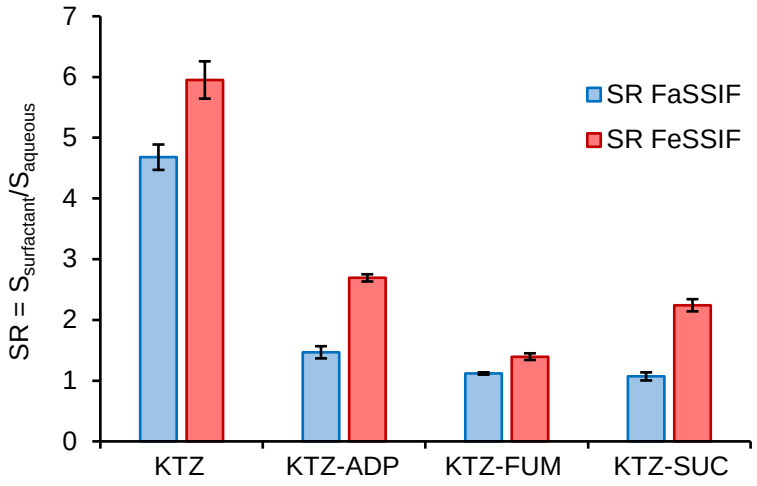

(b)

Figure 3.1. (a) KTZ cocrystals and drug experimental solubility in FaSSIF, FeSSIF, blank FaSSIF, and blank FeSSIF media. Numbers above the columns indicate equilibrium pH. (b) Solubilization ratio (SR) of KTZ drug and cocrystals in surfactant vs aqueous media. SR is calculated according to equations: $SR_{FaSSIF} = \frac{S_{FaSSIF}}{S_{BlankFaSSIF}}$ and $SR_{FeSSIF} = \frac{S_{FeSSIF}}{S_{BlankFeSSIF}}$. Cocrystals demonstrated higher solubility values and smaller SR compared to the drug in different media. This indicates that the cocrystals are less sensitive to pH and surfactants than the drug. Error bars indicate standard errors.

Solubilization ratio (SR) is defined here as the ratio of the solubility of drug or cocrystal in surfactant media and their solubility in the corresponding blank aqueous buffer ($SR = S_{surf}/S_{aq}$). Both drug and cocrystal solubility values were observed to increase in surfactant containing media from the corresponding blank media. KTZ drug SR_{FaSSIF} (solubility ratio of FaSSIF vs blank FaSSIF) was 4.7 and SR_{FeSSIF} was 6 (figure 3.1b). Cocrystal SR_{FaSSIF} values are between 1.1 and 1.4 and SR_{FeSSIF} values are between 1.4 and 2.7.

In previous publications from Rodriguez lab, we have established a simple relationship between cocrystal and drug solubilization ratios, where a 1:1 cocrystal solubilization ratio will equal the square root of the drug solubilization ratio.[14, 16] This relationship applies to cases where coformer is not solubilized by solubilizing agents. Based on the experimental drug solubility and solubilization ratio (SR_{drug}) values in figure 3.1, one would expect that the

cocrystal solubilization ratio (SR_{cc}) to be about 2.2 for FaSSIF and 2.4 for FeSSIF. However, the experimental cocrystal SR ratios were different from the expected values due to (equilibrium) pH differences during cocrystal and drug solubility measurements. Table 3.3 compares the predicted vs. experimental SR_{cc} values under the same pH conditions.

Table 3.3. KTZ cocrystal and drug predicted vs. experimental solubilization ratio (SR).

Cocrystal	Media	pH_{eq}	SR_{drug} [a]	SR_{cc} pred[b]	SR_{cc} exp[c]
KTZ-ADP	Blank FaSSIF	4.43 ± 0.02	1.31	1.14	1.47
	FaSSIF	4.50 ± 0.02			
	Blank FeSSIF	4.59 ± 0.02	4.98	2.23	2.69
	FeSSIF	4.67 ± 0.03			
KTZ-FUM	Blank FaSSIF	4.00 ± 0.01	1.27	1.13	1.11
	FaSSIF	4.07 ± 0.02			
	Blank FeSSIF	4.26 ± 0.07	1.73	1.32	1.40
	FeSSIF	4.37 ± 0.04			
KTZ-SUC	Blank FaSSIF	4.40 ± 0.01	1.35	1.16	1.07
	FaSSIF	4.43 ± 0.03			
	Blank FeSSIF	4.62 ± 0.01	5.40	2.32	2.24
	FeSSIF	4.63 ± 0.01			

a. SR_{drug} calculated with equation $SR_{drug} = \left(\frac{S_{surf}}{S_{aq}}\right)_{drug}$, using drug eutectic concentration from table 3.2, which is equal to the solubility of drug at that pH and surfactant concentration.
b. SR_{cc} predicted using the relationship: $SR_{cc} = \sqrt{SR_{drug}}$, under the assumption that coformer solubilization is negligible.
c. SR_{cc} determined from experimental solubility values using equation: $SR_{cc} = \left(\frac{S_{surf}}{S_{aq}}\right)_{cc}$.

Decreases of media pH from initial pH values (pH 6.5 and 5) due to coformer ionization have increased drug solubility and made the effect of surfactants on drug and cocrystal solubility

less prominent. The SR_{cc} values predicted from the square root of SR_{drug} are in excellent agreement with the experimentally observed SR_{cc} values under the same pH conditions. This shows that the simple relationship between drug and cocrystal SR holds true for the KTZ cocrystals, and it can be used to quickly assess cocrystal solubility behavior in surfactant containing media based on drug solubility behavior. Smaller SR_{cc} compared to SR_{drug} can lead to reduced food-effects, and can also reduce the risk of cocrystal conversion to drug in solution by decreasing cocrystal solubility advantage.

Predicting Cocrystal Solubility as a Function of pH and Solubilizing Agents

Although the ionization properties of cocrystal components make measuring their solubility under certain conditions (pH > 5) difficult, the equations derived in the theoretical section can be used to predict drug and cocrystal solubility in solutions of different surfactant and pH conditions. Cocrystal K_{sp}, component pK_a, and K_s values are needed for the calculations. K_{sp} values for the three KTZ cocrystals have been determined and reported in Chapter 2. The component pK_a values are readily available in the general literature. The drug and coformer solubilization constants ($K_{s,T}$) are specific to each component, solubilizing agent, and solution conditions (temperature, pH, etc.), and it can be determined experimentally.

Differences in pH will lead to different extents of ionization for the drug and coformer, therefore $K_{s,T}$ value of each cocrystal component determined in the presence of the surfactants is specific for that pH. In order to determine $K_{s,T}$ values for KTZ and coformers, single component solubilities were measured in surfactant and blank media and reported in table 3.4.

Table 3.4. Cocrystal component solubility in different media conditions. Errors are standard errors.

Cocrystal component	Media	Initial pH	pH_{eq}	Solubility (mM)	SR S_{surf}/S_{blank}
KTZ	Blank FaSSIF	6.50 ± 0.04	6.48 ± 0.01	7.5 (± 0.2) $x10^{-3}$	4.7 ± 0.2
	FaSSIF	6.50 ± 0.04	6.45 ± 0.01	3.5 (± 0.1) $x10^{-2}$	
	Blank FeSSIF	5.00 ± 0.03	4.99 ± 0.04	0.205 ± 0.009	6.0 ± 0.3
	FeSSIF	5.00 ± 0.03	5.00 ± 0.01	1.22 ± 0.03	
ADP	Blank FeSSIF	5.00 ± 0.03	3.88 ± 0.01	193 ± 2	0.97 ± 0.05
	FeSSIF	5.00 ± 0.03	3.91 ± 0.06	190 ± 10	
FUM	Blank FeSSIF	5.00 ± 0.03	3.08 ± 0.01	135.7 ± 0.8	1.20 ± 0.03
	FeSSIF	5.00 ± 0.03	3.04 ± 0.02	162 ± 5	
SUC	Blank FeSSIF	5.00 ± 0.03	3.04 ± 0.02	580 ± 10	1.1 ± 0.1
	FeSSIF	5.00 ± 0.03	3.00 ± 0.01	660 ± 10	

One can observe in table 3.4 that the drug solubility was enhanced to a larger extent than the coformers from blank FeSSIF to FeSSIF media. KTZ solubility is 6 times higher in FeSSIF than blank FeSSIF, whereas the coformer solubility values changed by ≤ 1.2 fold. High solubility and ionization of the acidic coformers caused the pH of the solution to drop 1 to 2 pH

units in FeSSIF and blank FeSSIF from the initial pH 5. KTZ solubility values were higher in pH 5 (FeSSIF and blank FeSSIF) than pH 6.5 (FaSSIF and blank FaSSIF), due to increase in drug solubility with decreasing pH. The SR of KTZ was also higher in FeSSIF than FaSSIF, which could be due to higher level of surfactants in FeSSIF.

Equations 3.15 and 3.28 can be combined and rearranged to solve for $K_{s,T}^{KTZ}$

$$K_{s,T}^{KTZ} = \frac{\frac{[KTZ]_T}{[B]_{aq}} - 1 - 10^{pK_{a2,KTZ} - pH} - 10^{pK_{a1,KTZ} + pK_{a2,KTZ} - 2pH}}{[M]} \tag{3.33}$$

where $[KTZ]_T$ is the total (non-ionized and ionized species in both aqueous and micellar pseudophases) KTZ concentration, and $[B]_{aq}$ is the non-ionized drug concentration in solution. Equations 3.27 and 3.29 can be combined and rearranged to solve for $K_{s,T}^{CF}$

$$K_{s,T}^{CF} = \frac{\frac{[CF]_T}{[H_2A]_{aq}} - 1 - 10^{pH - pK_{a1,CF}} - 10^{2pH - pK_{a1,CF} - pK_{a2,CF}}}{[M]} \tag{3.34}$$

where $[CF]_T$ is the total coformer concentration and $[H_2A]_{aq}$ is the non-ionized coformer concentration in solution. $K_{s,T}$ values for KTZ cocrystal components were calculated using equations 3.33 and 3.34, with the pK_a and experimental solubility values of the components at the corresponding pH (table 3.4). $K_{s,T}$ values for drug and coformers are reported in table 3.5.

Table 3.5. KTZ cocrystal component $K_{s,T}$ values.

	pH		$K_{s,T}$ (M^{-1})
	Initial	Final	
KTZ	5.00 ± 0.03	5.00 ± 0.01	14400 ± 400
	6.48 ± 0.02	6.45 ± 0.01	1600 ± 70
ADP	5.00 ± 0.03	3.91 ± 0.06	0
FUM	5.00 ± 0.03	3.04 ± 0.02	29.1 ± 0.2
SUC	5.00 ± 0.03	3.00 ± 0.01	9.5 ± 0.2

$K_{s,T}$ values of KTZ are much larger compared to the coformers, and this supports our expectation that the surfactants will preferentially solubilize the more lipophilic drug over the more hydrophilic coformers. ADP does not appear to be solubilized by the surfactant micelles, resulting in its $K_{s,T}$ being 0. FUM and SUC are both slightly solubilized by the surfactants.

$K_{s,T}$ is calculated at a specific pH. Using $K_{s,T}$ determine at one pH to predict solubility at a different pH can lead to incorrect solubility evaluations. KTZ and CF can each ionize into 3 species, which can be solubilized by surfactants to different extent. The value of $K_{s,T}$ will depend on the distribution and concentration of the ionized species. Figure 3.2 illustrates the fraction distribution of the ionized species of KTZ and CF as a function of pH.

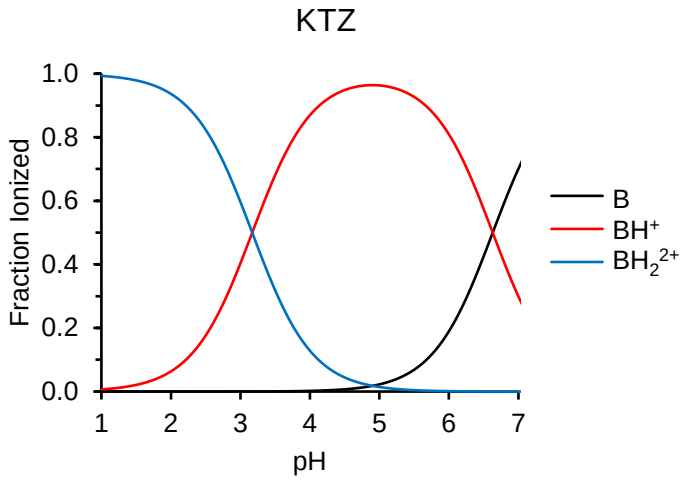

(a)

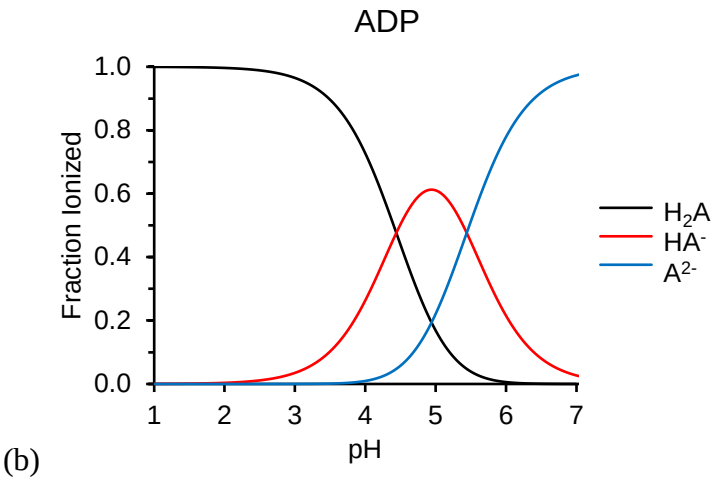

(b)

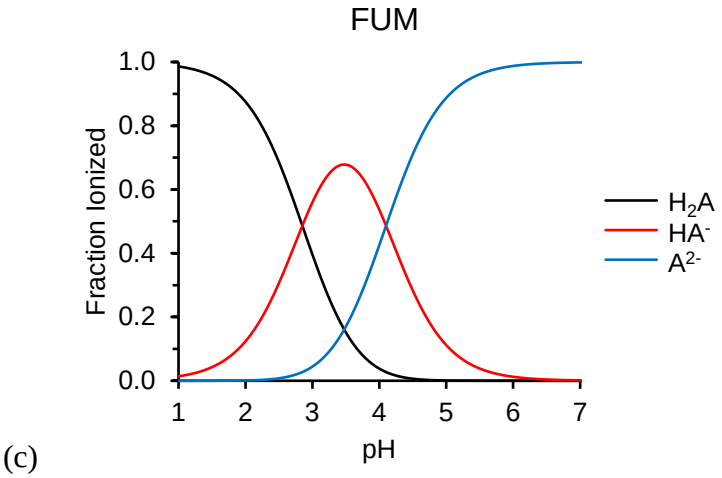

(c)

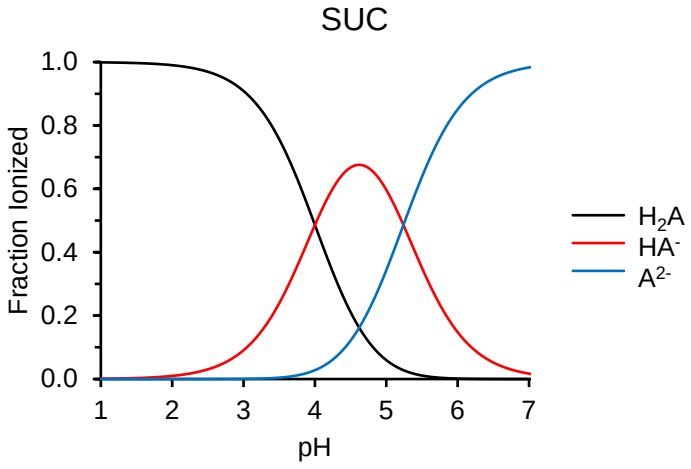

(d)

Figure 3.2. Distribution of different ionization states for drug and coformer as a function of pH.

KTZ goes from being nearly entirely in BH^+ form at pH 5 to about half non-ionized (B) and half BH^+ forms at pH 6.5. Based on the $K_{s,T}$ values of KTZ in table 3.5, it appears that the ionized form of KTZ is solubilized to a higher extent than the non-ionized drug. The reason for this is not clear. One of the possibilities could be the ionic interaction between positively charged drug and taurocholate anions,[39] but further studies are needed to confirm this hypothesis. In this study, however, pH 5 and 6.5 are the most relevant for our purposes. The effect of KTZ ionization states on its $K_{s,T}$ value across different pH ranges is not within the scope of this study and not investigated here.

Figure 3.2 shows that the coformer fraction ionized can range from < 10% ionized to 100% ionized from pH 3 to 6.5. The coformer $K_{s,T}$ values were determined between pH 3.00 and 3.91, and the $K_{s,T}$ values were used for predictions in the pH range studied (pH 5 to 6.5). The assumption here is that the coformer $K_{s,T}$ dependence on pH is negligible and will have little to no impact on cocrystal solubility predictions. One would expect the coformer $K_{s,T}$ to decrease with increasing pH (due to higher extent of coformer ionization). Because the coformer $K_{s,T}$ values were already quite small to begin with (at pH 3 to 4), we expect the assumption is reasonable in this case. One of the potential consequences is overestimating cocrystal solubility in our predictions if the assumption is not justified.

Predicted cocrystal and drug solubility values were calculated with equations 3.15 and 3.31 based on media conditions (pH and [M]) and the corresponding parameter values of K_{sp}, pK_a, and $K_{s,T}$. Figure 3.3 shows that the predicted cocrystal and drug solubility values are in excellent agreement with the experimentally determined values. This means that the solubility equations and associated parameters can quantitatively predict cocrystal solubility, which can in

turn provide valuable information on cocrystal solubility and stability behavior without the need for extensive experimentation.

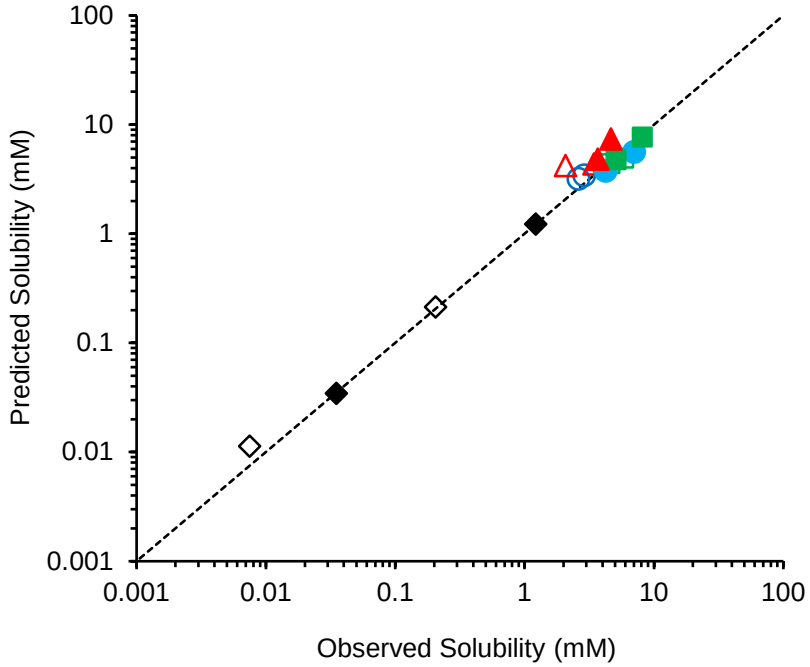

Figure 3.3. Predicted vs. observed solubility of KTZ drug and cocrystals in surfactant containing media (closed symbols) of FeSSIF and FaSSIF, and in blank media (open symbols). KTZ drug is represented by (◊), KTZ-ADP is represented by (○), KTZ-FUM is represented by (□), and KTZ-SUC is represented by (Δ). Predicted solubility values for drug and cocrystals were calculated with equations 3.15 and 3.31 using appropriate $K_{s,T}$ values from table 3.5. Observed solubility values were determined experimentally at the eutectic point using equation 3.32. The dotted line represents where the predicted and experimental solubilities are equal. Observed solubility standard error values are less than 4% and are within the data points.

Cocrystal K_{eu}

For metastable cocrystals with higher solubility than their parent drugs, cocrystal equilibrium solubility can be determined at the eutectic point.[3, 40] In this study, the eutectic points between the drug and cocrystal were used to determine the stoichiometric solubility of KTZ cocrystals under various media conditions. Eutectic concentrations of KTZ and CF are plotted in figure 3.4, and they are useful in assessing cocrystal SA and thermodynamic stability.

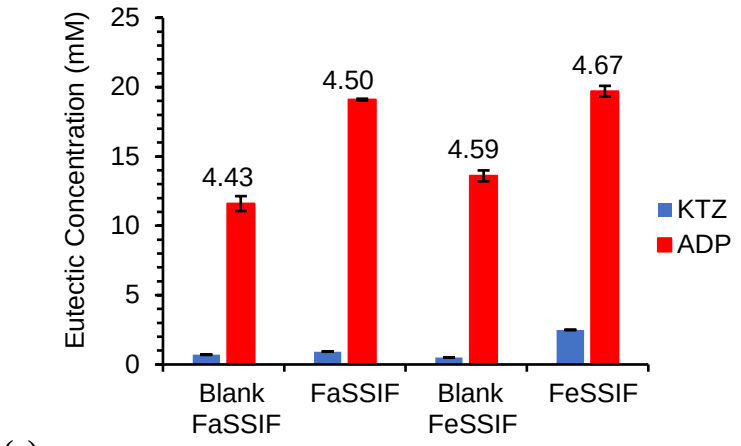

(a)

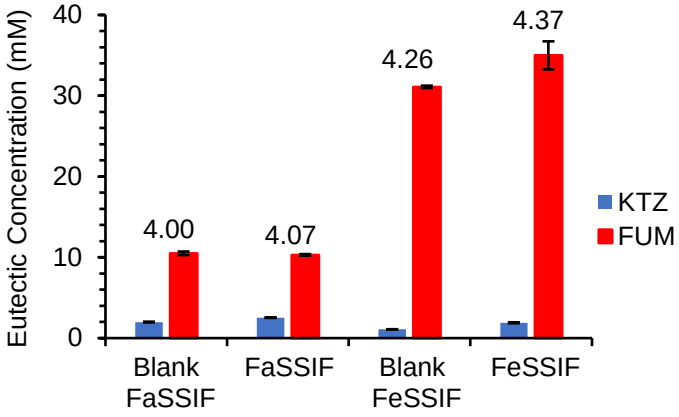

(b)

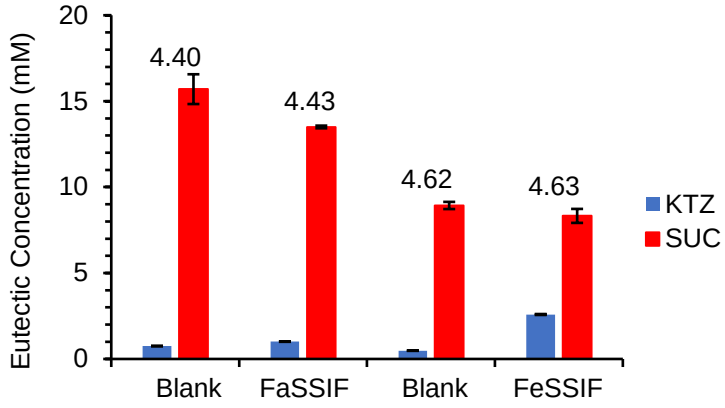

(c)

Figure 3.4. Cocrystal component eutectic concentrations in FaSSIF, FeSSIF, blank FaSSIF, and blank FeSSIF media. Numbers on top of the columns indicate equilibrium pH. (a) KTZ-ADP (b) KTZ-FUM (c) KTZ-SUC. Error bars indicate standard error.

CF eutectic concentrations are higher than that of KTZ for all cocrystals under conditions studied. For cocrystals with 1:1 stoichiometry, which are the cases of the KTZ cocrystals, this

means that the cocrystals are more soluble than the drug. The ratio of coformer to drug eutectic concentrations is used to approximate the eutectic constant, K_{eu}, which is defined as the activity ratio of coformer to drug at the eutectic point.

$$K_{eu} = \frac{a_{CF,eu}}{a_{KTZ,eu}} \approx \frac{[CF]_{eu,T}}{[KTZ]_{eu,T}} \tag{3.35}$$

The notation "a" represents the activity of coformer or drug.

$K_{eu} > 1$ for a 1:1 cocrystal indicates $S_{cc} > S_{drug}$, and the cocrystal is thermodynamically unstable with respect to drug, and vice versa.[3, 11, 38, 41] In general, K_{eu} values are larger in blank media than in surfactant containing media. K_{eu} can be related to cocrystal SA, and this relationship is expressed in the following equation for a 1:1 cocrystal.[11, 41-42]

$$K_{eu} = \left(\frac{S_{cc}}{S_{drug}} \right)^2 = SA^2 \tag{3.36}$$

This relationship for KTZ cocrystals is illustrated in figure 3.5, and the experimentally observed values are in excellent agreement with this prediction. All K_{eu} values are > 1, and this means that all the cocrystals are more soluble than the drug under the conditions studied.

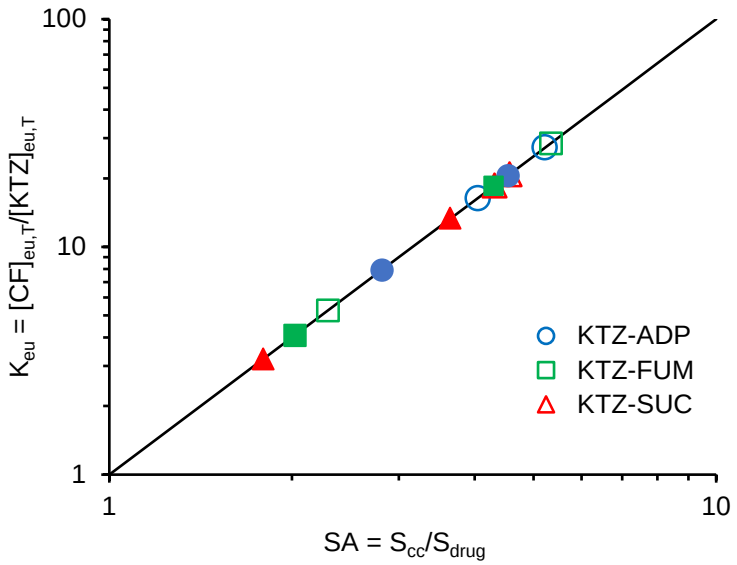

Figure 3.5. Relationship between K_{eu} and cocrystal solubility advantage (SA) for KTZ cocrystals. Line was generated from the logarithmic form of equation 3.36, $\log K_{eu} = 2\log(SA)$. Open symbols correspond to blank media, and closed symbols correspond to surfactant containing media (FeSSIF and FaSSIF). K_{eu} standard errors are less than 6% and are within the data points.

Effect of Surfactants on Cocrystal Dissolution Behavior

Preferential solubilization of drug over coformer reduces cocrystal SA, and it can help stabilize cocrystal in solution and slow its conversion to less soluble forms (usually the drug) during kinetic studies.[11-12, 14-17] Bile salts present in the GI tract and simulated intestinal fluids (FeSSIF and FaSSIF) can act as drug solubilizing agents and have been shown in the previous sections to reduce KTZ cocrystal SA by up to 60%. To evaluate the influence of cocrystal SA on dissolution and conversion to KTZ, dissolution studies were conducted in FeSSIF, FaSSIF, and corresponding blank media. The mass of drug and cocrystals used for dissolution is 1 mg KTZ equivalent per mL to reflect the KTZ dose (200 mg) dissolving in 200 mL of water, which corresponds to 1.9 mM. At this dose, the cocrystals are fully dissolved under the conditions of this study, but the KTZ drug solubility is below that value and therefore not expected to fully dissolve.

For clarity, only KTZ concentrations (not CF concentrations) were plotted in the figures of this section to compare cocrystal dissolution advantage over the pure drug. Both CF and KTZ concentrations were measured during cocrystal dissolution, and CF concentrations during dissolution confirmed that the cocrystals were fully dissolved. CF concentrations during dissolution in blank media are presented in appendix 2C, where pH 6.5 media = blank FaSSIF and pH 5.0 media = blank FeSSIF. CF concentrations in surfactant media (FeSSIF and FaSSIF) are presented in appendix 3A.

Figure 3.6 compares the dissolution of drug and cocrystals between FaSSIF and blank FaSSIF media (initial pH = 6.5). Cocrystals showed clear dissolution advantages compared to the drug in every case except for KTZ-FUM in blank FaSSIF. Dissolution of pure drug showed that the drug dissolved and reached a plateau corresponding to its solubility (~0.01 mM in blank FaSSIF and ~0.04 mM in FaSSIF). Cocrystals generated supersaturation levels of KTZ ($\sigma = (C/S)_{drug}$) up to 30 times above drug solubility during dissolution. Although the cocrystals were fully dissolved, supersaturation of drug in solution led to KTZ precipitation. This explains why the measured KTZ concentration never reached 1.9 mM, which corresponds to $\sigma \approx 170$ in blank FaSSIF and $\sigma \approx 56$ in FaSSIF.

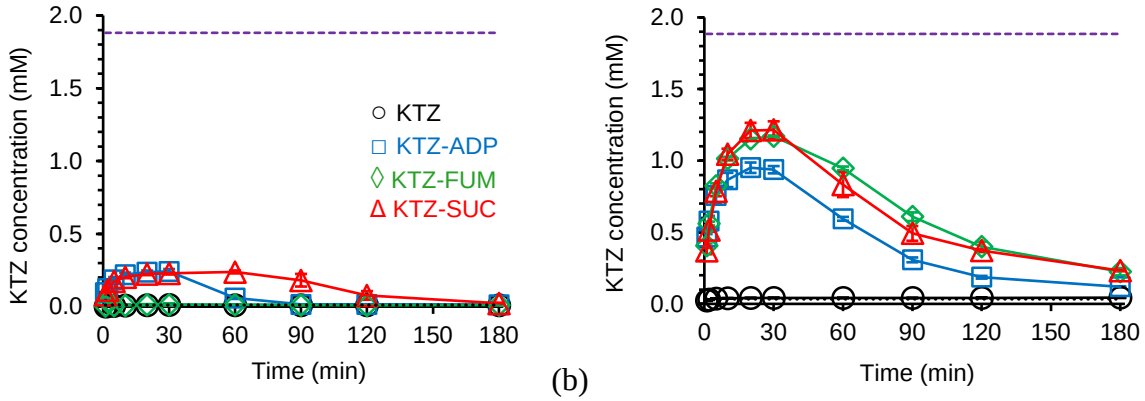

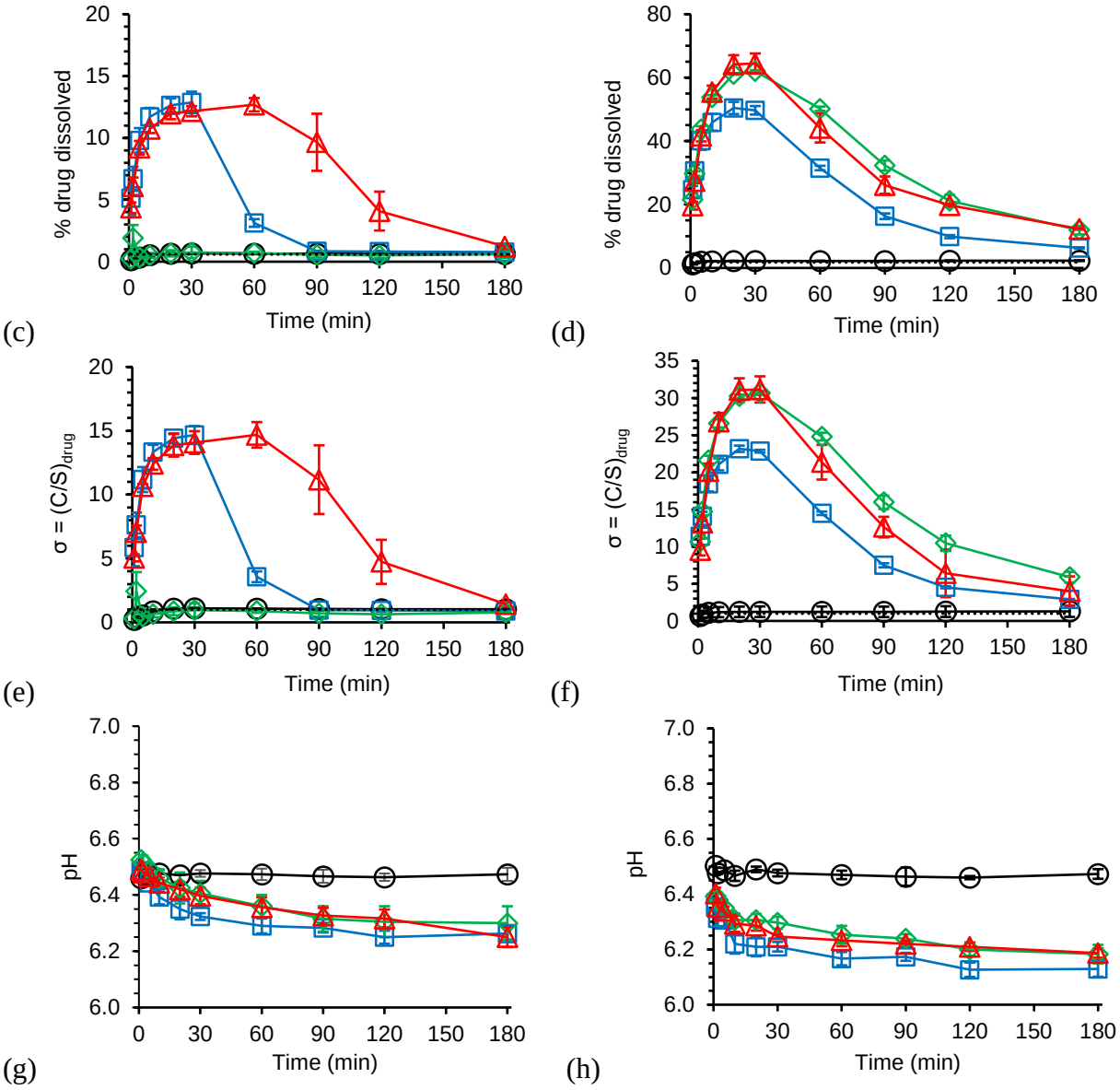

Figure 3.6. KTZ drug and cocrystal dissolution in blank FaSSIF and FaSSIF (initial pH 6.5). KTZ concentration vs. time in (a) blank FaSSIF and (b) FaSSIF. % drug dissolved vs. time in (c) blank FaSSIF and (d) FaSSIF. Supersaturation with respect to drug (σ) vs. time in (e) blank FaSSIF and (f) FaSSIF. Bulk solution pH vs. time in (g) blank FaSSIF and (h) FaSSIF. Purple dashed line in (a) and (b) represents the KTZ concentration if cocrystal/drug were fully dissolved (1.9 mM). Black dotted line in (a) and (b) represents drug solubility (S_{drug}), in (c) and (d) represents 100 × (S_{drug} / 1.9 mM), and in (e) and (f) represents σ = 1 (no supersaturation). Error bars indicate standard errors.

Cocrystal dissolution in FaSSIF achieved higher drug concentrations, % drug dissolved, and σ values compared to dissolution in blank FaSSIF, indicating that the presence of surfactants enhanced cocrystal dissolution and slowed cocrystal conversion to drug. This is especially pronounced for KTZ-FUM cocrystal, which demonstrated little to no dissolution advantage compared to drug in blank FaSSIF (~0.01 mM or 0.6 % drug dissolved), but in FaSSIF KTZ-FUM generated near supersaturation level near 30. KTZ-ADP and KTZ-SUC also showed improvements from blank FaSSIF to FaSSIF, with maximum supersaturation level (σ_{max}) increasing from about 15 (blank FaSSIF) to 23 and 30 (FaSSIF), respectively.

Figure 3.7 illustrates KTZ cocrystal dissolution in FeSSIF and blank FeSSIF. Lower pH (pH 5) of FeSSIF and blank FeSSIF media increases KTZ solubility and decreases cocrystal SA (by 30 to 100 fold) compared to the pH 6.5 media (FaSSIF and blank FaSSIF). Higher surfactant concentration in FeSSIF compared to FaSSIF can further enhance solubility and dissolution of KTZ drug and cocrystals. The cocrystals were observed to outperform the drug during dissolution in FeSSIF and blank FeSSIF.

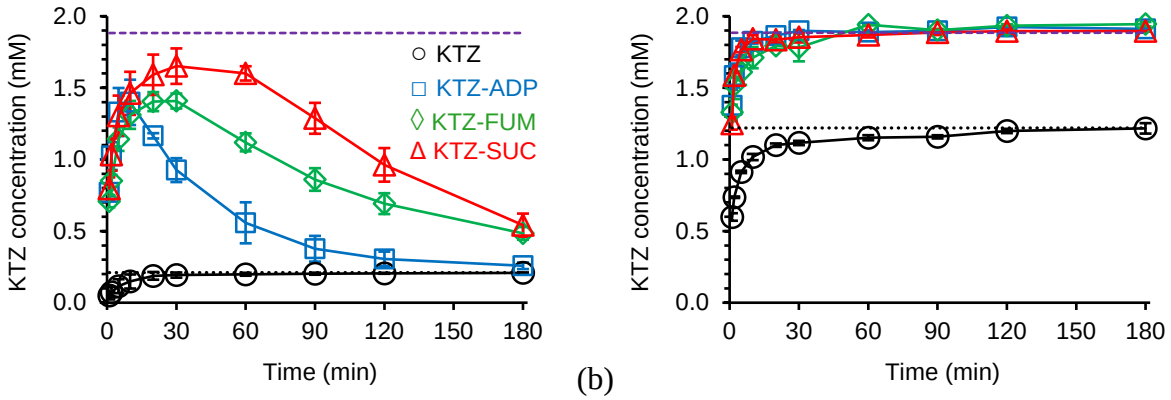

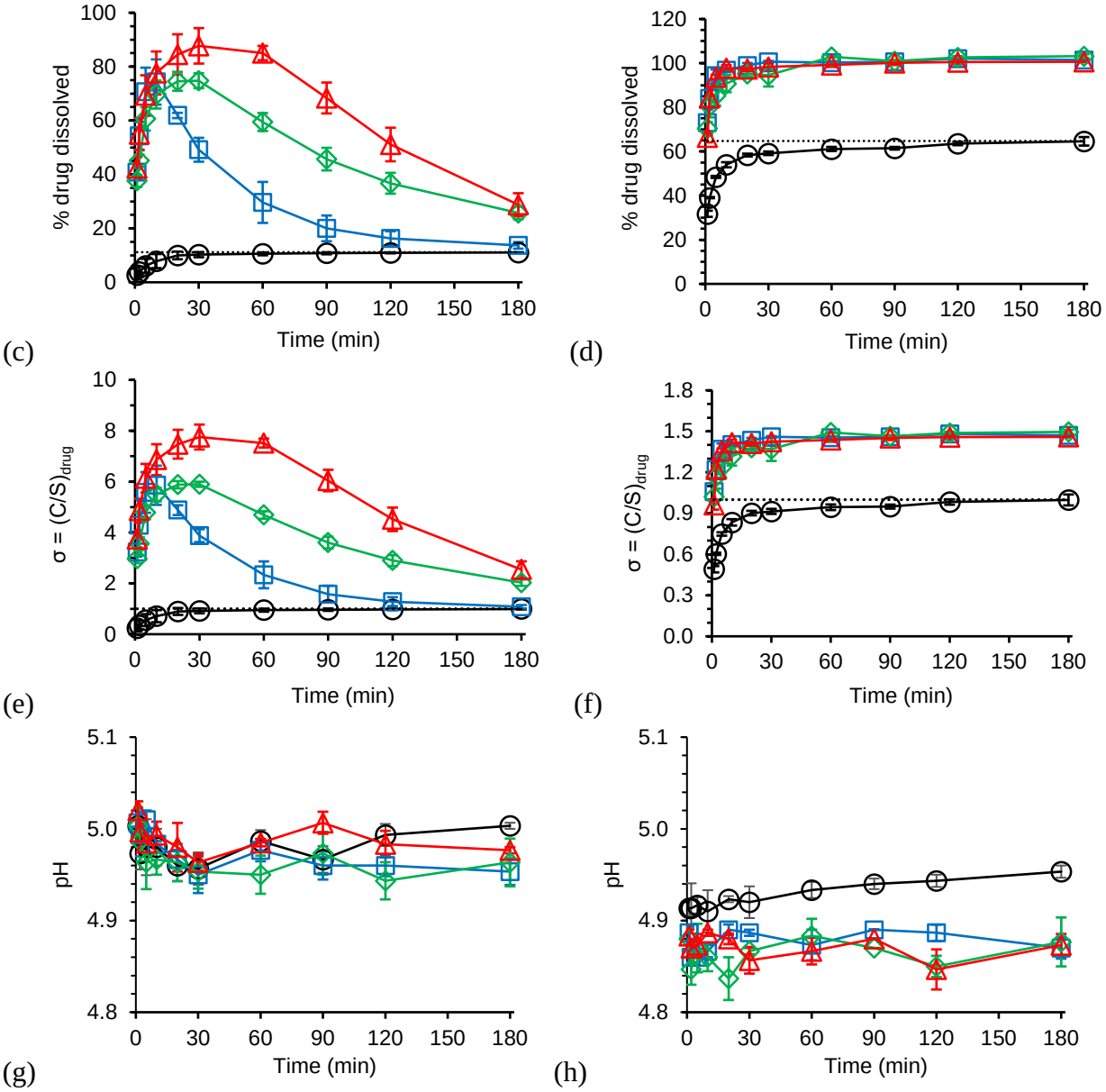

Figure 3.7. KTZ drug and cocrystal dissolution in blank FeSSIF and FeSSIF (initial pH 5.0). KTZ concentration vs. time in (a) blank FeSSIF and (b) FeSSIF. % drug dissolved vs. time in (c) blank FeSSIF and (d) FeSSIF. Supersaturation with respect to drug (σ) vs. time in (e) blank FeSSIF and (f) FeSSIF. Bulk solution pH vs. time in (g) blank FeSSIF and (h) FeSSIF. Purple dashed line in (a) and (b) represents the KTZ concentration if cocrystal/drug were fully dissolved (1.9 mM). Black dotted line in (a) and (b) represents drug solubility (S_{drug}), in (c) and (d) represents 100 × (S_{drug} / 1.9 mM), and in (e) and (f) represents σ = 1 (no supersaturation). Error bars indicate standard errors.

In figure 3.7a, cocrystals show clear dissolution advantage over drug in blank FeSSIF, reaching 74 – 88% drug dissolved (compare to 11% dissolved from pure drug) and generating σ up to 7.8 at C_{max}. Conversion from cocrystal to drug occurred in blank FeSSIF, indicated by decreasing KTZ concentrations over time. In FeSSIF, cocrystals remained fully dissolved and sustained $\sigma \approx 1.5$ for the entire duration of the study. This relatively low supersaturation may help explain why no drug precipitation was observed during dissolution in FeSSIF.

Tables 3.6 and 3.7 summarize results from cocrystal and drug dissolution and corresponding SA values. C_{max} and σ_{max} show the ability of the cocrystals to generate supersaturation during dissolution. AUC provides information on the ability of the cocrystals to sustain supersaturation. SA is the main driving force for cocrystal to drug conversion and affects C_{max}, σ_{max}, and AUC values achieved during dissolution. The largest SA values were observed in blank FaSSIF (pH 6.5, no surfactants), ranging from 440 to 3118. The smallest SA values were observed in FeSSIF (pH 5.0, with surfactants), ranging from 5 to 13. SA has an inverse relationship with C_{max} and AUC, with the lowest SA corresponding to the highest C_{max} and AUC achieved for each cocrystal, and vice versa.

Table 3.6. Cocrystal supersaturation index ($SA=S_{cc}/S_{drug}$), drug C_{max}, AUC, and maximum supersaturation ($\sigma_{max} = C_{max}/S_{drug}$) during dissolution in blank FaSSIF and FaSSIF (pH 6.5) media.

	Media	Final pH	SA[a]	C_{max} (mM)	T_{max} (min)	σ_{max} [a]	AUC (mM×min)
KTZ	Blank FaSSIF	6.48 ± 0.01	--	0.012 ± 0.001	--	--	2.11 ± 0.08
	FaSSIF	6.48 ± 0.01	--	0.043 ± 0.002	--	--	7.5 ± 0.4
KTZ-ADP	Blank FaSSIF	6.23 ± 0.02	440	0.24 ± 0.03	30	14.7 ± 0.9	13.3 ± 0.5
	FaSSIF	6.13 ± 0.03	221	0.95 ± 0.03	20	22.5 ± 0.8	78 ± 3
KTZ-FUM	Blank FaSSIF	6.30 ± 0.09	3118	0.04 ± 0.03	2	2 ± 2	2.1 ± 0.4
	FaSSIF	6.18 ± 0.03	1418	1.17 ± 0.01	30	28.7 ± 0.1	119 ± 4
KTZ-SUC	Blank FaSSIF	6.24 ± 0.05	822	0.24 ± 0.02	60	14.7 ± 0.6	26 ± 3
	FaSSIF	6.19 ± 0.02	461	1.22 ± 0.06	30	30 ± 1	118 ± 1

a. SA values predicted at corresponding final pH of dissolution for each drug and cocrystal, calculated with equations 3.15 and 3.31.

From blank FaSSIF to FaSSIF, SA values decrease roughly by a half for each cocrystal, while C_{max}, σ_{max}, and AUC values all increased. The most dramatic improvement is the KTZ-FUM cocrystal, with about 30 times higher C_{max}, 14 times higher σ_{max}, and 57 times higher AUC from blank FaSSIF to FaSSIF. KTZ-ADP and KTZ-SUC also showed improvements in C_{max} (4 to 5 fold), σ_{max} (1.5 to 2 fold), and AUC (4.5 to 5.9 fold) in FaSSIF.

Table 3.7. Cocrystal supersaturation index ($SA=S_{cc}/S_{drug}$), drug C_{max}, AUC, and maximum supersaturation ($\sigma_{max} = C_{max}/S_{drug}$) during dissolution in blank FeSSIF and FeSSIF (pH 5.0) media.

	Media	Final pH	SA[a]	C_{max} (mM)	T_{max} (min)	σ_{max} [a]	AUC (mM×min)
KTZ	Blank FeSSIF	5.01 ± 0.02	--	0.208 ± 0.001	--	--	35 ± 2
	FeSSIF	4.95 ± 0.01	--	1.22 ± 0.03	--	--	206 ± 3
KTZ-ADP	Blank FeSSIF	4.94 ± 0.02	13	1.4 ± 0.3	10	5.9 ± 0.7	98 ± 9
	FeSSIF	4.88 ± 0.01	5.0	1.93 ± 0.01	--	1.48 ± 0.01	339 ± 1
KTZ-FUM	Blank FeSSIF	4.94 ± 0.06	36	1.41 ± 0.09	30	5.9 ± 0.2	160 ± 10
	FeSSIF	4.86 ± 0.03	13	1.95 ± 0.01	--	1.49 ± 0.01	337 ± 3
KTZ-SUC	Blank FeSSIF	4.99 ± 0.02	21	1.7 ± 0.2	30	7.8 ± 0.6	210 ± 20
	FeSSIF	4.87 ± 0.01	7.1	1.91 ± 0.01	--	1.46 ± 0.01	335 ± 3

a. SA values predicted at corresponding final pH of dissolution for each drug and cocrystal, calculated with equations 3.15 and 3.31.

Cocrystal SA values in FeSSIF and blank FeSSIF are much smaller ($SA \leq 36$) comparing to in pH 6.5 media (FaSSIF and blank FaSSIF). C_{max} and AUC in pH 5 media were also higher. Cocrystals were fully dissolved and no drug precipitation occurred during dissolution in FeSSIF, and the highest AUC and C_{max} values were observed in this media.

Figure 3.8 illustrates C_{max} and AUC from drug and cocrystal dissolution under different media conditions. The cocrystals (except for KTZ-FUM in blank FaSSIF) generated higher KTZ

concentrations compared to pure drug dissolution. Although drug precipitation occurred in all media except FeSSIF, the cocrystals still outperformed the drug in most cases.

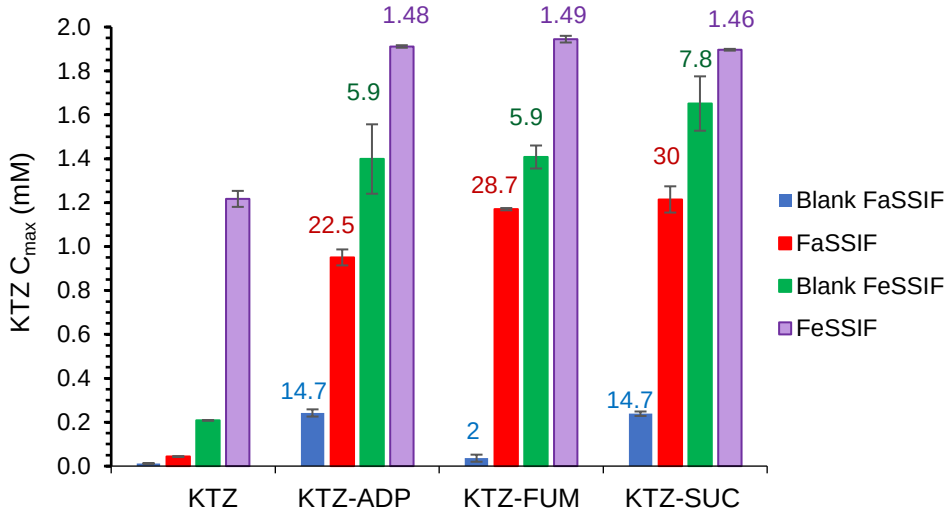

(a)

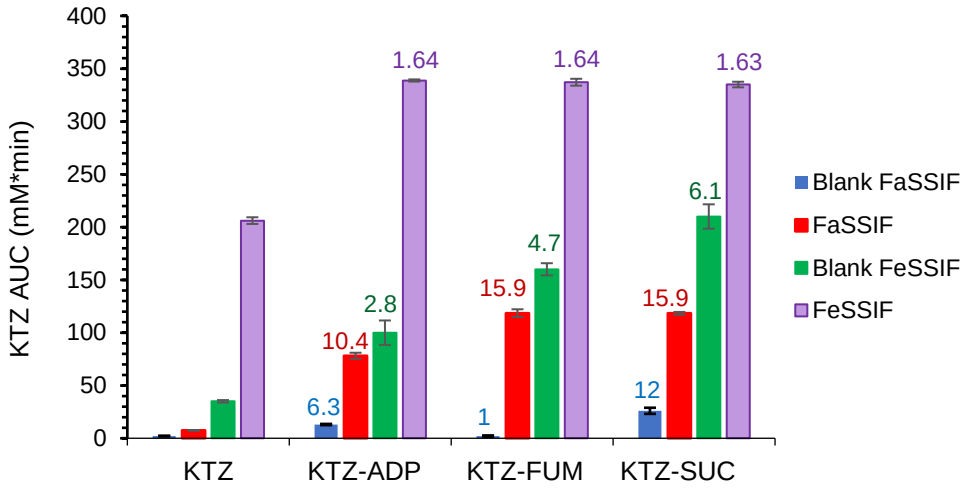

(b)

Figure 3.8. (a) KTZ C_{max} and (b) AUC during dissolution of drug and cocrystals in different media. Numbers on top of the columns indicates (a) σ_{max}, which is defined as C_{max}/S_{drug} and (b) AUC ratio of cocrystal to drug ($AUC_{cc/drug}$). Error bars indicate standard errors.

KTZ cocrystals improve dissolution by generating supersaturation in solution. However, any system that can generate supersaturation has the potential to precipitate.[11, 17, 43-45] SA can provide important information on the risk of cocrystal conversion and supersaturation behavior.

Figure 3.9 shows the maximum supersaturation level achieved and AUC enhancement by cocrystal dissolution in relation with SA.

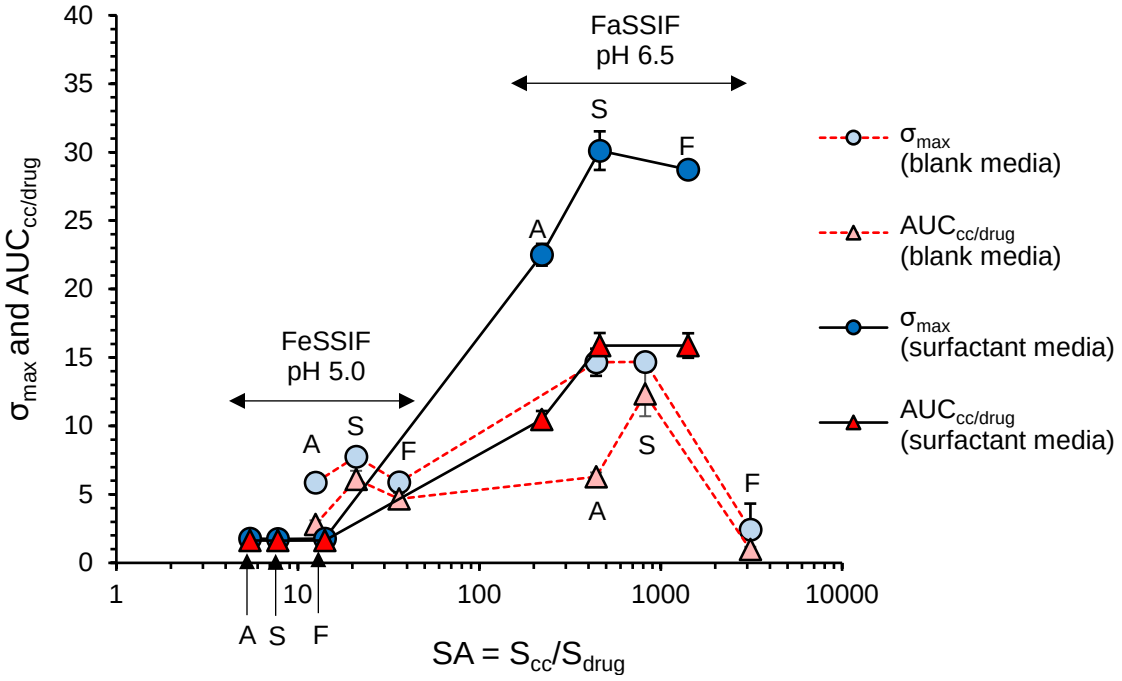

Figure 3.9. Cocrystal σ_{max} and $AUC_{cc/drug}$ as a function of cocrystal supersaturation index (SA). Letters "A", "S", and "F" by the symbols represent cocrystals KTZ-ADP, KTZ-SUC, and KTZ-FUM, respectively. pH 5.0 represents FeSSIF and blank FeSSIF media, and pH 6.5 represents FaSSIF and blank FaSSIF media. Error bars indicate standard error. Error bars that are not seen is due to error within data points.

Figure 3.9 shows the advantage of KTZ cocrystals compared to drug. In FaSSIF, σ_{max} values (22 – 30) are 1.5 to 15 times higher than in blank FaSSIF. $AUC_{cc/drug}$ values (10-15) are 5 to 57 times higher than in blank. In FeSSIF, the cocrystals fully dissolved and no drug precipitation occurred. σ_{max} and $AUC_{cc/drug}$ values in FeSSIF are lower than in blank FeSSIF due to higher S_{drug} in FeSSIF. S_{cc} also increases in FeSSIF, but to a lesser extent than S_{drug}.

The highest σ_{max} and $AUC_{cc/drug}$ values in FaSSIF indicate that higher supersaturation levels are more difficult to sustain over time. σ_{max} and $AUC_{cc/drug}$ increase with SA up to a

critical supersaturation value (about 800 to 1400 in both blank and FaSSIF). Rapid nucleation occurs at SA ~ 3000 in blank FaSSIF at $\sigma_{max} > 14$.

The relationship between kinetic dissolution behavior of KTZ cocrystals and SA values showed how the cocrystal with the highest solubility and largest SA did not necessarily show superior dissolution behavior. SA represents the driving force for drug precipitation. Phase conversion between cocrystal and its constituent drug can be described by the following equation[46]

$$\Delta G_{cocrystal \rightarrow drug} = -RT \ln(SA) \tag{3.37}$$

ΔG is the Gibbs free energy change for the process, and it is negative for a spontaneous process. Cocrystal to drug conversion is favored when $S_{cocrystal} > S_{drug}$. The rate of drug nucleation is proportional to ΔG, which is in turn proportional to the logarithmic of SA. An extremely large SA can lead to fast conversion of cocrystal to a less soluble form, and it is undesirable for generating and maintaining supersaturation. One must find the right balance between solubility enhancement and risk of precipitation in order to optimize drug supersaturation behavior.

Conclusion

Cocrystals and drugs can encounter both endogenous and synthetic solubilizing agents during the pharmaceutical development process and in the GI environment. Solubilizing agents that preferentially solubilize the drug over coformer can reduce cocrystal SA and improve dissolution by enhancing and sustaining supersaturation of the drug in solution. Understanding cocrystal solubility and stability in the presence of solubilizing agents is crucial for correct interpretation of experimental results and rational selection of additives to achieve better *in vitro* and *in vivo* performance. The equations derived in this chapter provide a material-sparing and

time-efficient approach for quantitative evaluation of metastable cocrystal solubility and SA. KTZ cocrystals were shown to be more soluble than drug under all media conditions used in this study, although the cocrystal solubility enhancement in biorelevant media were not as high as that of the drug. We have shown that surfactants in biorelevant media reduced cocrystal SA and improve drug solution levels by slowing cocrystal conversion to drug during dissolution.

Acknowledgement

Research reported in this publication was partially supported by the National Institute of General Medical Sciences of the National Institutes of Health under award number R01GM107146. The content is solely the responsibility of the authors and does not necessarily represent the official views of the National Institutes of Health. We also gratefully acknowledge partial financial support from the College of Pharmacy at the University of Michigan.

References

1. Basavoju, S.; Boström, D.; Velaga, S., Indomethacin–Saccharin Cocrystal: Design, Synthesis and Preliminary Pharmaceutical Characterization. *Pharmaceutical Research* **2008,** *25* (3), 530-541.

2. Cheney, M. L.; Weyna, D. R.; Shan, N.; Hanna, M.; Wojtas, L.; Zaworotko, M. J., Coformer selection in pharmaceutical cocrystal development: A case study of a meloxicam aspirin cocrystal that exhibits enhanced solubility and pharmacokinetics. *Journal of Pharmaceutical Sciences* **2011,** *100* (6), 2172-2181.

3. Good, D. J.; Rodríguez-Hornedo, N. r., Solubility Advantage of Pharmaceutical Cocrystals. *Crystal Growth & Design* **2009,** *9* (5), 2252-2264.

4. Jung, M.-S.; Kim, J.-S.; Kim, M.-S.; Alhalaweh, A.; Cho, W.; Hwang, S.-J.; Velaga, S. P., Bioavailability of indomethacin-saccharin cocrystals. *Journal of Pharmacy and Pharmacology* **2010,** *62* (11), 1560-1568.

5. McNamara, D. P.; Childs, S. L.; Giordano, J.; Iarriccio, A.; Cassidy, J.; Shet, M. S.; Mannion, R.; O'Donnell, E.; Park, A., Use of a Glutaric Acid Cocrystal to Improve Oral Bioavailability of a Low Solubility API. *Pharmaceutical Research* **2006,** *23* (8), 1888-1897.

6. Smith, A. J.; Kavuru, P.; Wojtas, L.; Zaworotko, M. J.; Shytle, R. D., Cocrystals of Quercetin with Improved Solubility and Oral Bioavailability. *Molecular Pharmaceutics* **2011,** *8* (5), 1867-1876.

7. Childs, S. L.; Rodriguez-Hornedo, N.; Reddy, L. S.; Jayasankar, A.; Maheshwari, C.; McCausland, L.; Shipplett, R.; Stahly, B. C., Screening strategies based on solubility and solution composition generate pharmaceutically acceptable cocrystals of carbamazepine. *CrystEngComm* **2008,** *10* (7), 856-864.

8. Childs, S. L.; Chyall, L. J.; Dunlap, J. T.; Smolenskaya, V. N.; Stahly, B. C.; Stahly, G. P., Crystal Engineering Approach To Forming Cocrystals of Amine Hydrochlorides with Organic Acids. Molecular Complexes of Fluoxetine Hydrochloride with Benzoic, Succinic, and Fumaric Acids. *Journal of the American Chemical Society* **2004,** *126* (41), 13335-13342.

9. Weyna, D. R.; Cheney, M. L.; Shan, N.; Hanna, M.; Zaworotko, M. J.; Sava, V.; Song, S.; Sanchez-Ramos, J. R., Improving Solubility and Pharmacokinetics of Meloxicam via Multiple-Component Crystal Formation. *Molecular Pharmaceutics* **2012,** *9* (7), 2094-2102.

10. Bethune, S. J.; Huang, N.; Jayasankar, A.; Rodríguez-Hornedo, N. r., Understanding and Predicting the Effect of Cocrystal Components and pH on Cocrystal Solubility. *Crystal Growth & Design* **2009,** *9* (9), 3976-3988.

11. Kuminek, G.; Cao, F.; Bahia de Oliveira da Rocha, A.; Gonçalves Cardoso, S.; Rodríguez-Hornedo, N., Cocrystals to facilitate delivery of poorly soluble compounds beyond-rule-of-5. *Advanced Drug Delivery Reviews* **2016,** *101*, 143-166.

12. Huang, N.; Rodríguez-Hornedo, N. r., Effect of Micellar Solubilization on Cocrystal Solubility and Stability. *Crystal Growth & Design* **2010,** *10* (5), 2050-2053.

13. Lipert, M. P. Predicting the Influence of Drug Solubilizing Agents on Cocrystal Solubility, Stability, and Transition Points. Dissertations and Theses, University of Michigan, 2015.

14. Lipert, M. P.; Rodríguez-Hornedo, N., Cocrystal Transition Points: Role of Cocrystal Solubility, Drug Solubility, and Solubilizing Agents. *Molecular Pharmaceutics* **2015**.

15. Huang, N.; Rodríguez-Hornedo, N., Engineering cocrystal solubility, stability, and pHmax by micellar solubilization. *Journal of Pharmaceutical Sciences* **2011,** *100* (12), 5219-5234.

16. Lipert, M. P.; Roy, L.; Childs, S. L.; Rodriguez-Hornedo, N., Cocrystal Solubilization in Biorelevant Media and its Prediction from Drug Solubilization. *Journal of Pharmaceutical Sciences* **2015**.

17. Roy, L.; Lipert, M. P.; Rodriguez-Hornedo, N., Co-crystal Solubility and Thermodynamic Stability. In *Pharmaceutical Salts and Co-crystals*, The Royal Society of Chemistry: 2012; pp 247-279.

18. Huang, N. C. Engineering cocrystal solubility and stability via ionization and micellar solubilization. University of Michigan, 2011.

19. Galia, E.; Nicolaides, E.; Hörter, D.; Löbenberg, R.; Reppas, C.; Dressman, J. B., Evaluation of Various Dissolution Media for Predicting In Vivo Performance of Class I and II Drugs. *Pharmaceutical Research* **1998,** *15* (5), 698-705.

20. Jantratid, E.; Janssen, N.; Reppas, C.; Dressman, J. B., Dissolution Media Simulating Conditions in the Proximal Human Gastrointestinal Tract: An Update. *Pharmaceutical Research* **2008,** *25* (7), 1663-1676.

21. Kostewicz, E. S.; Brauns, U.; Becker, R.; Dressman, J. B., Forecasting the Oral Absorption Behavior of Poorly Soluble Weak Bases Using Solubility and Dissolution Studies in Biorelevant Media. *Pharmaceutical Research* **2002,** *19* (3), 345-349.

22. Hörter, D.; Dressman, J. B., Influence of physicochemical properties on dissolution of drugs in the gastrointestinal tract1. *Advanced Drug Delivery Reviews* **2001,** *46* (1–3), 75-87.

23. Dressman, J. B., Dissolution testing of immediate-release products and its application to forecasting in vivo performance. *Drugs and the pharmaceutical sciences* **2000,** *106*, 155-182.

24. Nikoletta Fotaki, M. V., Biorelevant Dissolution Methods and Their Applications in In Vitro In Vivo Correlations for Oral Formulations *The Open Drug Delivery Journal* **2010,** *4*, 2-13.

25. Mazer, N. A.; Benedek, G. B.; Carey, M. C., Quasielastic light-scattering studies of aqueous biliary lipid systems. Mixed micelle formation in bile salt-lecithin solutions. *Biochemistry* **1980,** *19* (4), 601-615.

26. Avdeef, A., *Absorption and drug development solubility, permeability, and charge state*. 2nd ed.; John Wiley & Sons: Hoboken, N.J., 2012; p xli, 698 p.

27. Smith, R. M.; Martell, A. E.; SpringerLink, *Critical Stability Constants Second Supplement*. Springer US : Imprint: Springer: Boston, MA, 1989; p XVIII, 643 p.

28. Serjeant, E. P.; Dempsey, B., *Ionisation constants of organic acids in aqueous solution*. Pergamon Press: Oxford ; New York, 1979; p xi, 989 p.

29. Zhu, C.; Jiang, L.; Chen, T.-M.; Hwang, K.-K., A comparative study of artificial membrane permeability assay for high throughput profiling of drug absorption potential. *European Journal of Medicinal Chemistry* **2002,** *37* (5), 399-407.

30. Hansch, C.; Leo, A.; Hoekman, D.; Livingstone, D., *Exploring QSAR: hydrophobic, electronic, and steric constants*. American Chemical Society Washington, DC: 1995; Vol. 48.

31. Dressman, J. B.; Reppas, C., In vitro–in vivo correlations for lipophilic, poorly water-soluble drugs. *European Journal of Pharmaceutical Sciences* **2000,** *11, Supplement 2*, S73-S80.

32. Calafato, N. R.; Picó, G., Griseofulvin and ketoconazole solubilization by bile salts studied using fluorescence spectroscopy. *Colloids and Surfaces B: Biointerfaces* **2006,** *47* (2), 198-204.

33. Yamashita, T.; Yamamoto, E.; Kushida, I., Frozen water phase method for logD measurement using a 96-well plate. *Talanta* **2011,** *84* (3), 809-813.

34. Rodríguez-Hornedo, N.; Nehm, S. J.; Seefeldt, K. F.; Pagán-Torres, Y.; Falkiewicz, C. J., Reaction Crystallization of Pharmaceutical Molecular Complexes. *Molecular Pharmaceutics* **2006,** *3* (3), 362-367.

35. Nehm, S. J.; Rodríguez-Spong, B.; Rodríguez-Hornedo, N., Phase Solubility Diagrams of Cocrystals Are Explained by Solubility Product and Solution Complexation. *Crystal Growth & Design* **2005,** *6* (2), 592-600.

36. Naylor, L. J. B., V.; Rodriguez-Hornedo, N.; Weiner, N. D.; Dressman, J. B., Dissolution of steroids in bile salt solutions is modified by the presence of lecithin. *Eur. J. Pharm. Biopharm.* **1995,** *41* (6), 346-353.

37. Naylor, L. J. B., Vassiliki; Dressman, Jennifer B., Comparison of the Mechanism of Dissolution of Hydrocortisone in Simple and Mixed Micelle Systems. *Pharmaceutical Research* **1993,** *10* (6), 865-870.

38. Good, D. J.; Rodríguez-Hornedo, N. r., Cocrystal Eutectic Constants and Prediction of Solubility Behavior. *Crystal Growth & Design* **2010,** *10* (3), 1028-1032.

39. Moore, E. W.; Celic, L.; Ostrow, J. D., Interactions Between Ionized Calcium and Sodium Taurocholate: Bile Salts Are Important Buffers for Prevention of Calcium-Containing Gallstones. *Gastroenterology 83* (5), 1079-1089.

40. Good, D. J. Pharmaceutical Cocrystal Eutectic Analysis: Study of Thermodynamic Stability, Solubility, and Phase Behavior. The University of Michigan, 2010.

41. Alhalaweh, A.; Roy, L.; Rodríguez-Hornedo, N.; Velaga, S. P., pH-Dependent Solubility of Indomethacin–Saccharin and Carbamazepine–Saccharin Cocrystals in Aqueous Media. *Molecular Pharmaceutics* **2012,** *9* (9), 2605-2612.

42. Kuminek, G.; Rodriguez-Hornedo, N.; Siedler, S.; Rocha, H. V. A.; Cuffini, S. L.; Cardoso, S. G., How cocrystals of weakly basic drugs and acidic coformers might modulate solubility and stability. *Chemical Communications* **2016,** *52* (34), 5832-5835.

43. Brouwers, J.; Brewster, M. E.; Augustijns, P., Supersaturating drug delivery systems: The answer to solubility-limited oral bioavailability? *Journal of Pharmaceutical Sciences* **2009,** *98* (8), 2549-2572.

44. Schultheiss, N.; Newman, A., Pharmaceutical Cocrystals and Their Physicochemical Properties. *Crystal Growth & Design* **2009,** *9* (6), 2950-2967.

45. Augustijns, P.; Brewster, M. E., Supersaturating drug delivery systems: Fast is not necessarily good enough. *Journal of Pharmaceutical Sciences* **2012,** *101* (1), 7-9.

46. Kuminek, G., Cavanagh, K., Rodríguez-Hornedo, N., Measurement and mathematical relationships of cocrystal thermodynamic properties. In *Pharmaceutical Crystals: Science and Engineering*, John Wiley & Sons: 2017, Submitted.

Appendix 3A

Cocrystal Dissolution in FaSSIF

Both KTZ and CF concentrations were monitored during dissolution to assess the extent of cocrystal dissolution and conversion in solution (figure 3A.1).

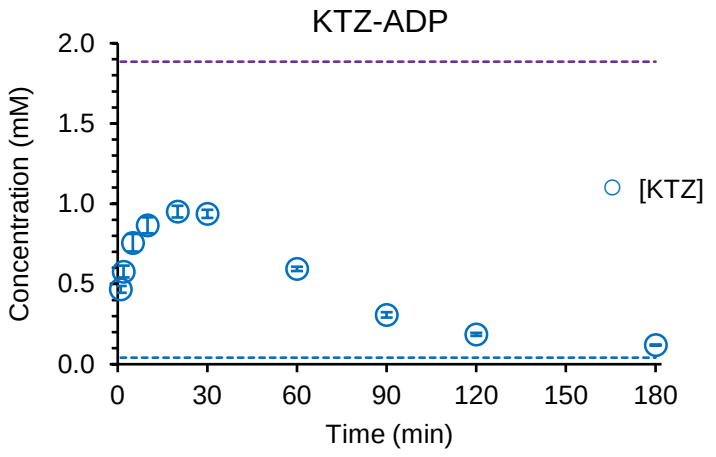

(a)

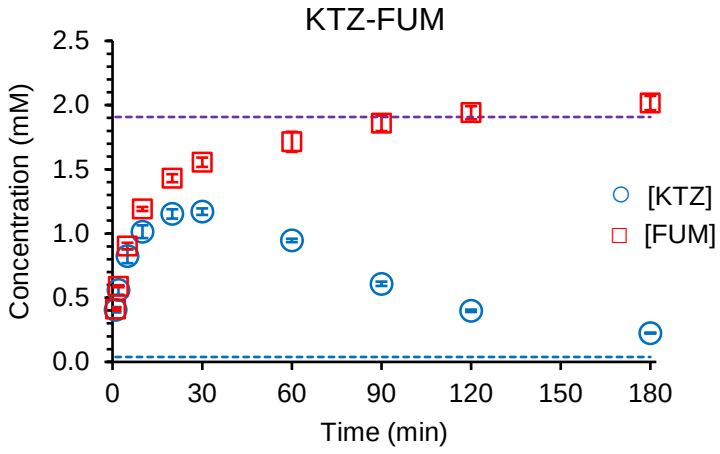

(b)

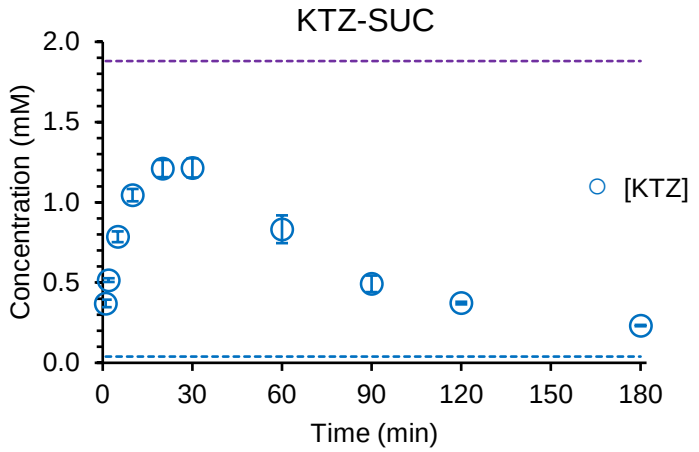

(c)

Figure 3A.1. KTZ cocrystal component concentrations during dissolution in FaSSIF media. Purple dashed line indicates the concentration at which the cocrystal is fully dissolved. Blue dashed line indicates KTZ drug solubility. Error bars on the symbols indicate standard errors.

As cocrystal dissolved, both CF and KTZ were released into solution. FUM concentrations increased with time and reached full dissolution around 90 min. This shows that KTZ-FUM cocrystal was fully dissolved in FaSSIF and KTZ drug was precipitating out of the solution during dissolution. Poor UV absorption of SUC and ADP led to their solution concentrations not able to be determined during dissolution. However, KTZ-SUC and KTZ-ADP cocrystal solubilities are between 5 and 10 times above the concentration at full dissolution (1.9 mM), therefore the cocrystals are expected to be able to fully dissolve.

Cocrystal Dissolution in FeSSIF

During dissolution in FeSSIF, no precipitation of any solid forms was observed for any of the cocrystals. All three cocrystals remained fully dissolved and maintained σ level of about 1.8 for the entire duration of the study (figure 3A.2).

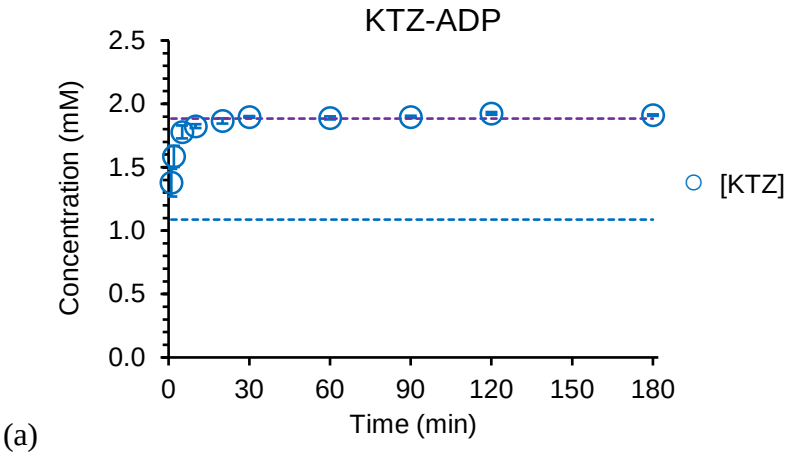

(a)

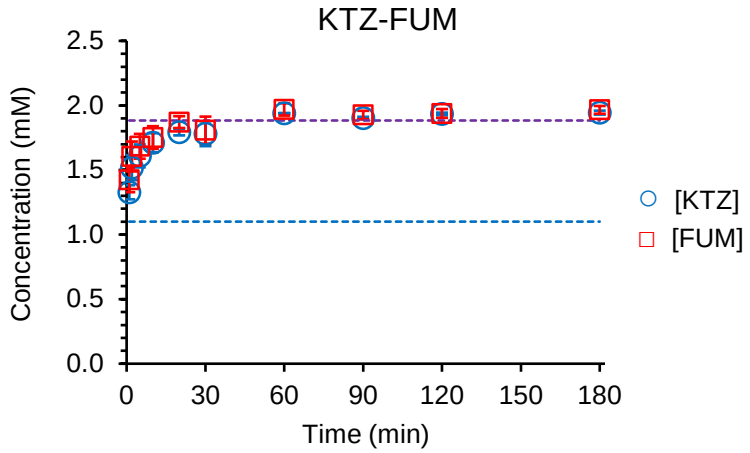

(b)

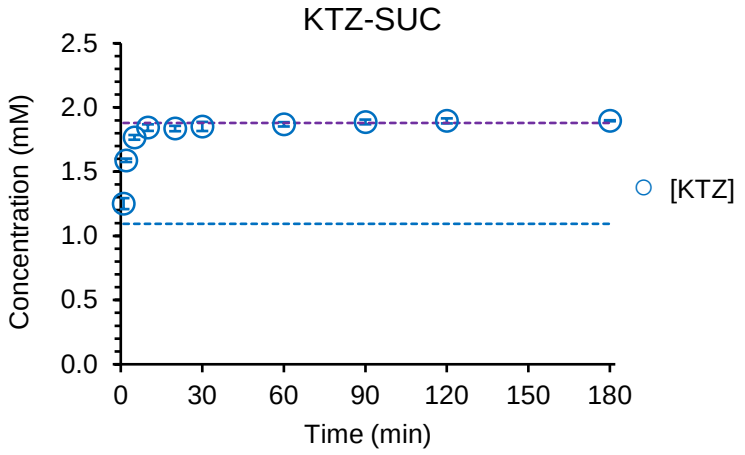

(c)

Figure 3A.2. KTZ cocrystal component concentrations during dissolution in FeSSIF media. Purple dashed line indicates the concentration at which the cocrystal is fully dissolved. Blue dashed line indicates KTZ drug solubility. Error bars on the symbols indicate standard errors.

FUM is the only coformer which concentration could be measured during dissolution in FeSSIF. The FUM concentrations can be seen to overlap that of KTZ during KTZ-FUM dissolution, and this indicates that the cocrystal remained fully dissolved and did not convert to drug during dissolution.

Appendix 3B

Cocrystal powder dissolution in FaSSIF and FeSSIF media were also conducted with magnetic stirring (200 rpm) to see how different conditions might affect the dissolution and conversion rate of these cocrystals. The total dissolution volume used was 21 mL, the mass of cocrystal and drug used was 0.8 mg KTZ equivalent/mL, which corresponds to the dose of KTZ (200 mg in 250 mL of water/stomach volume), at 24.5 (± 0.5) °C. The drug and cocrystal powders used were sieved and collected between 106 – 125μm particle size. Sampling procedure and HPLC methods used were the same as the other dissolution studies with overhead propellers, as described in the Materials and Methods section.

Cocrystal Dissolution in FaSSIF (Magnetic Stirring)

Figure 3B.1 illustrates the drug and cocrystal dissolution behavior in FaSSIF media. If the full mass of drug/cocrystal added to solution were dissolved, the solution concentration of KTZ would be equal to 1.5 x 10^{-3} M. In figure 3B.1a, one can observe that KTZ drug dissolved to its solubility in FaSSIF (3.5 x 10^{-5} M at pH 6.5) in 10 to 20 min and plateaued for the remainder of the dissolution. The KTZ cocrystals reached σ values between 20 and 30 at C_{max}.

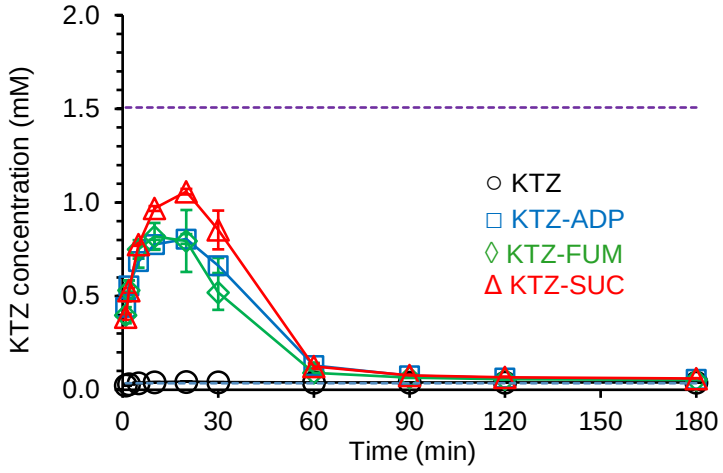

(a)

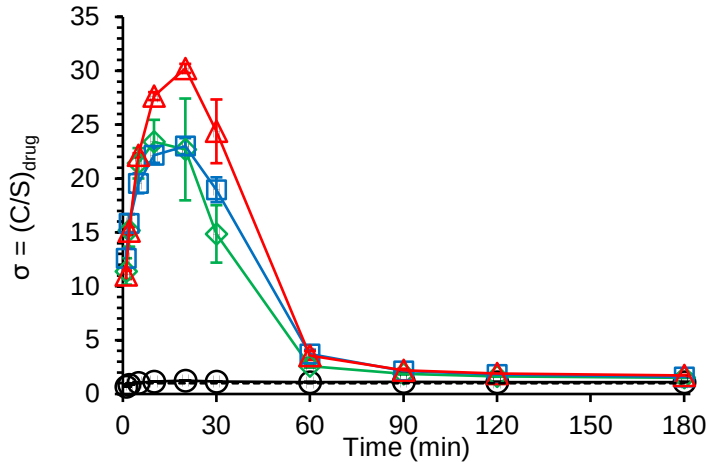

(b)

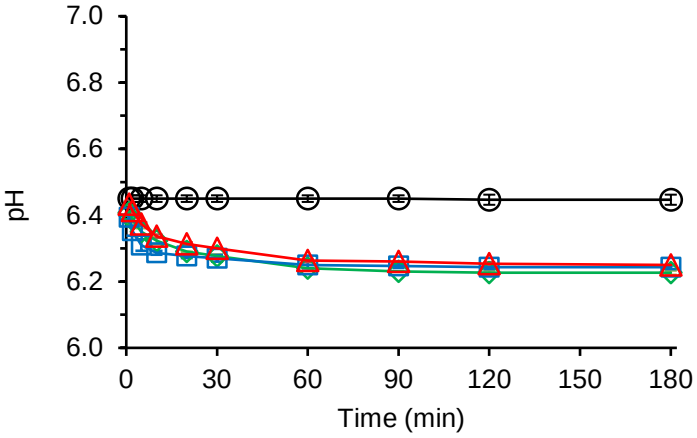

(c)

Figure 3B.1. KTZ drug and cocrystal dissolution in FaSSIF with magnetic stirring. (a) KTZ concentration vs. time. The purple dashed line indicates the KTZ concentration if the cocrystal or drug added were fully dissolved. The black dotted line indicates the solubility of KTZ in FaSSIF. (b) σ with respect to KTZ solubility. The black dotted line indicates where σ = 1, or no supersaturation. (c) Bulk pH during dissolution.

In comparison to dissolution conducted with overhead propeller studies, which also used a larger volume (30 mL) and slightly more drug/cocrystal (1.9×10^{-3} M), dissolution using magnetic stirring appeared to achieve lower drug C_{max} values and have a faster conversion rate. The C_{max} from the cocrystals decreased 12 - 30% in dissolution with magnetic stirring, and σ_{max} decreased 0.7 - 24%. The T_{max} of KTZ-FUM and KTZ-SUC were also affected, and they were 20 and 10 min earlier in comparison to previous dissolution studies, respectively. KTZ-ADP appeared to be the least affected out of the three cocrystals. KTZ-ADP C_{max} in both sets of

dissolution studies occurred at the same time point, the C_{max} value decreased about 15% compared to dissolution with overhead stirring, and it exhibited only 0.7% decrease in σ_{max}.

Cocrystal Dissolution in FeSSIF (Magnetic Stirring)

Cocrystal dissolution in FeSSIF with magnetic stirring was able to achieve full dissolution in less than 20 min and remained fully dissolved for the duration of the experiment (figure 3B.2). The σ values from cocrystal dissolution were small (about 1.3), and the cocrystals were able to maintain this supersaturation and no drug precipitation was observed. In this case, there appeared to be no large variation in cocrystal dissolution/conversion behavior between the two sets of dissolution conditions.

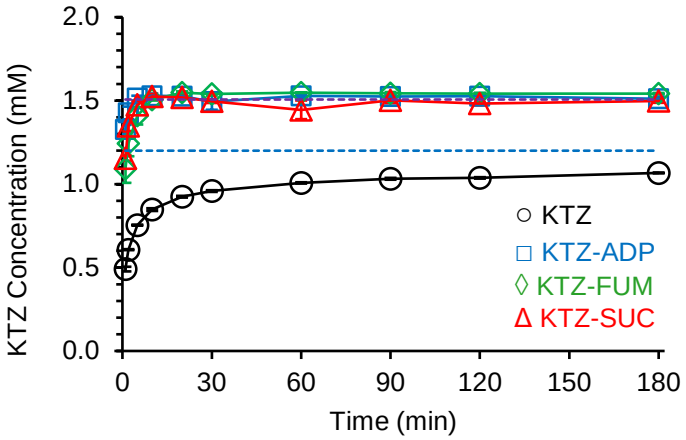

(a)

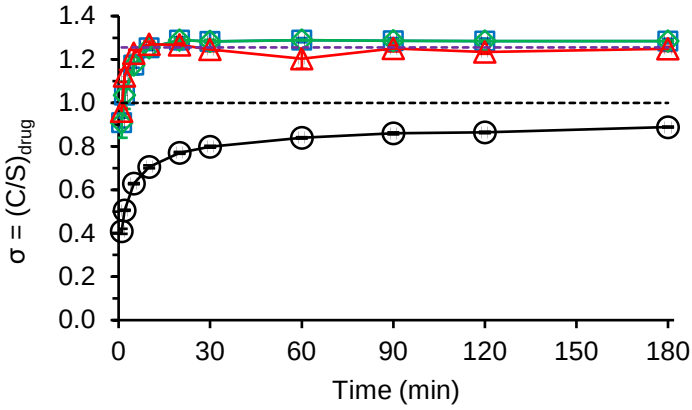

(b)

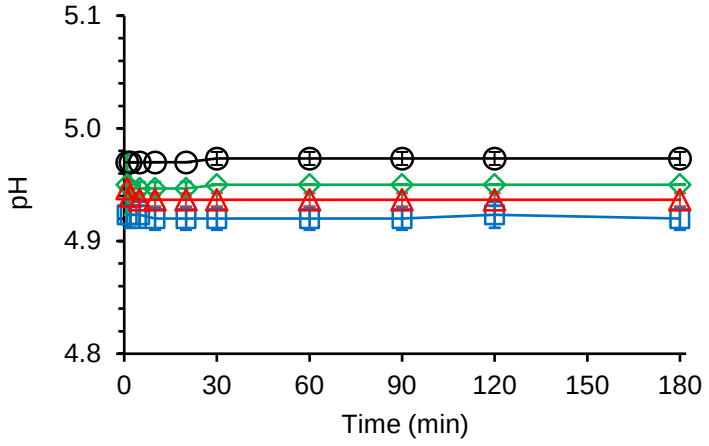

(c)

Figure 3B.2. KTZ drug and cocrystal dissolution in FeSSIF with magnetic stirring. (a) KTZ concentration vs. time. The purple dashed line indicates the KTZ concentration if the cocrystal or drug added were fully dissolved. The black dotted line indicates the solubility of KTZ in FeSSIF. (b) σ with respect to KTZ solubility. The black dotted line indicates where σ = 1, or no supersaturation. (c) Bulk pH during dissolution.

CHAPTER 4

ASSESSING SUPERSATURATION AND CONVERSION BEHAVIOR OF COCRYSALS OF A BASIC DRUG USING pH-SHIFT DISSOLUTION TEST

Introduction

Weakly basic drugs with low solubility under high pH conditions can have impaired oral absorption in patients whose gastric pH is elevated.[1-8] A young and healthy individual usually has a fasting gastric pH of around 2, but in patients with hypochlorhydria conditions caused by diseases (AIDS, gastric cancer) or medications (gastric acid suppressing agents) the fasting gastric pH can increase to above 7.[9-13] Ketoconazole (KTZ) is a broad-spectrum antifungal drug that has been effective in treating fungal infections and was commonly used in AIDS patients.[14-18] The FDA has issued a warning in 2013 regarding hepatotoxicity caused by oral KTZ and has since restricted its use to severe cases or when alternatives are unavailable.[18-20] Although the clinical use of KTZ has become less frequent, the solution properties of this drug and its cocrystals were found to be quite interesting. KTZ drug and cocrystals can serve as model compounds to improve understanding of systems with similar physicochemical properties.

KTZ is a lipophilic, weakly basic drug, whose primary dissolution site is the stomach. Fasting gastric pH is expected to play a major role in assisting or inhibiting its dissolution behavior. Kostewicz et al. demonstrated that when gastric pH is elevated, incomplete dissolution of the dose occurred and oral absorption was reduced for the weakly basic compounds studied.[5] In another study of pH-dependent dissolution and absorption of two weakly basic drugs,

dipyridamole and ketoconazole, Zhou et al. found that *in vitro* dissolution and drug plasma concentration profiles in dogs decreased as media and gastric pH increased. Decrease in treatment efficacy due to poor oral drug absorption can have detrimental effects on patient health and prognosis.

Cocrystals with ionizable components are known to impart or alter solubility-pH dependence compared to the parent drug.[21-24] Previous chapters demonstrated how cocrystals of KTZ with acidic coformers can improve solubility and dissolution under elevated pH (pH > 4) conditions. Coformer ionization properties altered the solubility-pH profiles of KTZ cocrystals from that of the parent drug, resulting in reductions in pH-sensitivity in cocrystal solubility and the existence of solubility transition points, pH_{max}. pH_{max} is an important parameter that defines pH regions where cocrystals are thermodynamically stable and where cocrystals have solubility advantage over drug.[22-27] Similar solubility behavior has been observed for other cocrystals consist of basic and acidic components, or components with amphoteric properties in previous studies from Rodriguez lab.[22-24]

KTZ cocrystals demonstrated the ability to generate and maintain supersaturation for up to 30 times above drug solubility during *in vitro* dissolution at pH above pH_{max} (3.6 – 3.8). To better understand how these dissolution advantages can translate to *in vivo* absorption and bioavailability, pH-shift dissolution studies were used to simulate the solution environments the cocrystals are expected to encounter during oral dosing. A simple *in vitro* microdissolution test was developed to assess the pH-dependent absorption risk for weakly basic drugs by Mathias et al. in a 2013 publication.[28] KTZ was one of the drugs used in the study. KTZ dissolved rapidly in SGF pH 2 and was able to remain fully dissolved after the addition of FaSSIF at a supersaturation level around 10 until 75 minutes, after which KTZ slowly precipitated.[28] In the

SGF pH 6 to FaSSIF study, KTZ dissolution was poor and was not able to reach drug solubility during the test.[28] The *in vitro* pH-effect of KTZ was calculated by taking the ratio of the AUC of SGF_{pH6}→FaSSIF and SGF_{pH2}→FaSSIF dissolution.[28] The results are in good agreement with reported clinical (human) pH-effect AUC ratio of KTZ, demonstrating that this dissolution test can provide a quick and effective assessment to predict drug *in vivo* behavior.[28] KTZ cocrystals demonstrated less sensitivity to pH than the drug, and pH-shift dissolution test can help us to better understand and predict how KTZ cocrystals might behave in the gastrointestinal tract.

This study aims to (1) conduct pH-shift dissolution test on KTZ drug and cocrystals to determine the effect of gastric pH on dissolution and supersaturation behavior, (2) assess the potential solution advantages the cocrystals can provide during dissolution and transfer from the gastric to intestinal compartment, and (3) determine KTZ precipitation behavior during dissolution.

Materials and Methods

Materials

Ketoconazole (lot # BS1203355108, 98% purity) was purchased from Bosche Scientific (New Brunswick, NJ) and used as received. Adipic acid (lot # 06807BE, 99% purity), succinic acid (lot # 037K0021, 99% purity), fumaric acid (lot # 09426EE, 99+% purity), acetic acid (lot # 074K3658, 99%), sodium acetate anhydrous (lot # 100K0272), potassium phosphate monobasic (ACS reagent), and sodium chloride (NaCl) (lot # 094K0183, ACS reagent) were purchased from Sigma-Aldrich (St. Louis, MO) and used as received. FaSSIF/FeSSIF/FaSSGF powder was purchased from biorelevant.com (London, United Kingdom) and used as received. HPLC grade methanol, HPLC grade 2-propanol, sodium phosphate monobasic ($NaH_2PO_4 \bullet H_2O$) (lot #

017316), and hydrochloric acid (lot # 2AJK15038, ACS grade) were purchased from Fisher Scientific (Fair Lawn, NJ). Acetone (ACS reagent 99.5%) and phosphoric acid (lot # B0506524, 85+%) were purchased from Acros Organics (NJ) and used as received. Trifluoroacetic acid (spectrophometric grade, 99%) was purchased from Aldrich Company (Milwaukee, WI). NaOH (pellets) was purchased from J.T. Baker (Philipsburg, NJ). Water used in this study was filtered through a Milli-Q Reference Water System from Millipore Co. (Bedford, MA).

Cocrystal Synthesis

1:1 cocrystals of KTZ and the dicarboxylic acid coformers were prepared by reaction crystallization method at room temperature.[29] KTZ-FUM and KTZ-SUC were synthesized in acetone. KTZ-ADP was synthesized in 2-propanol. Full conversion of drug to cocrystal was observed between 24 to 48 hours. The solid phases were verified by X-ray powder diffraction (XRPD) and differential scanning calorimetry (DSC); cocrystal component stoichiometry was verified by HPLC.

Dissolution Media

All aqueous media were prepared at room temperature with DI water filtered by Milli-Q Reference Water System. Simulated gastric fluid (SGF) of two different pH values was prepared. 0.01 M of HCl solution was prepared for SGF at pH 2.08 ± 0.04. Phosphate buffer was prepared with potassium phosphate monobasic and NaOH for SGF at pH 6.03 ± 0.03 to represent elevated gastric pH condition. Concentrated FaSSIF was prepared by using 1.5 times the concentrations of each media component based on the method and composition described by Dressman and coworkers.[30-31] The surfactants used in FaSSIF (lecithin and sodium taurocholate) were from premade FaSSIF/FeSSIF/FaSSGF powders purchased from Biorelevant.com.

Concentrated blank FaSSIF (1.5x) was prepared with the same ingredients and procedure as FaSSIF, except blank FaSSIF did not contain lecithin and sodium taurocholate.

pH-Shift Dissolution

Dissolution setup is based on the Microdissolution pH-Shift Test described in the 2013 publication by Mathias et al.[28] The pH-shift dissolution was conducted in two stages, in order to mimic the transfer from gastric to intestinal compartment. KTZ drug and cocrystals were first dissolved in 7 mL of simulated gastric fluid (SGF) at pH 2 (normal) or pH 6 (elevated) for 20 minutes (min).[28, 30-31] At 20 min, 14 mL of the concentrated (1.5 x) FaSSIF or blank FaSSIF was added to cause a pH-shift to pH 6.5, and dissolution continued till 180 min. The mass of solid used for drug and cocrystal dissolution translates to concentrations between 1.5×10^{-3} and 1.6×10^{-3} M (corresponding to the 200 mg KTZ dose/250 mL) in the initial SGF media, and becomes approximately 5×10^{-4} M following dilution by the addition of the second media.

Dissolution was conducted in 25 mL beaker with magnetic stirring (200 rpm) set in a water bath at 24.8 ± 0.02 °C. Powder of drug or cocrystal used was sieved between 106 – 125 μm. Solution samples (approximately 0.4 mL) were taken with syringe at selected time points both prior and following pH-shift. Sample volume was not replaced. Loss in volume of the initial dissolution media was accounted for in the calculation of theoretical maximum concentrations (fully dissolved). The solution samples were filtered using syringe filter with PVDF membrane of 0.45 μm pore size. The solution concentrations of drug and coformers were analyzed with HPLC after proper dilution with mobile phase. pH during dissolution was also monitored.

High Performance Liquid Chromatography (HPLC)

Solution concentrations of the drug and coformer were analyzed by a Waters HPLC equipped with an UV spectrometer detector. A Waters Atlantis C18 column with the dimensions of 250 x 4.6 mm and 5 µm particle size was used for separation at ambient temperature. The flow rate was set at 1mL/min. Injection volume of 20µL was used for KTZ and FUM, and injection volume of 100µL was used for SUC and ADP. For KTZ-ADP and KTZ-FUM cocrystals and their components, the mobile phase used composed of 60% methanol and 40% water with 0.1% trifluoroacetic acid (TFA). The KTZ component of KTZ-SUC cocrystal was analyzed using mobile phase composed of 60% methanol and 40% water with 0.1% TFA. The SUC component was analyzed using a gradient method with flow rate of 1mL/min starting with mobile phase composed of 25% methanol and 75% water with 0.1% TFA. The composition changes to 80% methanol and 20% water with 0.1% TFA after 2.5 min then reverts back to 25% methanol and 75% water with 0.1% trifluoroacetic acid after 6 min. The wavelengths used for the analytes were as follows: 230 nm for KTZ, 220 nm for FUM, and 210 nm for SUC and ADP.

X-Ray Powder Diffraction (XRPD)

A Rigaku Miniflex X-ray diffractometer (Danverse, MA0) using Cu-Kα radiation, a tube voltage of 30 kV, and a tube current of 15 mA was utilized for analysis and characterization of cocrystals synthesized prior to the dissolution experiments. Measurements were taken from 5° to 40° at a continuous scan rate of 2.5°/min.

Thermal Analysis

TA instrument differential scanning calorimetry (DSC) (Newark, DE) was used to analyze and characterize the solids collected from the cocrystal synthesis via RCM. The heating

rate of the experiments was at 10°C/min under dry nitrogen atmosphere. Standard aluminum sample pans and lids were used for these measurements.

Light Microscopy Studies

KTZ phase separation/precipitation behavior in supersaturated solutions was studied under bright field microscopy using a Leica DMi8 microscope. Sample solution was prepared by dissolving 8 mg of KTZ in 10 mL of 0.01 M HCl solution (pH 2) in a scintillation vial with magnetic stirring. After all solid drug was dissolved, 1.1 mL of 0.1 M NaOH solution was added to solution to raise the pH to 6.5 ± 0.1 and induce supersaturation of drug. 200 μL of the solution was sampled and transferred into a 96-well plate to be observed under the microscope. 20x magnification objective lens was used for the observations.

Results and Discussion

SGF pH 2 to Blank FaSSIF

First, the effect of pH-shift from pH 2 to 6.5 without surfactants was examined. Low gastric pH is favorable for KTZ dissolution and absorption, and at pH 2, the drug is more soluble than the cocrystals. Figure 4.1 shows the KTZ concentration and supersaturation level during cocrystal and drug pH-shift dissolution from SGF pH 2 to blank FaSSIF (pH 6.5) if full dissolution was achieved. The mass of drug and cocrystals used in dissolution is 0.8 mg KTZ equivalent per mL in the initial media, which corresponds to the oral dose of KTZ (200 mg) dissolving in gastric volume of 250 mL.[11, 32-33] This corresponds to KTZ concentrations (fully dissolved) of 1.5 mM in the initial media before pH-shift and 0.5 mM after pH-shift.

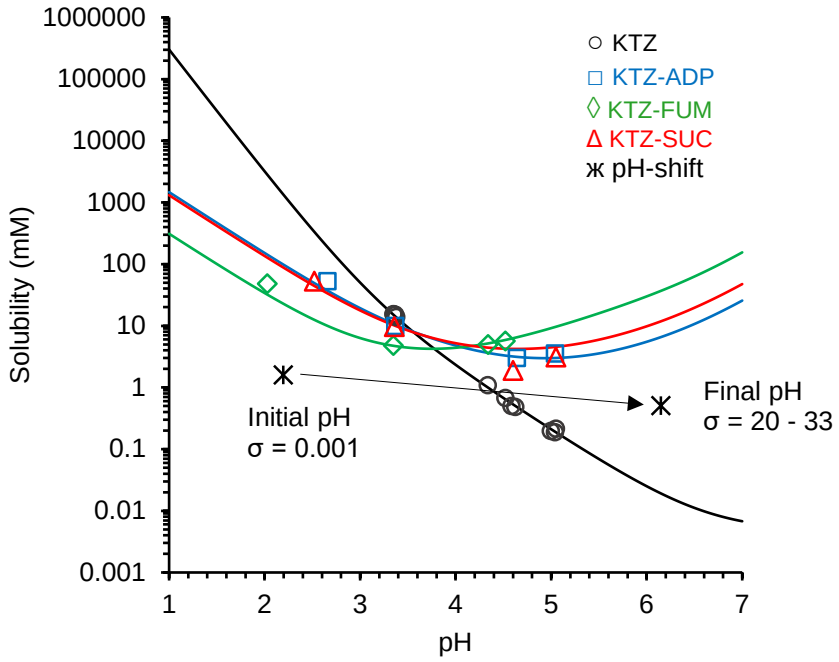

Figure 4.1. KTZ concentration that can be achieved during cocrystal and drug pH-shift dissolution from SGF pH 2 to blank FaSSIF (pH 6.5). KTZ drug and cocrystal solubility-pH profiles (solid lines) from pH 1 to 7 were generated using equations 2.2 and 2.3 and parameter values reported in Chapter 2. Experimental solubility values for drug and cocrystals are presented as symbols: KTZ (○), KTZ-ADP (□), KTZ-FUM (◊), and KTZ-SUC (Δ). The standard errors of experimental solubility values are less than 4% and are within the data symbol. Concentrations of drug and cocrystal before and after pH-shift are indicated by "ж", and pH-shift is indicated by "→". σ in this plot represents the theoretical supersaturation level ($\sigma_{theoretical}$) of KTZ if drug or cocrystal is fully dissolved, and it is equal to $(C/S)_{drug}$. The range of σ values is due to the slight pH variations from the dissolution studies.

Figure 4.1 shows that at initial pH (pH ~ 2.2), both drug and cocrystals can fully dissolve. After the pH-shift (final pH 6.0 - 6.3), KTZ solubility drops dramatically (≤ 0.025 mM), and the drug and cocrystals, if fully dissolved, will generate supersaturations between 20 and 33 with respect to drug. This theoretical supersaturation with respect to drug is represented by $\sigma_{theoretical}$. $\sigma_{theoretical} > 1$ indicates that the solution is supersaturated with KTZ and precipitation of drug is favorable.

The kinetics of precipitation can vary greatly due to many factors including supersaturation, solute concentration, pH, solution composition, stirring, and temperature.[34-38] Supersaturation is a major driving force of KTZ precipitation. As supersaturation levels increase, so does drug precipitation, resulting in lower levels of drug concentration.[25, 27, 38] If drug precipitation is relatively slow, supersaturation can be achieved and maintained for longer periods of time. The ability of drug and cocrystals to maintain supersaturation following pH-shift from pH 2.2 to between pH 6.0 – 6.3 is shown in figure 4.2.

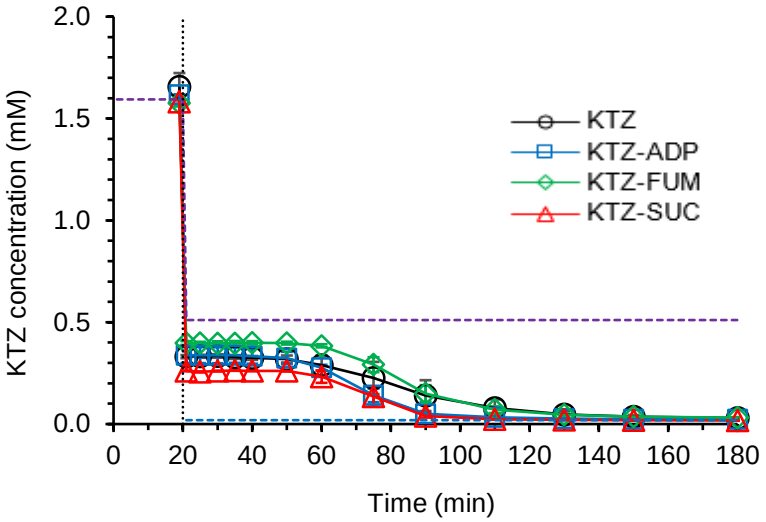

(a)

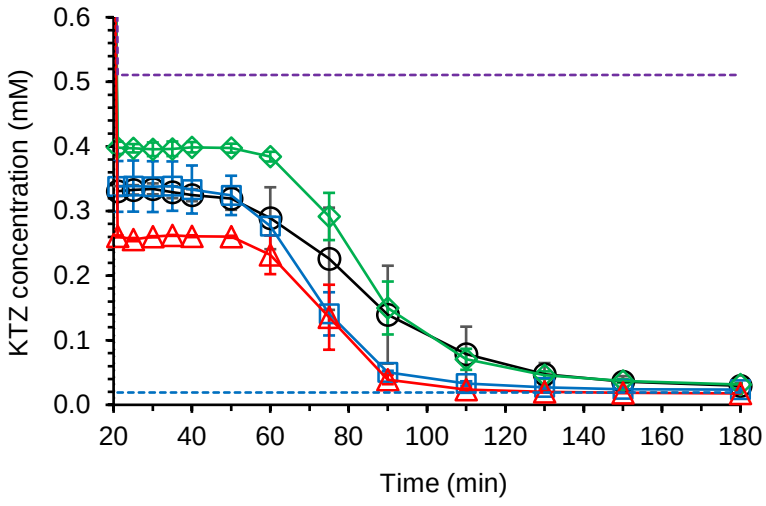

(b)

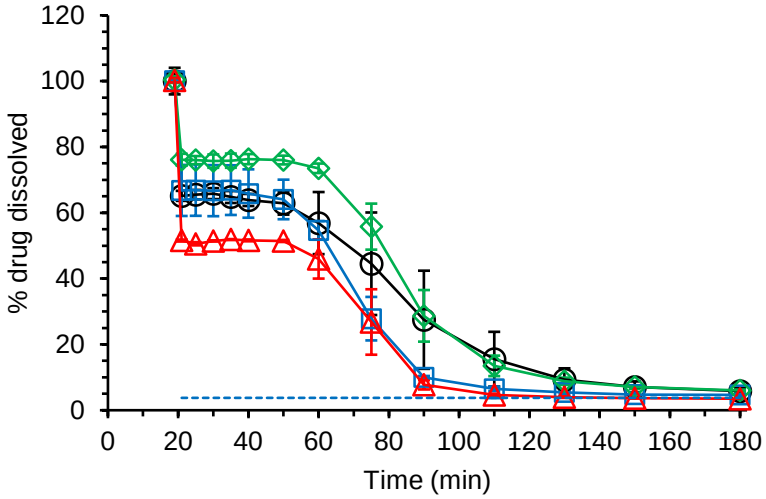

(c)

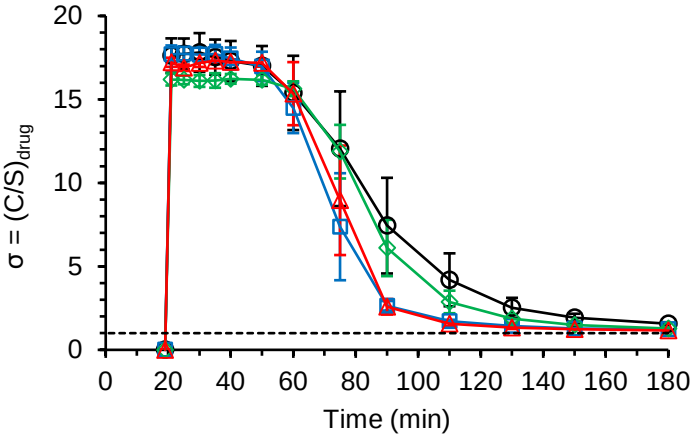

(d)

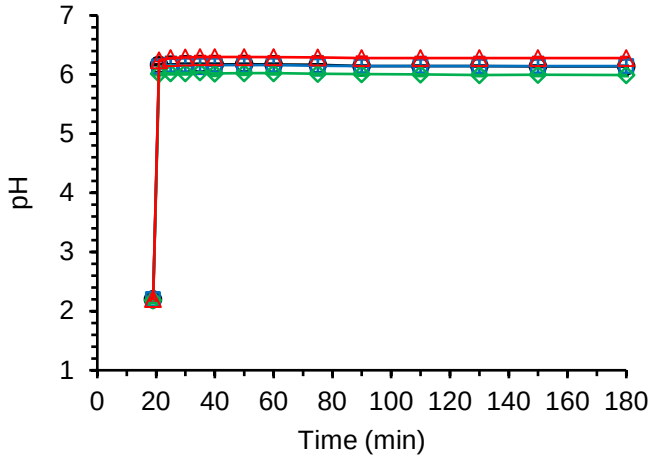

(e)

Figure 4.2. pH-shift dissolution of SGF pH 2 to blank FaSSIF (pH 6.5) for KTZ drug and cocrystals. (a) KTZ concentration-time profile during dissolution. (b) KTZ concentration-time

profile after pH-shift (20 – 180min). (c) Percent drug dissolved (100 × [KTZ] / 0.5 mM after pH-shift) vs. time. (d) KTZ supersaturation vs. time. (e) Solution pH during dissolution. Black dotted vertical line in (a) represents where pH-shift occurred. Purple dashed lines in (a) and (b) indicate the concentration if drug and cocrystals fully dissolve. The drop in theoretical concentration at 20 min indicates the dilution. Blue dashed line in (a) and (b) represents S_{drug} in blank FaSSIF, and in (c) represents 100 × (S_{drug} / 0.5 mM). The black dashed line in (d) indicates where $\sigma = 1$.

Figure 4.2 shows that the cocrystals and drug exhibited similar experimental supersaturation levels (σ_{exp}) and KTZ precipitation behavior during dissolution. Cocrystal or drug added to the initial media dissolved within minutes and remained fully dissolved prior to pH-shift. Concentrations of drug and coformers were measured at 19 min, right before the pH-shift, and the concentrations confirmed full dissolution of drug and cocrystals. Coformer concentrations during dissolution can be found in appendix 4A.

Immediately after pH-shift into blank FaSSIF, a slight cloudiness was observed in the bulk solution. KTZ concentrations dropped below the full dissolution concentration at 0.5 mM ($\sigma_{theoretical} = 20 – 33$) to between 0.25 – 0.4 mM but still generated σ_{exp} between 16 and 18 up to the 50 min time point (about 30 min after the pH-shift). At and after 60 min, KTZ concentrations were observed to decrease, indicating crystallization of drug was occurring.

The presence of a supersaturated plateau region immediately following pH-shift that is below full dissolution but above drug solubility suggests an initial precipitation state. This phase that forms in this state was further evaluated to be a metastable phase, that over time converts to crystalline KTZ, which will be discussed in a subsequent section.

SGF pH 2 to FaSSIF

The differences between gastric and intestinal compartment is not only pH but also the presence of solubilizing agents as physiologically relevant surfactants. In Chapter 3, we have demonstrated that sodium taurocholate and lecithin present in FaSSIF and FeSSIF can enhance

solubility and slow cocrystal to drug conversion. In this section, FaSSIF was used for the pH-shift study to determine the effect of endogenous surfactants on cocrystal conversion kinetics. Figure 4.3 shows the observed and predicted influence of pH with and without surfactants on KTZ drug and cocrystal solubility.

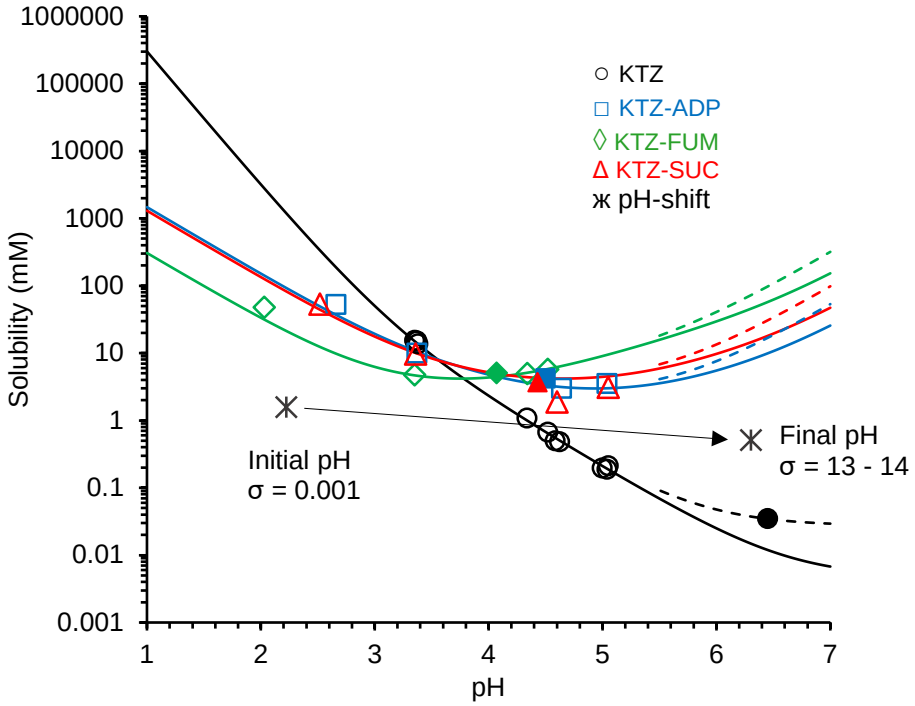

Figure 4.3. KTZ concentration that can be achieved during cocrystal and drug pH-shift dissolution from SGF pH 2 to FaSSIF. Solid curves represent KTZ drug and cocrystal solubility-pH profiles from pH 1 to 7. The influence of surfactants in FaSSIF on drug and cocrystal solubility is represented as dashed lines. Experimental solubility values for drug and cocrystals are presented as symbols: KTZ (○), KTZ-ADP (□), KTZ-FUM (◊), and KTZ-SUC (Δ). Open symbols indicate solubility in aqueous buffer, and closed symbols represent solubility in FaSSIF. The standard errors of experimental solubility values are less than 4% and are within the data symbol. Concentrations of drug and cocrystal before and after pH-shift are indicated by "ж", and pH-shift is indicated by "→". σ in this plot represents the theoretical supersaturation level ($\sigma_{theoretical}$) of KTZ if drug or cocrystal is fully dissolved, and it is equal to $(C/S)_{drug}$. The range of σ values is due to the slight pH variations from the dissolution studies.

Figure 4.3 shows the pH conditions before and after pH-shift, as well as the concentration of drug and cocrystals used in dissolution study relative to their solubility. Drug and cocrystal solubilities are higher in FaSSIF than in blank buffer of the same pH. Both the cocrystals and

drug are fully soluble before the pH-shift. After the pH-shift, cocrystals remain fully soluble but the drug solubility drops below 0.5 mM, with $\sigma_{theoretical}$ between 13 and 14 at full dissolution. $\sigma_{theoretical}$ in FaSSIF is lower than blank FaSSIF due to higher S_{drug}, and this can lead to a slower rate of drug precipitation.

Figures 4.4a and 4.4b show that KTZ concentrations immediately after pH-shift falls to theoretical concentration of 0.5 mM, which indicates full cocrystal and drug dissolution. Bulk pH values were similar for drug and cocrystal dissolution studies, and they increased from around 2.2 to about 6.3 before and after the pH-shift. Unlike blank FaSSIF, the bulk solution remained clear and no cloudiness or precipitation was observed immediately following the pH-shift.

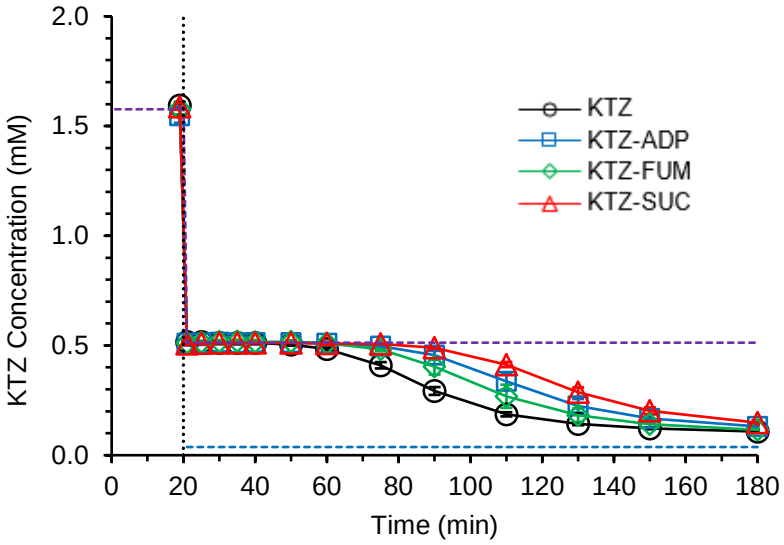

(a)

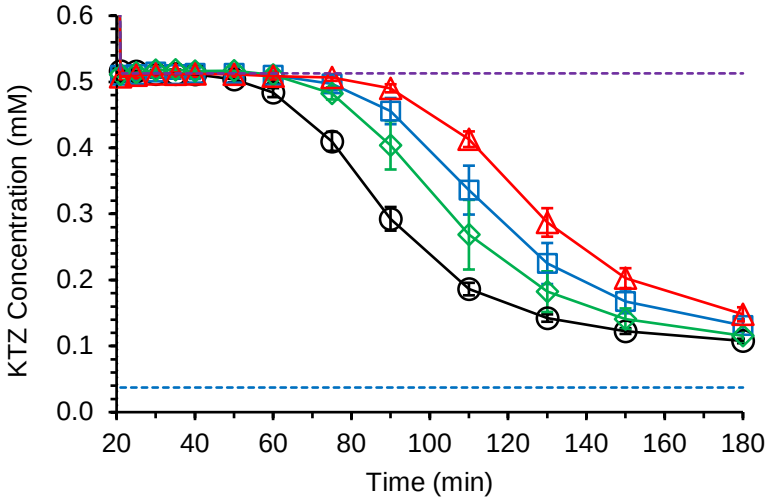
KTZ Concentration (mM)
0.6
0.5
0.4
0.3
0.2
0.1
0.0
20
40
60
80
100
120
140
160
180
Time (min)

(b)

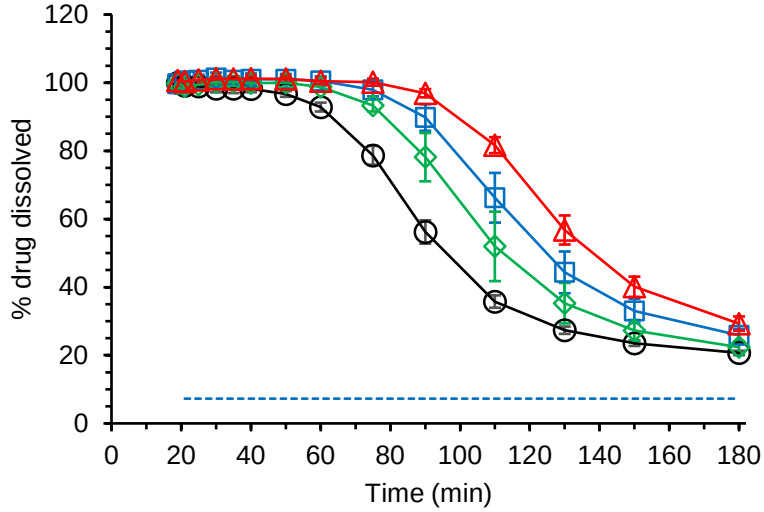
% drug dissolved
120
100
80
60
40
20
0
0
20
40
60
80
100
120
140
160
180
Time (min)

(c)

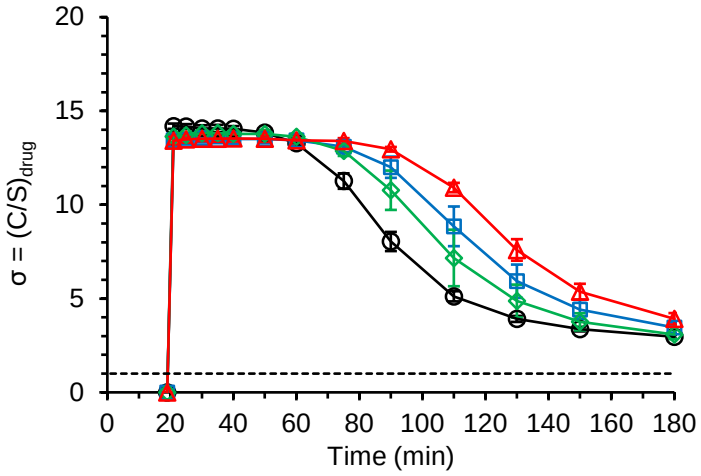
σ = (C/S)drug
20
15
10
5
0
0
20
40
60
80
100
120
140
160
180
Time (min)

(d)

(e)

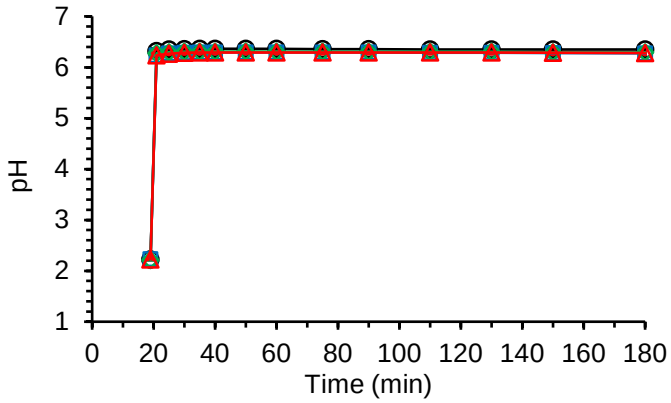

Figure 4.4. pH-shift dissolution of SGF pH 2 to FaSSIF for KTZ drug and cocrystals. (a) KTZ concentration-time profile during dissolution. (b) KTZ concentration-time profile after pH-shift (20 – 180min). (c) Percent drug dissolved (100 × [KTZ] / 0.5 mM after pH-shift) vs. time. (d) KTZ supersaturation vs. time. (e) Solution pH during dissolution. Black dotted vertical line in (a) represents where pH-shift occurred. Purple dashed lines in (a) and (b) indicate the concentration if drug and cocrystals fully dissolve. The drop in theoretical concentration at 20 min indicates the dilution. Blue dashed line in (a) and (b) represents S_{drug} in FaSSIF, and in (c) represents 100 × (S_{drug} / 0.5 mM). The black dashed line in (d) indicates where $\sigma = 1$.

Surfactants in FaSSIF appeared to have a positive effect on cocrystal and drug pH-shift dissolution. KTZ concentrations were higher, supersaturations were lower (13 – 15 in FaSSIF vs. 16 – 18 in blank FaSSIF) and were sustained longer. The initial supersaturation levels (σ_{exp} between 13 and 15) were sustained until the 75 min time point (55 min after pH-shift) for KTZ-SUC and KTZ-ADP, 60 min time point (40 min after pH-shift) for KTZ-FUM, and 50 min time point (30 min after pH-shift) for KTZ drug. By the end of the dissolution (180 min), KTZ concentrations did not drop to drug solubility, but remained supersaturated with σ_{exp} values between 3 and 4.

KTZ drug pH-shift dissolution from SGF pH 2 to FaSSIF from this study was compared with the results from the Mathias et al. study (gastric pH 2 to FaSSIF) at 37°C temperature in figure 4.5.[28]

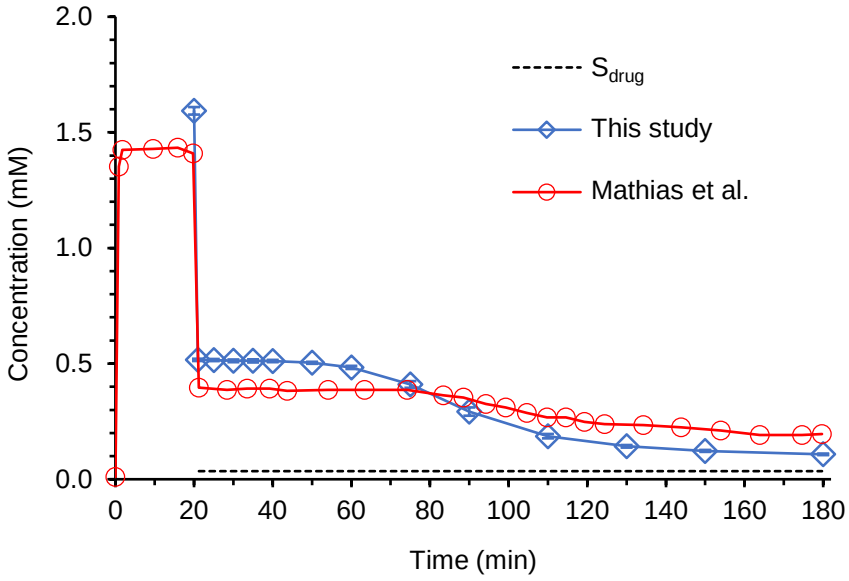

Figure 4.5. KTZ pH-shift dissolution (SGF pH 2 to FaSSIF) comparison between this study and study published by Mathias et al.[28]

The results from this study are in very good agreement with those from Mathias et al. In both cases, KTZ drug dissolved rapidly and completely in the initial media, then remained fully dissolved initially after pH-shift ([KTZ] ≈ 0.5 mM in this study and ≈ 0.4 mM in Mathias et al. study). KTZ was observed to begin precipitating between 60 min and 75 min, reaching final concentration values (at 180 min) of 0.1 mM in both studies.[28] The main differences between the two studies were temperature (25°C in this study vs. 37°C in Mathias et al. study) and analytical methods (HPLC vs. UV probe) for drug concentration measurements.[28]

SGF pH 6 to FaSSIF

Unlike in the previous section pH-shift studies, the dose of KTZ drug is not fully soluble in the initial media of SGF pH 6 (figure 4.6). This resulted in undissolved solid in solution before pH-shift for both cocrystal and drug dissolution studies. The solid could either be from undissolved drug/cocrystal or from cocrystal conversion to drug. In this case, the pH difference from initial to final media was relatively small (< 0.5 pH unit increase), and drug solubility is

higher in final media (FaSSIF) compared to in initial media (SGF pH 6) due to the solubilizing effect of FaSSIF surfactants. Although KTZ has demonstrated poor solubility, dissolution, and oral absorption at this gastric pH,[2, 4-5, 39] all three cocrystals have higher solubilities and can have dissolution advantages over the drug.

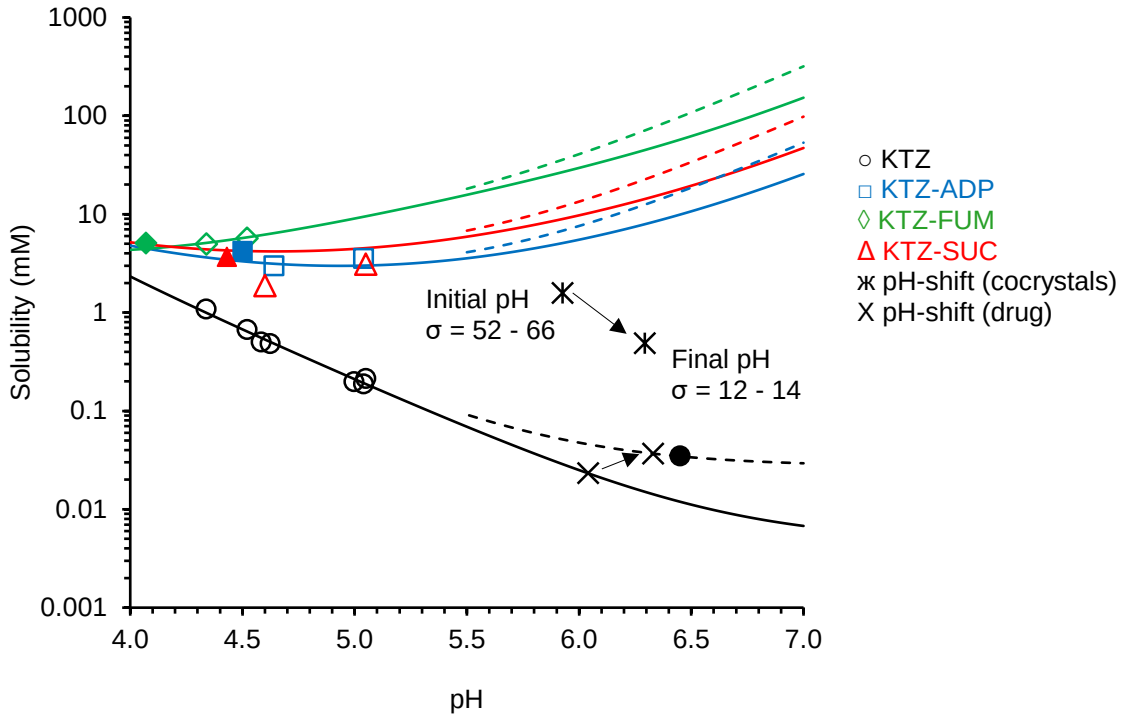

Figure 4.6. KTZ concentration that can be achieved during cocrystal and drug pH-shift dissolution from SGF pH 6 to FaSSIF. Solid curves represent KTZ drug and cocrystal solubility-pH profiles from pH 4 to 7. The influence of surfactants in FaSSIF on drug and cocrystal solubility is represented as dashed lines. Experimental solubility values for drug and cocrystals are presented as symbols: KTZ (○), KTZ-ADP (□), KTZ-FUM (◊), and KTZ-SUC (Δ). Open symbols indicate solubility in aqueous buffer, and closed symbols represent solubility in FaSSIF. The standard errors of experimental solubility values are less than 4% and are within the data symbol. Concentrations of cocrystal before and after pH-shift are indicated by "ж", concentrations of drug before and after pH-shift are indicated by "×", and pH-shift is indicated by "→". σ in this plot represents the theoretical supersaturation level ($\sigma_{theoretical}$) of KTZ if cocrystal is fully dissolved, and it is equal to $(C/S)_{drug}$. The range of σ values is due to the slight pH variations from the dissolution studies. Since KTZ drug cannot dissolve above its thermodynamic solubility, the drug is not expected to achieve supersaturation during dissolution.

Figure 4.6 shows that before pH-shift (pH 5.9 - 6.1), the mass of cocrystal and drug used would be 52 and 66 times above the drug solubility if fully dissolved. This means that cocrystal dissolution can generate supersaturation and undergo solution-mediated conversion to drug prior to pH-shift. After pH-shift, $\sigma_{theoretical}$ values decreased to between 12 and 14.

Drug supersaturation generated by cocrystal dissolution in the initial media can be maintained after pH-shift, and any undissolved solid cocrystals could continue to dissolve in FaSSIF and generate more dissolution advantage (figure 4.7).

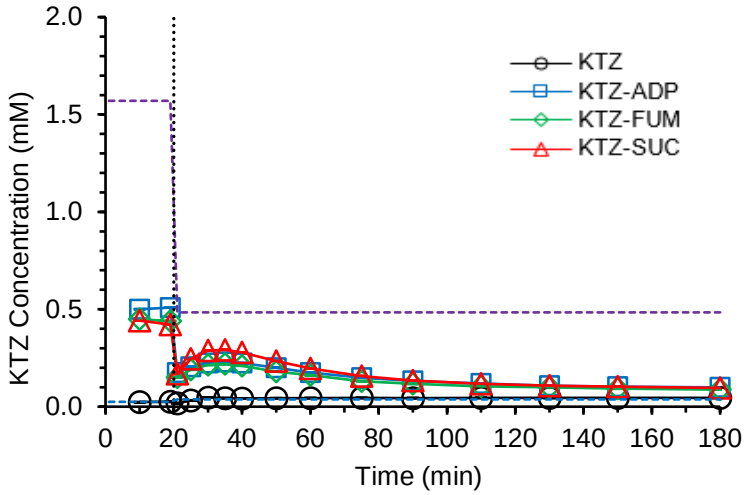

(a)

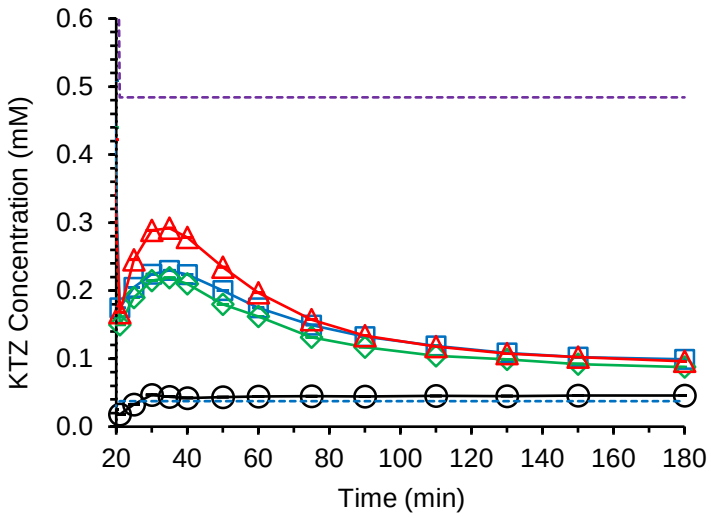
KTZ Concentration (mM)
0.6
0.5
0.4
0.3
0.2
0.1
0.0
20
40
60
80
100
120
140
160
180
Time (min)

(b)

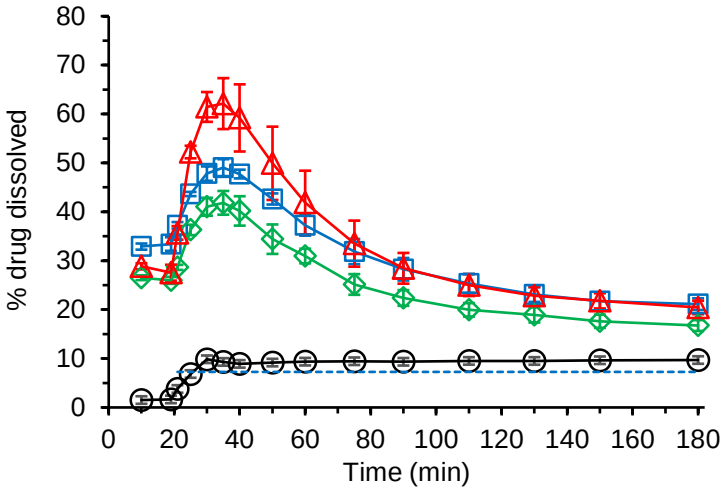
% drug dissolved
80
70
60
50
40
30
20
10
0
0
20
40
60
80
100
120
140
160
180
Time (min)

(c)

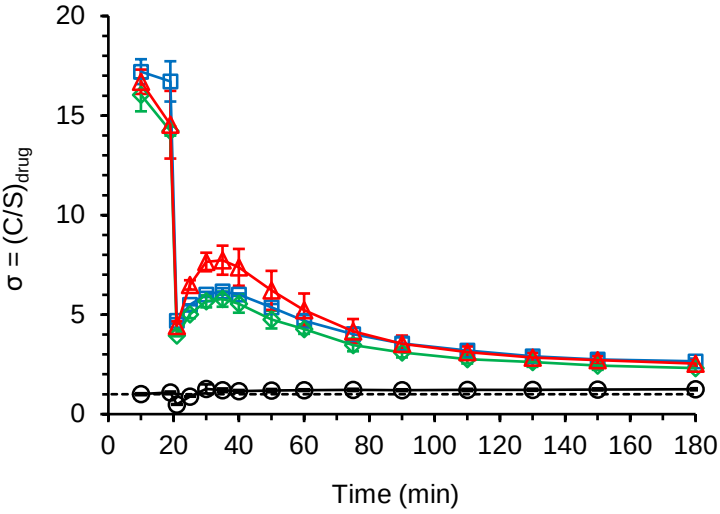
σ = (C/S)drug
20
15
10
5
0
0
20
40
60
80
100
120
140
160
180
Time (min)

(d)

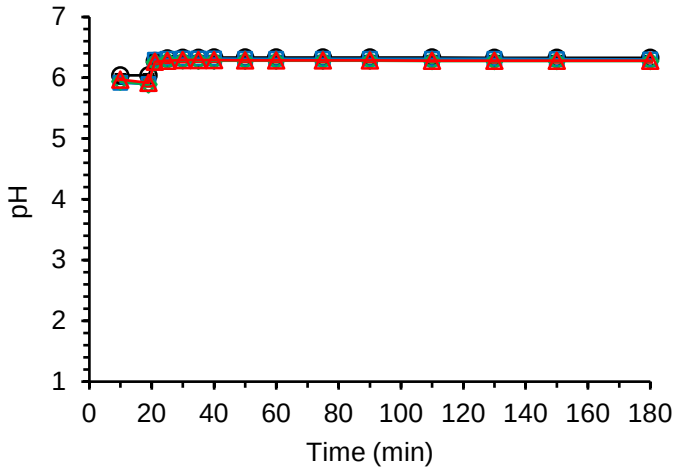

(e)

Figure 4.7. pH-shift dissolution of SGF pH 6 to FaSSIF for KTZ drug and cocrystals. (a) KTZ concentration-time profile during dissolution. (b) KTZ concentration-time profile after pH-shift (20 – 180min). (c) Percent drug dissolved (100 × [KTZ] / 1.5 mM before pH-shift and 100 × [KTZ] / 0.5 mM after pH-shift) vs. time. (d) KTZ supersaturation vs. time. (e) Solution pH during dissolution. Black dotted vertical line in (a) represents where pH-shift occurred. Purple dashed lines in (a) and (b) indicate the concentration if drug and cocrystals fully dissolve. The drop in theoretical concentration at 20 min indicates the dilution. Blue dashed line in (a) and (b) represents S_{drug} in FaSSIF, and in (c) represents 100 × (S_{drug} / 0.5 mM) after pH-shift. The black dashed line in (d) indicates where $\sigma = 1$.

Figure 4.7 shows that cocrystal dissolution generated much higher KTZ concentrations in solution compared to pure drug dissolution. KTZ concentrations from cocrystal dissolution were observed to increase immediately following the pH-shift, indicating that there might have been some undissolved cocrystal prior to pH-shift. Cocrystals generated σ_{exp} values between 14 and 18 before the pH-shift and between 5 and 8 after the pH-shift at C_{max} (figure 4.7d). The cocrystals also maintained σ_{exp} between 2 and 3 by the end of dissolution (180 min).

Pure drug dissolution in SGF pH 6 to FaSSIF showed much lower concentrations of KTZ compared to the dissolution starting with low initial pH (SGF pH 2), and similar observation can also be seen in the study by Marthias et al. (figure 4.8).[28]

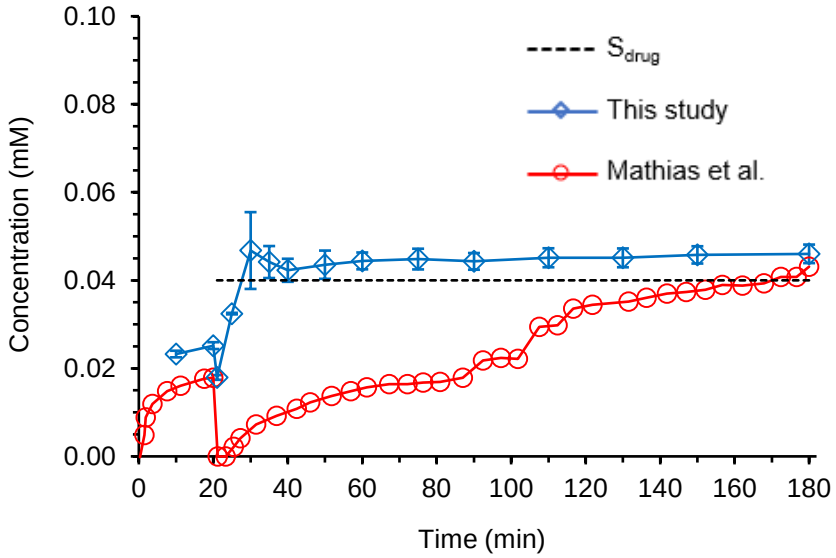

Figure 4.8. KTZ pH-shift dissolution (SGF pH 6 to FaSSIF) comparison between this study and study published by Mathias et al.[28]

In this study, KTZ concentration in FaSSIF quickly reached 0.046 mM (within 10 min) after pH-shift, and remained around drug solubility for the duration of the study. In the Mathias et al. study, KTZ concentration initially appeared to drop to zero after pH-shift, then slowly increased over time toward drug solubility, reaching final concentration around 0.043 mM by the end of dissolution.[28] Both studies reached similar final drug concentration values by 180 min, which corresponds to KTZ solubility in FaSSIF (between 0.026 and 0.05 mM).[31, 40-42] Although the two studies appeared to exhibit some differences in KTZ concentrations during dissolution, it is important to note that the concentration values measured are very small (≤ 0.05 mM) making accurate quantifications more difficult. This may have contributed to some of the differences observed.

Elevated gastric pH condition is where the KTZ cocrystals truly demonstrated advantages over the drug. While the basic drug struggled to dissolve under the high pH conditions, the

cocrystals were able to generate much higher drug levels both before and after pH-shift. KTZ cocrystals reduced the negative impact of elevated pH on drug dissolution behavior.

Drug and Cocrystal Dissolution C_{max} and AUC

Values of solution pH, KTZ C_{max}, and σ_{max} (C_{max}/S_{drug}) before pH-shift are summarized in table 4.1.

Table 4.1. Dissolution pH, KTZ C_{max}, and σ_{max} before pH-shift under different media conditions.

Drug/ Cocrystal	Media	pH	C_{max} (mM)	% drug dissolved[a]
KTZ	pH 2 → Blank FaSSIF	2.20 ± 0.01	1.66 ± 0.07	100
	pH 2 → FaSSIF	2.23 ± 0.01	1.59 ± 0.02	100
	pH 6 → FaSSIF	6.04 ± 0.02	0.025 ± 0.001	2
KTZ-ADP	pH 2 → Blank FaSSIF	2.21 ± 0.06	1.616 ± 0.002	100
	pH 2 → FaSSIF	2.23 ± 0.02	1.55 ± 0.03	100
	pH 6 → FaSSIF	5.90 ± 0.03	0.51 ± 0.02	34
KTZ-FUM	pH 2 → Blank FaSSIF	2.18 ± 0.05	1.58 ± 0.02	100
	pH 2 → FaSSIF	2.21 ± 0.01	1.58 ± 0.02	100
	pH 6 → FaSSIF	5.89 ± 0.03	0.449 ± 0.008	27
KTZ-SUC	pH 2 → Blank FaSSIF	2.20 ± 0.02	1.58 ± 0.01	100
	pH 2 → FaSSIF	2.23 ± 0.01	1.59 ± 0.01	100
	pH 6 → FaSSIF	5.92 ± 0.06	0.44 ± 0.01	29

a. % drug dissolved calculated with 100 × $[KTZ]_{Cmax}$ before pH-shift / 1.5 mM.

Table 4.1 shows that before pH-shift, KTZ drug and cocrystals were 100% dissolved in SGF pH 2 media. Full dissolution did not occur in SGF pH 6, the cocrystals were able to

achieve between 27% and 34% drug dissolved before pH-shift, which are much improved compared to pure drug, which only achieved about 2% dissolved in SGF pH 6.

Values of final solution pH, KTZ C_{max}, σ_{max} (supersaturation at C_{max}), AUC, and cocrystal to drug AUC ratio after the pH-shift are summarized in table 4.2. Drug and cocrystal dissolution achieved similar C_{max}, σ_{max}, and AUC values after pH-shift from SGF pH 2. In dissolution SGF pH 6 → FaSSIF, the cocrystals demonstrated dissolution advantages over drug, achieving 3 – 4 times higher AUC values and σ_{max} values between 5 and 8 after pH-shift. Higher extent of KTZ dissolution achieved by the cocrystals under elevated pH condition can lead to higher drug levels (5 – 8 fold increase) in the intestinal compartment for oral absorption.

Table 4.2. Final dissolution pH, KTZ C_{max}, σ_{max}, AUC, and cocrystal to drug AUC ratio following pH-shift under different media conditions.

Drug/ Cocrystal	Media	pH	C_{max} (mM)	σ_{max} [a]	AUC (mM × min)	$AUC_{cc/drug}$
KTZ	pH 2 → Blank FaSSIF	6.16 ± 0.01	0.334 ± 0.008	17.8 ± 0.5	24 ± 5	--
	pH 2 → FaSSIF	6.36 ± 0.01	0.516 ± 0.005	14.3 ± 0.1	46 ± 1	--
	pH 6 → FaSSIF	6.33 ± 0.01	0.046 ± 0.002	1.25 ± 0.06	7.0 ± 0.4	--
KTZ-ADP	pH 2 → Blank FaSSIF	6.15 ± 0.01	0.339 ± 0.004	18 ± 2	20 ± 1	0.8 ± 0.2
	pH 2 → FaSSIF	6.29 ± 0.01	0.515 ± 0.008	13.6 ± 0.2	57 ± 2	1.23 ± 0.06
	pH 6 → FaSSIF	6.31 ± 0.01	0.230 ± 0.008	6.2 ± 0.2	23 ± 1	3.2 ± 0.2
KTZ-FUM	pH 2 → Blank FaSSIF	6.01 ± 0.01	0.399 ± 0.008	16.2 ± 0.3	29 ± 2	1.2 ± 0.2
	pH 2 → FaSSIF	6.30 ± 0.01	0.518 ± 0.008	13.8 ± 0.2	53 ± 3	1.14 ± 0.07
	pH 6 → FaSSIF	6.28 ± 0.01	0.22 ± 0.01	5.8 ± 0.3	20 ± 1	2.9 ± 0.2
KTZ-SUC	pH 2 → Blank FaSSIF	6.29 ± 0.01	0.262 ± 0.001	17.32 ± 0.05	16 ± 1	0.7 ± 0.1
	pH 2 → FaSSIF	6.29 ± 0.01	0.512 ± 0.004	13.6 ± 0.1	61.2 ± 0.8	1.33 ± 0.04
	pH 6 → FaSSIF	6.29 ± 0.01	0.29 ± 0.02	7.7 ± 0.7	24 ± 2	3.5 ± 0.4

b. $\sigma_{max} = C_{max}/S_{drug}$. S_{drug} values are predicted using equations and parameter values established in Chapter 2 and Chapter 3.

A comparison of KTZ C_{max} from drug and cocrystal pH-shift dissolution studies in figure 4.9 shows the advantages of KTZ cocrystals.

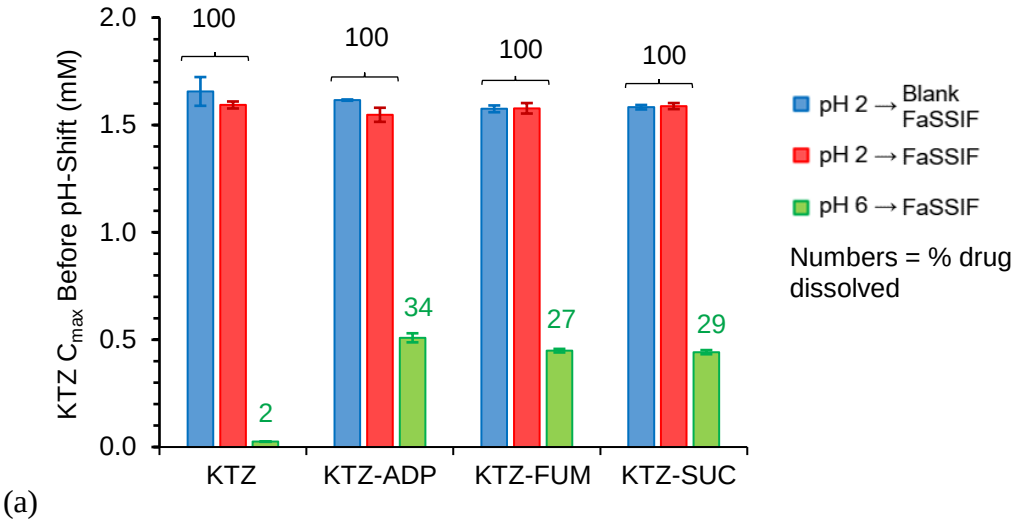

(a)

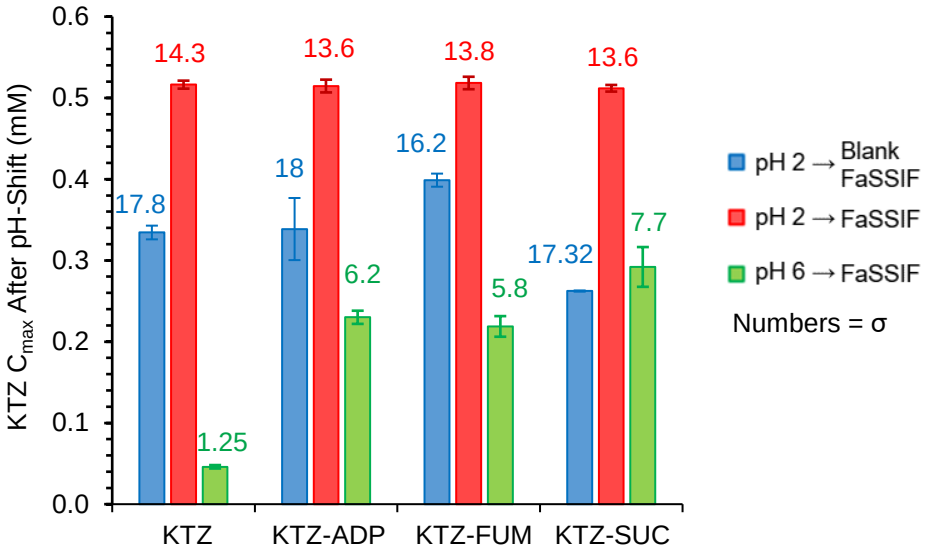

(b)

Figure 4.9. KTZ C_{max} (a) before and (b) after pH-shift for drug and cocrystal dissolution. Numbers on top of columns in (a) indicate % drug dissolved at C_{max} which is equal to 100 × $[KTZ]_{Cmax}$ / 1.5 mM, and in (b) indicate σ_{max} values (C_{max}/S_{drug}). pH values in legend indicate initial media pH. Error bars indicate standard errors.

The cocrystals and drug had similar performance during dissolution when the initial media pH was low (figures 4.2, 4.4, and 4.9). Cocrystals, in most cases, exhibited similar C_{max} values as the drug for dissolution starting with SGF pH 2. The exception being KTZ-SUC in blank FaSSIF, which achieved a lower C_{max} value compared to the drug. C_{max} values in blank

FaSSIF are lower than those in FaSSIF following pH-shift from SGF pH 2 for both drug and cocrystals. This correlates with the initial drop in drug concentration to below full dissolution immediately after pH-shift into blank FaSSIF, and the formation of metastable drug forms during this time. High levels of supersaturation in solution can cause phase separation and metastable forms to occur prior to drug crystallization.[35, 43-44] This precipitation behavior is described in the next section.

AUC values for cocrystals and drug were calculated between time points 21 and 180 min (after pH-shift) and shown in figure 4.10a. AUC can be an indicator of KTZ oral absorption and bioavailability since it quantifies the overall exposure of drug under pH and endogenous surfactants conditions of the small intestine, where the KTZ is absorbed. Cocrystals show superior performance in FaSSIF following pH-shift from SGF pH 6, and their AUC values are 3 to 4 times higher than the drug. This suggests that cocrystals may improve oral absorption of KTZ, in particular under elevated gastric pH conditions.

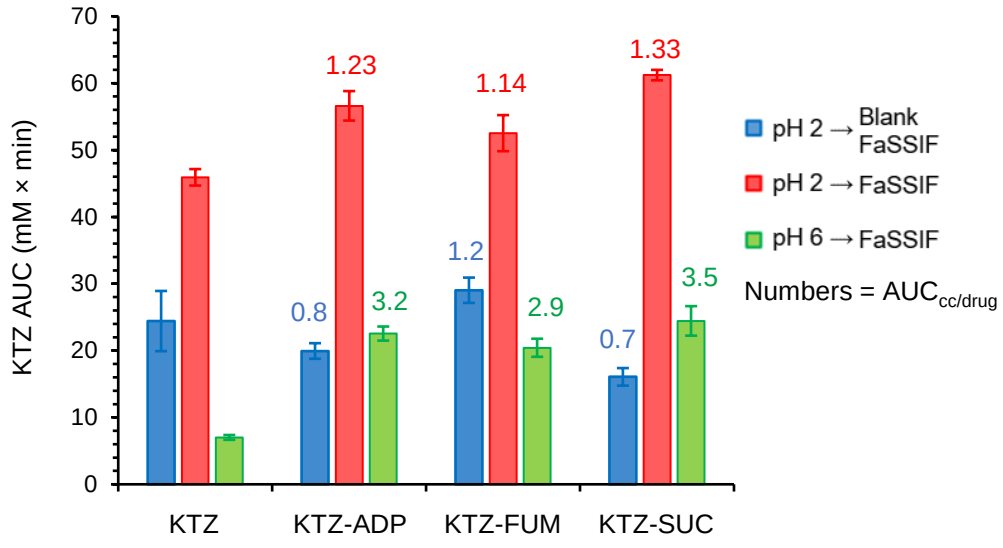

(a)

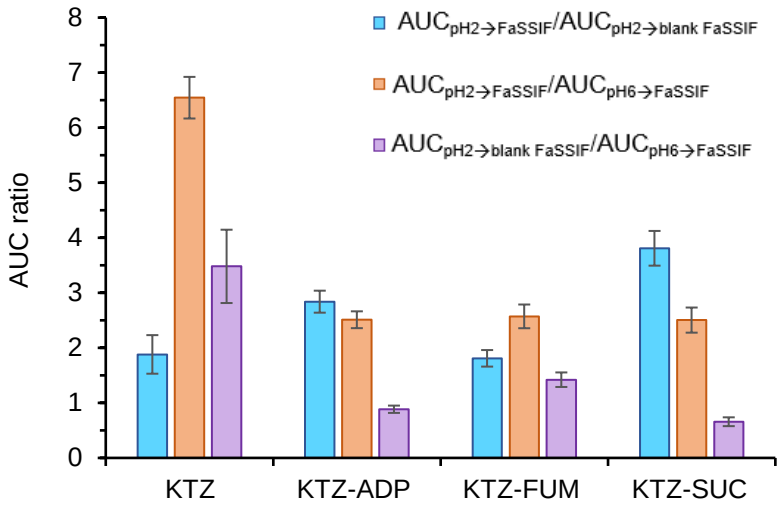

(b)

Figure 4.10. (a) KTZ AUC after pH-shift (21 – 180 min) for drug and cocrystal dissolution. Number on top of the column indicates AUC ratio of cocrystal to drug ($AUC_{cc/drug}$). (b) Cocrystal and drug AUC ratio in different media.

Dissolution in SGF pH 6 to FaSSIF exhibited the lowest σ_{max} values, and cocrystal dissolution led to supersaturation that was sustained for the entire duration of this study. As a result, cocrystal AUC in pH 6 → FaSSIF were 3 – 4 times higher than the drug (figure 4.10a). Cocrystal and drug AUC ratios in figure 4.10b show that cocrystal dissolution appears to be less sensitive to pH than the drug. Drug dissolution showed more than 6 fold difference between $AUC_{pH2\rightarrow FaSSIF}$ and $AUC_{pH6\rightarrow FaSSIF}$, while the cocrystal AUC values changed only about 2.5 fold. Cocrystal $AUC_{pH2\rightarrow blank\ FaSSIF}/AUC_{pH6\rightarrow FaSSIF}$ and $AUC_{pH2\rightarrow FaSSIF}/AUC_{pH6\rightarrow FaSSIF}$ ratios are less than half of those of the drug, and this implies that the cocrystals may exhibit less variability in dissolution and bioavailability based on gastric pH conditions than the drug.

Cocrystal $AUC_{pH2\rightarrow FaSSIF}/AUC_{pH2\rightarrow blank\ FaSSIF}$ ratios show more variability for KTZ-ADP and KTZ-SUC, while KTZ-FUM exhibited a similar AUC ratio as the drug. Since KTZ cocrystals and drug were fully dissolved in SGF pH 2, the variability of AUC after pH-shift is dependent on the precipitation kinetic of the drug rather than cocrystal dissolution. KTZ

cocrystals have shown clear advantages with elevated gastric pH condition, which is known to pose serious problems for KTZ oral absorption.[2, 4, 39]

The study of Mathias et al. reported KTZ pH-effect ratio of the AUC values of the full dissolution profiles (0 to 180 min) from gastric to intestinal transfer ($AUC_{SGFpH6\rightarrow FaSSIF}/AUC_{SGFpH2\rightarrow FaSSIF}$) to be 0.22, and this was compared to the clinical ratio of 0.19.[28] The AUC in our work was determined after pH shift (21 to 180 min), but they can still be used to understand the effect of gastric pH on KTZ exposure in the intestinal environment. The after pH-shift AUC ratios (SGF pH6 → FaSSIF vs. SGF pH2 → FaSSIF) for KTZ drug, KTZ-ADP, KTZ-FUM, and KTZ-SUC are: 0.15, 0.40, 0.39, and 0.40, respectively. Larger AUC ratio values of the cocrystals indicate that the pH-effect on cocrystals are less pronounced than the drug.

Metastable Phases of KTZ During Precipitation

The solution behavior of KTZ in blank FaSSIF immediately following pH-shift suggested that metastable form of KTZ have formed. A highly supersaturated solution can undergo liquid-liquid phase separation, which is a process also known as spinodal decomposition, prior to crystallization.[35, 43-49] This liquid-liquid phase separation can be induced by rapid generation of high supersaturation with respect to drug.[43-44, 46, 50] In the case of KTZ, this can be accomplished by rapidly increase pH of a drug solution from 2 to 6.5 with the addition of NaOH, generating high supersaturation level of drug ($\sigma = 150$). The previously clear drug solution immediately turned cloudy upon NaOH addition, similar to what was observed during pH-shift dissolution from pH 2 to blank FaSSIF. A sample of this solution was taken and observed under the microscope. A few of those images are presented below to show the progression of KTZ precipitation.

Sample solution under the microscope was initially too cloudy to make out any clear image. After about 10 to 15 min, the solution was settled enough that liquid-like droplets could be seen on the bottom of the well. This confirmed that KTZ does indeed undergo liquid-liquid phase separation under high supersaturation conditions. The phase separated droplets gradually increased in size and began merging with each other, as can be observed in figure 4.11 as the island-like formations. Also present were smaller spherical phases, which gradually increased in size and number with time but did not appear to merge with each other. During this time period, no crystalline drug was observed.

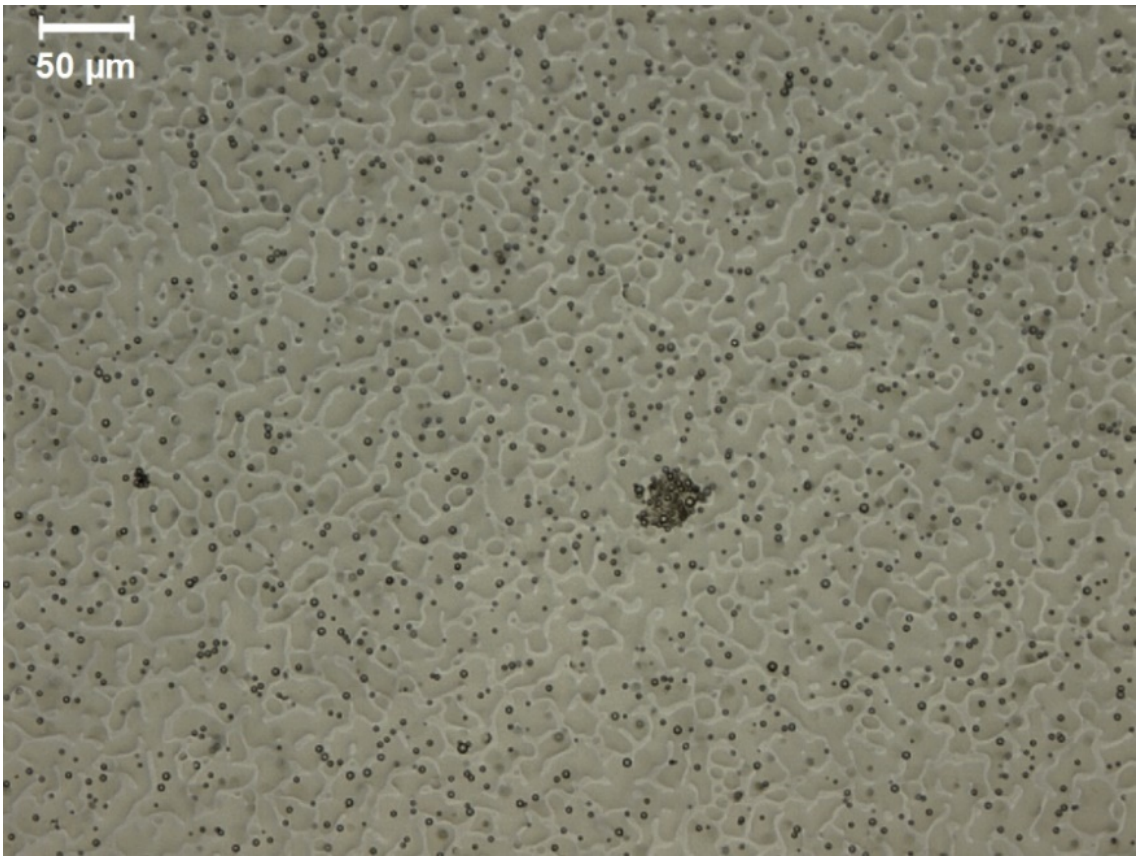

Figure 4.11. Islands and spherical domains of phase separated KTZ. The photo was taken at 40 min following the pH shift from 2 to 6.5.

At 180 min (figure 4.12), the liquid-like phases formed islands as droplets merged, while the spherical phase grew in size and number. Small KTZ crystals began to form (< 30 μm) by this time. Figure 4.12 shows two of the crystals.

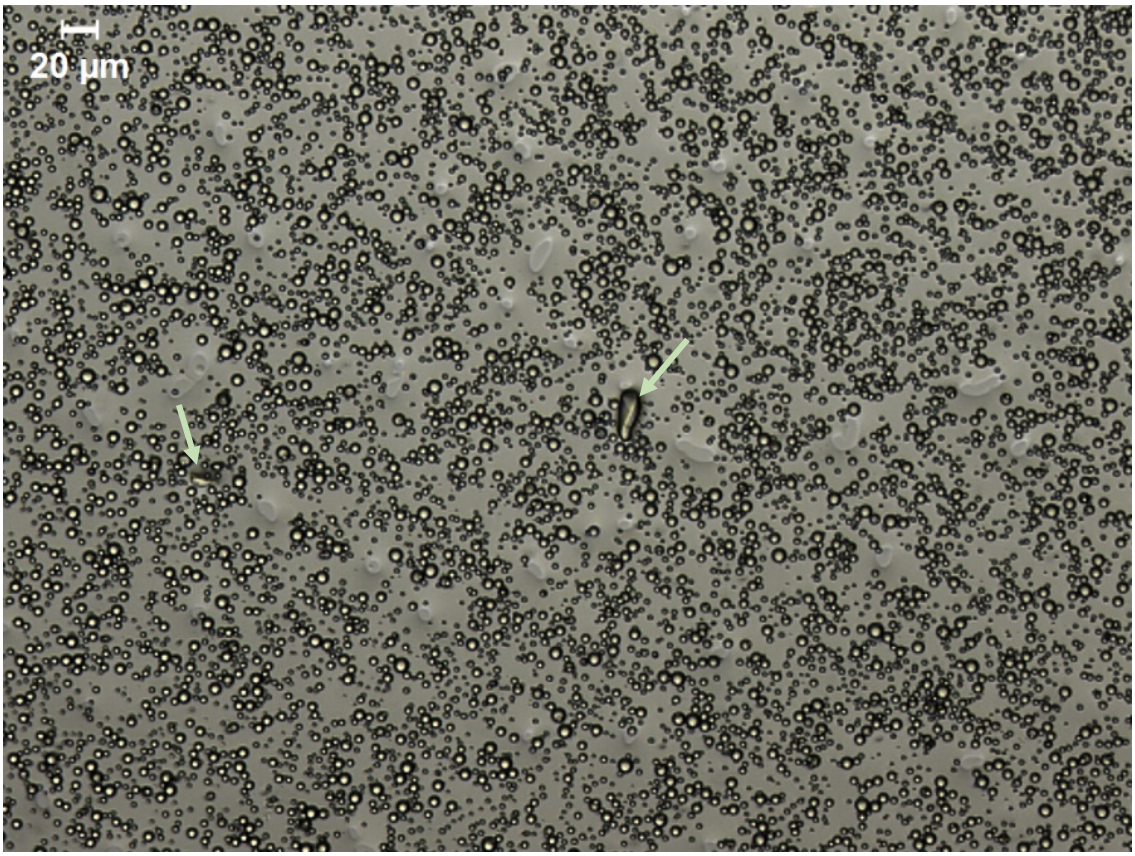

Figure 4.12. Metastable forms of KTZ observed 3 hours after pH-shift. The liquid phase has merged into islands. The spheres are larger in size and more numerous. Drug crystals began to form (indicated by arrows).

The small crystals of KTZ grew in solution over time, and they became clearly visible and much larger in size (60 – 90 μm) by 6 hours (figure 4.13). As the crystals grew, the liquid-like phase receded from the growing crystals, and the spheres also disappeared from that area. This is likely due to the metastable phases converting to drug crystals.

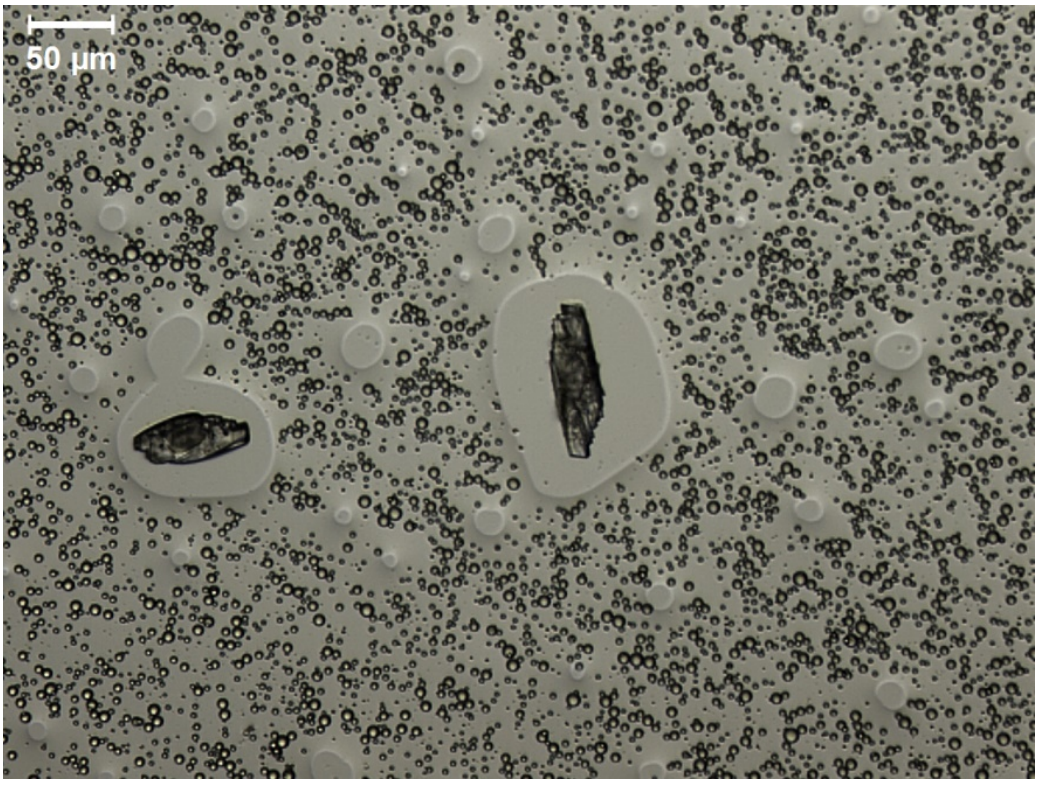

Figure 4.13. Metastable phases formed at high supersaturations convert to crystals. After 6 hours, the KTZ crystals have grown significantly in size. As crystals grew, the surrounding metastable phases are depleted.

Formation of metastable drug forms may be favorable for oral absorption *in vivo*. These metastable KTZ phases exhibit higher solubility than the crystalline form, and their formation can delay the onset of crystallization thus allowing higher levels of drug exposure. Future studies will investigate the conditions under which these metastable states form, and their compositions and structures. This is beyond the scope of this chapter.

Conclusion

pH-shift dissolution studies that simulated fasting gastric and intestinal pH conditions demonstrated the advantages of KTZ cocrystals over the dug. The most important improvements in dissolution behavior were shown by cocrystals under SGF pH 6 condition, where the drug

dissolution was very poor and could lead to poor oral absorption *in vivo*. Supersaturation of KTZ achieved by cocrystals (between 5 and 8 fold) can lead to oral absorption enhancement under elevated gastric pH conditions and improve bioavailability for this drug. Under normal fasting gastric pH conditions (pH 2), the cocrystal and drug dissolution exhibited similar solution behavior with some differences in KTZ concentration vs time profiles following the pH-shift in FaSSIF. These studies suggest that cocrystals may enhance the oral absorption of KTZ and mitigate the effect of elevated gastric pH.

KTZ goes through metastable phases during its precipitation prior to crystallization of the drug at high supersaturation levels induced by pH changes. These metastable phases exhibit higher solubility than crystalline drug, and may also enhance oral absorption. Additional studies are needed to determine the properties of these metastable phases and what conditions are required for their formation.

Acknowledgment

Research reported in this publication was partially supported by the National Institute of General Medical Sciences of the National Institutes of Health under award number R01GM107146. The content is solely the responsibility of the authors and does not necessarily represent the official views of the National Institutes of Health. We also gratefully acknowledge partial financial support from the College of Pharmacy at the University of Michigan.

References

1. Mitra, A.; Kesisoglou, F., Impaired Drug Absorption Due to High Stomach pH: A Review of Strategies for Mitigation of Such Effect To Enable Pharmaceutical Product Development. *Molecular Pharmaceutics* **2013,** *10* (11), 3970-3979.

2. Zhou, R.; Moench, P.; Heran, C.; Lu, X.; Mathias, N.; Faria, T. N.; Wall, D. A.; Hussain, M. A.; Smith, R. L.; Sun, D., pH-Dependent Dissolution in Vitro and Absorption in Vivo of Weakly Basic Drugs: Development of a Canine Model. *Pharmaceutical Research* **2005,** *22* (2), 188-192.

3. Kostewicz, E. S.; Wunderlich, M.; Brauns, U.; Becker, R.; Bock, T.; Dressman, J. B., Predicting the precipitation of poorly soluble weak bases upon entry in the small intestine. *Journal of Pharmacy and Pharmacology* **2004,** *56* (1), 43-51.

4. Van der Meer, J. W. M.; Keuning, J. J.; Scheijgrond, H. W.; Heykants, J.; Van Cutsem, J.; Brugmans, J., The influence of gastric acidity on the bio-availability of ketoconazole. *Journal of Antimicrobial Chemotherapy* **1980,** *6* (4), 552-554.

5. Kostewicz, E. S.; Brauns, U.; Becker, R.; Dressman, J. B., Forecasting the Oral Absorption Behavior of Poorly Soluble Weak Bases Using Solubility and Dissolution Studies in Biorelevant Media. *Pharmaceutical Research* **2002,** *19* (3), 345-349.

6. Sugawara, M.; Kadomura, S.; He, X.; Takekuma, Y.; Kohri, N.; Miyazaki, K., The use of an in vitro dissolution and absorption system to evaluate oral absorption of two weak bases in pH-independent controlled-release formulations. *European Journal of Pharmaceutical Sciences* **2005,** *26* (1), 1-8.

7. Budha, N. R.; Frymoyer, A.; Smelick, G. S.; Jin, J. Y.; Yago, M. R.; Dresser, M. J.; Holden, S. N.; Benet, L. Z.; Ware, J. A., Drug Absorption Interactions Between Oral Targeted Anticancer Agents and PPIs: Is pH-Dependent Solubility the Achilles Heel of Targeted Therapy? *Clinical Pharmacology & Therapeutics* **2012,** *92* (2), 203-213.

8. *Oral Drug Absorption: Prediction and Assessment*. Marcel Dekker, Inc: 2000.

9. Feldman, M.; Barnett, C., Fasting gastric pH and its relationship to true hypochlorhydria in humans. *Digestive Diseases and Sciences* **1991,** *36* (7), 866-869.

10. Dressman, J.; Berardi, R.; Dermentzoglou, L.; Russell, T.; Schmaltz, S.; Barnett, J.; Jarvenpaa, K., Upper Gastrointestinal (GI) pH in Young, Healthy Men and Women. *Pharmaceutical Research* **1990,** *7* (7), 756-761.

11. Mudie, D. M.; Amidon, G. L.; Amidon, G. E., Physiological parameters for oral delivery and in vitro testing. *Molecular pharmaceutics* **2010,** *7* (5), 1388-1405.

12. Lake-Bakaar, G.; Quadros, E.; Beidas, S.; Elsakr, M.; Tom, W.; Wilson, D. E.; Dincsoy, H. P.; Cohen, P.; Straus, E. W., Gastric Secretory Failure in Patients with the Acquired Immunodeficiency Syndrome (AIDS). *Annals of Internal Medicine* **1988,** *109* (6), 502-504.

13. Welage, L. S.; Carver, P. L.; Revankar, S.; Pierson, C.; Kauffman, C. A., Alterations in Gastric Acidity in Patients Infected with Human Immunodeficiency Virus. *Clinical Infectious Diseases* **1995,** *21* (6), 1431-1438.

14. Oji, C.; Chukwuneke, F., Evaluation and treatment of oral candidiasis in HIV/AIDS patients in Enugu, Nigeria. *Oral and Maxillofacial Surgery* **2008,** *12* (2), 67-71.

15. Barchiesi, F.; Giacometti, A.; Arzeni, D.; Branchesi, P.; Crescenzi, G.; Ancarani, F.; Scalise, G., Fluconazole and Ketoconazole in the Treatment of Oral and Esophageal Candidiasis in AIDS Patients. *Journal of Chemotherapy* **1992,** *4* (6), 381-386.

16. Lake-Bakaar, G.; Tom, W.; Lake-Bakaar, D.; Gupta, N.; Beidas, S.; Elsakr, M.; Straus, E., Gastropathy and ketoconazole malabsorption in the acquired immunodeficiency syndrome (AIDS). *Ann Intern Med* **1988,** *109* (6), 471-473.

17. Gupta, A. K.; Sauder, D. N.; Shear, N. H., Antifungal agents: an overview. Part I. *Journal of the American Academy of Dermatology* **1994,** *30* (5), 677-698.

18. Gupta, A. K.; Lyons, D. C. A., The Rise and Fall of Oral Ketoconazole. *Journal of Cutaneous Medicine and Surgery* **2015,** *19* (4), 352-357.

19. FDA Drug Safety Communication: FDA limits usage of Nizoral (ketoconazole) oral tablets due to potentially fatal liver injury and risk of drug interactions and adrenal gland problems. https://www.fda.gov/Drugs/DrugSafety/ucm362415.htm.

20. FDA Drug Safety Communication: FDA warns that prescribing of Nizoral (ketoconazole) oral tablets for unapproved uses including skin and nail infections continues; linked to patient death. https://www.fda.gov/Drugs/DrugSafety/ucm500597.htm.

21. Alhalaweh, A.; Roy, L.; Rodríguez-Hornedo, N.; Velaga, S. P., pH-Dependent Solubility of Indomethacin–Saccharin and Carbamazepine–Saccharin Cocrystals in Aqueous Media. *Molecular Pharmaceutics* **2012,** *9* (9), 2605-2612.

22. Bethune, S. J.; Huang, N.; Jayasankar, A.; Rodríguez-Hornedo, N. r., Understanding and Predicting the Effect of Cocrystal Components and pH on Cocrystal Solubility. *Crystal Growth & Design* **2009,** *9* (9), 3976-3988.

23. Reddy, L. S.; Bethune, S. J.; Kampf, J. W.; Rodríguez-Hornedo, N., Cocrystals and Salts of Gabapentin: pH Dependent Cocrystal Stability and Solubility. *Crystal Growth & Design* **2009,** *9* (1), 378-385.

24. Kuminek, G.; Rodriguez-Hornedo, N.; Siedler, S.; Rocha, H. V. A.; Cuffini, S. L.; Cardoso, S. G., How cocrystals of weakly basic drugs and acidic coformers might modulate solubility and stability. *Chemical Communications* **2016,** *52* (34), 5832-5835.

25. Kuminek, G.; Cao, F.; Bahia de Oliveira da Rocha, A.; Gonçalves Cardoso, S.; Rodríguez-Hornedo, N., Cocrystals to facilitate delivery of poorly soluble compounds beyond-rule-of-5. *Advanced Drug Delivery Reviews* **2016,** *101*, 143-166.

26. Huang, N.; Rodríguez-Hornedo, N., Engineering cocrystal solubility, stability, and pHmax by micellar solubilization. *Journal of Pharmaceutical Sciences* **2011,** *100* (12), 5219-5234.

27. Roy, L.; Lipert, M. P.; Rodriguez-Hornedo, N., Co-crystal Solubility and Thermodynamic Stability. In *Pharmaceutical Salts and Co-crystals*, The Royal Society of Chemistry: 2012; pp 247-279.

28. Mathias, N. R.; Xu, Y.; Patel, D.; Grass, M.; Caldwell, B.; Jager, C.; Mullin, J.; Hansen, L.; Crison, J.; Saari, A.; Gesenberg, C.; Morrison, J.; Vig, B.; Raghavan, K., Assessing the Risk of pH-Dependent Absorption for New Molecular Entities: A Novel in Vitro Dissolution Test, Physicochemical Analysis, and Risk Assessment Strategy. *Molecular Pharmaceutics* **2013,** *10* (11), 4063-4073.

29. Rodríguez-Hornedo, N.; Nehm, S. J.; Seefeldt, K. F.; Pagán-Torres, Y.; Falkiewicz, C. J., Reaction Crystallization of Pharmaceutical Molecular Complexes. *Molecular Pharmaceutics* **2006,** *3* (3), 362-367.

30. Jantratid, E.; Janssen, N.; Reppas, C.; Dressman, J. B., Dissolution Media Simulating Conditions in the Proximal Human Gastrointestinal Tract: An Update. *Pharmaceutical Research* **2008,** *25* (7), 1663-1676.

31. Galia, E.; Nicolaides, E.; Hörter, D.; Löbenberg, R.; Reppas, C.; Dressman, J. B., Evaluation of Various Dissolution Media for Predicting In Vivo Performance of Class I and II Drugs. *Pharmaceutical Research* **1998,** *15* (5), 698-705.

32. Amidon, G.; Lennernäs, H.; Shah, V.; Crison, J., A Theoretical Basis for a Biopharmaceutic Drug Classification: The Correlation of in Vitro Drug Product Dissolution and in Vivo Bioavailability. *Pharmaceutical Research* **1995,** *12* (3), 413-420.

33. Nizoral (Ketoconazole) Tablets Drug Label. https://www.accessdata.fda.gov/drugsatfda_docs/label/2014/018533s041lbl.pdf.

34. ter Horst, J. H.; Schmidt, C.; Ulrich, J., 32 - Fundamentals of Industrial Crystallization A2 - Rudolph, Peter. In *Handbook of Crystal Growth (Second Edition)*, Elsevier: Boston, 2015; pp 1317-1349.

35. Beckmann, W., Mechanisms of Crystallization. In *Crystallization: Basic Concepts and Industrial Applications*, 2013; pp 7-33.

36. Sangwal, K., Kinetics and Mechanism of Crystal Growth: An Overview. *Additives and Crystallization Processes: From Fundamentals to Applications*, 65-107.

37. De Yoreo, J. J.; Vekilov, P. G., Principles of crystal nucleation and growth. In *Reviews in mineralogy and geochemistry*, 2003; Vol. 54, pp 57-93.

38. Rodríguez-hornedo, N.; Murphy, D., Significance of controlling crystallization mechanisms and kinetics in pharmaceutical systems. *Journal of Pharmaceutical Sciences* **1999,** *88* (7), 651-660.

39. Dressman, J. B.; Reppas, C., In vitro–in vivo correlations for lipophilic, poorly water-soluble drugs. *European Journal of Pharmaceutical Sciences* **2000,** *11, Supplement 2*, S73-S80.

40. Kalantzi, L.; Persson, E.; Polentarutti, B.; Abrahamsson, B.; Goumas, K.; Dressman, J. B.; Reppas, C., Canine Intestinal Contents vs. Simulated Media for the Assessment of Solubility of Two Weak Bases in the Human Small Intestinal Contents. *Pharmaceutical Research* **2006,** *23* (6), 1373-1381.

41. Clarysse, S.; Brouwers, J.; Tack, J.; Annaert, P.; Augustijns, P., Intestinal drug solubility estimation based on simulated intestinal fluids: Comparison with solubility in human intestinal fluids. *European Journal of Pharmaceutical Sciences* **2011,** *43* (4), 260-269.

42. Taupitz, T.; Dressman, J. B.; Klein, S., In Vitro Tools for Evaluating Novel Dosage Forms of Poorly Soluble, Weakly Basic Drugs: Case Example Ketoconazole. *Journal of Pharmaceutical Sciences* **2013,** *102* (10), 3645-3652.

43. Rodríguez-Spong, B.; Acciacca, A.; Fleisher, D.; Rodríguez-Hornedo, N., pH-Induced Nanosegregation of Ritonavir to Lyotropic Liquid Crystal of Higher Solubility than Crystalline Polymorphs. *Molecular Pharmaceutics* **2008,** *5* (6), 956-967.

44. Tung, H.-H.; Paul, E. L.; Midler, M.; McCauley, J. A., Critical Issues in Crystallization Practice. In *Crystallization of Organic Compounds: An Industrial Perspective*, John Wiley & Sons, Inc.: 2009.

45. Emilie Deneau, G. S., An In-Line Study of Oiling Out and Crystallization. *Organic Process Research & Development* **2005,** *9* (6), 943-950.

46. Veesler, S.; Lafferrère, L.; Garcia, E.; Hoff, C., Phase Transitions in Supersaturated Drug Solution. *Organic Process Research & Development* **2003,** *7* (6), 983-989.

47. Lafferrère, L.; Hoff, C.; Veesler, S., Study of liquid–liquid demixing from drug solution. *Journal of Crystal Growth* **2004,** *269* (2), 550-557.

48. Bonnett, P.; Carpenter, K.; Dawson, S.; Davey, R., Solution crystallisation via a submerged liquid–liquid phase boundary: oiling out. *Chemical communications* **2003,** (6), 698-699.

49. Cahn, J. W., On spinodal decomposition. *Acta Metallurgica* **1961,** *9* (9), 795-801.

50. Indulkar, A. S.; Box, K. J.; Taylor, R.; Ruiz, R.; Taylor, L. S., pH-Dependent Liquid–Liquid Phase Separation of Highly Supersaturated Solutions of Weakly Basic Drugs. *Molecular Pharmaceutics* **2015,** *12* (7), 2365-2377.

Appendix 4A

To confirm that the cocrystals were fully dissolved, both drug and coformer concentrations were monitored during dissolution. The figures in this appendix show the cocrystal component concentrations during dissolution.

pH-Shift Dissolution: pH 2 → Blank FaSSIF

Drug and coformer concentrations from figure 4A.1 show that full dissolution of cocrystals was achieved in the initial media prior to pH-shift. This can be observed as the ADP, FUM, and SUC concentrations were the same as that of the drug, and both were at full dissolution concentration (purple dashed lines). Following the pH-shift, KTZ concentrations were observed to drop slightly below full dissolution, while the coformers ADP and FUM concentrations were seen to remain at full dissolution. SUC has very poor UV absorption, and its concentration could not be detected by HPLC after pH-shift. The coformer concentrations remained at full dissolution for the entire duration of the dissolution, indicating that the cocrystal was fully dissolved. The differences between coformer and drug concentrations immediately after the pH-shift also suggested that the lower KTZ concentrations were likely due to drug precipitation behavior instead of experimental or instrumental errors.

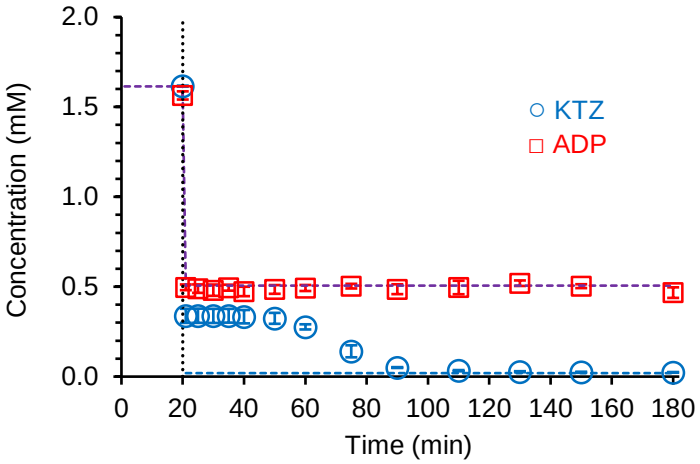

(a)

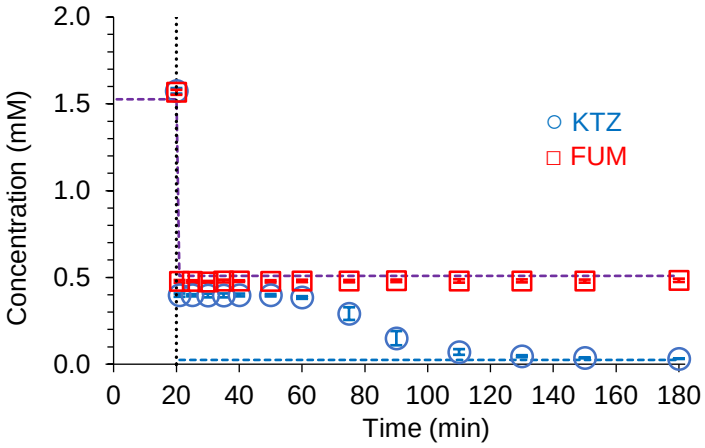

(b)

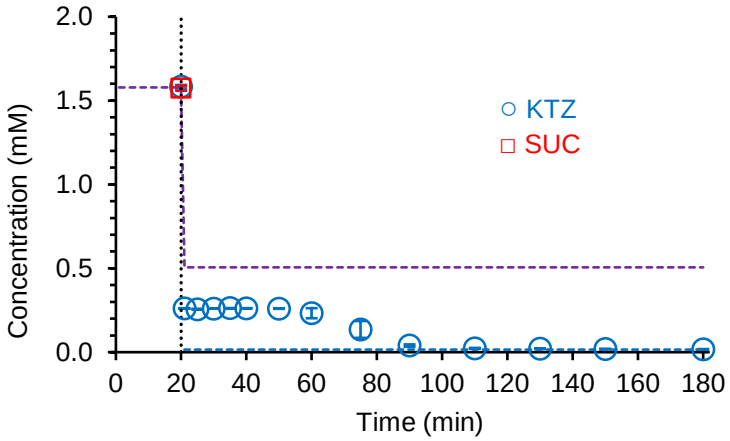

(c)

Figure 4A.1. Cocrystal component concentrations measured during pH-shift dissolution from SGF pH 2 to blank FaSSIF (pH 6.5, no surfactant). (a) KTZ-ADP. (b) KTZ-FUM. (c) KTZ-SUC. The purple dashed lines indicate the fully dissolved cocrystal/component concentration. The blue dashed lines indicate KTZ drug solubility. The dotted vertical black lines indicate where the pH-shift occurred.

pH-Shift Dissolution: pH 2 → FaSSIF

Cocrystal component concentrations in the initial media (SGF pH 2) indicated full dissolution of the cocrystals. As can be seen in figure 4A.2, drug concentrations were initially at full dissolution in FaSSIF. FUM was the only coformer that could be analyzed by HPLC in FaSSIF. FUM concentrations overlapped with KTZ concentrations until the drug began to precipitate out of the solution after 60 min, while the coformer remained fully dissolved.

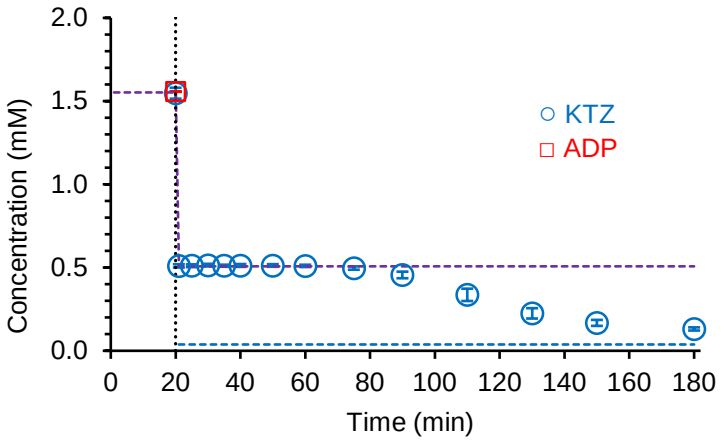

(a)

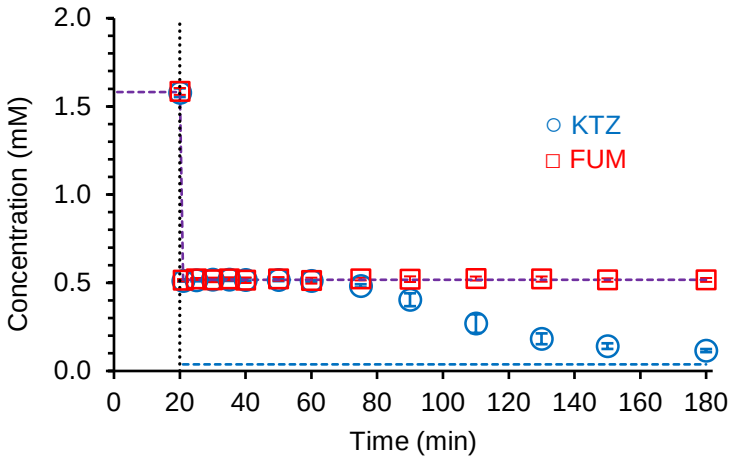

(b)

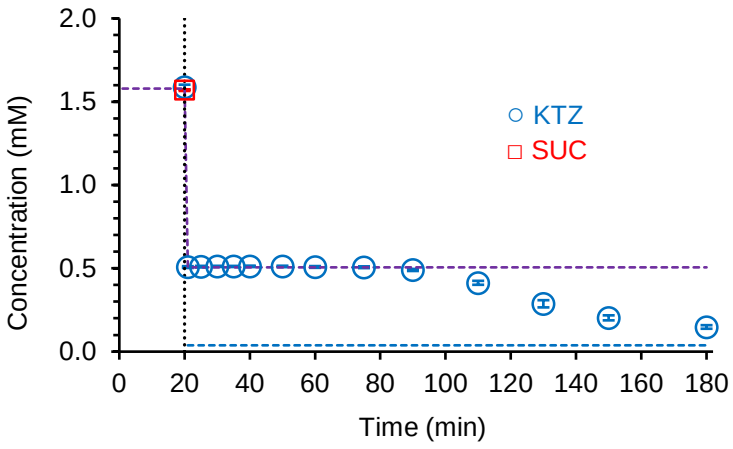

(c)

Figure 4A.2. Cocrystal component concentrations measured during pH-shift dissolution from SGF pH 2 to FaSSIF (pH 6.5). (a) KTZ-ADP. (b) KTZ-FUM. (c) KTZ-SUC. The purple dashed lines indicate the concentration at which the cocrystal is fully dissolved. The blue dashed lines indicate KTZ drug solubility. The dotted vertical black lines indicate where the pH-shift occurred.

pH-Shift Dissolution: pH 6 → FaSSIF

In pH 6 media, the cocrystals are fully soluble but the drug is not. In figures 4A.3(a) and 4A.3(b), ADP and FUM concentrations in the initial media suggest that the cocrystals may not have been fully dissolved prior to transferring into FaSSIF. SUC concentration was too low to be detected. ADP and FUM concentrations were higher than KTZ concentration in the SGF pH 6 media, indicating that drug precipitation may already be occurring. Only FUM was able to be detected in FaSSIF, and its concentration-time profile in FaSSIF indicates that the cocrystal was still dissolving in FaSSIF. Although coformers ADP and SUC concentrations could not be measured in FaSSIF, the drug concentration in FaSSIF exhibited initial increases before dropping down over time. This also suggest that there are still solid cocrystals left to dissolve in FaSSIF even as KTZ precipitated.

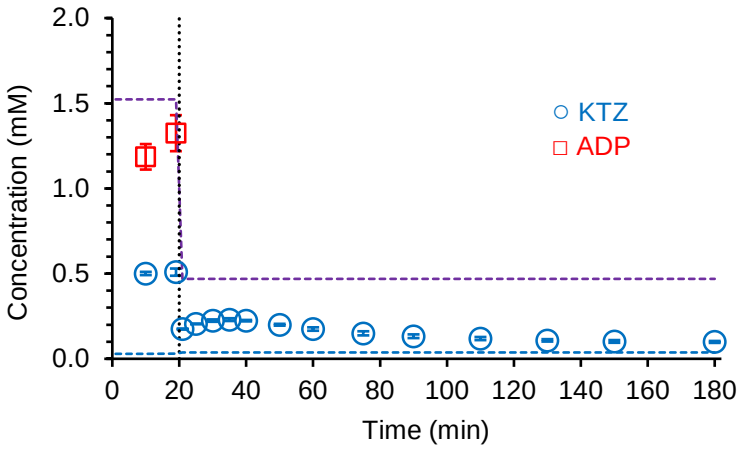

(a)

(b)

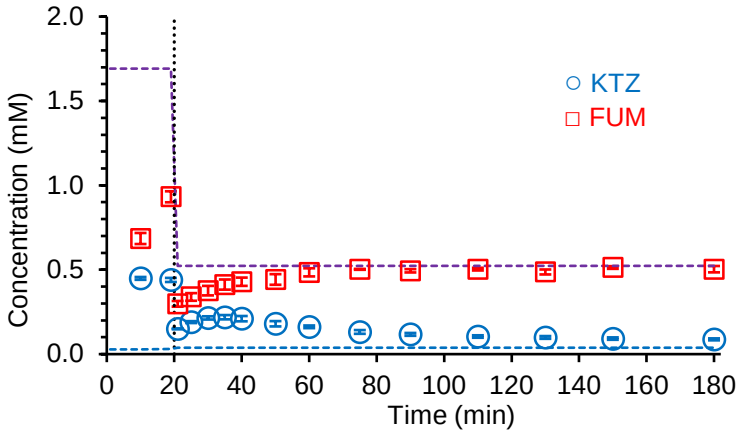

(c)

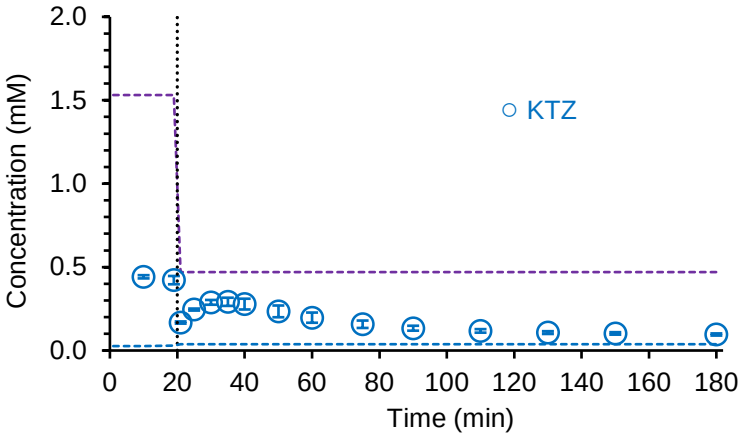

Figure 4A.3. Cocrystal component concentrations measured during pH-shift dissolution from SGF pH 6 to FaSSIF (pH 6.5). (a) KTZ-ADP. (b) KTZ-FUM. (c) KTZ-SUC. SUC concentration was too low to be detected in (c). The purple dashed lines indicate the concentration at which the cocrystal is fully dissolved. The blue dashed lines indicate KTZ drug solubility. The dotted vertical black lines indicate where the pH-shift occurred.

CHAPTER 5

CONCLUSIONS AND FUTURE WORK

This dissertation determined the mechanisms by which cocrystals of basic drugs with acidic coformers enhance solubility and dissolution under elevated pH conditions. The objectives of this work were to (1) understand the effect of pH and physiologically relevant surfactants on cocrystal solubility, supersaturation index (SA), and dissolution behavior; (2) derive mathematical models that describe cocrystal solubility behavior based on cocrystal dissociation, component ionization and solubilization equilibria; and (3) provide better understanding of cocrystal kinetic behavior based on SA and thermodynamic stability. Overall, this work aimed to expand current knowledge of the relationship between cocrystal thermodynamic and kinetic behaviors, and how this knowledge may be applied to optimize the advantages of cocrystals.

Cocrystals of a poorly water soluble, weakly basic drug ketoconazole (KTZ) with acidic coformers adipic acid (ADP), fumaric acid (FUM), and succinic acid (SUC) were used as model compounds to determine the effect of cocrystallization on solubility-pH behavior. Equations were derived to quantitatively predict cocrystal solubility under different pH conditions from cocrystal K_{sp} and component K_a. These predictions were validated with experimental solubility values of the cocrystals, and the equations were also capable of predicting solubility beyond the experimentally accessible pH range. In addition, these equations can be expanded to incorporate the effect of solubilizing agents in solution, such as endogenous bile salts present in the

gastrointestinal (GI) tract. The equations allow for accurate predictions of cocrystal solubility and SA without the need for extensive experimentation, saving both time and materials.

KTZ cocrystals exhibited distinctive solubility-pH behavior compared to the parent drug. While the basic drug solubility decreased with increasing pH to a constant value, the cocrystals have U-shaped solubility curves with pH. Different solubility-pH dependence resulted in the cocrystals having lower solubility than the drug at low pH conditions (pH < 3) and becoming more soluble as pH increased (pH > 4). Each of the cocrystals has a pH_{max}, ranging from pH 3.6 to 3.8, where $S_{cocrystal}$ is equal to S_{drug}. This pH_{max} identifies pH region (pH > pH_{max} for these cocrystals) where the cocrystal can provide solubility and dissolution advantage compared to the parent drug. Dissolution conducted at pH > pH_{max} led to supersaturation of the drug and can provide enhancement of oral drug absorption under elevated pH condition in the GI tract. KTZ cocrystal supersaturation index (SA) values increased from 1 at pH_{max} to 900 – 6000 at pH 6.5. Larger SA can increase the rate of drug precipitation and lead to no dissolution advantage. KTZ-FUM cocrystal in pH 6.5 buffer had SA > 3000, which resulted in rapid solution-mediated transformation back to the less soluble drug. This shows that cocrystal SA, which is a thermodynamic value, can be used to assess the kinetic behavior of cocrystals and risk of conversion.

Cocrystals and drugs can encounter many different types of solubilizing agents during the development process and oral dosing. Both the synthetic additives in the formulation and the endogenous surfactants and lipids present in the GI tract can alter the solubility of drug and cocrystals. Preferential solubilization of the more lipophilic drug component (KTZ) over the more hydrophilic coformers (ADP, FUM, and SUC) led to reduction of SA in the surfactant containing media (FeSSIF and FaSSIF). In other words, the cocrystal solubility enhancement

was less pronounced (1 – 3 fold) than that of the pure drug (4 – 6 fold) by these surfactants. The total solubilization constants ($K_{s,T}$) were determined for each component under relevant pH conditions and used in the prediction of drug and cocrystal solubility behavior. The reduction in SA caused by solubilizing agents allowed KTZ cocrystals to achieve higher drug concentrations and sustained supersaturation during dissolution in FeSSIF and FaSSIF compared to blank media of the same pH. Drug solubilizing agents that reduce SA can enhance cocrystal stability in solution and improve dissolution behavior.

Dissolution studies that mimic the pH change along the GI tract showed that the cocrystals performed much better than the drug under conditions where the gastric pH is elevated. Basic drugs like KTZ often have poor dissolution and oral absorption when gastric acidity is compromised, leading to highly variable bioavailability with pH. The cocrystals greatly improved the overall drug levels during dissolution following pH-shift from SGF pH 6 to FaSSIF media, achieving about 3 fold higher AUC than drug under the same media conditions. The cocrystals showed similar solution behavior as the drug under low gastric pH condition (pH 2), even though their solubilities are lower than that of the drug at that pH 2. The pH-shift studies provided a quick and effective way to assess the potential advantages these cocrystals can have *in vitro* and *in vivo*, and they also allowed us to observe the precipitation behavior of the drug.

During the pH-shift studies, we also observed that the KTZ drug can undergo spinodal decomposition (liquid-liquid phase separation) under high supersaturation levels, resulting in the formation of metastable drug phases during precipitation. These metastable phases of KTZ appeared to have higher solubility compared to the crystalline form and can delay the onset of crystallization. The presence of metastable KTZ forms in solution can lead to higher sustained

drug supersaturation (with respect to crystalline drug solubility), which can in turn improve oral absorption. Microscopic studies showed two distinct metastable forms of KTZ. One form resembled a droplet-like phase, and the other form has spherical shapes that would grow in number and size over time but do not appear to merge with each other. These two distinct phases of KTZ were observed to coexist in solution prior to the formation of drug crystals, and they can be induced by rapid generation of high supersaturation level of drug through increasing solution pH.

The findings in this work supported that cocrystals of basic drugs with acidic coformers can improve solubility and dissolution under elevated pH conditions in the GI tract and reduce pH-sensitivity. The unique solid and solution chemistry of cocrystals allows their solubility and dissolution advantages to be fine-tuned to optimize drug absorption. The mathematical relationships developed in this work can be used as quick and effective tools to quantitatively assess cocrystal solubility and potential for supersaturation under a wide range of media conditions. SA can be used to aid the interpretation of kinetic dissolution results, and it is a useful tool for a quick assessment of the risk of cocrystal conversion and drug precipitation.

A preliminary model for KTZ precipitation behavior is under development. This work is still in an early stage and further studies are required to validate and optimize this model. Further studies that involve a wider selection of drugs, cocrystals, additives, and solution conditions are needed to establish the relationship between cocrystal SA values and the kinetic behaviors. The influence of cocrystals on drug supersaturation, permeability, and absorption *in vivo* remains to be established. This knowledge will aid in developing better predictions for *in vivo* behavior based on *in vitro* studies.